**Instituto de Agroquímica y Tecnología de Alimentos**

**(IATA-CSIC)**

**Grupo de Envases**


# EFECTO DE DISTINTOS TRATAMIENTOS DE CONSERVACIÓN DE ALIMENTOS SOBRE LA MORFOLOGÍA Y PROPIEDADES DE MATERIALES POLIMÉRICOS DE ENVASE

Memoria presentada por:

**AMPARO LÓPEZ RUBIO**

PARA OPTAR AL GRADO DE DOCTOR EN TECNOLOGÍA DE ALIMENTOS

**Valencia, Febrero de 2006**

## LISTA DE PUBLICACIONES

Esta tesis es una compilación de las siguientes publicaciones:

I. "Morphological alterations induced by temperature and humidity in ethylene-vinyl alcohol copolymers". **A. López-Rubio**, J.M. Lagarón*, E. Giménez, D. Cava, P. Hernandez-Muñoz, T. Yamamoto and R. Gavara. *Macromolecules* 36, pp. 9467-9476 (2003)

II. "Gas barrier changes and morphological alterations induced by retorting in ethylene-vinyl alcohol based food packaging structures". **A. López-Rubio**, P. Hernández-Muñoz, E. Giménez, T. Yamamoto, R. Gavara and J.M. Lagarón*. *Journal of Applied Polymer Science* 96, issue 6, pp. 2192-2202 (2005)

III. "Characterization of the effect of retorting on blends of EVOH with amorphous polyamide and nylon-containing ionomer". Artículo en preparación

IV. "Gas barrier changes and structural alterations induced by retorting in a high barrier aliphatic polyketone terpolymer". **A. López-Rubio**, E. Giménez, R. Gavara and J.M. Lagarón*. Aceptado para publicación en el *Journal of Applied Polymer Science*

V. "On the unexpected crystallization of amorphous polyamide as induced by a packaged food retorting treatment and its implications in barrier properties". **A. López-Rubio**, R. Gavara and J.M. Lagarón*. Aceptado para publicación en el *Journal of Applied Polymer Science*

VI. "Effects of high pressure treatments on the properties of food packaging materials". **A. López-Rubio**, P. Hernández-Muñoz, E. Almenar, J.M. Lagarón, R. Catalá, R. Gavara* and M.A. Pascall. *Innovative Food Science and Emerging Technologies* 6, issue 1, pp. 51-58 (2005)

VII. "Radiation-induced oxygen scavenging activity in EVOH copolymers". Artículo en preparación

VIII. "Improving Packaged Food Quality and Safety by Synchrotron X-Ray Analysis". **A. López-Rubio,** P. Hernández-Muñoz, R. Catalá, R. Gavara and J.M. Lagarón*. *Food Additives and Contaminants 22*, issue 10, pp. 988-993 (2005).

# 1 INTRODUCCIÓN

## 1.1 ANTECEDENTES

Los envases alimentarios han dejado de ser un mero medio de transporte y protección para pasar a formar parte del propio producto, percibiéndose hoy como un elemento esencial en el actual estilo de vida de las sociedades desarrolladas. Desde un punto de vista comercial se lo considera tan importante como el alimento (producto) propiamente dicho, el precio, el canal de venta (place) o la promoción. Muchos especialistas lo llaman "la quinta p", en alusión al nombre inglés packaging. Entre los factores vinculados a este fenómeno figuran los nuevos hábitos de consumo de comidas rápidas (precocinadas) y congeladas, las formas de comercialización y la notable dinámica que ha cobrado la industria alimentaria, que cada año lanza al mercado miles de productos alimenticios nuevos.

La introducción de los polímeros como materiales para el envasado de alimentos ha supuesto toda una revolución a lo largo de las últimas décadas. Las ventajas de los materiales plásticos frente a otros más tradicionales como el vidrio o la hojalata son muchas. Una de las más importantes es la diversidad de materiales y composiciones disponibles que permiten adaptar de una manera aceptable las propiedades del envase a las necesidades específicas de cada producto. Otras características muy relevantes de estos materiales son su ligereza, bajo coste, facilidad de impresión y termosoldabilidad, propiedad que permite la formación de envases herméticos sin necesidad de elementos de cierre adicionales. Es también una ventaja el hecho de que sean fácilmente conformables en una variedad ilimitada de formas y tamaños, y que éstas sean muy fácilmente accesibles y modificables por los transformadores. Es bien conocido que las propiedades ópticas de los materiales plásticos en términos de transparencia y brillo pueden adecuarse a los requisitos específicos de un producto. Esto facilita la visión del producto envasado por el consumidor y confiriéndole una apariencia muy atractiva, al tiempo que puede ser opaco a un intervalo determinado de longitudes de onda para proteger al producto. Las propiedades térmicas y mecánicas también pueden ser modificadas en gran medida, si bien siempre dentro de las limitaciones inherentes a los plásticos, para obtener materiales de envase que permitan construir desde estructuras muy flexibles para fabricar bolsas, sacos y

envolturas, pasando por semirrígidos (bandejas y tarrinas), hasta materiales más rígidos constitutivos de botellas, depósitos, tapones, etc.. En cuanto a las propiedades térmicas, se pueden producir materiales con mayor resistencia térmica para, por ejemplo, fabricar envases esterilizables u otros con menor punto de fusión que pueden actuar como termosoldables. Otra característica también muy relevante de los plásticos como materiales de envase y que se apoya en la termosoldabilidad anteriormente mencionada, es la posibilidad de incorporarlos en procesos integrados, donde la formación del envase, el llenado y posterior sellado ocurren en línea de manera muy ventajosa desde un punto de vista económico y de rapidez de fabricación, evitando el transporte de envases vacíos.

Sin duda, el mayor inconveniente de los plásticos, al compararlos con otros materiales de envase tradicionalmente utilizados (como el vidrio o la hojalata), deriva de su estructura. Los materiales utilizados en el envasado de alimentos son amorfos o semicristalinos. Estos últimos constan de una fase cristalina, en la que las cadenas poliméricas se encuentran ordenadas en una configuración muy compacta formando cristales y que a efectos prácticos se puede considerar impermeable, y una fase amorfa en la que las cadenas poliméricas están desordenadas, dejando entre ellas volumen libre disponible para el transporte de compuestos de bajo peso molecular como gases o vapores, fenómeno responsable de las interacciones del envase con el alimento y el exterior del envase, tan relevantes para la calidad y seguridad de los alimentos. La permeabilidad al oxígeno, en concreto, es un parámetro crítico para la conservación de muchos productos alimentarios. El oxígeno es un elemento que concurre en muchas de las causas de deterioro de los alimentos, tales como la alteración microbiológica por mohos u otros microorganismos aerobios, el deterioro enzimático (pardeamiento enzimático, oxidación de la vitamina C y pérdida de aromas), o el deterioro bioquímico (enranciamiento de grasas). Para otros alimentos, sin embargo, su presencia es necesaria, como es el caso de frutas y verduras frescas, que requieren de oxígeno para poder mantener su actividad fisiológica, o en carnes rojas para mantener una pigmentación adecuada.

En consecuencia, numerosos estudios se han centrado en entender los mecanismos de transporte de masa en polímeros para así poder diseñar materiales con la permeabilidad adecuada al tipo de aplicación. Para el envasado de alimentos

sensibles al oxígeno se necesitan materiales poliméricos que restrinjan de manera sustancial el paso de gases y vapores. A estos materiales con baja permeabilidad se los conoce como materiales de alta barrera[1]. Estos materiales llegan en la actualidad a presentarse como una alternativa a los materiales tradicionales utilizados en la fabricación de conservas, como el vidrio y la hojalata. En el caso de frutas y verduras frescas, diversos estudios se han centrado en el diseño de materiales u envases que, permitan el intercambio de gases y vapores de forma controlada para asegurar que dichos productos vegetales frescos puedan mantener un metabolismo postcosecha durante la etapa de comercialización.

Por otro lado, en muchas industrias agroalimentarias, para optimizar la velocidad de procesado y minimizar la manipulación de los productos alimentarios, las líneas de producción llevan incorporada una línea de envasado, de tal forma que los tratamientos de conservación se aplican al producto ya envasado. La esterilización en el envase (o apertización) es uno de los tratamientos clásicos más empleados y para los que los envases clásicos de vidrio y hojalata cumplen la mayoría de los requisitos a la hora de asegurar la vida útil de las conservas. También para estos tratamientos, existen envases alternativos construidos con materiales poliméricos. Los requisitos más importantes incluyen la utilización de envases herméticos de alta barrera a los gases construidos con materiales que soporten adecuadamente el proceso de esterilización. El material alta barrera más empleado para este tipo de aplicaciones es el copolímero de etileno-alcohol vinílico (EVOH), ya que además de tener unas excelentes propiedades barrera a gases y compuestos de bajo peso molecular (como los aromas) y de poder ser transformado con los mismos procesos que otros materiales comunes como las poliolefinas, muestra una alta resistencia química a disolventes, excelentes propiedades ópticas y físicas, buena resistencia térmica y altísima velocidad de cristalización[2,3].

Las excelentes propiedades barrera de estos copolímeros se derivan de la presencia en su estructura de grupos hidroxilo que le confieren una elevada cohesión intermolecular, reduciendo el volumen libre entre las cadenas disponible para el intercambio de gases. Pero a su vez, estos grupos hidroxilo hacen que este material sea altamente hidrofílico, de manera que en presencia de agua sus propiedades barrera se ven en gran medida deterioradas[4]. Por esta razón en la mayoría de

aplicaciones de envasado de alimentos se utilizan estructuras multicapa en las cuales el EVOH se encuentra franqueado entre dos láminas de materiales hidrófobos, como por ejemplo, polietileno, polipropileno, etc.

El EVOH lo podemos encontrar formando parte tanto de envases flexibles como semirrígidos y rígidos[5,6]. Estos últimos, bien sean bandejas, tarrinas o botellas, se utilizan básicamente para envasar alimentos sensibles al oxígeno que pueden además ser sometidos a procesos tales como llenado en caliente, envasado aséptico ó esterilización dentro del envase. Los procesos de esterilización suelen tener lugar en presencia de vapor de agua a presión, por lo que los envases se ven expuestos a altas temperaturas y altas humedades relativas. En estas condiciones, el agua es capaz de atravesar la capa externa de polipropileno, sorbiéndose en la capa intermedia de EVOH y causando una plastificación del material. Esto provoca un aumento del volumen libre permitiendo el paso de oxígeno hacia el interior del envase. Este fenómeno ha sido descrito por diversos autores[7,8,9], si bien se desconocía el efecto de estos procesos sobre la morfología de estos copolímeros, efecto que es objeto de estudio en este trabajo. El elevado paso de oxígeno a través de las paredes del envase tras la esterilización se traduce en una reducción de la vida útil del alimento envasado, especialmente si éste es susceptible de sufrir oxidaciones, ya que, aparte de la potencial alteración microbiológica que con la presencia de oxígeno puede verse favorecida, el producto puede sufrir cambios sensoriales inaceptables induciendo al rechazo por parte del consumidor.

Algunas de las soluciones que podrían plantearse al anterior problema son, por ejemplo, reforzar la estructura del EVOH mediante tratamientos térmicos de forma que se reduzca su sensibilidad a la elevada humedad que atraviesa las capas externas del envase durante la esterilización, o bien reducir su carácter hidrófilo mezclándolo con otros materiales más hidrófobos, en las proporciones adecuadas para que su permeabilidad a gases se mantenga baja.

Existen otros materiales poliméricos de alta barrera a gases como son algunas composiciones de poliamidas o las policetonas que potencialmente podrían sustituir al EVOH en este tipo de aplicaciones y que, por tanto, también se han considerado para este estudio.

Por otra parte, los consumidores actualmente prefieren alimentos más frescos y naturales y, por tanto, con tratamientos de conservación menos agresivos, como son las altas presiones hidrostáticas o la irradiación. Los envases plásticos juegan un papel fundamental en la aplicación de estos tratamientos novedosos de conservación, ya que pueden aplicarse al alimento ya envasado y, por ejemplo, en el caso de la alta presión, es necesario utilizar envases flexibles para que la presión se transmita adecuadamente al alimento. Como en el caso de la esterilización, los envases utilizados para envasar los productos antes del tratamiento requieren que al menos uno de los materiales poliméricos constitutivos de la estructura posea una baja permeabilidad a los gases. El copolímero de etileno y alcohol vinílico, debido a sus excelentes propiedades sería un buen material para este tipo de aplicaciones, pero es necesario estudiar qué efectos tienen estos tratamientos sobre su estructura y propiedades, con el fin de asegurar la calidad y vida útil del alimento envasado.

## 1.2 POLÍMEROS Y ALIMENTOS

De un modo sencillo podemos describir los polímeros como moléculas muy largas (macromoléculas) construidas a partir de unidades más pequeñas o monómeros. La organización de dichas unidades, los diferentes tipos de cadenas que pueden sintetizarse y las diferentes conformaciones que pueden adoptar las cadenas, hacen de los polímeros una clase de materiales con un rango de propiedades amplísimo y de gran interés en aplicaciones de envasado de alimentos dada su capacidad para adecuarse y dar respuesta a la complejidad y variedad de productos a envasar.

El uso de plásticos (polímeros que pueden ser conformados utilizando calor, presión y tiempo[10]) en el envasado de alimentos es bastante reciente, pero los avances científicos y tecnológicos en el campo han sido y siguen siendo tremendos y fascinantes.

Grandes avances han tenido lugar desde que A. Parker desarrollara el primer plástico sintético en 1838, una forma de nitrato de celulosa al que se denominó “parkesine”, con el que se reemplazaron materiales naturales como el marfil en algunas aplicaciones. Pero hasta casi un siglo después ni siquiera se intuyó la verdadera naturaleza macromolecular de los plásticos. En aquel entonces se pensaba que estos materiales de elevado peso molecular consistían en pequeñas moléculas en suspensiones estables que constituían sistemas coloidales[7].

La verdadera revolución de los polímeros sintéticos tuvo lugar en la década de los 40 del siglo pasado, a raíz de la extensa investigación llevada a cabo durante la Segunda Guerra Mundial, en la que la ligereza de estos materiales fue, probablemente, una de las claves de su éxito. De los años 50 a los 70, el descubrimiento de los catalizadores Ziegler-Natta (por los que ambos descubridores fueron agraciados con sendos premios Nobel) que permitían una síntesis polimérica controlada (con capacidad para regular tanto el peso molecular, como la secuencia de monómeros y, por tanto, la arquitectura macromolecular) a baja presión y temperatura, así como el desarrollo de nuevas tecnologías de síntesis impulsaron el, desde entonces imparable, desarrollo de nuevos materiales poliméricos[10].

Como ya se ha comentado brevemente en los antecedentes, los materiales poliméricos, han ido desplazando progresivamente a otros materiales de envase tradicionalmente utilizados como la hojalata o el vidrio. Hoy en día, prácticamente todos los alimentos que encontramos en los supermercados, tanto frescos como procesados, se comercializan en algún tipo de envase, que en una gran parte están constituidos por materiales poliméricos. Como puede observarse en la figura 1.1, los materiales plásticos suponen alrededor de un 70% de los materiales de envases para alimentos. Desde el punto de vista comercial, en el que la máxima es "reducción de costes" para conseguir maximizar el beneficio, parece que, de nuevo, la ligereza de estos materiales tendría una importancia considerable en su introducción inicial como materiales para el diseño de envases de alimentos.

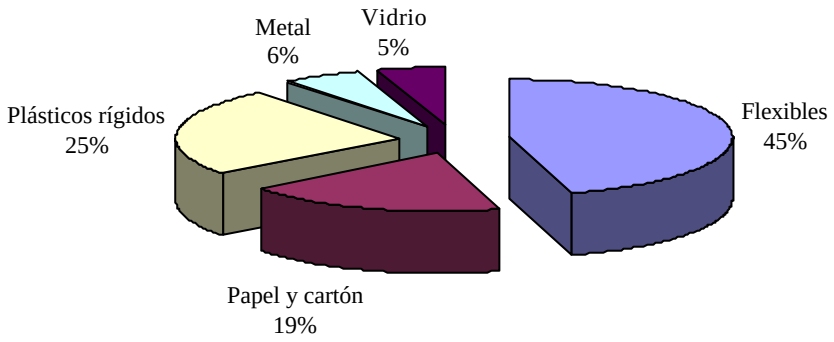


**Figura 1.1** Materiales utilizados en envases de alimentos en Europa occidental

Otra de las grandes ventajas de los plásticos como materiales de envase radica en su enorme versatilidad. Estos pueden diseñarse, modificarse, mezclarse, "ensamblarse" formando estructuras multicapa, moldearse y hasta funcionalizarse para satisfacer las necesidades del producto a envasar, lo cual permite comercializar prácticamente cualquier tipo de producto alimenticio y además proveerlo de una vida útil razonable, ya que no olvidemos que los polímeros en su concepción de envases deben de "contener, proteger e identificar" el producto desde su fabricación hasta su consumo[11]. Para conseguir este objetivo los envases plásticos, a diferencia de los

envases de vidrio y hojalata, suelen estar constituidos por diversas capas, cada una de las cuales aporta al menos una característica deseable al conjunto. En la capa externa del envase suelen utilizarse materiales con capacidad de impresión y que proporcionen consistencia y propiedades mecánicas adecuadas, como el polietiléntereftalato (PET) o la poliamida orientada (oPA). La capa intermedia suele ser la que proporciona propiedades de alta barrera a gases y compuestos de bajo peso molecular (siempre que la aplicación concreta de envasado lo requiera). Los materiales más empleados como capa intermedia son los copolímeros EVOH, también algunos tipos de poliamida, así como aluminio en el caso de que se requiera además opacidad. Por último, la capa interna del envase debe de proporcionar propiedades como termosoldabilidad e inercia química, en la que los materiales más utilizados son, sin duda, poliolefinas tales como el polipropileno (PP) o el polietileno (PE).

La amplia variedad de formas en que pueden conformarse, así como su capacidad de ser decorados o serigrafiados mediante impresión hacen de los materiales plásticos de envase muy atractivos, actuando de vendedor silencioso frente al consumidor, otorgando incluso un valor añadido al producto envasado.

Otras de las ventajas de estos materiales en el campo del envasado de alimentos son sus propiedades ópticas (transparencia), capacidad de termosellado eliminando la necesidad de adicionar elementos de cierre, así como su inercia química que asegura el mantenimiento de sus propiedades durante el almacenamiento y conservación de los productos envasados[12]. Sin embargo, esta inercia química, que a priori es una ventaja, plantea en la práctica serios problemas medioambientales, ya que la enorme cantidad de envases plásticos comercializados a nivel mundial genera, a su vez, una cantidad ingente de residuos que es necesario gestionar. A este respecto, durante las dos últimas décadas ha existido un interés creciente en el desarrollo de materiales comestibles y biodegradables que queda reflejado en una intensa actividad investigadora[13,14,15].

Pero, sin lugar a dudas, la propiedad más relevante de los plásticos en el envasado de alimentos, como también ha quedado patente en el apartado de antecedentes, se deriva de la presencia de un volumen libre entre las cadenas poliméricas que permite

el transporte de sustancias de bajo peso molecular a través de la matriz polimérica y que se manifiesta en fenómenos como el intercambio de gases entre el exterior y el interior del envase (como la permeación del oxígeno desde el exterior al interior del envase o de componentes del aroma alimentario que supondría una pérdida de calidad sensorial del alimento envasado), así como la sorción de componentes del alimento o la migración de aditivos o residuos desde el envase, que pueden alterar la calidad y salubridad del alimento envasado. Este tema lo trataremos en mayor profundidad en el apartado de "propiedades barrera en polímeros".

En la actualidad muchos envases hacen uso de estas últimas propiedades de forma positiva, dando lugar a un nuevo concepto de envase, el envase activo, que en contraposición al concepto clásico de envase alimentario que lo define como "barrera pasiva que separa el alimento del medio ambiente y evita o retrasa los efectos adversos del entorno para mantener su seguridad y calidad", está pensado para actuar como un sistema coordinado con el producto y el entorno para mejorar la seguridad y calidad del mismo y alargar su vida útil[16]. Así, para muchos alimentos, estos envases activos controlan el intercambio de gases para mantener al alimento en una atmósfera adecuada. Estos nuevos sistemas de envasado se desarrollaron como una tecnología emergente de procesado de alimentos que da respuesta a la tendencia de los consumidores hacia el consumo de alimentos mínimamente procesados, frescos, naturales y con elevada vida útil. Adicionalmente, la globalización de los mercados, que implica mayores distancias de distribución, plantea contínuos retos al sector del envase actuando como fuerza impulsora para el desarrollo de nuevos y mejorados conceptos de envasado que aumenten la vida útil de los productos sin disminuir su seguridad y calidad.

## 1.3 POLÍMEROS Y TRATAMIENTOS DE CONSERVACIÓN DE ALIMENTOS

### 1.3.1 Esterilización en autoclave

Los plásticos entraron en la fabricación de conservas con el desarrollo de las técnicas de envasado aséptico y de las bolsas esterilizables en la década de los años 60 del siglo pasado. El camino recorrido desde esas fechas, en los intentos de encontrar materiales plásticos resistentes a las temperaturas de esterilización sin problemas tecnológicos, ha sido muy largo, con avances muy significativos en diversas líneas de actuación, hasta culminar en años recientes con los nuevos materiales plásticos de alta barrera esterilizables a alta temperatura que ya constituyen una realidad comercial[17]. En el desarrollo de los envases plásticos esterilizables pueden establecerse tres etapas bien definidas, que han dado lugar a diferentes tecnologías que coexisten en la actualidad con diferente grado de penetración comercial[18]:

- Bolsas flexibles esterilizables
- Envases rígidos esterilizables
- Envases semirrígidos de plásticos alta barrera, entre los que encontramos: bandejas con tapa de complejos termosellables y tarrinas con tapa metálica con doble cierre.

En la línea de sustitución de los envases metálicos clásicos para alimentos esterilizados, la primera y más significativa alternativa hasta años recientes ha sido la bolsa flexible esterilizable, cuyo desarrollo se inició en los años 50. En su diseño generalizado, la bolsa flexible esterilizable tiene forma de sobre plano con cuatro costuras laterales y está constituída por laminados de alta barrera y resistentes a temperaturas de esterilización. El diseño y las características del material permite una rápida y eficaz esterilización del producto envasado, con la mínima sobrecocción de las zonas periféricas, así como un rápido calentamiento del alimento para el consumo[19].

El éxito tecnológico e incluso comercial de los primeros años de su desarrollo se debió a las substanciales ventajas que, en principio, aporta esta tecnología,

particularmente su ligereza y perfil plano que permite una rápida esterilización y, por tanto, una excelente calidad del producto envasado. No obstante, presentaba también ciertos inconvenientes prácticos, como por ejemplo[20]:

- Difícil llenado y manipulación en caliente de las bolsas
- Bajas velocidades de producción
- Necesidad de control muy estricto en la esterilización

Estos inconvenientes han limitado su desarrollo comercial, sólo apreciable en algunos países como Japón. En los últimos años se han desarrollado las bolsas flexibles autosustentables como las que se muestran en la figura 1.2, diseñadas para facilitar el llenado y manipulación y aumentar las velocidades de producción.


**Figura 1.2** Ejemplo comercial de bolsas flexibles esterilizables autosustentables

Por otro lado, las dificultades tecnológicas de las bolsas flexibles esterilizables y el interés de los fabricantes de envases impulsaron el desarrollo como alternativa en los años 70 de las bandejas esterilizables. Uno de los primeros ejemplos de estos envases fue el Lamipack, desarrollado en Japón. Se trata de una bandeja esterilizable constituída por una multicapa coextruída de polipropileno(PP)/policloruro de vinilideno (PVdC)/PP. Posteriormente se comercializaron otras tecnologías si bien

usando copolímeros de etileno y alcohol vinílico (EVOH) como sistema barrera alternativo al PVdC[21]. Básicamente las diversas alternativas actuales consisten en bandejas planas termoformadas de baja profundidad, de composición PP/EVOH/PP, con distintos formatos, en algunos casos multicompartimentadas para contener varias partes de una comida. En la figura 1.3 se muestra esquemáticamente la estructura de este tipo de bandejas así como de los materiales que se emplean en las tapas.

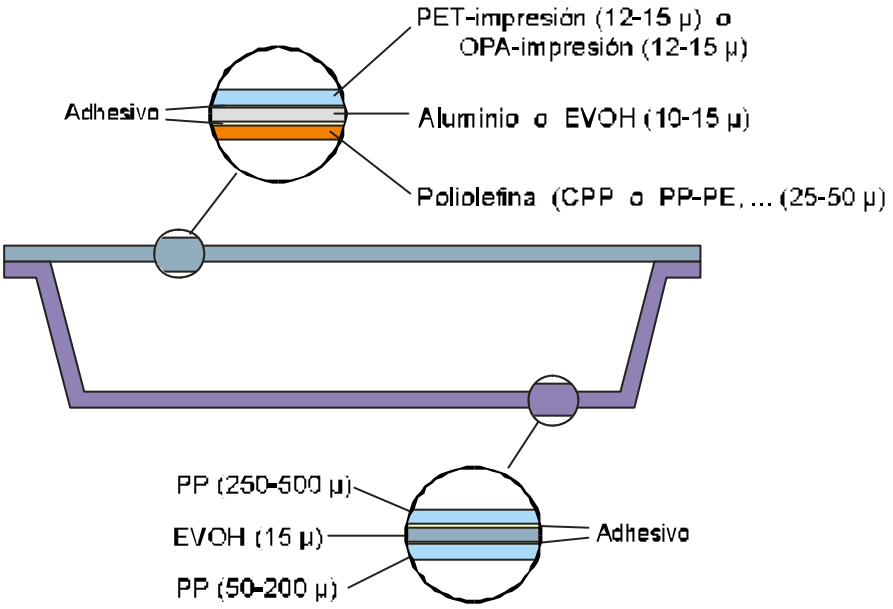


**Figura 1.3** Estructuras de envase comúnmente utilizadas como cuerpo y tapa de bandejas esterilizables

Como ya se ha comentado previamente, diversos estudios realizados con éstas y otras estructuras multicapa conteniendo EVOH como material barrera[8,9], han demostrado un aumento en la permeabilidad al oxígeno del mismo como consecuencia de los procesos de esterilización. La pérdida de propiedades barrera de estos materiales, así como el tiempo que tarda el material en recuperar su permeabilidad original, son datos indispensables para conocer la cantidad de oxígeno que atraviesa el envase y que puede alterar las propiedades de los alimentos envasados e, incluso, comprometer su vida útil.

### 1.3.2 Tratamiento con altas presiones hidrostáticas

El procesado mediante altas presiones hidrostáticas es una tecnología de conservación emergente que está alcanzando relevancia comercial como consecuencia de las tendencias actuales de consumo, que llevan a la producción de productos de alta calidad que mantengan sus propiedades naturales, de frescura y sin la adición de conservantes[22].

Excepto en el caso de alimentos líquidos que pueden ser tratados con altas presiones sin necesidad de estar envasados (aunque necesitarán un envasado aséptico posterior), los envases son un factor clave en el procesado por altas presiones, ya que deben de conservar las propiedades de los alimentos sin perder ni la integridad, ni las propiedades barrera y mecánicas.

La conservación de alimentos mediante altas presiones hidrostáticas consiste básicamente en la aplicación de presiones hidrostáticas entre 100 y 1000 MPa durante un determinado período de tiempo (generalmente entre 1 y 30 minutos) a temperatura ambiente (aunque en la práctica se puede aplicar desde temperaturas bajo cero hasta más de 100ºC[23]). La presión se aplica a través de un fluido donde el alimento previamente envasado es sumergido, y la extensión de la vida útil se consigue mediante la inactivación de microorganismos y enzimas.

Los tratamientos de conservación por altas presiones hidrostáticas presentan innumerables ventajas frente a los tratamientos térmicos convencionales, resaltando el que se aplican a bajas temperaturas, lo cual favorece el mantenimiento de los atributos de calidad del producto envasado. Además, este tratamiento es independiente del tamaño y geometría del producto a tratar, y su efecto es instantáneo y uniforme, y a pesar de que se ha probado que afecta en cierto modo la textura de algunos productos alimentarios, el sabor, color y propiedades nutricionales se mantienen prácticamente inalteradas[17].

A parte de los requerimientos típicos de los envases para alimentos como son hermeticidad, interacciones envase/alimento mínimas y propiedades barrera y ópticas adecuadas, el envase debe de ser capaz de transmitir la presión hidrostática al

producto envasado. Estudios previos han demostrado que los envases flexibles son más adecuados que los rígidos para los tratamientos con altas presiones. Los envases rígidos, tales como los botes metálicos o de vidrio tienden a fracturarse o deformarse como resultado de la elevada presión aplicada[24]. Por el contrario, la mayor parte de los envases flexibles soportan este tipo de tratamientos de conservación sin mostrar signos visibles de pérdida de integridad. Unos de los factores más importantes que han contribuido al éxito de los envases plásticos es la posibilidad de utilizar estructuras multicapa. Dicho complejo multicapa, adecuado para preenvasar alimentos que van a ser tratados con altas presiones, debe de poseer la suficiente flexibilidad, elasticidad y resistencia a delaminación durante el proceso de compresión, ya que la pérdida de integridad estructural puede implicar un deterioro en la calidad y seguridad del alimento envasado[25].

Es, por tanto, de suma importancia entender los efectos de las altas presiones sobre propiedades relevantes de los materiales plásticos que aseguren la seguridad y calidad de los productos alimentarios a lo largo de su vida útil.

### 1.3.3 Esterilización mediante irradiación

La conservación de los alimentos mediante radiaciones ionizantes consiste, en esencia, en un proceso mediante el cual el alimento es sometido a un tipo de radiación que provoca en sus componentes y en sus contaminantes cambios moleculares que mejoran la calidad higiénico-sanitaria del alimento y prolongan su vida útil[26]. Las radiaciones ionizantes son aquellas capaces de transmitir al material irradiado energía suficiente para provocar su ionización. El fenómeno de la ionización consiste básicamente en el desplazamiento de electrones fuera de sus órbitas habituales. Cuando la energía transmitida es suficiente se produce incluso la expulsión de electrones y, en ocasiones, la rotura de enlaces moleculares. De este modo se generan[27]:

-*partículas excitadas* (desplazamiento de un electrón sin expulsión del átomo),
-*iones* (partículas cargadas eléctricamente), o
-*radicales libres* (en los que quedan desapareados electrones en el orbital externo de las moléculas, convirtiéndose en partículas neutras altamente reactivas).

Cuando la energía del electrón expulsado es suficiente, éste puede generar el mismo efecto en moléculas próximas ("ionización secundaria"). El tipo de partícula formada, depende, además del nivel energético de la radiación, de la naturaleza del material irradiado[28].

La dosis de radiación se define como la cantidad de energía absorbida por un producto durante su irradiación. La unidad de medida es el Gray (Gy) = tratamiento capaz de transmitir 1 Julio de energía /Kg de producto irradiado. El rango habitual de la irradiación de los alimentos va de 50 Gy a 10 kGy. Una dosis de irradiación de 10 kGy equivaldría a la cantidad de energía necesaria para que el agua aumentase 2,4ºC su temperatura. Por ello, algunos autores[21,29] se han referido a la irradiación de alimentos como *esterilización fría*.

Las fuentes de irradiación son:

- Los rayos gamma

- Los rayos X de energía inferior a 5 MeV
- Los electrones acelerados de energía inferior a 10 MeV.

Si los niveles de energía de la radiación fueran excesivamente elevados, podría producirse un fenómeno de radiactividad inducida: algunos componentes de los alimentos se convertirían a su vez en elementos radiactivos. Seguramente esta posibilidad y los conocidos dramáticos efectos de las radiaciones en el cuerpo humano son las razones por las que el consumidor ha desarrollado tal rechazo a los alimentos irradiados.

Para evitar el riesgo de la radiactividad inducida, el Comité Mixto de expertos en irradiación de alimentos (ICGFI: International Consultative Group of Food Irradiation), integrado por miembros de la FAO/AIEA/OMS, basándose en estimaciones teóricas y centenares de estudios realizados en diversos países por laboratorios gubernamentales y privados, acordó en 1981 autorizar para el tratamiento de alimentos, tan sólo fuentes de radiación con energía muy inferior a la necesaria para inducir radiactividad. Este comité mixto de expertos concluyó de modo taxativo que la irradiación de alimentos con dosis inferiores a 10 kGy no presenta riesgos toxicológicos, ni introduce riesgos desde un punto de vista nutricional o microbiológico[30]. Recientemente (1997), la OMS, como consecuencia de los resultados favorables de gran número de investigaciones sobre el consumo de alimentos irradiados con dosis muy superiores a los 10 kGy, se ha declarado en favor de la utilización de dosis de radiación más elevadas[31].

De acuerdo con su intensidad la radiación se clasifica en:

| Tratamiento | Aplicaciones | Dosis | Productos |
|---|---|---|---|
| **Dosis baja (Hasta 1 kGy)** | **Inhibición de la germinación** | **0,05-0,15** | **Patatas, cebollas, ajos, boniatos, etc.** |
| | **Desinfestación e inactivación parasitaria** | **0,15-0,5** | **Cereales, frutas frescas y deshidratadas, carne pescado deshidratado, cerdo fresco** |
| | **Ralentización de los procesos fisiológicos (maduración, etc.)** | **0,25-1,0** | **Frutas y vegetales frescos** |
| **Dosis media (1-10 kGy)** | **Extensión de la vida útil** | **1,0-3,0** | **Pescado fresco, fresas, setas, etc.** |
| | **Eliminación de microorganismos contaminantes y patógenos** | **1,0-7,0** | **Marisco fresco y congelado, pollo y carne crudo y congelado, etc.** |
| | **Mejora de las propiedades tecnológicas de los alimentos** | **2,0-7,0** | **Uva (incrementado zumo), vegetales deshidratados (reduciendo el tiempo de cocción), etc.** |
| **Dosis alta (10-50 kGy)** | **Esterilización industrial (en combinación con calor)** | **30-50** | **Carne, pollo, marisco, alimentos preparados, dietas esterilizadas para hospitales.** |
| | **Reducción de la carga microbiana de aditivos e ingredientes** | **10-50** | **Especias, preparación de enzimas, goma natural, etc.** |

El uso de radiaciones ionizantes ha sido aprobado para diversos productos alimentarios. Con el fin de aumentar la protección que ofrece este tipo de tratamiento, y como ya se ha comentado brevemente en los antecedentes, los alimentos son envasados en envases flexibles previo a la irradiación, para así evitar una posible recontaminación[32]. Sin embargo, el número de polímeros aprobados por

la legislación para este tipo de aplicaciones es todavía limitado ya que durante la irradiación se generan en los polímeros subproductos de radiólisis que pueden migrar al alimento deteriorando, de ese modo, sus propiedades sensoriales e incluso su seguridad. Los cambios inducidos en los polímeros como consecuencia de la irradiación, dependen de su naturaleza química, de los aditivos utilizados para fabricar el material, de la historia térmica del mismo, así como de las condiciones empleadas en la irradiación. Los principales cambios que tienen lugar son:

- Escisión y entrecruzamiento de las cadenas poliméricas
- Formación de gases y productos de radiólisis de bajo peso molecular
- Formación de enlaces insaturados

Si la irradiación se aplica en presencia de oxígeno, pueden tener lugar otro tipo de reacciones de degradación oxidativa con la consiguiente formación de diversos compuestos de bajo peso molecular como peróxidos, aldehídos, cetonas, etc[33].

Actualmente también se utiliza la irradiación mediante electrones acelerados para la esterilización de materiales plásticos para envasado aséptico.

Es, por tanto, de suma importancia estudiar los cambios físicos y químicos que tienen lugar en los plásticos como consecuencia de estos procesos para asegurar una calidad óptima del producto envasado.

## 1.4 PROPIEDADES DE INTERÉS EN LOS POLÍMEROS PARA SU APLICACIÓN EN EL ENVASADO DE ALIMENTOS

Como ya se ha comentado previamente, existen un gran número de ventajas por las que los materiales poliméricos van desplazando paulatinamente a otros materiales en aplicaciones de envasado de alimentos. Estas ventajas derivan de las propiedades físicas, mecánicas y químicas de los plásticos. De entre las propiedades de interés que presentan los plásticos como materiales de envase de alimentos, nos centraremos en las propiedades barrera (claves para la conservación) y en las térmicas, y en cómo éstas se ven influenciadas por la estructura y morfología de los polímeros. Otras propiedades relevantes en la aplicación que nos compete son las propiedades mecánicas, que no comentaremos por encontrarse fuera del alcance de este estudio, pero sobre las que existe una amplia bibliografía que puede ser consultada en caso de interés[34,35].

### 1.4.1 Propiedades barrera en polímeros

El concepto de "barrera" hace referencia a la capacidad de un material para oponerse a fenómenos de transporte de masa que, con mayor o menor intensidad provocan el intercambio de gases y otros compuestos de bajo peso molecular en el sistema alimento/envase/entorno. Una "alta barrera" es, sin duda alguna, una propiedad muy deseable e incluso imprescindible en algunas de las aplicaciones de envasado de alimentos. El término "alta barrera" suele emplearse en los casos en que los valores de permeabilidad de los materiales a compuestos de bajo peso molecular, como gases o aromas alimentarios, son bajos o muy bajos. Los polímeros normalmente poseen una estructura relativamente "abierta" con un empaquetado molecular pobre y un elevado volumen libre, el cual, favorece el paso de gases y vapores a través de la matriz polimérica. En la figura 1.4 se muestra la permeabilidad a oxígeno de diversos materiales utilizados en envases para alimentos. Como puede observarse, los copolímeros de etileno y alcohol vinílico, materiales objeto de esta tesis, son uno de los materiales plásticos con mejor barrera a oxígeno en condiciones de sequedad.

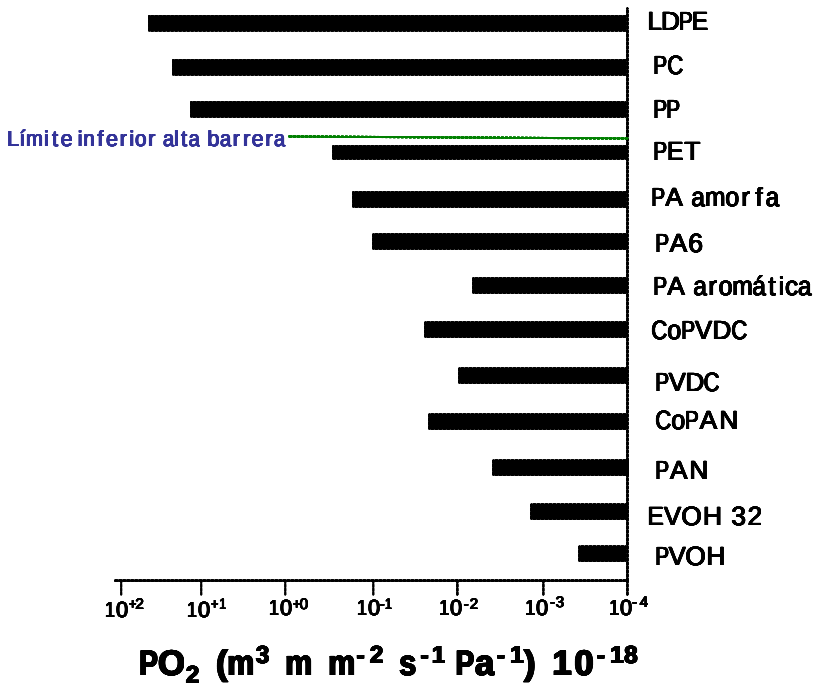


**Figura 1.4** Permeabilidad al oxígeno de diversos materiales poliméricos de envase

Para conseguir una permeabilidad al oxígeno baja es necesario que la fracción de volumen libre del material sea la menor posible, y que la densidad de energía cohesiva sea lo mayor posible, para que de este modo las cadenas poliméricas se mantengan fuertemente unidas impidiendo el paso de sustancias a su través. A continuación se describe con más detalle como se produce el transporte de masa.

### 1.4.1.1 Transporte de masa en polímeros

El transporte de masa de un compuesto a través de la sección transversal de un filme polimérico que separa dos ambientes con diferente concentración del compuesto permeante se caracteriza por la permeabilidad o coeficiente de permeabilidad (P), que a su vez es el resultado de la combinación de dos procesos, disolución (o sorción) y difusión[36], que vienen descritos por los respectivos coeficientes de solubilidad (S) y difusión (D) siendo:

$$P = DS \qquad \text{(Ec. 1)}$$

El coeficiente de solubilidad describe la disolución del permeante en el polímero y es una constante termodinámica del sistema polímero/permeante, mientras que el coeficiente de difusión describe el movimiento de las moléculas del permeante dentro del polímero y es una constante cinética del sistema polímero/permeante[37].

Si nos fijamos en la ecuación 1, es obvio que una baja permeabilidad se obtiene manteniendo la difusividad del soluto (D) o la solubilidad del soluto (S) baja.

#### 1.4.1.1.1 Sorción

La capacidad de sorción de un permeante en un polímero depende de la compatibilidad termodinámica entre ambos[38], y puede expresarse matemáticamente a través de leyes de equilibrio. En sistemas en los que el polímero está rodeado de una fase gaseosa, este equilibrio puede describirse en su forma más simple por el coeficiente de solubilidad (S) definido por la ley de Henry:

$$C = pS \qquad \text{(Ec. 2)}$$

Donde $C$ es la concentración en el equilibrio del permeante en el polímero y $p$ es la presión parcial del permeante en la fase gaseosa. En el caso de polímeros, sin embargo, esta ley sólo se cumple para bajas presiones de permeante, es decir, en el intervalo en el que el coeficiente de solubilidad es independiente de la concentración o de la presión parcial.

Como alternativas a para describir el equilibrio de sorción en aquellos sistemas en los que la ley de Henry no se sustenta, suelen emplearse otras expresiones para describir isotermas de sorción, siendo una de las más utilizadas la isoterma de Langmuir:

$$C = \frac{C_h bp}{1 + bp} \qquad \text{(Ec. 3)}$$

donde $p$ es la presión, $C_h$ es la constante de saturación de los huecos y $b$ es la llamada constante de afinidad de huecos y que tiene unidades de [presión$^{-1}$]. Este modelo de isoterma describe la sorción de algunos gases en sólidos. La solubilidad va aumentando a medida que aumenta la presión parcial hasta que todos los sitios disponibles están ocupados por el permeante y el material deja de adsorber, alcanzándose entonces un estado de saturación[39].

Un aspecto a resaltar es que los mecanismos de transporte de masa varían en función de que el polímero se encuentre por encima o por debajo de su temperatura de transición vítrea ($T_g$), es decir, en estado gomoso o vítreo respectivamente. Cuando el polímero se encuentra en estado gomoso, los tiempos de relajación son muy cortos y tras la adsorción de pequeñas moléculas de permeante, las cadenas poliméricas rápidamente se reorganizan para alcanzar un nuevo estado de equilibrio. Adicionalmente suelen mostrar aumentos en la permeabilidad al aumentar la presión parcial del permeante debido a que sufren fenómenos de plastificación. Un ejemplo de este tipo de comportamiento es el que muestra el *d*-limoneno (componente de aromas de zumos de fruta) como permeante en poliolefinas como el polietileno o el polipropileno[40]. Las isotermas de sorción se desvían positivamente de la ley de Henry como consecuencia de la plastificación y pueden describirse mediante expresiones exponenciales tales como las que describe la ley de Flory-Huggins. Por el contrario, en el caso de polímeros en estado vítreo y, por tanto, con tiempos de relajación largos se propone un modelo de sorción dual, en el que la disolución de moléculas del penetrante en el polímero tiene lugar de dos formas distintas[41,42]:

- Moléculas que se disuelven mediante un mecanismo “ordinario”. La concentración de las cuales está relacionada con la presión en el equilibrio del penetrante mediante la ley de Henry.
- Moléculas que se disuelven en el volumen libre del polímero. La concentración de estas moléculas está relacionada con la presión de equilibrio del penetrante mediante la isoterma de Langmuir.

Se asume que ambas formas de sorción suceden simultáneamente y la concentración de gas en el polímero es la suma de los dos modos de sorción. Se han postulado modelos de sorción más complejos para determinados polímeros en estado vítreo,

como por ejemplo un modelo dual modificado que incluye las ecuaciones de Langmuir y Flory-Huggins fue utilizado para describir la sorción de agua en poliamida amorfa[43].

#### 1.4.1.1.2 Difusión

El coeficiente de difusión (D) caracteriza la velocidad de una molécula de permeante sorbida para desplazarse a través de las cadenas poliméricas y se describe habitualmente mediante las leyes de Fick[44,45].

$$F = -D\left(\frac{\partial c}{\partial x}\right) \qquad \text{(Ec. 4)}$$

$$\frac{\partial c}{\partial t} = D\left(\frac{\partial^2 c}{\partial x^2}\right) \qquad \text{(Ec. 5)}$$

Pero éstas solo pueden aplicarse cuando el polímero es homogéneo e isotrópico, es decir cuando el coeficiente de difusión es independiente de la posición dentro del volumen del polímero. Cuando nos encontramos ante polímeros heterogéneos, el problema de la difusión es mucho más complejo, pero ha sido abordado por gran número de investigadores[46,47,48]. Dicho coeficiente de difusión está estrechamente relacionado con el tamaño molecular del penetrante y con la naturaleza y condiciones del polímero y, como en el caso de la solubilidad, se han propuesto diversos modelos para describir la difusión de gases en diversos materiales en función de si éstos se encuentran en estado vítreo[42,49] o gomoso[41,47].

Por otro lado, manteniendo la temperatura, presión, la diferencia de concentraciones y el flujo de permeante constante, el cálculo del coeficiente de difusión a partir de un experimento de permeación se simplifica en gran medida, tal y como se explica en el siguiente apartado.

#### 1.4.1.1.3 Permeación

La permeación es el intercambio de sustancias a través de un filme que separa dos fases fluidas. Para caracterizar el transporte de masas a través de polímeros es necesario obtener al menos dos de los tres coeficientes que describen el proceso: permeabilidad (P), difusividad o difusión (D) y solubilidad (S). Mediante experimentos de permeación controlados, tales como los llevados a cabo en el presente estudio, es posible obtener los valores de P y D y, por tanto, indirectamente podemos conocer S[45]. Aunque hay diversos métodos para realizar experimentos de permeación, normalmente en la bibliografía encontramos dos, el llamado método isostático o de flujo contínuo y el método cuasi-isostático. En este trabajo se ha utilizado el método isostático, en el que se mantiene un gradiente de oxígeno constante a través de la película polimérica que separa las dos cámaras de la célula de ensayo. Para ello, en una de las cámaras se mantiene una atmósfera rica en el permeante (oxígeno puro) mediante un flujo constante de este gas. En la segunda cámara un flujo de gas inerte (nitrógeno) va purgando las moléculas de permeante conforme éstas llegan manteniéndola, de este modo, libre de permeante. Las moléculas de permeante empiezan a ser adsorbidas y a difundir por la estructura del material polimérico hasta llegar a la superficie contraria del filme que está en contacto con la segunda cámara. A este periodo inicial del ensayo se le conoce como estado de transición, y en él, el flujo de permeante que va alcanzando la segunda cámara va incrementándose con el tiempo hasta que se alcanza el estado estacionario, momento en el que el flujo de permeante se hace constante.

Registrando el flujo de permeante que atraviesa la película ensayada es posible obtener información de los coeficientes que describen el transporte de masa. El coeficiente de permeabilidad (P) se obtiene en el estado estacionario, mientras que el coeficiente de difusión (D) se calcula a partir del estado de transición del experimento[50]. Para ello, es necesario resolver las leyes de Fick teniendo en cuenta las condiciones de contorno del experimento. Para un experimento de permeación isostático como el anteriormente descrito, el valor del flujo de permeante que alcanza la segunda cámara de la célula a cualquier tiempo ($F_t$) del experimento de

permeación varía desde cero a tiempo igual a cero, hasta alcanzar el valor $F_\infty$ que es el flujo en el estado estacionario y viene expresado por la siguiente ecuación[51]:

$$\frac{F_t}{F_\infty} = \left(\frac{4}{\sqrt{p}}\right)\left(\sqrt{\frac{l^2}{4Dt}}\right)\sum_{n=1,3,5}^{\infty} \exp\left(\frac{-n^2 l^2}{4Dt}\right) \qquad \text{(Ec. 6)}$$

Donde D es el coeficiente de difusión, t es el tiempo de experimento y $l$ es el espesor del filme. En esta ecuación se asume que D es independiente del tiempo y de la concentración. A tiempos cortos el proceso de permeación puede ser razonablemente bien descrito tan sólo utilizando el primer término del sumatorio, con lo cual la ecuación anterior puede simplificarse:

$$\frac{F_t}{F_\infty} = f = \left(\frac{4}{\sqrt{p}}\right) X^{1/2} \exp(-X) \qquad \text{(Ec. 7)}$$

Esta última ecuación describe correctamente el proceso de permeación desde tiempo cero hasta que se alcanza el 95% del flujo en estado estacionario, y como además se observa, el valor de X ($l^2$/4Dt) depende únicamente de $\phi$ ($F_t$/ $F_\infty$) y, por tanto, para cada valor de $\phi$ habrá un solo valor de X. Utilizando el método de Newton-Raphson[52] pueden obtenerse los valores de X para valores de flujo de 1/4, 1/2 y 3/4 del flujo en estado estacionario ($\phi$=0.25, 0.50 y 0.75 respectivamente), los cuales nos permiten, simplemente con conocer el tiempo que tarda el permeante en alcanzar dichos flujos, despejar el valor del coeficiente de difusión[53]:

$$X_{1/4} = \left(\frac{l^2}{4D}\right)\left(\frac{1}{t_{1/4}}\right) = 2.6961 \qquad \text{(Ec. 8)}$$

$$X_{1/2} = \left(\frac{l^2}{4D}\right)\left(\frac{1}{t_{1/2}}\right) = 1.8013 \qquad \text{(Ec. 9)}$$

$$X_{3/4} = \left(\frac{l^2}{4D}\right)\left(\frac{1}{t_{3/4}}\right) = 1.1877 \qquad \text{(Ec. 10)}$$

Despejando de estas fórmulas y aplicando los tests de consistencia dados por Gavara y Hernández[53] para confirmar que el cálculo del tiempo en el que se alcanza el estado estacionario ha sido correcto, se obtiene de un modo sencillo el coeficiente de difusión D, que junto con el valor de P obtenido del flujo en estado estacionario nos permiten calcular S a partir de la ecuación 1.

### 1.4.2 Propiedades térmicas

El conocimiento de las propiedades térmicas de los polímeros es indispensable para entender su comportamiento a la temperatura de servicio, o bien para predecir qué ocurriría en otras condiciones de almacenamiento o uso.

La calorimetría diferencial de barrido (DSC) nos permite conocer los parámetros más importantes que describen las propiedades térmicas de un polímero, a saber:

- Temperaturas de fusión ($T_m$) y cristalización ($T_c$): Estas temperaturas representan transiciones térmicas de primer orden. Nos indican la temperatura a la que funden o cristalizan la mayor parte de los cristales del polímero. Por tanto, ambas transiciones van asociadas a polímeros semicristalinos y no se observarán en aquellos cuya estructura sea totalmente amorfa. En el caso de pequeñas moléculas, la temperatura de fusión está bien definida y se caracteriza por un pico endotérmico (absorción de energía necesaria para la fusión) estrecho, manteniéndose la temperatura durante la transición relativamente constante hasta que todo el material sólido pasa a estado líquido. Por el contrario, en el caso de los polímeros, existe una distribución de tamaños y grado de perfección de los cristales en su estructura que queda reflejada en una endoterma relativamente ancha (tanto mayor cuanto más heterogénea sea su morfología cristalina). El punto de fusión, en este caso, es el máximo del pico, que indica la temperatura a la que funde el mayor porcentaje de cristales. Además, este pico de fusión variará en función de la historia térmica de la muestra, la velocidad de calentamiento y el espesor del filme[54].

- Entalpías de fusión y cristalización (? $H_m$ y ? $H_c$ respectivamente): se calculan a partir del área bajo las curvas de fusión y cristalización, y nos dan una idea de la

fracción de masa cristalina en la muestra polimérica que funde (en el caso de la entalpía de fusión) durante un barrido de calentamiento y que cristaliza (en el caso de la entalpía de cristalización) durante un barrido de enfriamiento.

- Temperatura de transición vítrea ($T_g$): transición de segundo orden relacionada con la relajación o incremento en la movilidad de segmentos de cadena de la fase amorfa. Por debajo de esta temperatura el polímero se encuentra en estado vítreo en el cual las cadenas no tienen la suficiente energía térmica para realizar movimientos cooperativos. Se encuentran como "congeladas" y, como hemos visto previamente, el tiempo de respuesta del polímero en estado vítreo a cambios conformacionales como consecuencia de la adsorción de un permeante es bastante largo, si lo comparamos con el tiempo de respuesta cuando el polímero se encuentra en estado gomoso (por encima de la $T_g$), en el que los segmentos de cadena en la fase amorfa del polímero alcanzan un alto grado de movilidad e incrementan considerablemente sus grados de libertad.

En la figura 1.5, se muestran las transiciones térmicas anteriormente mencionadas tal y como aparecerían en un termograma de DSC.

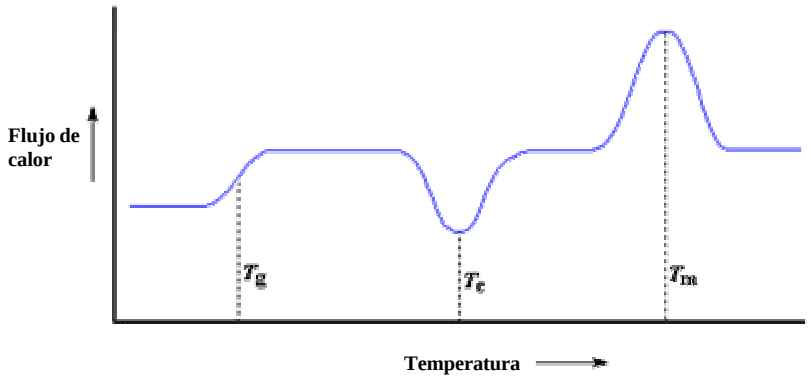


**Figura 1.5** Gráfico de DSC mostrando las diferentes transiciones térmicas que tienen lugar en un polímero semicristalino

La velocidad de calentamiento o enfriamiento durante los experimentos influye en los resultados obtenidos y, en consecuencia, a la hora de realizar estudios comparativos, se debe utilizar siempre la misma. Una velocidad de enfriamiento muy elevada ("quenching"), por ejemplo, conduce a una estructura mucho más metaestable y de menor cristalinidad, ya que las cadenas no disponen del tiempo suficiente para reorganizarse tridimensionalmente (la formación de cristales requiere de temperatura y tiempo).

### 1.4.3 Polímeros y morfología

El término morfología hace referencia a la estructura fina del plástico, que engloba la presencia, forma, organización y estado físico de las regiones cristalinas y amorfas que normalmente coexisten en el polímero. Los plásticos usados en el envasado de alimentos son, bien sólidos amorfos (como en el caso de la poliamida amorfa), o más comúnmente semicristalinos (como los copolímeros de etileno y alcohol vinílico o las policetonas) que contienen ambas regiones (cristalina y amorfa) entremezcladas[10].

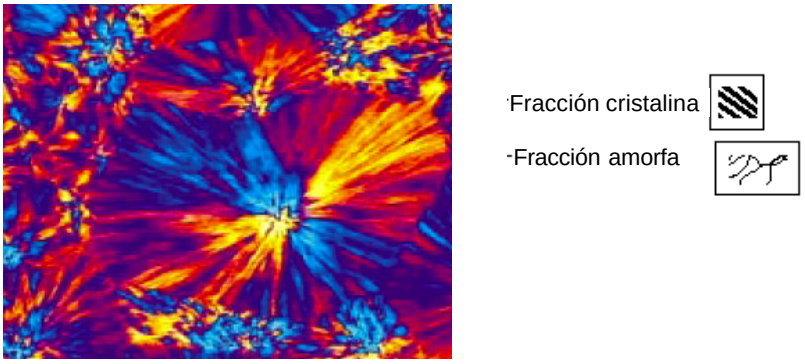


**Figura 1.6** Imagen de la morfología de un polímero semicristalino

La morfología de un polímero depende principalmente de 3 factores: composición química, grado de polimerización y configuración de las cadenas, si bien, otros

parámetros como la historia térmica del material y el método de procesado también influencian el estado físico de la muestra polimérica[55]. En general, los cristales poliméricos se organizan en lamelas que a su vez se constituyen en superestructuras más o menos esféricas denominadas esferulitas y que tienen una morfología en la mesofase como la que aparece en la figura 1.6.

### 1.4.3.1 Cristalinidad

La cristalinidad supone el ordenamiento regular y repetitivo de las moléculas poliméricas. A pesar de que en teoría las moléculas poliméricas tienden hacia la configuración que suponga menor energía libre (lo cual implica ordenarse en forma de cristal), en la práctica para que un polímero pueda cristalizar necesita una ordenación regular de átomos en la cadena. Irregularidades comunes en las cadenas poliméricas que pueden impedir la cristalización o, al menos, limitarla son, por ejemplo, las ramificaciones en la cadena o irregularidades estereoquímicas[10].

El grado de cristalinidad de un polímero refleja la cantidad de regiones cristalinas y amorfas que posee y se determina principalmente mediante DSC y difracción de rayos X. La mayor precisión en la determinación de la estructura cristalinina y cristalinidad de un material se obtiene mediante difracción de rayos X. Otra forma de determinar cristalinidad es calcularla a partir de medidas de densidad, para lo cual es necesario conocer los valores de densidad del material en estado amorfo y del cristal puro, lo cual plantea dificultades en el caso de polímeros que no se han podido obtener ni amorfos ni totalmente cristalinos como es el caso del EVOH. En la práctica la determinación de la estructura cristalina en polímeros es bastante compleja dada la heterogeneidad de formas y tamaños que pueden encontrarse en estas macromoléculas y que dan como resultado patrones de difracción relativamente complejos, sobretodo si los comparamos con los obtenidos en el caso de materiales de bajo peso molecular en los que es posible obtener cristales simples[56]. En el caso de materiales no poliméricos, por debajo del punto de fusión se obtienen los patrones cristalinos, mientras que por encima del punto de fusión se observa el patrón amorfo. Cuando se trata de polímeros, por debajo del punto de fusión ambos patrones (el de la fase amorfa y el de la fase cristalina) se observan a la vez y superpuestos, lo cual

complica aún más la correcta dilucidación morfológica[57]. De un modo general, se puede afirmar que, cuanto menores sean los cristales, más anchos serán los picos de difracción obtenidos.

Pero a pesar de lo dificultoso que puede resultar el análisis de los datos obtenidos por difracción, para el estudio de la morfología cristalina es una técnica indispensable y que ha tenido un papel fundamental en el desarrollo de esta tesis. Como veremos más adelante, los resultados de difracción se obtuvieron principalmente mediante radiación sincrotrón, que presenta unas propiedades únicas para el análisis de materiales y un número considerable de ventajas respecto a los equipos de difracción de laboratorio. La utilidad de la técnica, junto con las características más importantes y algunos ejemplos de aplicación se recogen en el último de los artículos recopilados.

### 1.4.3.2 Importancia de la morfología en las propiedades barrera

Sin lugar a dudas, la estructura química del polímero determina en gran medida las propiedades del mismo. Con respecto a la permeabilidad, normalmente la presencia de grupos apolares voluminosos dan lugar a materiales muy permeables, mientras que la introducción de grupos químicos polares que establezcan fuertes interacciones entre si proporcionando una elevada cohesividad, tendrá como resultado una disminución de la permeabilidad[38]. Una elevada cohesividad y la consiguiente disminución en el volumen libre disponible para el transporte de permeantes lo proporcionan, por ejemplo, los grupos hidroxilo presentes en la estructura de los copolímeros de etileno y alcohol vinílico (EVOH).

Para una determinada estructura química, la importancia fundamental de la presencia de cristales en la misma con respecto a las propiedades barrera, radica en que éstos son considerados “impermeables” al paso de gases y sustancias de bajo peso molecular. En la fase cristalina del polímero, el empaquetamiento molecular es mucho más eficiente, y de un modo generalizado se considera que los fenómenos de permeación tienen lugar únicamente a través de la fase amorfa[58].

Adicionalmente, la existencia de cristales en la estructura polimérica dificulta el transporte a través de la fase amorfa por que impone un camino más tortuoso a las moléculas del permeante, introduciendo un factor conocido como factor de tortuosidad. Las moléculas del permeante ya no siguen un camino recto para atravesar el espesor del filme, sino que tienen que sortear los diferentes cristalitos encontrados a su paso y, por tanto, el camino a recorrer por las mismas se incrementa, disminuyendo así los coeficientes de transporte vistos anteriormente. Por otro lado, los cristales también imponen una dificultad añadida al paso de permeantes por que inducen en general restricciones conformacionales sobre la fase amorfa adyacente, introduciendo un nuevo factor, conocido como factor de inmovilización[38].

Como conclusión, y teniendo en cuenta las implicaciones de la cristalinidad y su morfología en las propiedades barrera, es posible mejorar estas últimas mediante un procesado adecuado, optimizando los parámetros que influyen en la formación de cristales mediante el control de la historia térmica del material.

## REFERENCIAS

[1] W.J. Koros. *Barrier Polymers and Structures: Overview*. ACS Symp. Ser., Washington (1990)

[2] E.B. Schaper. *High Barrier Plastics Packaging and Ethylene Vinyl Alcohol Resins (a marriage).* Food Packaging Technology, ASTM STP 1113. D. Henyon Ed., Philadelphia (1991)

[3] W.E. Brown. *Plastics in Food Packaging. Properties, Design and Fabrication.* Marcel Dekker, Inc., Nueva York (1992)

[4] T. Iwanami, Y. Hirai. *Ethylene vinyl alcohol resins for gas-barrier material.* TAPPI J., 66(10), 85 (1983)

[5] J.A. Watchel, B.C. Tsai, C.J. Farrel. *Plastics Engineering, 41* (2), 41 (1985)

[6] N. Hata, H. Shimo. *New EVOH development in flexible applications.* Presented at Future-Pack'96, the Thirteenth International Schroeder Conference on Packaging Innovations, Chicago, IL (1996)

[7] Z. Zhang, I.J. Britt, M.A. Tung. *Plastic Film and Sheeting 14*, 287 (1998)

[8] B.C. Tsai, J.A. Wachtel. *Barrier Polymers and Structures*. Ed. J. Koros. American Chemical Society, Washington (1990)

[9] M.M. Alger, T.J. Stanley, J. Day. *Barrier Polymers and Structures*. Ed. J. Koros. American Chemical Society, Washington (1990)

[10] R.J. Hernandez, S.E.M. Selke, J.D. Culter. *Plastics Packaging. Properties, Processing, Applications and Regulations.* Hanser Publishers, Munich (2000)

[11] F.A. Paine, H.Y. Paine. *Manual de envasado de alimentos.* A. Madrid Vicente Editores. (1994)

[12] W.E. Brown. *Plastics in Food Packaging. Properties, Design and Fabrication.* Harold A. Hugues Ed. Marcel Dekker Inc., Nueva York (1992)

[13] M. Anker. *Edible and biodegradable films and coatings for food packaging. A literature review.* Chalmers University of Technology: Göteborg (1996)

[14] S. Guilbert, B. Cuq, N. Gontard. *Food Additives and Contaminants 14* (6), 741 (1997)

[15] Scout, G. *Polymer Degradation and Stability 68*, 1 (2000)

[16] M.L. Rooney. *Active Food Packaging*; M.L. Rooney, Ed.; London (1995)

[17] S. Ranganna. *Thermal processing - from appertization to aseptic packaging.* Conference Proceedings. India, Association of Food Scientists & Technologists. International Symposium (1988)

[18] Anon. *Food Engineering International 5* (6), 28 (1980)

[19] A. López. *A Complete Course in Canning*. A. López, Ed., The Canning Trade Inc. Publ., 62 (1987)

[20] R.A. Roop, P.E. Nelson. *Journal of Food Science 47* (1), 303 (1982)

[21] G.L. Schulz. *Journal of Food Protection 41* (6), 464 (1978)

[22] E. Palou, A. López-Malo, G.V. Barbosa-Cánovas, B.G. Swanson. *Handbook of Food Preservation*. Rahman, M.S., Ed., Marcel Dekker, Inc., Nueva York (1999)

[23] J. Yuste, R. Pla, E. Beltran, M. Mor-Mur. *High Pressure Research 22* (3-4), 673 (2002)

[24] C. Caner, R.J. Hernandez, M.A. Pascall. *Packaging Technology and Science 13* (5), 183 (2000)

[25] C. Caner, R.J. Hernandez, M.A. Pascall, J. Riemer. *Journal of the Science of Food and Agriculture 83* (11), 1095 (2003)

[26] E.S. Josephson. *Journal of Food Safety 5*, 161 (1983)

[27] R.J. Woods, A.K. Pikaev. *Applied Radiation Chemistry: Radiation Processing*. John Wiley and Sons, Nueva York (1994)

[28] T. Calderón García. La irradiación de Alimentos. Principios, realidades y perspectivas de futuro. McGraw-Hill, Madrid. (2000)

[29] M.J. Jay. *Microbiología moderna de los alimentos.* Acribia, Zaragoza (1994)

[30] OMS. Serie de informes técnicos nº659. *La comestibilidad de los alimentos irradiados: Informe de un Comité Mixto FAO/OIEA/OMS de expertos.* Organización Mundial de la Salud, Ginebra (1981)

[31] FAO/OIEA/OMS. Serie de informes técnicos nº890. *High-dose irradiation: wholesomeness of food irradiated with doses above 10KGy*. Organización Mundial de la Salud, Ginebra (1997)

[32] A. Kothapalli, G. Sadler. *Nuclear Instruments and Methods in Physics Research B 208*, 340 (2003)

[33] K.A. Riganakos, W.D. Koller, D.A.E. Ehlermann, B. Bauer, M.G. Kontominas. *Radiation Physics and Chemistry 54*, 527 (1999)

[34]L.E. Nielsen, R.F. Landel. *Mechanical Properties of Polymers and Composites*. 2nd Edition, Marcel Dekker, Inc., Nueva York (1994)

[35]I.M. Ward. *Mechanical Properties of Solid Polymers*. 2nd Edition, John Wiley and Sons, Chischester (1990)

[36] J. Crank, G.S. Park. *Difussion in polymers.* New York, Academic Press (1968)

[37] J. Koszinowski, O. Piringer. *Journal of Plastic Film and Sheeting 3*, 96 (1987)

[38] M. Mulder. *Basic Principles of Membrana Technology*. Kluwer Academic Publishers, Dordrech, Holanda (1991)

[39] R.H. Perry, D.W. Green. *Perry's Chemical Engineers' Handbook*. McGraw-Hill, Nueva York (1984)

[40] J.M. Lagarón, R. Catalá, R. Gavara. *Materials Science and Technology 20*, 1 (2004)

[41] S.A. Stern, S. Trohalaki. *Barrier Polymer and Structures.* Ed. J. Koros, American Chemical Society, Washington (1990)

[42] S.A. Stern, H.L. Frisch. *Annual Reviews of Material Science 11*, 523 (1981)

[43] R.J. Hernández, J.R. Giacin, E.A. Grulke. *Journal of Membrane Science 65*, 187 (1992)

[44] C.E. Rogers. *Physics and Chemistry of the Organic Solid State*. Labes, M.M., Weissberg, A., Eds. Interscience, Nueva York (1965)

[45] J. Crank. *The Mathematics of Difussion.* Ed. Clarendon, Oxford (1975)

[46] C.E. Rogers. *Physics and Chemistry of the Organic Solid State*. D. Fox, M.M. Labes, A. Weissberg, Eds., Interscience, Nueva York (1965)

[47] H.L. Frisch, S.A. Stern. *Critical Reviews of the Solid State and Material Science 11*, 123 (1983)

[48] R.M. Barrer. *Difussion in Polymers*. J. Crank, G.S. Park, Eds., New York Academic, Nueva York (1968)

[49] W.J. Koros, R.T. Chern. *Handbook of Separation Process Technology.* R.H.Rousseau, Ed., Wiley & Sons, Nueva York (1987)

[50] R. Gavara, R. Catalá, P. Hernández-Muñoz, R.J. Hernández. *Packaging Technology and Science 9*, 215 (1996)

[51]R.A. Pasternak, J.F. Schimscheimer, J. Heller. *Journal of Polymer Science, part A-2 8*, 467 (1970)

[52] S.C. Chapra, R.P. Canale. *Numerical Methods for Engineers with Personal Computer Applications.* McGraw-Hill, Inc., Nueva York (1985)

[53] R. Gavara, R.J. Hernández. *Journal of Plastic Film and Sheeting 9*, 126 (1993)

[54] J.A. de Saja, M.A. Rodríguez, M.L. Rodríguez. *Materiales. Estructura, propiedades y aplicaciones.* Thomson Editores Spain, Madrid (2005)

[55] D.C. Basset. *Principles of Polymer Morphology*. Cambridge University Press, Cambridge (1981)

[56] P.C. Painter, M.M. Coleman. *Fundamentals of Polymer Science. An Introductory Text.* Technomic Publishing Company, Inc., Pennsylvania (1997)

[57] H. Tadokoro. *Structure of Crystalline Polymers*. John Wiley & Sons, Nueva York (1979)

[58]D.W. Weinkauf, D.R. Paul. *Barrier Polymer and Structures*. Ed. J. Koros, American Chemical Society, Washington (1990)

## 2 OBJETIVOS Y PLAN DE TRABAJO

Los copolímeros de etileno y alcohol vinílico (EVOH), como ya se ha comentado previamente, presentan unas excelentes propiedades para el envasado de alimentos, entre las que destaca su elevada barrera a gases y compuestos de bajo peso molecular. Sin embargo, cuando se someten a procesos de esterilización industrial (121ºC durante 20 minutos en autoclave), estos copolímeros, incluso protegidos entre polipropileno en estructuras multicapa típicamente utilizadas en envases esterilizables, sufren un considerable aumento en la permeabilidad a oxígeno (factor clave en la conservación de muchos alimentos). Con estos antecedentes, el objetivo general de la tesis fue:

***Entender el mecanismo de deterioro que conduce al aumento de la permeabilidad a oxígeno durante la esterilización de los copolímeros EVOH y proponer soluciones o alternativas que aseguren la calidad y salubridad de los alimentos de larga duración envasados en materiales poliméricos.***

Para alcanzar este objetivo general, se plantearon una serie de objetivos parciales. El primer objetivo que se planteó fue, por tanto, dilucidar cuáles eran los **efectos de este tratamiento combinado de temperatura y vapor de agua a presión sobre la estructura, permeabilidad y características térmicas de los copolímeros EVOH**. Entender la relación entre estructura y propiedades de estos plásticos de alta barrera se planteaba como una tarea esencial para poder, más tarde, proponer soluciones al deterioro de las propiedades barrera de los materiales.

Una vez entendido el mecanismo de deterioro inducido por la esterilización industrial sobre estos materiales, el siguiente paso o segundo objetivo fue el **diseño de estrategias para paliar los efectos negativos de la esterilización sobre los copolímeros EVOH**.

El tercer objetivo planteado fue el de **estudiar el comportamiento de otros materiales de alta y media-alta barrera (policetonas y poliamida amorfa) frente a la esterilización**, con la intención de encontrar materiales alternativos al EVOH para dichas aplicaciones de envasado.

Como último objetivo y teniendo en cuenta la tendencia que presentan los mercados actuales hacia la comercialización de productos más frescos y naturales a los que se les aplican tratamientos de conservación menos agresivos, se quiso investigar la **influencia de otros tratamientos de conservación emergentes, como son las altas presiones hidrostáticas y la irradiación**, sobre los copolímeros EVOH y compararlos con los efectos de la esterilización.

Para la consecución de los anteriores objetivos se elaboró un **plan de trabajo** en el que se utilizaron técnicas de caracterización de la estructura y de las propiedades barrera descritas en la sección de materiales y métodos.

® *Estudio de los efectos de la esterilización sobre la morfología y propiedades de los copolímeros de etileno y alcohol vinílico*

Mediante la utilización de la calorimetría diferencial de barrido (DSC) se estudian cambios en el punto de fusión, la entalpía de fusión y la anchura del pico de fusión que indican cambios en la morfología del material. Los cambios potenciales en la estructura cristalina se analizaron tanto mediante espectroscopía infrarroja y Raman, como mediante técnicas de difracción de rayos X utilizando una fuente de radiación sincrotrón de alta energía. Esta técnica además fue utilizada para simular in-situ el proceso de esterilización y observar cómo se modifica la estructura cristalina del material en función de la temperatura. También se planteó la realización de medidas de permeabilidad a oxígeno y, por último, se seleccionó la técnica de microscopía electrónica de barrido (SEM) para la observación de cambios morfológicos en la sección transversal de los filmes tras los diferentes tratamientos.

En cuanto al segundo objetivo, algunas de las estrategias esbozadas para paliar los efectos negativos de la esterilización sobre los copolímeros se detallan a continuación:

® *Modificación de la historia térmica de los materiales*

Una de las hipótesis que se plantearon fue que mediante el refuerzo de la estructura cristalina del EVOH mediante tratamientos de templado o recocido ("annealing"), podrían paliarse los efectos perjudiciales de la esterilización.

® *Desarrollo de mezclas*

Se estudió el comportamiento frente a la esterilización de diversas mezclas de EVOH con poliamidas y con ionómeros con el fin de observar si se conseguía disminuir la sensibilidad a la humedad del copolímero y, por tanto, mejorar la resistencia de los mismos al someterlos a dichos tratamientos.

Posteriormente, y de acuerdo con los objetivos 3 y 4 se plantearon las siguientes tareas:

® *Estudio del comportamiento de otros polímeros barrera al ser sometidos a tratamientos de esterilización*

Esterilizar en el autoclave diversos plásticos de interés en aplicaciones de envasado de alimentos, tales como poliamidas amorfas y policetonas alifáticas, con el objetivo de seleccionar para un estudio más en profundidad aquellos que potencialmente podrían sustituir al EVOH en aplicaciones de esterilización de alimentos en el propio envase.

® *Efecto de otros tratamientos emergentes de conservación sobre la estructura y propiedades de los copolímeros de etileno y alcohol vinílico*

Dada la tendencia actual en las industrias agroalimentarias hacia la utilización de métodos de conservación menos agresivos y que conserven en mayor medida las propiedades nutritivas y de calidad de los alimentos, en este estudio también se pretendía analizar sus efectos sobre los copolímeros EVOH. Para ello, estos materiales de alta barrera se sometieron a tratamientos de altas presiones e irradiación y, posteriormente, se analizaron mediante las técnicas antes mencionadas. En el caso concreto de la irradiación también se empleó la técnica de cromatografía de gases acoplada a la espectroscopía de masas para analizar los productos de radiólisis consecuencia de dicho tratamiento.

# 3 PARTE EXPERIMENTAL

## 3.1 MATERIALES

### 3.1.1 Copolímeros de etileno y alcohol vinílico (EVOH)

En este estudio se han empleado 6 grados comerciales de copolímero de etileno y alcohol vinílico (Soarnol®) que serán referenciados con la siguiente nomenclatura: EVOH26, EVOH29, EVOH32, EVOH38, EVOH44 y EVOH48, donde el número indica el porcentaje en moles de etileno en la composición. Estos materiales fueron suministrados por la empresa Nippon Synthetic Chemical Industry Co., Ltd. (Osaka, Japón). Estos materiales se recibieron en forma de película, co-extruidos entre dos capas de polipropileno tanto con adhesivo (típica estructura multicapa utilizada en envases esterilizables para alimentos sensibles al oxígeno, en adelante identificada como PP//EVOH//PP), como sin adhesivo (estructura pensada para poder delaminar la capa barrera intermedia, identificada como PP/EVOH/PP). Los espesores de las estructuras multicapa empleadas fueron PP/adhesivo/EVOH/adhesivo/PP = 90/10/10/10/90 micras y PP/EVOH/PP = 100/10/100.

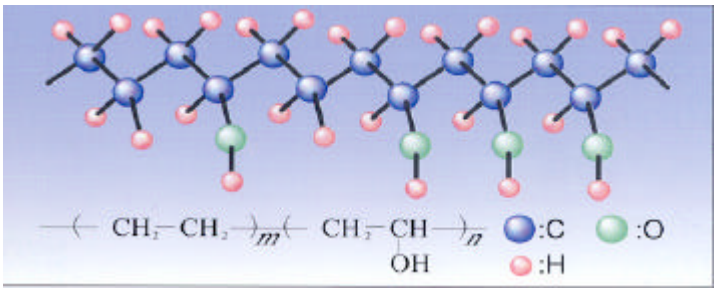


**Figura 3.1** Estructura química de los copolímeros de etileno y alcohol vinílico

Además de los filmes de EVOH, para la realización de algunos experimentos se emplearon láminas más gruesas del copolímero obtenidas mediante moldeo por compresión en una prensa de platos calientes hidroneumática a partir de varios

gramos de granza de los diferentes copolímeros. Estas láminas, a su vez, fueron obtenidas de dos formas: mediante enfriamiento brusco en agua (quenching) tras el fundido para imitar las condiciones de procesado que dan lugar a la morfología obtenida por extrusión, y mediante enfriamiento lento entre las placas de la prensa (a unos 15$^{o}$C/minuto) para la obtención de materiales con morfología cristalina más estable.

### 3.1.2 Poliamida amorfa (aPA)

La poliamida amorfa utilizada en este estudio fue suministrada en forma de película de unos 45 micras de espesor por la empresa E.I. Du Pont de Nemours and Co. (Wilmington, DE, EEUU), bajo el nombre comercial Selar® PA UX-2034. El polímero es una copoliamida aromática amorfa obtenida a partir de la síntesis por condensación de la hexametilenodiamina y una mezcla de ácidos isoftálico y tereftálico (70/30). Se simularon estructuras multicapa PP/aPA/PP mediante envasado a vacío de película de aPA en una bolsa de polipropileno de 100 micras de espesor. Al no utilizarse ningún tipo de adhesivo, tras los diferentes tratamientos, la estructura podía delaminarse con facilidad para la caracterización de la poliamida.

### 3.1.3 Policetonas alifáticas (PKs)

Los materiales caracterizados en este estudio se sintetizaron en BP Chemicals (GB) utilizando un catalizador metalocénico de paladio patentado. Los materiales se suministraron en forma de polvo, tal y como se obtuvieron en el reactor.

Se utilizó un terpolímero de etileno/propileno/monóxido de carbono (PK). El peso molecular promedio ($M_w$) es de alrededor de 130000 y el índice de polidispersidad es de 2.1. Estos materiales son terpolímeros perfectamente alternantes con un contenido molar de monóxido de carbono (CO) del 50%. La segunda olefina, es decir, el propileno, sustituye al azar al etileno a lo largo de la cadena.

Se obtuvieron filmes de aproximadamente 120 micras de espesor mediante moldeo por compresión utilizando una prensa de platos calientes hidroneumática y enfriando bajo presión a unos 15º/minuto hasta temperatura ambiente.

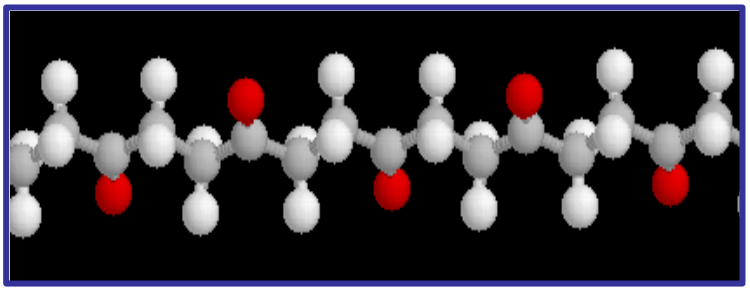

**Figura 3.2** Representación esquemática de la estructura química de una policetona en la que las bolas grises representan las moléculas de carbono, las blancas son las moléculas de hidrógeno y las rojas son moléculas de oxígeno

### 3.1.4 Mezclas en base EVOH

Se estudiaron también filmes extruídos de mezclas binarias de EVOH32/aPA y EVOH32/Ionómero con composición 80/20 en ambos casos y una mezcla ternaria de EVOH32/aPA/Ionómero en proporciones 80/10/10. El ionómero utilizado en estas mezclas (de nombre comercial Surlyn® AM 7938) corresponde a un nuevo producto desarrollado por E.I. Du Pont de Nemours and Co. (Wilmington, DE, EEUU). Se trata de una mezcla con un copolímero de etileno-ácido metacrílico parcialmente neutralizado y poliamida-6 (N-Ionómero). Esta mezcla fue diseñada exclusivamente como aditivo para los copolímeros EVOH con la finalidad de aumentar su transparencia, alcanzar una mayor resistencia a la flexión, excelente termoconformabilidad y barrera a gases (oxígeno) en presencia de humedades elevadas, sin un gran detrimento de la excelente barrera al oxígeno del EVOH seco.

## 3.2 MÉTODOS

### 3.2.1 Acondicionamiento de las muestras

Dado que tanto los copolímeros EVOH como la poliamida amorfa presentan un marcado carácter hidrófilo y que el contenido en agua afecta significativamente a sus propiedades, previo al análisis, a menos que se indique lo contrario, todas las muestras fueron secadas en estufa de vacío a 70ºC durante una semana.

### 3.2.2 Diferentes tratamientos aplicados a los materiales

3.2.2.1 Tratamientos térmicos

Los materiales fueron tratados térmicamente tanto en presencia de agua (esterilización en autoclave) como en seco en un horno convencional. El tratamiento estándar dado a las muestras tanto en el horno como en el autoclave fue de 120ºC durante 20 minutos. Se aplicaron también, sobre algunos de los polímeros estudiados, otro tipo de tratamientos térmicos que se especifican en cada caso.

3.2.2.2 Tratamiento con altas presiones hidrostáticas (HPP)

Este tratamiento de conservación, así como la irradiación (apartado 3.2.2.3), únicamente se aplicó a los copolímeros de etileno y alcohol vinílico como alternativa a la esterilización. Los filmes de EVOH fueron cortados en trozos de 10×10 centímetros y, posteriormente, se introdujeron en bolsas de polietileno. Cada bolsa se llenó con 150 mililitros de agua y se selló, sin dejar espacio de cabeza, utilizando una selladora Multivac 021-336 (Busch, Suiza). Por tanto, los filmes tratados no tuvieron contacto directo con el fluido utilizado para la transmisión de las altas presiones hidrostáticas.

Los tratamientos con altas presiones hidrostáticas se llevaron a cabo en un QFP-6 “Flow Batch High Pressure Food Processor” (Flow Autoclave System, Columbus, OH). Este equipo cuenta con una cámara de un litro para trabajar a escala piloto cuyas dimensiones son 6 centímetros de diámetro y 18.8 centímetros de largo. El fluido utilizado para transmitir la presión fue una mezcla de agua y glicerol cuyo nombre comercial es Houghton-Safe 620-TY (Houghton Internacional, Valley Forge,

PA). Las condiciones de los diferentes tratamientos aplicados fueron 400 y 800 MPa, durante 5 y 10 minutos, a 40 y 75ºC de temperatura.

3.2.2.3 Irradiación

Películas 10 y 60 µm de EVOH29 se irradiaron utilizando una fuente de electrones acelerados a dosis de 30 y 90 KGy. La irradiación se llevó a cabo a temperatura ambiente y en presencia de aire con un equipo Electrocurtain CB250/15/180L (Eye Graphics Co. Ltd.) en los laboratorios centrales de investigación de la empresa Nippon Gohsei (Japón). El voltaje de aceleración empleado fue de 200 KV y una corriente de irradiación de 1.4 mA.

### 3.2.3 Calorimetría diferencial de barrido (DSC)

Las propiedades térmicas de los materiales empleados en el estudio, antes y después de los diferentes tratamientos de conservación aplicados fueron estudiadas mediante calorimetría diferencial de barrido. Los experimentos de DSC se llevaron a cabo mediante un calorímetro diferencial de barrido Perkin Elmer DSC-7 (Perkin Elmer CETUR Instruments, Norwalk, CT). La calibración del equipo se realizó utilizando indio como sustancia de referencia ($T_m$=156.6ºC, ? $H_m$ =108.37 J/g, siendo $T_m$ y ? $H_m$ la temperatura y entalpía de fusión respectivamente). El peso nominal de las muestras osciló entre 4 y 8 mg y la velocidad de barrido empleada fue de 10ºC/minuto en atmósfera de nitrógeno. Los ciclos térmicos aplicados variaron en función del polímero a analizar y se especifican a lo largo del estudio. De un modo general y sin especificar temperaturas, se realizó un primer calentamiento hasta fusión (primer barrido), manteniéndose a esa temperatura durante 1 minuto, se enfrió hasta temperatura ambiente, manteniéndose otro minuto y, por último, se dio un segundo calentamiento hasta fusión (segundo barrido). El primer barrido se utilizó para estimar los cambios producidos durante los diferentes tratamientos, mientras que el segundo barrido fue útil para constatar si los cambios inducidos eran o no reversibles.

Los parámetros estudiados fueron, en la mayor parte de los casos, la temperatura de fusión ($T_m$) que se calculó como el máximo de la endoterma de fusión, la entalpía de

fusión (? $H_m$) calculada como el área bajo la curva de fusión, la temperatura de transición vítrea ($T_g$) definida como el punto medio de la transición y la temperatura y entalpía de cristalización ($T_c$ y ? $H_c$, respectivamente).

También se utilizó el equipo con una unidad de subenfriamiento (con nitrógeno líquido) para el estudio de transiciones térmicas subambiente.

### 3.2.4 Velocidad de transmisión de oxígeno

La velocidad de transmisión de oxígeno ($O_2$TR) a través de los polímeros tanto aislados como de las estructuras multicapa se llevaron a cabo en un equipo OX-TRAN® 2/20 (Mocon Inc., Minneapolis, MN) a 0% de humedad relativa y a 45ºC de temperatura (en algunos casos también a 21ºC). Los ensayos se realizaron a alta temperatura para aumentar la permeabilidad de los materiales y, de ese modo, discernir con mayor precisión los efectos de los tratamientos sobre los materiales, dado el carácter alta barrera de los materiales empleados. En la mayoría de los casos se presenta el valor de $O_2$TR en lugar de dar el coeficiente de permeabilidad ya que muchas de las muestras medidas eran estructuras multicapa. Estos valores de velocidad de transmisión de oxígeno son directamente comparables, siempre que las muestras a comparar tengan igual espesor.

### 3.2.5 Espectroscopía infrarroja con transformada de Fourier

Una de las técnicas empleadas para analizar cambios estructurales inducidos por los diferentes tratamientos en los materiales poliméricos fue la espectroscopía infrarroja. La caracterización mediante esta técnica se realizó utilizando un equipo FT-IR Tensor 37 (Bruker, Darmstadt, Alemania). Se llevaron a cabo tanto medidas en transmisión, generalmente en filmes de poco espesor (~10 µm), como medidas con el accesorio de medidas por reflexión (ATR, Golden Gate, Specac) con el que se analiza únicamente la estructura en las primeras micras de la superficie del material. Para los experimentos en transmisión, la cámara del infrarrojo se mantuvo purgada continuamente con un flujo abundante de nitrógeno para mantener una atmósfera

inerte y seca. En la mayor parte de las medidas, se seleccionó una resolución de 4 $cm^{-1}$ y un tiempo medio de adquisición de 4 segundos. Otras condiciones experimentales utilizadas se especifican a lo largo del trabajo.

### 3.2.6 Espectroscopía Raman

La espectroscopía Raman fue utilizada para contrastar los efectos de la esterilización sobre la estructura cristalina de los copolímeros EVOH. Espectros de Raman se obtuvieron con un equipo NIR-FT-Raman Perkin-Elmer Spectrum 2000 equipado con un láser de diodo Nd:YAG y con una resolución de 2 $cm^{-1}$.

### 3.2.7 Medidas de WAXS/SAXS

Para el estudio detallado de la estructura cristalina de los materiales antes y después de los tratamientos aplicados, se llevaron a cabo experimentos de difracción de rayos X a ángulos altos (wide angle X-ray scattering, WAXS) y a ángulos bajos (small angle X-ray scattering, SAXS) utilizando una fuente de radiación sincrotrón. Estos experimentos se realizaron en la estación A2 del Hasylab (DESY) en Hamburgo (Alemania). Los patrones de difracción se recogieron mediante un detector unidimensional y una longitud de onda de radiación incidente, ?, de 0.15 nm. La intensidad de los datos de WAXS y SAXS se corrigió con la respuesta del detector y la calibración se realizó con patrones de PET y colágeno de rata respectivamente. A los datos de SAXS se les aplicó la corrección de Lorentz.

Además de medidas puntuales sobre los materiales, se llevaron a cabo experimentos resueltos en el tiempo de calentamiento en seco y en presencia de humedad. Para este tipo de experimentos el filme polimérico se confinó entre láminas de aluminio o poliimida amorfa (kapton) en cápsulas especiales, diseñadas para medir líquidos. Estas cápsulas contaban además con unas gomas anulares que aseguraban la hermeticidad del cierre, de forma que, en los experimentos en presencia de humedad, impedían la salida del vapor de agua presurizada de la cápsula. De este modo se consiguió simular, in-situ, el proceso industrial de esterilización, ya que dicha

cápsula actuaba de “miniautoclave”. La presencia de agua en la cápsula tras finalizar los experimentos de esterilización in-situ fue indicativa de la validez de los ensayos. La velocidad de calentamiento y enfriamiento utilizada en los experimentos resueltos en el tiempo fue de 5ºC/minuto.

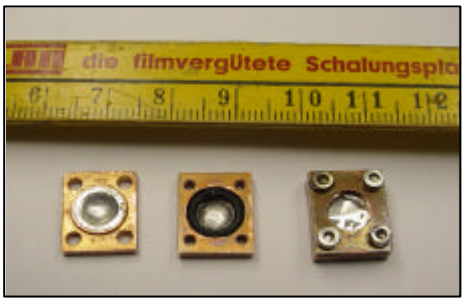


**Figura 3.3** Cápsulas para líquidos utilizadas en el sincrotrón para realizar los experimentos de esterilización in-situ

### 3.2.8 Microscopía electrónica de barrido (SEM)

Previo a la observación de la microestructura de las muestras mediante SEM, éstas fueron fracturadas en nitrógeno líquido y montadas en portamuestras inclinados. A la superficie de fractura se le aplicó entonces un recubrimiento de oro/paladio (sputtering) mediante una técnica de deposición a vacío. Las microfotografías fueron tomadas con un equipo SEM S41000 (Hitachi, Osaka, Japón) aplicando un voltaje de 10 keV.

# 4 RESULTADOS Y DISCUSIÓN

## 4.1 INTRODUCCIÓN A LOS RESULTADOS

Este apartado tiene la intención de dar cohesión y exponer brevemente una continuidad lógica a los capítulos de resultados que se presentan como una colección de artículos. Tal y como se explicó brevemente en el apartado de "Objetivos y plan de trabajo", esta tesis comenzó abordando el problema que planteaban los copolímeros de etileno y alcohol vinílico (EVOH), materiales ampliamente utilizados en envases plásticos esterilizables como capa de alta barrera a gases para envasar alimentos sensibles al oxígeno, al ser sometidos a procesos de esterilización industrial en autoclave.

En el primer artículo recopilado, se incluye el estudio de los efectos de la temperatura y humedad por separado, y del tratamiento combinado de temperatura y vapor de agua a presión (esterilización) sobre los copolímeros, y de cómo estos efectos dependen en gran medida de la composición del copolímero. Estos resultados, como se puede observar en el anexo 1, se publicaron en la revista científica *Macromolecules*.

A continuación, y una vez entendidos los efectos de estos tratamientos sobre la morfología de estos materiales poliméricos, se plantearon diversas alternativas para paliar el daño estructural que conducía a la pérdida de propiedades barrera de los materiales.

En primer lugar, se estudió el comportamiento frente a la esterilización de filmes de los copolímeros protegidos por materiales hidrofóbicos (polipropileno, en concreto) en estructuras multicapa como las que se utilizan normalmente en el envasado de alimentos. A pesar de que el daño morfológico se reduce mediante el uso de estas estructuras, el aumento de permeabilidad continúa siendo excesivo y la recuperación de las propiedades barrera es muy lenta, pudiendo por tanto comprometer la vida útil del producto envasado.

Por todo esto, se establecieron 3 estrategias diferentes para solventar el problema:

1. Secado posterior a la esterilización para eliminar el agua sorbida en la estructura del copolímero
2. Tratamiento térmico previo a la esterilización para reforzar la estructura de los materiales y que, de este modo, resistan mejor dichos tratamientos
3. Utilización de mezclas con poliamida amorfa y poliamida con ionómero

En el artículo 2, publicado en el *Journal of Applied Polymer Science* (ver Anexo 2) se recogen los resultados obtenidos para las estructuras multicapa polipropileno/EVOH/polipropileno, así como las mejoras inducidas mediante las dos primeras estrategias, es decir, mediante la aplicación de temperatura bien antes o después de la esterilización. Los efectos de este tratamiento de conservación de alimentos sobre las mezclas se presentan en el artículo 3 que se encuentra en fase de preparación.

Una vez analizadas las distintas posibilidades que existían para mejorar la resistencia de los copolímeros EVOH frente a la esterilización, nos planteamos el estudio del comportamiento de otros materiales de alta o media-alta barrera al someterlos a dicho tratamiento combinado de temperatura y humedad a presión. De entre los diferentes materiales analizados se seleccionaron aquellos que mostraban mejor comportamiento frente a la esterilización: una poliamida amorfa y un grado experimental de policetona.

Los datos referentes al efecto de la esterilización sobre las policetonas han sido aceptados para publicación en el *Journal of Applied Polymer Science*. Éstos se recopilan en el artículo IV, en el que se demuestra el mejor comportamiento de estos materiales utilizados incluso sin ningún tipo de protección.

En el artículo V se presentan los sorprendentes efectos de la esterilización sobre la poliamida amorfa. Este polímero amorfo es capaz de cristalizar durante la esterilización en autoclave. Los resultados obtenidos en este trabajo han sido aceptados para publicación en el *Journal of Applied Polymer Science.*

Finalmente y en vista de las nuevas tendencias de conservación de alimentos mediante tratamientos menos agresivos y que conserven mejor las propiedades nutritivas y organolépticas de los mismos, se quiso estudiar los efectos sobre los copolímeros de etileno y alcohol vinílico de dos tratamientos alternativos de conservación como son las altas presiones hidrostáticas (artículo VI) y la irradiación mediante electrones acelerados (artículo VII). Los datos referentes a los efectos de las altas presiones sobre los copolímeros EVOH han sido publicados en la revista científica *Innovative Food Science and Emerging Technologies*, tal y como puede observarse en el Anexo III.

Por último, nos ha parecido interesante añadir al final el artículo VIII, en el que se plasma la importancia de los estudios de difracción de rayos X utilizando una fuente de radiación sincrotrón en el estudio de la morfología de materiales poliméricos, así como el potencial de la técnica para llevar a cabo experimentos de simulación resueltos en el tiempo como los que se han realizado en la presente tesis. Este trabajo, tal y como se observa en el Anexo IV, ha sido publicado en la revista científica *Food Additives and Contaminants.*

**ARTÍCULO I**

# MORPHOLOGICAL ALTERATIONS INDUCED BY TEMPERATURE AND HUMIDITY IN ETHYLENE-VINYL ALCOHOL COPOLYMERS

## INTRODUCCIÓN AL ARTÍCULO I

Este artículo fue publicado en la revista *Macromolecules* tal y como puede observarse en el Anexo 1. En este artículo se presentan los resultados sobre la caracterización de los daños estructurales sufridos por los copolímeros EVOH como consecuencia de la esterilización en autoclave, cubriendo, por tanto, el primer objetivo de la tesis. Previo a este estudio, se analizan también cuáles son los efectos sobre la estructura de la temperatura (que como se verá "refuerza" la estructura mediante la inducción de formación de cristales) y la humedad (que conduce a la plastificación de la estructura) por separado. El estudio está centrado, fundamentalmente, en la caracterización estructural, en la que los estudios de espectroscopía infrarroja así como los experimentos de difracción de rayos X resueltos en el tiempo muestran su idoneidad para la comprensión de los cambios morfológicos que tienen lugar tras los diferentes tratamientos. Adicionalmente se presentan resultados de calorimetría diferencial de barrido (DSC), que muestran las modificaciones de las propiedades térmicas que, a su vez, ayudan a explicar los cambios en la estructura cristalina de estos materiales alta barrera al ser sometidos a tratamientos combinados de temperatura y vapor de agua a presión en autoclave.

**ABSTRACT**

The morphology of a number of high barrier ethylene-vinyl alcohol food packaging films with different ethylene contents have been evaluated by simultaneous WAXS/SAXS, FT-IR, DSC and Raman spectroscopy. This rather descriptive pioneering study was aimed at the understanding of the morphological changes that occur in these polymers as a result of temperature, humidity and combination of temperature and humidity treatments. From the results, the temperature effect was, as expected, found to improve polymer crystalline morphology leading to a higher, denser and more stable crystallinity. Lower ethylene content copolymers underwent partial solid-solid phase transition towards a more thermodynamically stable monoclinic morphology upon sufficient annealing. On the other hand, moisture sorption was found to result in melting of ill-defined crystals, particularly for the lowest ethylene content copolymers. This water sorption-induced crystal melting process has not been reported before and was seen to be largely suppressed by enhancing crystal stability. Combined temperature and humidity effects, as those for instance generated in retorting autoclaves, were found to dramatically deteriorate the polymer crystallinity, irrespective of initial crystal robustness. By making use of simultaneous time-resolved WAXS/SAXS experiments during in-situ retorting of a water saturated EVOH copolymer with 32mol% of ethylene, it was found that heated moisture weakened very readily the polymer crystalline morphology, which melted around 80$^{o}$C below its actual melting point.

**Keywords**: EVOH copolymers, temperature and humidity effects, structure/property relationship.

## INTRODUCTION

Ethylene-vinyl alcohol copolymers are a family of random semicrystalline materials with excellent barrier properties to gases and hydrocarbons, and with outstanding chemical resistance[1]. EVOH copolymers are commonly produced via a saponification reaction of a parent ethylene-co-vinyl acetate copolymer, whereby the acetoxy group is converted into a secondary alcohol. These materials have been increasingly implemented in many pipe and packaging applications where stringent criteria in terms of chemical resistance and in gas, water, aroma and hydrocarbon permeation are to be met. In particular, the copolymers with low contents of ethylene (below 38 mol% ethylene) have outstanding barrier properties, under dry conditions, compared to other polymeric materials. The crystalline morphology of these copolymers is relatively well-known across composition and has been the subject of two previous studies[2, 3].

An important application of these materials is as barrier layer in multilayer structures to be used in various packaging designs for foodstuffs. The presence of EVOH in the packaging structure is key to food quality and safety because it reduces the ingress of oxygen and the loss of aroma components during extended package shelf life. In spite of the low gas permeation, EVOH copolymers generally show poor moisture resistance. The appetite for water of these materials, which results in a high water uptake, leads to deterioration of the gas barrier performance in high relative humidity environments[4]. This deterioration is thought to derive from the fact that the inter- and intra-molecular hydrogen bonding (so-called self-association) provided by the hydroxyl groups is intercepted by water molecules. This interaction strongly reduces interchain cohesion and mechanical integrity, and increments the fractional free volume of the polymer (plasticization effect) for the permeants to travel across polymer packages. The plasticizing effect of water on the barrier properties of EVOH is time dependent, especially if the hydrophilic layer is protected by a water-barrier such as polypropylene as in the case of packages for food retorting. When such retortable packs (containing aqueous foodstuffs) are subjected to steam retorting, water passing through the protective hydrophobic layer is thought to be sorbed on the EVOH layer in such quantities that the barrier layer becomes quite permeable to oxygen. The rate of water release through the outer polypropylene layer becomes

very slow on cooling, so the oxygen permeability can remain elevated for many weeks[5]. Tsai and Jenkins[6] reported that the oxygen barrier of retortable packages containing an EVOH barrier layer was initially reduced by two orders of magnitude when these containers were subjected to steam or pressurized water during thermal processing, and during long term storage (>200 days) the barrier was partially recovered (by a factor of ten).

In spite of the extensive characterization of the effects on barrier properties that humidity and combined temperature and humidity environments can have on these materials, there is very little understanding of the actual morphological consequences. Yet, only a sound knowledge about these morphological effects can help designing appropriate and effective strategies to protect the materials from undesirable property damages. In this context, the main aim of this novel study is to shed light onto the fundamentals of the structural changes that occur in these copolymers upon direct exposure to (i) thermal treatments, (ii) moisture sorption and (iii) combination of temperature and humidity, i.e. during retorting processes.

## EXPERIMENTAL

*Materials*

Six different commercial ethylene-vinyl alcohol copolymer grades (Soarnol®) supplied by The Nippon Synthetic Chemical Industry Co., Ltd. (NIPPON GOHSEI) (Japan) were analyzed: EVOH26, EVOH29, EVOH32, EVOH38, EVOH44 and EVOH48, where the number indicates the mol percentage of ethylene in the copolymer composition.

Two types of sample morphologies were used in the present work: i) Coextruded EVOH films (ca. 10μm thickness) between polypropylene layers with no adhesive for easy delamination of the high barrier layer prepared at NIPPON GOHSEI and ii) compression moulded plates (ca. 1 mm thickness) obtained by both rapid cooling (quenched in water) to mimic extrusion conditions on crystalline morphology and slow cooling (15$^{o}$C/min) from the melt to obtain a more thermodynamically stable crystalline morphology. Samples were, unless otherwise stated, dried at 70$^{o}$C in vacuum during a week before undergoing testing. The reason for studying extruded thin film samples is that most food packaging applications of these materials are presented in this form.

*Methods*

The materials were thermally treated under dry and humid conditions in a conventional oven (annealing) and in a sterilization autoclave (retorting), respectively.

DSC experiments were carried out in a Perkin-Elmer DSC-7 calorimeter. The heating and cooling rate for the runs was 10ºC/min, being typical sample weight around 8 mg. Calibration was performed using an indium sample. All tests were carried out, at least, in duplicate.

Raman measurements were carried out with an NIR-FT-Raman Perkin-Elmer Spectrum 2000 instrument equipped with a diode pumped Nd:YAG laser PSU with a spectral resolution of 2 cm$^{-1}$. Transmission FT-IR experiments were recorded under a $N_2$ purged environment with a Bruker Tensor 37 equipment with 1 cm$^{-1}$ resolution.

Simultaneous WAXS and SAXS experiments were carried out at the synchrotron radiation source in the polymer beam A2 at Hasylab (DESY) in Hamburg (Germany). Scattering patterns were recorded using a one dimensional detector and an incident radiation wavelength, ?, of 0.15 nm. WAXS and SAXS data were corrected for detector response and beam intensity and calibrated against PET and rat tail standards, respectively. Determination of the long period was derived from background substracted and Lorentz corrected SAXS data[7]. Temperature scans were also carried out at 5$^{o}$C/min on dry (sandwiched between aluminum foil) and in water saturation conditions for EVOH32 films. Water saturation conditions during the temperature experiment were ensured by sealing a water saturated specimen in excess of moisture between “kapton” polyimide films and O-rings rubber seals inside typical screwed rectangular cell compartments designed for measuring liquids as a function of temperature, available at the station[8]. Experiment success was checked by observation of constant background intensity over the experiment and presence of moisture in the cell after termination of the thermal experiments, which indicated that moisture did not leak off the cell during the temperature run. The cited conditions are thought to closely simulate circumstances occurring during industrial retorting processes.

## RESULTS AND DISCUSSION

*Temperature effect*

Figure 1 shows WAXS and SAXS (as inset) patterns of the EVOH26 film after annealing during 20 minutes at different temperatures. These annealing steps reproduce potential retorting conditionings given to these materials but without the water vapor factor. From this Figure 1, a progressive strengthening of the WAXS crystalline and SAXS patterns and a shift to higher repeat distances of the SAXS peak maximum can be seen upon increasing annealing temperature. In fact, the crystalline morphology is seen to partially evolve from a defective orthorhombic morphology, result of crash cooling, towards the monoclinic unit cell typical of the slow cooled material[2] and thermodynamically more stable.

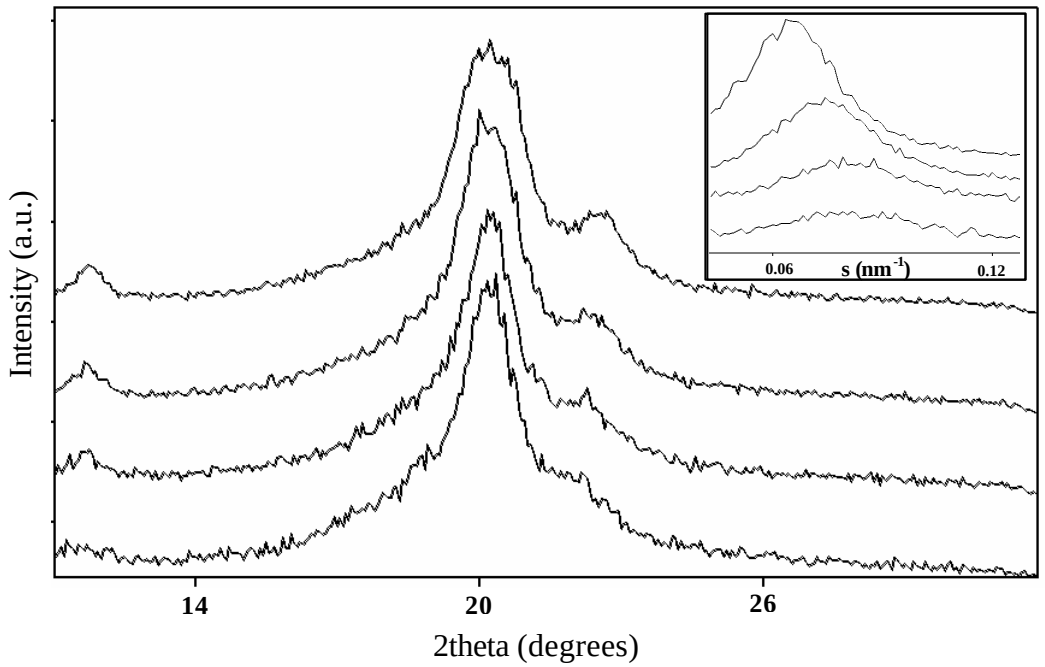


**Figure 1.** WAXS and SAXS raw patterns (inset) of annealed for 20 minutes EVOH26 at, from bottom to top, 100°C (dry sample), 120°C, 135°C, 160°C.

This kinetically slow thermally-induced solid-solid phase transition evolution is more clearly revealed at the highest annealing temperatures by both broadening of the (110) reflection and shift to higher angle of the (200) reflection, and has been reported before upon annealing of an EVOH32 sample during sufficient time at

relatively high temperature[9]. The above phase transformation evolution was only observed for EVOH26, EVOH29 and less clearly for EVOH32, remaining the other samples orthorhombic throughout annealing. The broadening of the (110) reflection is, in this case, due to early splitting of this into the two monoclinic reflections (110) and $(1\bar{1}0)$. These changes in the crystalline morphology can not be observed during a typical temperature scan of the samples, even at the relatively slow ramp speed of $5^oC$/min (see later in text), because of its rather slow kinetics. Quantification of crystallinity was attempted in compression moulded specimens but is not shown due to difficulties in setting a soundly justified position during curve-fitting for the amorphous halo. The complex issue of rigorous crystallinity determination for these polymers will be the topic of a separate study. Nevertheless, Figure 2 shows the evolution of the unit cell parameters a and b (the c axis is considered to be the fiber period of the planar zigzag chain conformation and is estimated from the literature to be a constant at 2.54 Å)[2,3] and the lattice volume as a function of ethylene content and annealing temperature. The a and b axes were determined from the (200) and (110) crystallographic planes at angles ca. $22^o$ and $21^o$, respectively.

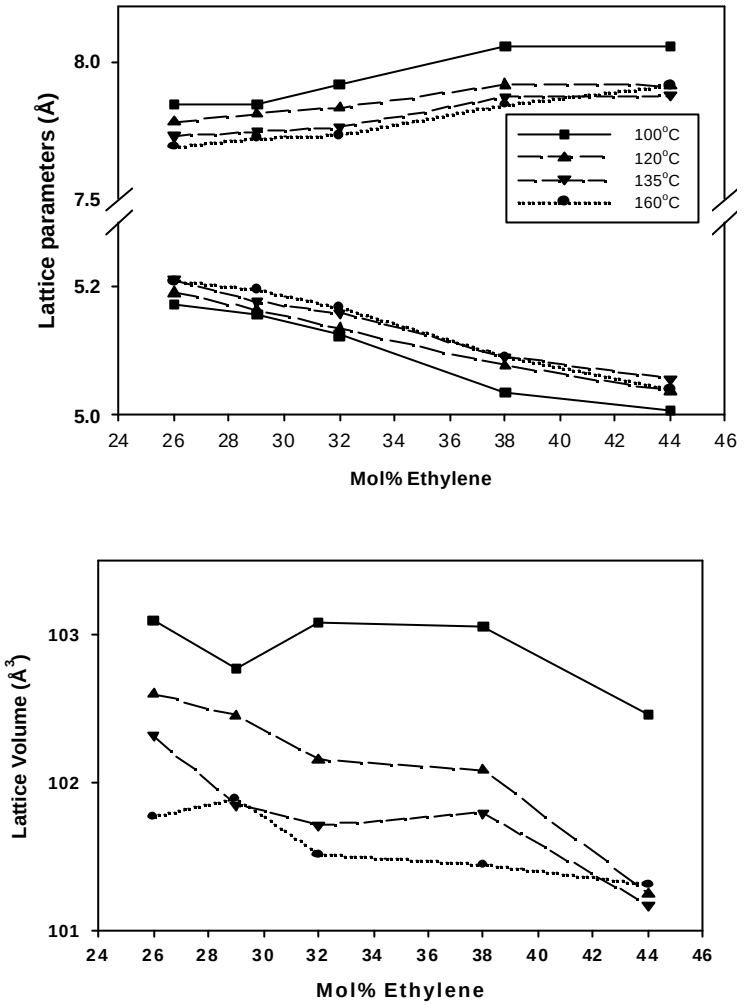


**Figure 2.** Evolution of a and b lattice parameters and lattice volume as a function of annealing temperature and ethylene content.

From this figure, it can be observed that a contraction of the a axis and a small expansion of the b axis occurs with increasing annealing temperature, leading therefore to an overall decrease in lattice volume. These results are consistent with an improvement in crystalline morphology towards thicker and more thermodynamically stable crystals in agreement with previous work[2].

Figure 3 plots the copolymers long period as determined from SAXS data as a function of annealing temperature and ethylene content. From this Figure, one can observe that the long period after annealing at 100°C is generally longer for the lower

ethylene content copolymers. The repeat distance increases with annealing temperature; this increase is larger for the high ethylene content copolymers because these materials have lower melting point (see copolymers melting point in the first column of Table 3) and, therefore, annealing is comparatively more aggressive for these particular samples. These observations are consistent with a general improvement in phase morphology and crystallinity development at expenses of the disappearance of the more defective crystals, resulting in a more homogeneous and sharply defined two phase architecture. However, samples EVOH38 and EVOH44, slow down increase and decrease long period respectively, at the highest annealing temperature, due to extensive melting during annealing and subsequent fast recrystallization upon sample removal from the oven, leading again to defects.

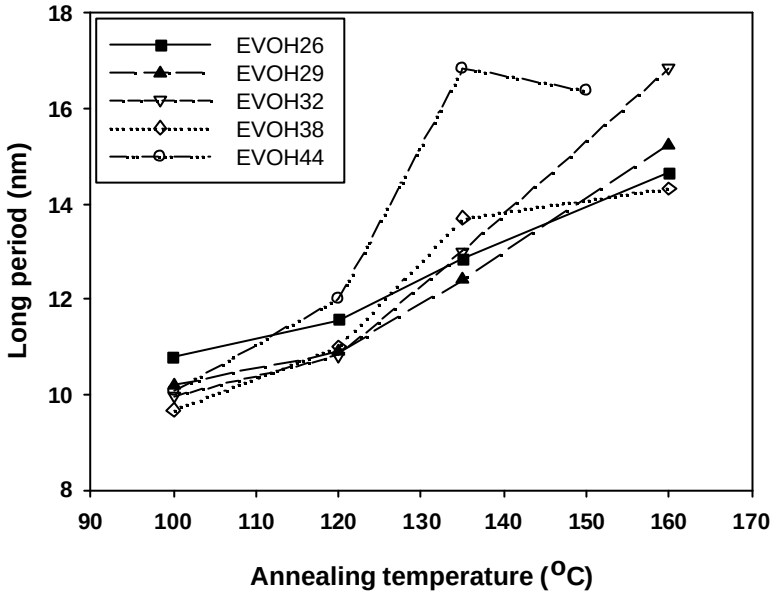


**Figure 3.** Long period as a function of annealing temperature for all copolymers.

Thus, a general picture of expected temperature-induced improvement in crystalline morphology and of a more regular stacking of the lamellae can be drawn from the above results upon annealing. This is a very general and well known response in crystalline polymers.

Further substantiation of these effects was alternatively gained by FT-IR experiments. From the results that follow, the FT-IR technique is uncovered as an extremely valuable characterization tool for these materials. The reasons being the high sensitivity of the technique to simultaneously detect changes in crystallinity and

water sorption levels. Figure 4 shows the effect of a stepwise annealing process on the infrared spectrum of an EVOH32 specimen. In this figure, the arrows indicate changes in the absorbance of some bands of interest with increasing temperature. To obtain the figure, a single specimen of the sample was cumulatively annealed at the various temperatures directly onto the FT-IR sample holder (to avoid changes in samples thickness or optical path), and, between annealing steps, it was taken out of the oven and FT-IR recorded. From the experiments, it can be observed that, upon annealing of this sample, a large increase in intensity of a band positioned at ca. 1140 $cm^{-1}$ becomes evident. Interestingly, the band at 1333 $cm^{-1}$ did not modify its intensity during the process and can, therefore, be potentially used as an internal standard during further experiments of this kind. A broad envelop peaked at 1092 $cm^{-1}$ was seen to decrease intensity because it hides the contribution of at least an amorphous band at ca. 1115 $cm^{-1}$.

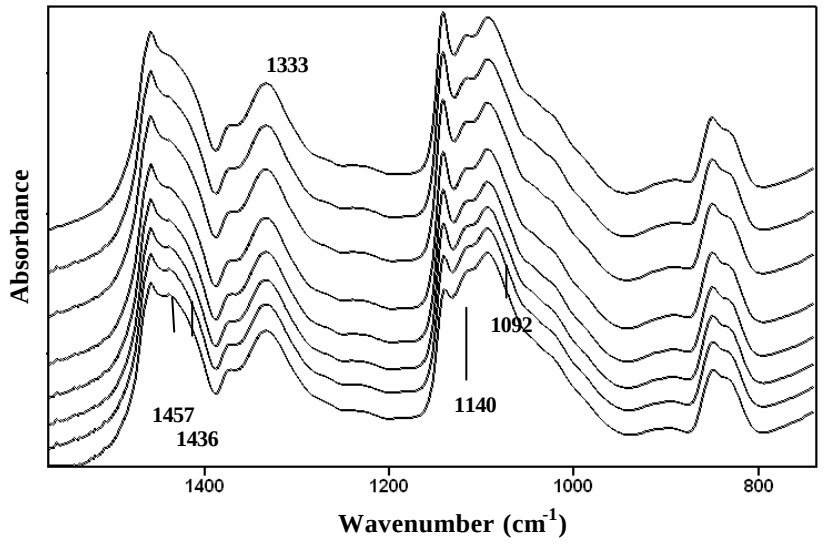


**Figure 4.** FT-IR spectra in the range 700-1600 $cm^{-1}$ of annealed for 20 minutes EVOH32 film at, from bottom to top, 70°C, 100°C, 120°C, 130°C, 140°C, 150°C, 160°C and 170°C.

The 1140 $cm^{-1}$ band (likely assigned to C-O-C or to C-C coupled with a CO stretching mode)[10,11], is known from previous works[11,12], to arise from all-trans conformation crystallizable chain segments, and is confirmed to be so throughout this work. Although in principle, all-trans conformers could be placed anywhere within the sample (as they are only ascribed to one dimensional order along the polymer chain) the vast majority of these must, in a good approximation, be within a

crystalline environment for unstretched semicrystalline polymer samples annealed (during drying) above $T_g$.

Despite the fact, that the coextrusion process may lead to some preferential orientation of the EVOH film in the machine direction this was not observed, by sample rotation, to affect the present FT-IR measurements throughout the work. Figure 5 shows more clearly the changes in the absolute absorbance of this band with annealing temperature. From this figure, it can be seen that the molecular order along the chain improves as the intensity of this band rises continuously with increasing annealing temperature. Note, however (thicker line in Figure 5), that annealing at the higher temperature (170$^o$C) results in a slight decrease of molecular order in line with analogous SAXS observations in Figure 3 for EVOH38 and EVOH44 at the highest temperatures. FT-IR becomes thus an excellent tool to ascertain phase structure modifications in molecular order, throughout the use of the 1140 cm$^{-1}$ band, for these particular materials.

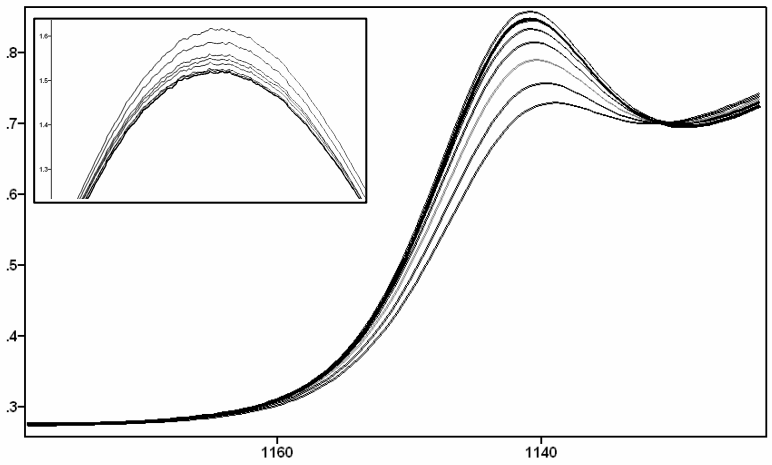


**Figure 5.** Absolute absorbance of the 1140 cm$^{-1}$ FT-IR band of annealed for 20 minutes EVOH32 specimen at, from lower to higher absorbance, 70$^o$C, 100$^o$C, 120$^o$C, 130$^o$C, 140$^o$C, 150$^o$C (overlap with 170$^o$C), 170$^o$C (thicker line), and 160$^o$C. Inset is the OH stretching band at 3347 cm$^{-1}$ in reverse temperature order.

Of particular relevance is also the inset in Figure 5, showing some changes of the OH stretching band upon stepwise annealing. From this figure, it is learnt that as annealing temperature is increased a decrease in band absorption occurs up to about 150$^o$C. Further annealing at higher temperatures does not lead to band shape nor intensity modifications. A feasible explanation for this particular behavior is the

progressive lost of remnant moisture present in the sample. Previous experiments by TGA suggested that some water molecules are very strongly linked to the polymer via hydrogen bonding and, therefore, to ensure an effective drying process a severe thermal treatment should be applied[9]. From the experiments being described in this study, there appears to be a close interrelation between temperature, molecular order and humidity (see later in text). From a fundamental point of view, to unleash these three effects appears to be virtually impossible, and this is, therefore, one of the main outcomes arising from the results as the paper develops.

*Humidity effect*

Sorption of water is known to have a severe plasticizing effect on the properties of these hydrophilic copolymers, particularly for the higher vinyl alcohol content copolymers. Most previous studies dealing with the characterization of moisture impact, have measured macroscopic properties like mechanical and barrier properties, and, therefore, there is a lack of morphological information on the effect of moisture sorption for these polymers[1,4,9,12,13,14,15]. Figure 6 shows the WAXS diffraction patterns of a dry (in vacuum at 70°C for a week) film specimen of EVOH32, of a specimen equilibrated at 100% relative humidity (RH).

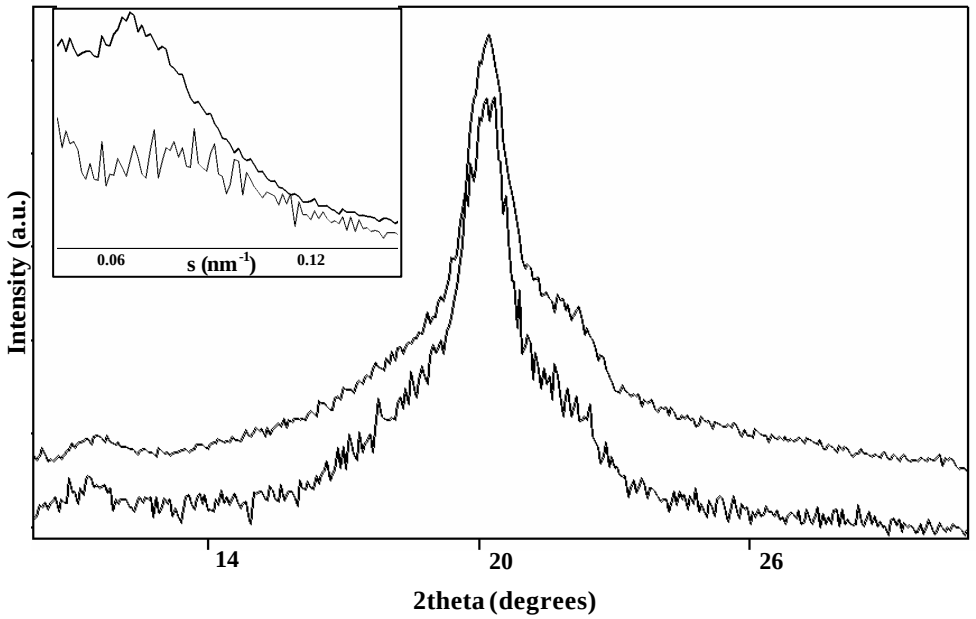


**Figure 6.** WAXS (normalized in intensity and shifted in the ordinate axis for comparison purposes) and raw SAXS patterns (inset, also slightly shifted in the ordinate axis) of EVOH32 dry (bottom) and saturated in water (top).

Figure 6 shows that the (200) diffraction plane at angle ca. 22$^{o}$ appears to resolve better upon moisture sorption. The inset in Figure 6 shows the raw SAXS patterns for these samples. From this, one can observe that the water saturated sample exhibits a more enhanced and shifted to lower angle peak maximum. The enhancement in intensity caused by the presence of moisture, could be attributed to an increase in phase contrast (scattering invariant is proportional to the square of the density contrast between amorphous phase and crystalline lamellae) due to presence of the plasticizing moisture in only the amorphous phase. Table 1 gathers the estimated long period for all dry and moisture saturated copolymers. From this, moisture sorption leads to increased long period, which is generally larger for lower ethylene content copolymers.

**Table 1.** Long period of EVOH films under dry and water saturation conditions.

| | **Dry (nm)** | **Water saturated (nm)** | **Difference** |
|---|---|---|---|
| **EVOH 26** | 10.8 | 13.3 | 2.5 |
| **EVOH 29** | 10.2 | 12.6 | 2.4 |
| **EVOH 32** | 10.0 | 12.7 | 2.7 |
| **EVOH 38** | 9.7 | 10.7 | 1.0 |
| **EVOH 44** | 10.1 | 10.9 | 0.8 |

Figure 7, shows the WAXS patterns of dry and water equilibrated specimens of EVOH26. From this figure a more clear strengthening and shift to higher angle of the (200) orthorhombic plane than in Figure 6 can be seen. This effect on the (200) reflection is most clearly seen for EVOH26 and less clearly observed for EVOH38 and EVOH44. Calculations of lattice parameters for the diffractogram in Figure 7 indicate that the a axis does indeed contract from 7.85 to 7.82 Å upon water equilibrium sorption. However, the b axis expands from 5.17 to 5.24 Å leading to an overall lattice volume expansion of about 1%. Contraction of the a axis and slight expansion of the b axis were indicative upon annealing in Figure 2 of progression of the crystalline phase towards a more thermodynamically stable morphology. Thus, the observations reported here appear to indicate that moisture sorption leaves a more stable arrangement of the lattice chains but with a slightly increased cell volume for

this sample. However, does this imply that higher molecular order is attained upon water sorption?

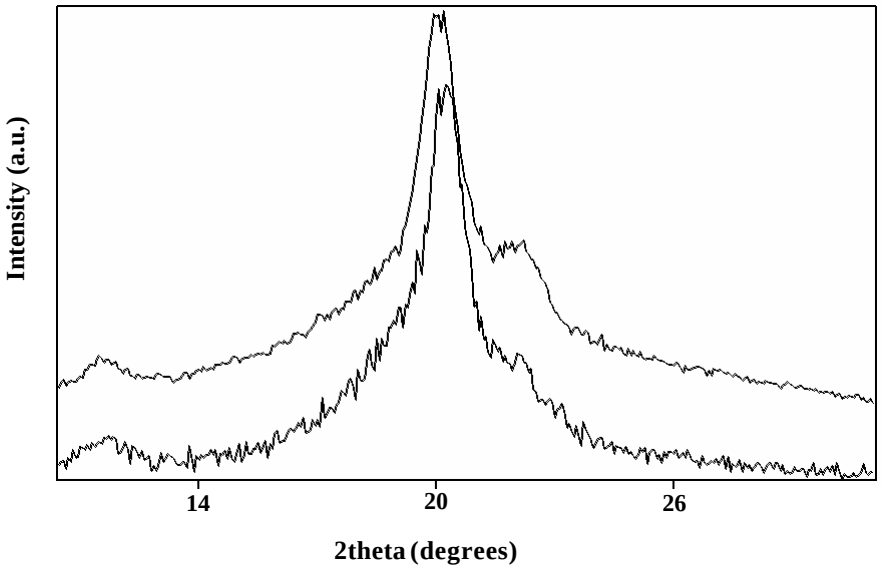


**Figure 7.** WAXS patterns (normalized in intensity and shifted in the ordinate axis for comparison purposes) of a film of EVOH26 dry (bottom) and water saturated (top).

To give answer to the above question, further experiments were also carried out by FT-IR on dry samples before and after water saturation. To do that however, a prior knowledge on the effect of moisture over the FT-IR spectrum is needed. This was derived by immersion in a 100%RH environment of specimens (not dried) of the various samples. After equilibrium sorption, these specimens were removed from the humidity conditions, wiped up the surface and then, measured by FT-IR, in-situ, during water desorption within the $N_2$ purged FT-IR chamber (see Figure 8).

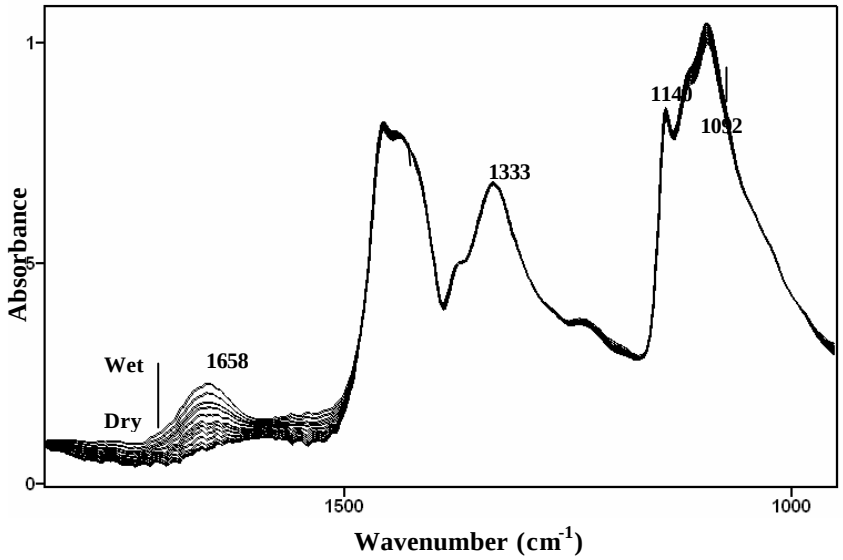


**Figure 8.** FT-IR spectra taken during desorption of a water equilibrated film of EVOH26. Arrows indicate the absolute absorbance changes upon water desorption. Note that this particular sample was not vacuum dried at 70°C before equilibrated in water.

Under these conditions, one can interpret absolute spectral modifications in the samples without interference from changes in thickness and optical path. Figure 8 shows the progressive decrease of the 1658 $cm^{-1}$ in-plane OH bending water band upon desorption. During this process, the band at 1333 $cm^{-1}$ remains completely unmodified and it is, therefore, further confirmed as an adequate internal standard for the experiments displayed here. The crystallinity band at 1140 $cm^{-1}$ also remains largely unmodified during desorption (see second and third rows in Table 2). However, the bands envelope with maximum at 1092 $cm^{-1}$ (having amorphous contributions)[11] appears to increase as moisture diffuses out of the sample, perhaps as a result of differences in absorption coefficients between dry and wet conditions for some of the corresponding modes in the amorphous phase.

With the above in mind, vacuum dry specimens of the different samples were measured by FT-IR before and after water saturation (see two bottom spectra in Figure 9 for EVOH26). The continuous arrow in Figure 9 indicates that water sorption in EVOH26 leads to a clear (larger than the changes seen in Figure 8) band

decrease of the 1140 $cm^{-1}$ crystallinity band. This is confirmed by observation of the data in Table 2. The fourth and fifth rows in Table 2 gather the normalized absorbance of the 1140 $cm^{-1}$ band of a dry specimen before and after water saturation for all copolymers. From this table, a crystallinity drop is found for the other copolymers, with a tendency for this to be lower in the highest ethylene content materials. Consequently, a partial dissolution of crystallinity is clearly happening for these samples upon water uptake, which from observation of Figure 8 and Table 2 is not recovered upon subsequent desorption.

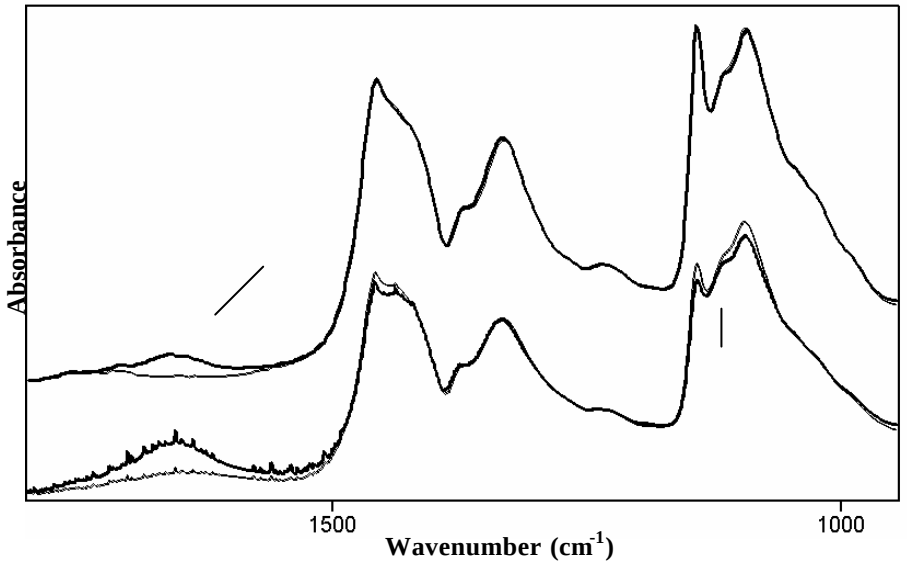


**Figure 9.** FT-IR spectra of EVOH26 dry at 70°C and dry and then water saturated (thicker spectrum) at the bottom, and annealed at 160°C and water saturated after annealing at 160°C (thicker spectrum) at the top. Continous arrow points to the 1140 $cm^{-1}$ crystallinity band and discontinuous arrow points to the 1658 $cm^{-1}$ OH in-plane bending of water.

**Table 2.** Normalized intensity of the 1140 $cm^{-1}$ (by subtracting the absorbance of the 1333 $cm^{-1}$ standard band and multiplying by 100) FT-IR band for the various materials after various treatments.

| Treatment | EVOH26 | EVOH29 | EVOH32 | EVOH38 | EVOH44 | EVOH48 |
|---|---|---|---|---|---|---|
| **Water Saturated** | 17 | 13 | 13 | 12 | 12 | 13 |
| **Fully Desorbed** | 15 | 14 | 14 | 13 | 12 | 13 |
| **Dry at 70°C** | 20 | 18 | 16 | 15 | 14 | 14 |
| **Dry and Water Sat.** | 14 | 13 | 13 | 13 | 12 | 13 |
| **Ann. At 120°C** | 23 | 21 | 20 | 19 | 17 | 17 |
| **†Ann. At 160°C** | 30 | 29 | 25 | 24 | 19 | 18 |
| **†Ann. At 160°C and Water Sat.** | 29 | 28 | 25 | 25 | 20 | 19 |

†EVOH44 and EVOH48 were annealed at 150°C instead of at 160°C.

Table 2 shows that upon water desorption of the as received materials equilibrated in water (therefore not previously dried), the intensity of the 1140 $cm^{-1}$ crystallinity band does not appear to have a clear trend with composition nor to change to a significant extend. It is worth noting that the absolute absorbances of the 1140 $cm^{-1}$ and internal standard bands are different for different copolymers and, as a result, the normalized intensity of the crystallinity band, although it approaches them all, is not necessarily comparable between different materials. Consequently, the numbers in Table 2 can only be compared in relative terms along columns (between treatments) and not across columns (between materials). After vacuum drying of the as received samples, all the materials increase crystallinity (compare second and fourth row in Table 2) due to the mild annealing treatment at 70°C given to them for a week. When the dry samples are equilibrated in water, there is a clear decrease in crystallinity for all copolymers, especially for the lowest ethylene content samples.

An interesting question rises however, from these observations: If sorption of water molecules leads to some reduction in crystallinity in fast cooled extruded EVOH specimens having a defective crystalline morphology; would this effect reproduce on

an annealed sample when undergoing water sorption? In other words, does crystal density and morphology matter in terms of moisture resistance? This question brings in another concern: Is the 1140 $cm^{-1}$ band drop observed by FT-IR upon moisture sorption in Figure 9 and Table 2 a true crystallinity reduction, or is just a result of the disappearance (due to moisture plasticization) of all-trans ordered chain segments present in the amorphous phase and being held up in all-trans conformation by intermolecular hydroxyl hydrogen bonding in the glassy state?

In order to assess these reasonable concerns, dry specimens of the various copolymers were stepwise annealed for 20 minutes in an oven at various temperatures (see top spectra in Figure 9 and Table 2). By doing so, higher and more robust crystallinity is generated. Thus, similarly as in Figure 4 for EVOH32, the band at 1140 $cm^{-1}$ ascribed to all-trans ordered conformers increases intensity with increasing annealing temperature for the copolymers, suggesting that thermally-induced higher molecular order is imprinted on the materials. However, after annealing at 160$^{o}$C (150$^{o}$C for EVOH44 and 48) the samples were exposed to a 100%RH environment until equilibrium sorption, and were then measured again by FT-IR at equilibrium sorption (see top spectra in Figure 9 and last row in Table 2) and during desorption inside a nitrogen purged FT-IR chamber (results not shown). From the latter experiments, it is found that the high molecular order achieved during annealing is now not being significantly disrupted by water sorption or subsequent desorption and, therefore, rules out the hypothesis of all-trans segments relaxing in the amorphous phase due to water sorption, and confirms the drop of the 1140$cm^{-1}$ band seen in Figure 9 and Table 2 as a genuine crystallinity destruction by dissolution.

Another supporting evidence for the above observations is the evolution of OH in-plane bending mode at 1658 $cm^{-1}$ (pointed by a discontinuous arrow) arising from the sorbed moisture in the sample in Figure 9. This band is seen smaller in the annealed at 160$^{o}$C water saturated sample, supporting that as annealing gives rise to a higher and more robust crystallinity in the sample the water uptake at equilibrium is clearly lower, e.g. 23% lower for EVOH26 from FT-IR measurements.

Figure 10 shows more clearly how as we increase annealing temperature of EVOH26 and, therefore, increase crystallinity and average crystalline density, lower reduction in crystallinity is observed for this specimen after equilibrium water sorption. In fact, the annealing process at 120$^{o}$C appears to produce sufficiently stable crystals in terms of moisture resistance for this EVOH26 sample, and, consequently, further annealing at higher temperatures has virtually no differentiating effect.

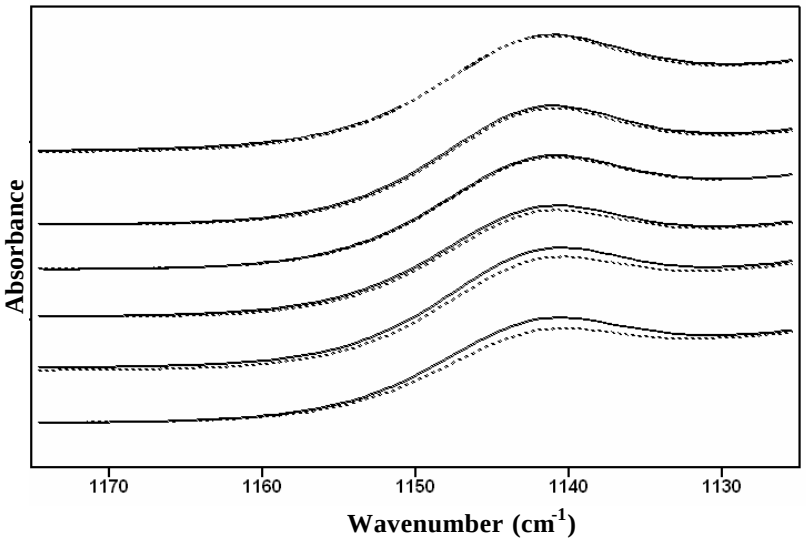


**Figure 10.** FT-IR spectra showing the 1140cm$^{-1}$ crystallinity band of annealed for 20 minutes at, from top to bottom, 140$^{o}$C, 130$^{o}$C, 120$^{o}$C, 110$^{o}$C, 90$^{o}$C and 80$^{o}$C EVOH26 specimens before (continuous) and after water saturation (discontinuous).

The overall results then suggest that water uptake leads to the dissolution of ill-defined (defective) crystallinity, most likely placed at the interphase between the crystalline lamellae and the amorphous phase. This leaves a lamellae core with improved crystalline morphology (see strengthening of the (200) plane in Figure 7) and with a slightly higher repeat distance as derived from the SAXS results due to expansion (dedensification) of the phase periodicity. The reported increase in cell volume for EVOH26 due to expansion of the b lattice parameter is thought to be the result of the plastizacing effect of the sorbed water in the amorphous phase resulting in swelling stresses on the crystalline morphology.

*Combined temperature and humidity effect*

In order to study the effect of the combination of the above two factors, temperature and moisture, on the morphology of EVOH copolymers, slow-cooled and crash-cooled compression moulded thicker plates were used. These samples were obtained as explained in the experimental section. Vacuum dried thicker plates were used in this part because the above polymer films, typically utilized in food packaging applications, did not withstand the treatment and irreversibly lost dimensional stability. The samples were conditioned in an autoclave at 120$^{o}$C during 20 minutes, typical industrial retorting conditions. It is worthy noting that in all cases treatments were carried out at temperatures well below the copolymers maximum of melting, albeit above their glass transition temperatures and around the a-relaxation temperatures[9]. The latter relaxation is picked up by dynamic-mechanical experiments and is related, by analogy to polyethylene, to relaxational motions within crystals.

**Table 3.** DSC maximum of melting ($T_m$), melting enthalpy (?H) and peak width at the base of crash-cooled and retorted crash-cooled specimens.

| | Untreated | | | 120ºC 20min, autoclave | | | Difference | | |
|---|---|---|---|---|---|---|---|---|---|
| | Tm (ºC) | ?H (J/g) | Width (ºC) | Tm (ºC) | ?H (J/g) | Width (ºC) | ?Tm (ºC) | ?(?H) (J/g) | ?Width (ºC) |
| EVOH26 | 200.1±0.2 | 90.6±13 | 16.8±0.5 | 193.2±0.1 | 96.0±0.3 | 23.6±2.6 | -6.9 | 5.5 | 6.8 |
| EVOH29 | 194.9±0.1 | 86.6±4.4 | 17.8±0.4 | 189.8±1.0 | 85.1±2.5 | 17.2±0.1 | -5.1 | -1.5 | -0.7 |
| EVOH32 | 187.0±0.1 | 83.5±0.1 | 13.6±5.4 | 183.3±4.0 | 82.2±4.7 | 22.0±0.3 | -3.7 | -1.3 | 8.4 |
| EVOH38 | 178.9±1.2 | 83.4±20 | 16.6±4.4 | 174.3±0.4 | 86.6±1.5 | 19.2±5.8 | -4.6 | 3.2 | 2.6 |
| EVOH44 | 167.3±0.1 | 84.6±6.0 | 17.5±0.1 | 165.7±1.4 | 83.0±12 | 20.1±3.8 | -1.7 | -1.6 | 2.7 |
| EVOH48 | 160.3±0.3 | 72.9± 25 | 13.9±0.7 | 158.5±3.3 | 72.6±6.0 | 16.5±0.7 | -1.8 | 7.9 | 2.6 |

**Table 4.** DSC maximum of melting ($T_m$), melting enthalpy (? H) and peak width at the base of slow-cooled and retorted slow-cooled specimens.

| | Untreated | | | 120ºC, 20min, Autoclave | | | Difference | | |
|---|---|---|---|---|---|---|---|---|---|
| | $T_m$ (ºC) | ? H (J/g) | Width (ºC) | $T_m$ (ºC) | ? H (J/g) | Width (ºC) | ? $T_m$ (ºC) | ?(?H) (J/g) | ?Width (ºC) |
| EVOH 26 | 198.2±0.1 | 94.5±3.9 | 8.0±0.1 | 194.3±1.4 | 83.6±1.3 | 19.5±0.4 | -3.9 | -10.9 | 11.5 |
| EVOH 29 | 193.3±0.3 | 97.1±1.9 | 8.4±2.9 | 188.7±3.4 | 91.0±0.1 | 17.7±0.1 | -4.7 | -6.1 | 9.2 |
| EVOH 32 | 185.7±0.7 | 92.8±0.3 | 8.1±6.5 | 186.1±0.2 | 88.7±0.5 | 23.5±0.0 | 0.4 | -4.1 | 15.4 |
| EVOH 38 | 176.8±0.1 | 91.5±6.6 | 9.8±0.6 | 176.1±0.0 | 92.5±10 | 17.3±4.7 | -0.8 | 0.9 | 7.5 |
| EVOH 44 | 166.8±0.7 | 91.0±5.2 | 10.1±1.9 | 165.6±0.6 | 83.7±21.5 | 17.9±3.4 | -1.3 | -7.3 | 7.8 |
| EVOH 48 | 160.9±0.1 | 86.0±0.3 | 12.5±0.3 | 160.3±0.1 | 78.3±0.7 | 15.3±0.3 | -0.7 | -7.8 | 2.9 |

From the first DSC heating scans (see Tables 3 and 4), it can be seen that the maximum of melting of the non-treated samples is higher than the melting point of the retorted samples. This is particularly the case for the copolymers with the higher vinyl alcohol contents. The samples appear, by visual inspection, to be dramatically damaged, with presence of voids and loss of transparency, i.e. intense whitening or hazing. These effects are attributed to pressurized water vapour having penetrated the amorphous phase but also diffusing through the crystal edges and inducing partial melting and fractionation of the crystalline morphology (see later). Voiding and loss of transparency could arise from bubbles formed by water evaporation as the pressure is released rapidly after retorting in the autoclave. From the above experiments, these damaging effects do not occur upon water exposure or uptake at room temperature and evidently neither due to annealing. High temperature and humidity, appear thus as a very severe aggressive combination of factors for these materials. Tables 3 and 4 gather, maximum of melting, peak width (at the base of the peak) and melting enthalpies for the various samples and conditionings recorded during the first run; and Figure 11 shows, as an example, the actual melting endotherms of crash-cooled EVOH26 and EVOH48. Although, the measured melting enthalpies (taken from the integrated area under the melting enthalpy covering from the endset of melting up to 70$^o$C below this) of treated and non-treated samples are only slightly smaller, pointing out that the overall degree of crystallinity may not have decreased so significantly, the melting peaks of the retorted samples have clearly broadened (particularly for the lower ethylene content samples and for the

slow-cooled samples) towards lower temperature, suggesting that a more heterogeneous crystalline structure with lower crystal size and/or perfection has occurred as a result of retorting and, irrespective, of whether a more robust crystalline morphology (as in slow-cooled samples) was originally present. It should be noticed that the samples were dried (70$^{o}$C in vacuum) immediately after the retorting processes and before the DSC run and that this conditioning may have to some extend re-annealed the structure.

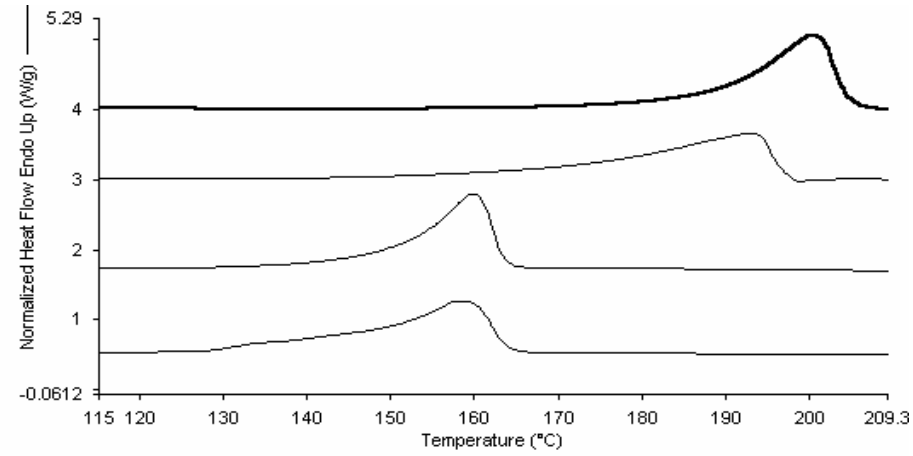


**Figure 11.** Melting endotherms of, from top to bottom, untreated and retorted EVOH26 and untreated and retorted EVOH48

WAXS experiments were also carried out on the slow-cooled and crash-cooled retorted samples. These samples were not reconditioned after retorting to avoid re-annealing and were just left to equilibrate at room temperature and 60%RH. Figure 12 shows the WAXS patterns of crash-cooled specimens before and after retorting. After retorting, the WAXS crystalline morphology has changed dramatically, particularly for the low ethylene content copolymers. The crystalline patterns are clearly less defined and the main diffraction peak (110) at angle 20$^{o}$ is much broader, suggesting crystal fractionation, heterogeneity and hence a more defective crystalline morphology. Note that Figure 1 showed also broadening of the (110) reflection at the highest annealing temperature, but there the broadening was a result of early splitting of this particular reflection into two monoclinic crystalline peaks as further suggested

by a strengthening and shift toward higher angle of the (200) reflection. Similar results were found (results not shown) for slow cooled samples, with a more stable initial crystalline morphology, suggesting that crystal robustness is not sufficient (as it was to avoid crystal dissolution during water sorption at room temperature) in terms of resistance to the process during direct exposure of EVOH to heated moisture.

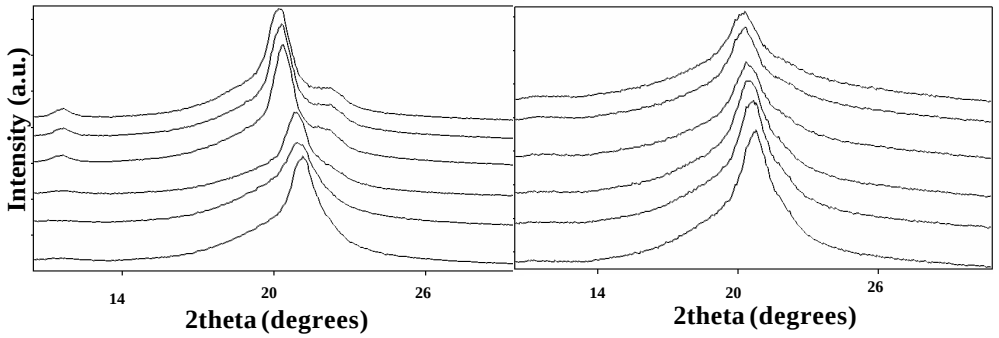


**Figure 12.** WAXS patterns of crash-cooled (left) and retorted crash-cooled (right) specimens of, from to top to bottom, EVOH26, EVOH29, EVOH32, EVOH38, EVOH44, EVOH48

Figure 13, shows the evolution of the a and b cell parameters after retorting of crash-cooled specimens as a function of ethylene content. From this figure, it can be clearly observed that retorting leads to clear expansion of the a (from sample EVOH26 to 38) and b (from sample 38 to 48) lattice parameters and, therefore, to an overall drop in crystalline density.

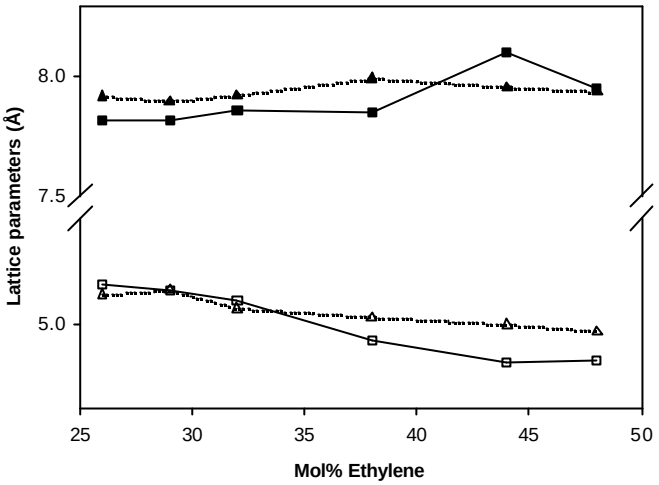


**Figure 13.** Evolution of lattice axis a and b of crash-cooled (squares) and retorted crash-cooled (triangles) specimens as a function of ethylene content.

No pseudohexagonal crystal lattice was found as a result of any of the treatments described above as the quantity $r=(3)^{1/2}b/a$ was always larger than unity[2]. Nevertheless, retorting imposes a very strong distorting effect on the crystalline lattice morphology of the samples as further proved by Figure 14. This figure shows the Raman spectrum in the -$CH_2$- bending range of slow cooled EVOH29, where factor group splitting features (see arrows) characteristic of an orthorhombic lattice are seen in the untreated specimen[16,17]. After retorting, a disappearance of the orthorhombic factor group splitting patterns indicates evolution towards a very distorted orthorhombic unit cell of lower crystalline density.

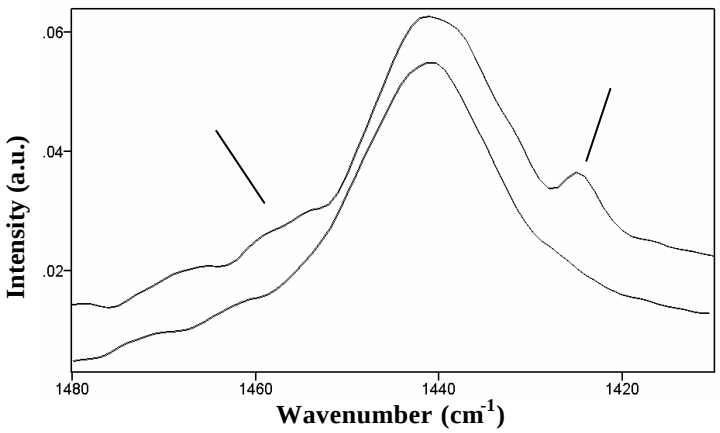


**Figure 14.** Raman -$CH_2$- bending range of crash-cooled (top spectrum) and retorted crash-cooled specimens of EVOH29. Arrows indicate bands evidencing a factor group splitting effect.

From the above, it is clear that EVOH monolayers are structures that even with high thicknesses are largely susceptible to alterations during combined temperature and humidity processes and, therefore, need to be protected between hydrophobic materials in commercial applications. But what are the actual changes taking place during direct retorting of an EVOH sample? In order to understand the transient occurrences during this combined temperature and humidity process a film sample of EVOH32 was scanned in temperature both dry and in the presence of excess saturating humidity conditions. Figure 15 shows the WAXS patterns of this sample under these conditions as a function of temperature.

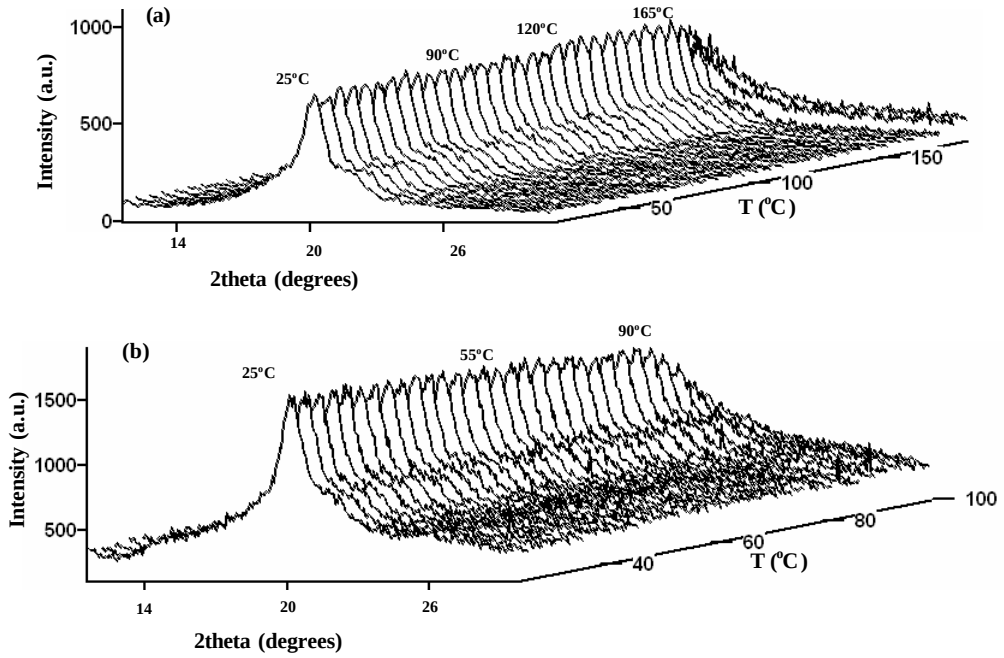


**Figure 15.** WAXS patterns as a function of temperature of (a) dry and (b) water saturated EVOH32 film specimens. Note the presence in Figure 15(b) of background signals underneath the crystalline EVOH patterns arising from the sample being measured in the cited liquid cell.

From this figure, it can be seen that under dry conditions the sample retains its crystalline morphology over temperature until it reaches melting at around 183°C, temperature at which the crystalline patterns disappear completely in agreement with its reported melting point. On the other hand, for a water saturated sample, the crystallinity decreases immediately above room temperature to completely disappear at around 100°C (83°C below its actual melting point). This is thought to be caused by pressurized heated water diffusing through thermally activated molecules within crystals disrupting the efficient crystalline intermolecular hydrogen bonding provided by the hydroxyl groups. The crystallinity decline appears more pronounced above 50°C and is very dramatic above 90°C. As a result, a saturated sample of EVOH32 appears to show very little moisture resistance at temperatures immediately above 50°C.

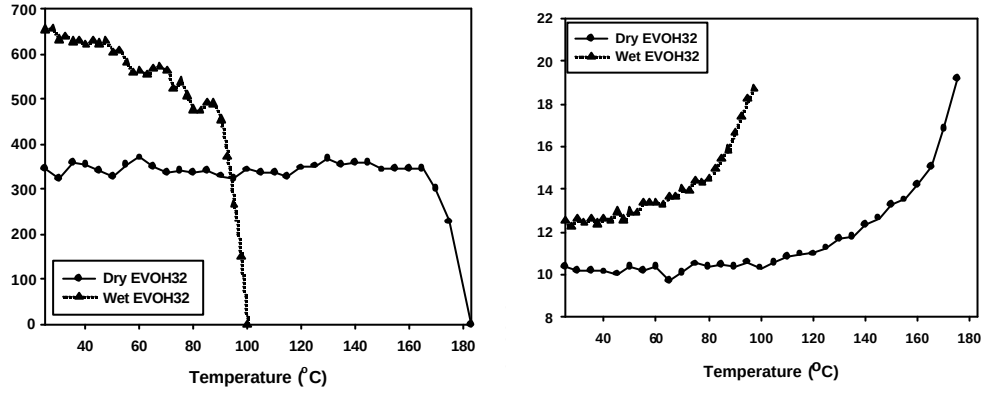


**Figure 16.** Intensity (left) of the (110) crystalline plane for the diffractograms plotted in Figure 15 and long period (right) as a function of temperature for a dry and water saturated film sample.

Figure 16 shows the evolution of the intensity of the (110) orthorhombic plane and of the long period (determined from the simultaneous SAXS patterns) with temperature. From this, it can be more clearly appreciated that under dry conditions the polymer morphology is largely retained until temperatures above 100°C, temperature in the vicinity of the polymer a-relaxation. Beyond this temperature, the long period begins to increase shallowly up to about 160°C and then markedly; concomitantly, the crystallinity appears to first increase slightly up to about 160°C (annealing effect)

and from then onwards to decrease to a fast pace (progressive melting). On the other hand, in the wet sample the long period is relatively retained up to about 50°C, but from there onwards it progressively increases in line with the observed decease of the crystallinity up to the complete melting of the sample. The above behavior does, of course, prevent the use of EVOH as monolayer packages in commercial food retortable packaging applications. In these particular applications, only adequate multilayer structures where a dry high gas barrier EVOH layer is sandwiched between high water barrier polymers have commercial interest. In this context, a more detailed description of the combined effect of temperature and humidity on the melting and crystallization behavior of these copolymers in monolayer and multilayer structures, as well as the role of crystal stability, as a function of temperature, humidity and composition is being currently under investigation.

**Acknowledgements**

The authors would like to thank The Nippon Synthetic Chemical Industry Co. Ltd. (NIPPON GOHSEI), Japan for financial support and Mr. Y. Saito, associate board director of Central Research Laboratory, NIPPON GOHSEI for helpful advice and suggestions during preparation of the manuscript. The work performed at the synchrotron facility in Hamburg (Hasylab, Germany) was supported by the IHP-Contract HPRI-CT-1999-00040/2001-00140 of the European Commission and the authors would like to acknowledge Dr. S. Funari and Mr. M. Dommach (Hasylab) for experimental support.

## REFERENCES

[1]Lagaron, J.M.; Powell, A.K.; Bonner, J.G. *Polymer Testing* **2001**, 20/5, 569-577.

[2]Cerrada, M.L.; Perez, E.; Pereña, J.M.; Benavente, R. *Macromolecules* **1998**, 31, 2559-2564.

[3] Takahashi, M.;Tashiro, K.; Amiya, S. *Macromolecules* **1999**, 32, 5860-5871.

[4] Aucejo, S.; Catala, R.; Gavara, R. *Food Sci. Technol. Int*. **2000**, 6, 159-164.

[5] Tsai, B.C.; Wachtel, J.A. In Barrier Polymers and Structures (W.J.Koros, Ed.), **1990**, American Chemical Society, Washington DC, p. 192-202.

[6] Tsai, B.C.; Jenkins, B.J. *J. Plastic Film and Sheeting* **1988**, 4, 63-71.

[7] Balta-Calleja, F.J.; Vonk, C.G. X-ray scattering of synthetic polymers, Amsterdam, Elsevier, 1980.

[8] http://www-hasylab.desy.de/science/groups/mpikgf.

[9] Lagaron, J.M.; Gimenez, E.; Saura J.J.; Gavara R. *Polymer* **2001**, 42, 7381-7394.

[10]Cooney, T.F.; Wang, L.; Sharma, S.K.; Gauldie, R.W.; Montana, A.J. *J. Polym. Sci., Part B: Polym. Phys*. **1994,** 32, 1163-1174.

[11] Xu, W.; Asai, S.; Sumita, M.; *Sen'i Gakkaishi* **1997**, 53(5), 174-182.

[12] Lagaron, J.M.; Gimenez, E.; Catala, R.; Gavara, R. *Macromol. Chem. Phys.* **2003**, 204, 704–713.

[13] Zhang, Z.; Britt, I.; Tung, M. *J. Polym. Sci., Part B: Polym Phys.* 1999, 37, 691-699.

[14] Aucejo, S.; Marco, C.; Gavara, R. *J Appl Polym Sci* **1999**, 74, 1201.

[15] Lagaron, J.M.; Gimenez, E.; Saura, J.J.; Gavara, R. *Polymer* **2001,** 42, 9531-9540.

[16] Lagaron, J.M. *J. Materials. Sci.* **2002**, 37, 4101-4107.

[17] Lagaron, J.M.; Powell, A.K.; Davidson, N.S. *Macromolecules* **2000**, 33, 1030-1035.

# GAS BARRIER CHANGES AND MORPHOLOGICAL ALTERATIONS INDUCED BY RETORTING IN ETHYLENE-VINYL ALCOHOL-BASED FOOD PACKAGING STRUCTURES

## INTRODUCCIÓN AL ARTÍCULO II

Para complementar los resultados sobre los efectos de la esterilización sobre los copolímeros de etileno y alcohol vinílico (EVOH), se muestran en el presente artículo (publicado en el *Journal of Applied Polymer Science* tal y como se muestra en el Anexo 2) los datos relativos a la pérdida de propiedades barrera y a su lenta recuperación. En el caso de los copolímeros con mayor contenido en alcohol vinílico y, por tanto, más hidrofílicos, se observa el daño irreversible causado por este proceso de conservación de alimentos, reflejado en una permeabilidad en el equilibrio considerablemente superior a la del material seco. También se muestran en este artículo las imágenes tomadas mediante microscopía electrónica de barrido (SEM) que desvelan la morfología inicial de los materiales y la inducida por los diferentes tratamientos dados a las muestras.

De acuerdo con el segundo objetivo de la tesis, se incluyen aquí los resultados referentes a la modificación térmica del material que busca paliar los anteriores efectos dañinos mostrados. Se llevaron a cabo dos tipos de tratamiento:

- Secado posterior a la esterilización: conduce a una mejora de la permeabilidad de los materiales, que sorprendentemente es incluso superior a la de los copolímeros secos. Sin embargo, la viabilidad de este tratamiento desde un punto de vista industrial es dudosa.
- "Annealing" previo a la esterilización: se calculó la temperatura óptima de recocido o "annealing", como aquella que inducía una mayor formación de cristales, y se observó la utilidad de este pretratamiento en los copolímeros más sensibles a la esterilización, es decir, con mayor contenido en alcohol vinílico.

Por otro lado, los datos de permeabilidad de muestras calentadas en estufa (sin humedad) demuestran que existen otros factores adicionales a la cristalinidad que influencian las propiedades barrera, y que no siempre una mayor cristalinidad está relacionada con menor permeabilidad (tal y como en principio sería de esperar).

**ABSTRACT**

Ethylene vinyl alcohol (EVOH)-based packaging structures were analyzed in terms of both barrier properties and morphological alterations after a retorting process and as functions of ethylene content. From the results, it was found that the samples do have a substantial decrease in oxygen barrier properties, and that the kinetics of recovery strongly depends on the copolymer ethylene fraction. A morphological deterioration was also observed as a result of retorting, particularly for packaging structures composed of EVOH copolymers of low ethylene contents. However, the polymer morphology and barrier properties were restored after a dry thermal treatment of the retorted samples. Interestingly, pre-annealing of low ethylene content copolymers rendered them more resistant to the retorting process by means of promoting both a more robust crystallinity and lower water sorption capacity.

Keywords: EVOH copolymers, barrier, food packaging, crystal structures, morphology

## INTRODUCTION

The ethylene vinyl alcohol (EVOH) copolymers are excellent gas barrier semicrystalline materials with very good chemical resistance and, as such, they are widely used in a number of packaging applications. One of the most widely implemented applications is as intermediate barrier layer in multilayer structures to be used in various packaging designs for foodstuffs. The presence of EVOH in the packaging structure is key to food quality and safety because, for instance, it delays the ingress of oxygen, agent responsible for a number of food deterioration processes.

The excellent barrier properties of EVOH copolymers derive from a high degree of crystallinity and the presence of hydroxyl groups in the polymer structure which confer them with both high intermolecular and intramolecular cohesive energy and a low fractional free volume between the polymer chains available for the mass exchange of low molecular weight substances. On the other hand, these hydroxyl groups make the materials highly hydrophilic, so that in the presence of water, their barrier performance is greatly reduced. Water molecules sorbed by EVOH in high relative humidity (HR) environments are believed to hydrogen bond to the hydroxyl groups present in the polymer and reduce the overall polymer self-association. Consequently, segmental mobility becomes greatly activated, thus facilitating diffusion of permeants[1].

As a result of the above, in many food packaging applications, multilayer structures are used, which comprise an intermediate layer of high barrier EVOH sandwiched between at least two layers of hydrophobic materials such as polypropylene (PP), polyethylene (PE), polystyrene (PS), and so forth. These multilayer structures are usually made by coextrusion or coinjection processes.

EVOH is commercially available in various grades with different ratios of ethylene/vinyl alcohol. The copolymers are used in flexible as well as in rigid and semirigid packages. Some of these packaging designs are used to pack $O_2$-sensitive foods and beverages that undergo processes like hot filling, aseptic packaging or sterilization inside the package. During typical industrial sterilization processes, which make use of heated water vapor as the heat transfer medium, it is believed that

some of the pressurized water vapor is capable of traversing the external hydrophobic layers, sorb into and subsequently plasticize the EVOH intermediate layer, leading to a decrease in barrier properties. In this context, many studies have been carried out to ascertain the effects of water sorption[2,3,4] and retorting[5,6,7] on the permeability and thermal properties of these copolymers. However, a search of the open literature reveals a lack of studies that focus on the potential morphological consequences of water sorption and sterilization for these polymers and their corresponding packaging structures. Over the last few years, several strategies have been devised to reduce the water sensitivity of EVOH, that is, blends of the copolymer with other materials[8,9,10,11], chemical modification[12], addition of desiccants[13], and even incorporation of nanoparticles on its structure[14]. In a more recent paper[15], it was reported that water sorption at room temperature does lead to a partial melting of defective crystals and, upon retorting of EVOH monolayers, a dramatic deterioration of the copolymer crystallinity was observed by synchrotron X-ray analysis immediately above room temperature, which resulted in earlier melting of the material 83$^{o}$C below its actual melting point. This deterioration was ascribed to pressurized water vapor sorbed in the amorphous phase, penetrating the crystalline phase through the interphase. It is very important to understand and control morphological alterations, because they are also responsible for changes in barrier properties through factors like crystallinity (impermeable phase to gases), tortuosity (or detour), and chain immobilization factors[16].

In this article, we report and interpret changes in the oxygen permeability of multilayer structures, having EVOH as barrier layer, after different thermal treatments and as a function of the ethylene content. From the results obtained, methodologies are proposed that seek to avoid or reduce the dramatic effects of combined temperature and humidity treatments in typical retortable PP/EVOH/PP packaging structures.

## EXPERIMENTAL

### Materials

Six different commercial ethylene vinyl alcohol (Soarnol®) copolymer grades supplied by The Nippon Synthetic Chemical Industry Co., Ltd. (NIPPON GOHSEI ,Japan) were analyzed: EVOH26, EVOH29, EVOH32, EVOH38, EVOH44 and EVOH48, where the numbers indicate the mol percentage of ethylene in the copolymer composition.

Films (~ 10 μm thick) of these EVOH materials were coextruded between polypropylene layers both with adhesive (typical commercial retortable multilayer structures, termed PP//EVOH//PP) and without adhesive (for easy of delamination of the high barrier layer, termed PP/EVOH/PP). Unless otherwise stated, all samples were dried at 70°C for 1 week in a vacuum oven. Structures of the tested multilayer films were PP/EVOH/PP = 100/10/100 μm and PP//EVOH//PP = 90/10/10/10/90.

### Thermal treatments

The materials were thermally treated under dry and humid conditions in a conventional oven (annealing) and in a sterilization autoclave (retorting), respectively. The standard treatment given to the samples, both in the oven and in the autoclave, was 120ºC during 20 minutes. Other thermal conditions applied are specifically cited throughout the article.

### Oxygen transmission rate

Oxygen transmission rate ($O_2$TR) measurements were performed in an OX-TRAN® 2/20 (Mocon Inc., Minneapolis, MN) at a temperature of 45°C and 0% RH. High-temperature assays were carried out to increase the permeability of the EVOH films and, thus, be able to measure it with higher certainty, given the very high barrier character of the materials with lower ethylene contents. $O_2$TR values are given instead of permeability coefficients because many of the samples measured were multilayer structures (PP//EVOH//PP). As the thickness of the samples (cut always from the middle of the co-extruded rolls section) was checked to be constant, the $O_2$TR values of the different specimens of the various samples can be directly compared.

**FT-IR experiments**

Transmission FT-IR experiments were recorded within a $N_2$-purged environment using a model Tensor37 equipment (Bruker, Darmstadt, Germany) with a resolution of 1 $cm^{-1}$.

**SEM observation**

For scanning electron microscopy (SEM) observation, the samples were fractured in liquid nitrogen and mounted on a sample holder. The fracture surface of the different samples was sputtered with Au/Pd in a vacuum. The SEM micrographs (S4100, Hitachi, Osaka, Japan) were taken with an accelerating voltage of 10 keV on the sample thickness.

**DSC experiments**

DSC experiments were carried out using a Perkin-Elmer DSC-7 calorimeter (Perkin-Elmer Cetus Instruments, Norwalk, CT). The rate of both heating and cooling for the runs was 10ºC/min, where a typical sample weight was around 8 mg. Calibration was performed using an indium sample. All tests were carried out, at least, in duplicate.

## RESULTS AND DISCUSSION

### Oxygen Transmission Rate

Figure 1 shows, as an example, the $O_2$TR evolution after retorting of three of the six multilayer materials analyzed versus the $O_2$TR values of the dry analogue. From this figure, it can be first seen that the dry $O_2$TR of EVOH increases with increasing the ethylene content in the copolymer, as expected and in agreement with all previous understanding of these materials. In this figure, it can also be observed that the barrier properties of the different EVOH materials, irrespective of their ethylene content, are largely deteriorated immediately after retorting.

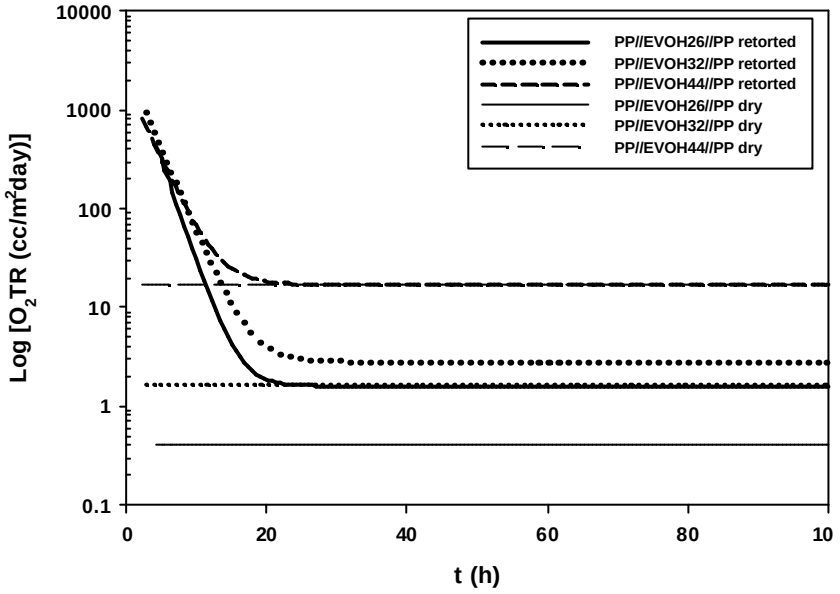


**Figure 1.** Oxygen Transmission Rate of retorted multilayer structures (PP//EVOH//PP) vs. time after retorting and $O_2$TR of the dry analogous

From the results, however, it appears that, after approximately 30 hours of testing, a considerably low $O_2$TR value has been reached for the materials, even though it was also expected that the kinetics of recovery would have clearly been slower had the experiments been carried out at room temperature. From the previous rationalization of this phenomenon, it is considered that water vapor penetrates the PP layers and plasticizes the intermediate EVOH barrier layer with a subsequent depletion in the overall barrier properties of the packaging structures. After sterilization, sorbed water is progressively eliminated from the copolymer structure; this phenomenon is reflected by observation of a continuous decrease in permeability with time. This

process of barrier recovery can be properly fitted to a simple exponential decay equation, expressed as:

$$OTR(t) = OTR_{\infty} + ae^{(-bt)} \qquad \text{(Equation 1)}$$

Where $a$ is approximately the transmission rate value of a freshly retorted sample and $OTR_{\infty}$ is that reached by the retorted sample at equilibrium. The parameter *b* is related to the kinetics of the OTR recovery: the lower the value, the slower the process. The parameters of the equation for the curves shown in Figure 1 are presented in Table 1. As can be seen in Table 1, the values of those parameters are, as expected, related to the ethylene content of the copolymers. With increasing ethylene content, the values of $a$ and *b* decrease, while $OTR_{\infty}$ values increase.

**Table 1.** Curve-fitting parameters for the permeability recovery data of the multilayer structures PP//EVOH26//PP, PP//EVOH32//PP and PP//EVOH44//PP to Eq. 1

| Estructure | $OTR_{\infty}$ | $a$ | b | $R^2$ |
|---|---|---|---|---|
| PP//EVOH 26//PP | 1.6 | 3222.28 | 0.4706 | 0.9863 |
| PP//EVOH 32//PP | 2.8 | 2681.87 | 0.3866 | 0.9809 |
| PP//EVOH 44//PP | 17 | 1885.14 | 0.3676 | 0.9755 |

Although, the equation that describes this process appears to fit well every multilayer material studied, substantial differences are observed related to the final $O_2$TR value achieved. While for the case of the EVOH44 the permeability value of the dry sample was reached after approximately 20 hours following retorting, for the other copolymers with higher content in vinyl alcohol, even after 300 hours of continuous testing at 45$^{o}$C in the transmission rate instrument analyzer, the barrier properties were not fully recovered. Moreover, the lower the ethylene content of the EVOH sample the higher the gap left (see Fig. 1) between the untreated and the retorted specimens. Most of the works reporting about oxygen permeability changes attributed to retorting treatments have been carried out in EVOH32 (most widely used commercial composition) and, as such, the behavior of other EVOH grades was not previously reported in published research articles. From experiments in all

samples, it was found (see Table 2) that the permeability plateau value reached after retorting appears to differ from that of the untreated specimens for samples with ethylene contents below 38% but does lead to improved barrier, already 20 hours after retorting, for EVOH44 and EVOH48.

In subsequent experiments, all samples, PP//EVOH//PP and PP/EVOH/PP, were retorted and then dried at 70°C for 1 week in a vacuum oven. The $O_2$TR results measured on these retorted and dry samples are displayed in Table 2, together with the oxygen transmission rate of dry and sterilized multilayer structures after 150 hours in the $O_2$TR instrument. In the case of the PP/EVOH/PP structures, the specimens were delaminated after retorting and only the EVOH layer was tested. Fortunately, the multilayer samples, were able to withstand the retorting process without delamination throughout the treatment. Samples which were accidentally delaminated during or before the treatment were severely damaged during retorting and were consequently discarded. Results on the effect of temperature and humidity over the structure of bare EVOH monolayers have been reported in an earlier work[15].

**Table 2.** Oxygen transmission rate (cc/m$^2$day) of the various EVOH grades after different treatments measured at 45ºC

| | EVOH 26 | EVOH 29 | EVOH 32 | EVOH 38 | EVOH 44 | EVOH 48 |
|---|---|---|---|---|---|---|
| **EVOH dry** | 0.45 | 0.82 | 1.97 | 5.35 | 17.55 | 32.00 |
| **EVOH retorted and dry** | 0.43 | 0.62 | 1.65 | 4.00 | 11.40 | 22.00 |
| **PP//EVOH//PP dry** | 0.40 | 0.70 | 1.65 | 5.00 | 17.37 | 34.30 |
| **PP//EVOH//PP retort. and dry** | 0.35 | 0.73 | 1.60 | 3.50 | 12.95 | 29.00 |
| **PP//EVOH//PP oven** | 0.37 | 0.60 | 1.57 | 5.32 | 18.45 | 35.50 |
| **PP//EVOH//PP ret (150h)*** | 1.62 | 1.68 | 2.80 | 4.96 | 17.00 | 28.55 |

*$O_2$TR of multilayer structures after 150 hours following retorting

Surprisingly, the $O_2$TR values of the retorted and then dried samples were found to be better than those of the untreated ones, being this improvement more pronounced for those copolymers with higher ethylene content. Also not entirely expected was the general observation that the samples with higher ethylene contents (EVOH38, EVOH44 and EVOH48), which were annealed in the oven at 120ºC during 20 minutes, did not show improved performance compared to retorted at 120°C and then

vacuum dried samples. From the above results, there appears to be more factors influencing barrier properties than just the well reported water-induced plasticization process.

**Morphological characterization**

In a novel approach to the study of the retorting effects over the EVOH copolymers, it was thought that potential structural modifications promoted by the humid thermal treatment could play a role in these permeability changes. This was further justified by observations from a previous work in which the combination of temperature and humidity factors was found to discernibly deteriorate the structure of these materials upon direct exposure. From this latter work, it also arose that an appropriate tool to study morphological alterations in these materials is the FT-IR spectroscopy technique, due to its high sensitivity to detect both, crystallinity alterations through the use of the 1140 $cm^{-1}$ band and the presence of humidity in the sample through observation of the OH in plane bending band at 1650 $cm^{-1}$. The 1140 $cm^{-1}$ band is likely attributable to C-O-C stretching or to C-C stretching coupled with a C-O stretching mode. The absorbance of this band (divided by that of the internal standard at 1333 cm-1) can thus give us an indication of potential alterations in crystallinity after the various treatments, irrespective of differences in optical path and of minor thickness variations between different specimens.

As an example of the sensitivity of this band to determine crystallinity changes on the samples, Figure 2 shows the effect of a stepwise annealing process on the infrared spectrum of an EVOH26 sample. To obtain this figure, a single specimen of the polymer was cumulatively annealed at 100, 120, 140 and 160ºC during 20 minutes directly onto the FT-IR sample holder (to avoid changes in sample thickness or optical path) and, between annealing steps, it was taken out of the oven and FT-IR recorded. It is well-known that the application of a thermal treatment below the melting point of semicrystalline polymeric materials and, particularly, above the a-relaxation of the material, favors the mobility of chain segments at the crystals' interphase and within the crystals toward the development of a more stable and thicker crystalline morphology, phenomenon known as annealing. Therefore, this phenomenon leads to the elimination of defects through partial melting and

recrystallization of the most ill-defined (less metastable) crystals, generating a more regular stacking of the lamellae and higher crystallinity. As a result, in Figure 2 it is observed that, as the annealing temperature increases, the crystallinity of the sample also increases and this is represented by the rise of the 1140 cm-1 band of the FT-IR spectrum.

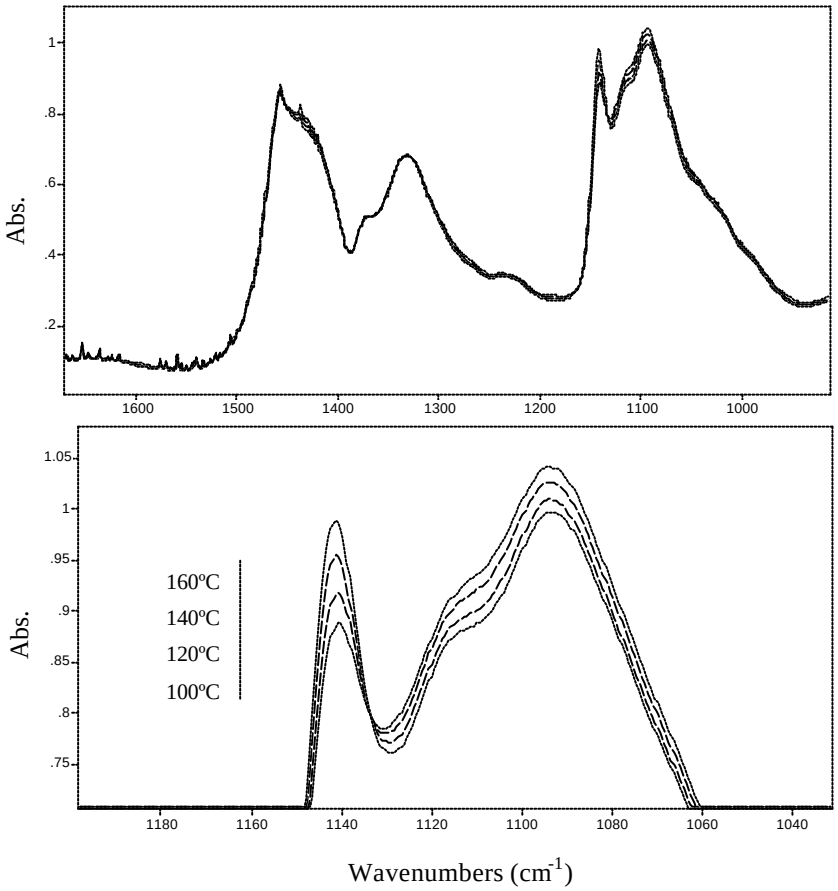


**Figure 2.** FT-IR spectra of an EVOH26 specimen annealed at various temperatures (top) and magnification of the range of the crystallinity band at 1140 $cm^{-1}$

Figure 3 shows, as an example, FT-IR spectra obtained for dry, retorted and retorted and dried PP/EVOH32/PP specimens. In agreement with the previous understanding of the retorting effects, it is now clearly seen that, as stated before, during the retorting process some moisture traverses the PP layers and sorbs onto the EVOH intermediate barrier layer, as it is clearly observed from the FT-IR spectrum of the retorted sample (see arrow in Figure 3). However, the water band is not so clearly seen in the dried samples, suggesting that drying is an effective process in reducing

sorption-induced polymer plasticization. Furthermore, from observation of this Figure 3, it can also be seen that upon retorting the crystallinity band at 1140 $cm^{-1}$ drops, effect which indicates that the crystallinity of the sample has undoubtedly decreased. On the other hand, the retorted and then dried sample does clearly show the highest absorbance for the crystallinity band, even higher than that of the unmodified sample, observation which points that the crystallinity is the highest for this specimen. Thus, pressurized water vapor, which penetrated the multilayer structure during retorting, is thought to melt and disrupt part of the EVOH crystalline morphology. The subsequent annealing process in the vacuum oven at 70ºC during 1 week, allowed the polymer chains to reorganize and anneal, giving rise to a significantly improved crystalline structure.

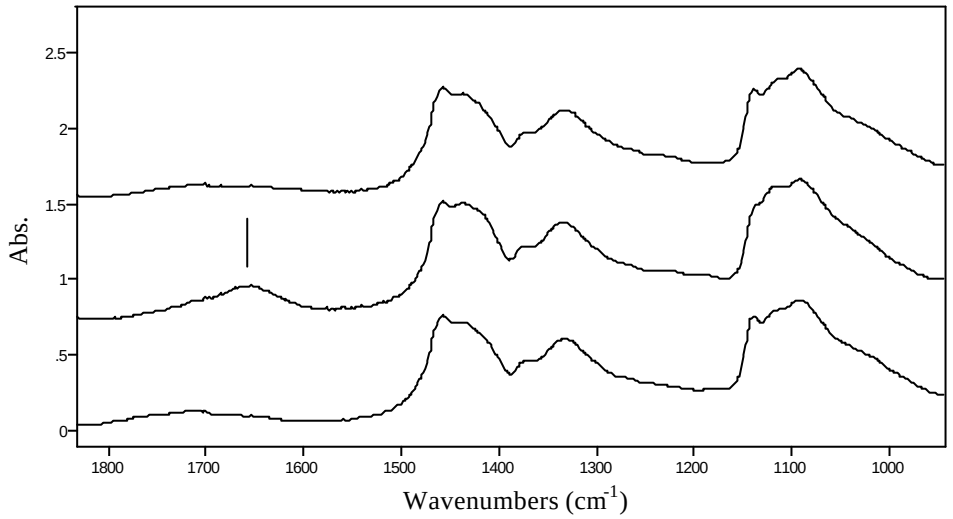


**Figure 3.** FT-IR spectra of, from top to bottom, untreated, retorted and retorted and then dried EVOH32 specimens, delaminated from PP/EVOH/PP structures

These observations appear to be supported by SEM microphotographs taken on the thickness of EVOH32 specimens. Figure 4 suggests that the polymer two-phase morphology can be revealed by this technique on 75 microns specimens without the need for etching. The spherical particles observed in some of the photomicrographs have previously been attributed to crystalline domains by Matsuyama et al[17]. In this Figure 4, the morphology of the untreated specimen is seen to be finer near to the surface [Figure 4(c)], likely due to faster cooling after coextrusion, and coarser (attributed to thicker crystals) at the core of the film. In Figure 4(b), this two-phase

morphology is seen to be more finely averaged and, thus, more homogeneous after retorting followed by drying at 70°C. Annealing at 120°C and at 160°C leads to a more homogeneous and, apparently, coarser granular morphology, suggesting higher crystallinity by crystal thickening.

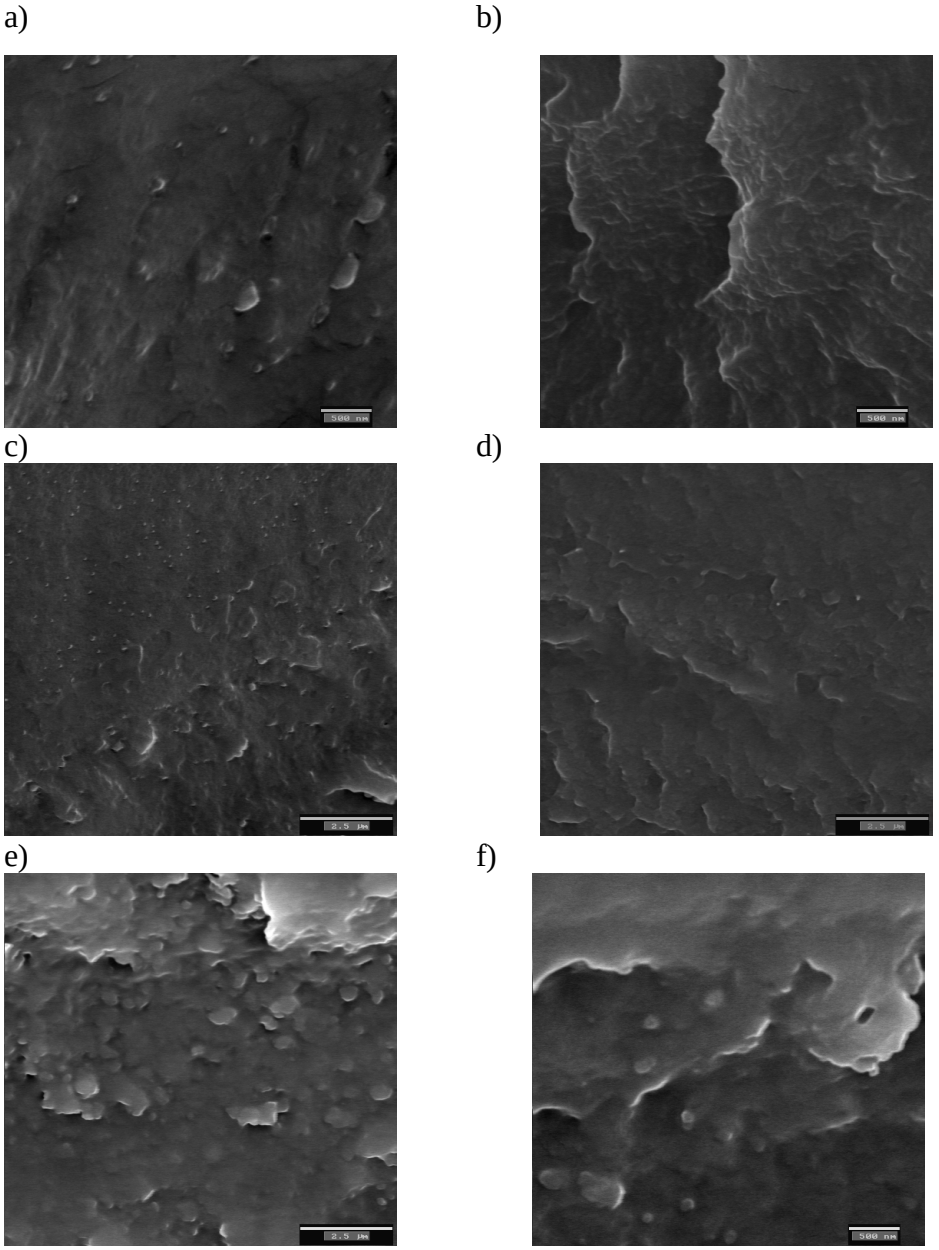


**Figure 4.** SEM micrographs of EVOH32 (75 microns) specimens of (a) untreated, (b) retorted and then dry, (c) untreated showing a skin/core morphology difference, (d) annealed at 120°C for 20 minutes, (e) and (f) annealed at 160°C for 20 minutes

Figure 5 unambiguously reveals that the 10-µm film is characterized by a much finer phase morphology than that of the 75-µm specimens seen in Figure 4. The micrographs in Figure 5, indicate that the two-phase morphology is more clearly resolved in retorted and then dried samples and in annealed specimens, and less defined (with a less regular crystalline morphology) in the untreated specimen. Figure 5(b) does clearly show the presence of extensive voiding in the retorted sample, supposedly, created by the ingress of water vapor during retorting, which appears to distort the polymer morphology and disrupts the crystallinity.

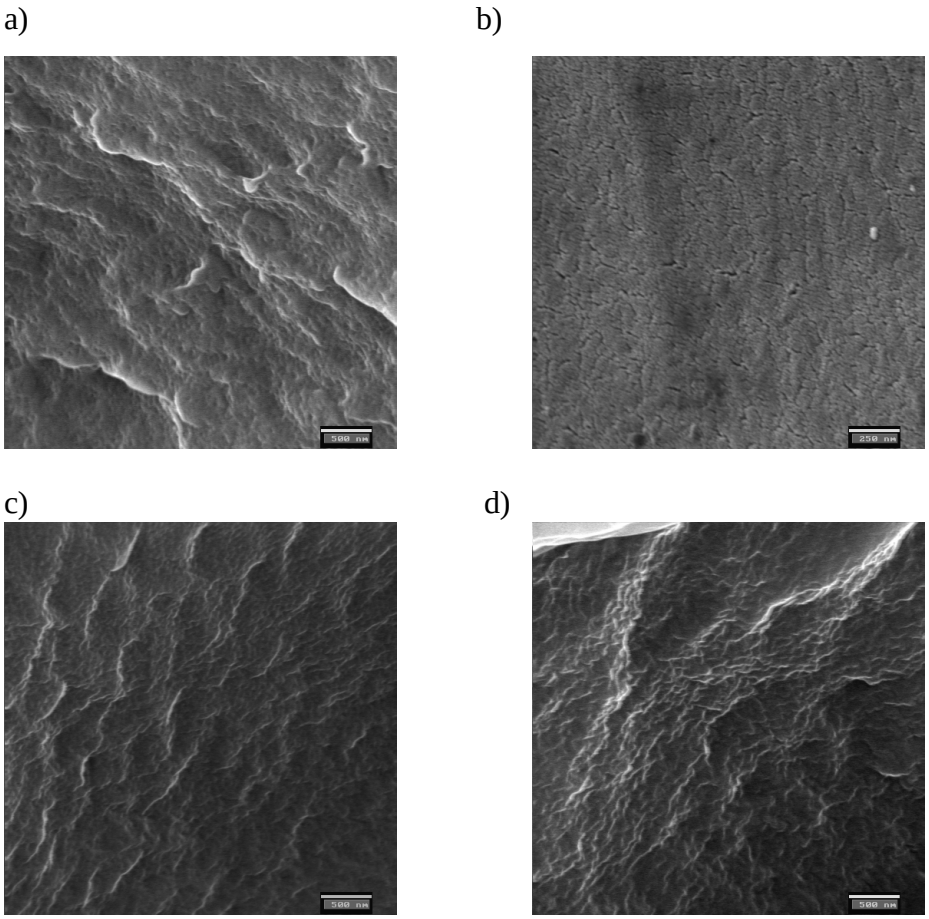


**Figure 5.** SEM micrographs of EVOH32 (10µm) specimens: (a) untreated, (b) retorted (c) retorted and then dried and (d) annealed at 160$^{o}$C for 20 minutes

The above observations can, thus, help explain the lower $O_2$TR values measured for the retorted and then dried samples in Table 2 ,compared to the untreated specimens, on the bases of both an increase in crystallinity and the more homogeneous and robust phase morphology attained: this phenomenon explained by the fact that

crystals are, in general, impermeable to the transport of most low molecular weight permeants and, consequently, an increase in crystallinity does usually result in an increase in barrier properties. Nevertheless, other particular morphological effects and features, including crystal shape, size, and orientation distribution[16], can also have a significant impact in barrier properties and may thus play a role in explaining some of the small permeability variations observed between annealed and retorted and then dry specimens. Thus, crystallinity and permeability do not necessarily follow a linear relationship[21]. For a given crystallinity, phase morphology, through mainly tortuosity and chain immobilization factors, can have unexpected outcomes for the barrier results.

FT-IR and morphological results can also help explain why a total recovery in barrier properties after retorting can not be achieved (see Fig. 1) for the most hydrophilic samples. This is explained by the morphological deterioration sustained by the material during the humid thermal treatment. However, and as opposed to this behavior, the barrier properties of the higher ethylene content copolymers (i.e. EVOH38, EVOH44 and EVOH48) seemed to improve after recovery from retorting. This change in trend is possibly related to the smaller morphological deterioration suffered by these latter materials during retorting (see later in text). However, it is difficult to understand on the sole account of this effect an improvement in barrier properties, unless a more favorable morphology regarding permeability is achieved after retorting. Nevertheless, it should be kept in mind that higher ethylene content copolymers have much lower oxygen barrier and, therefore, other circumstantial effects can have a stronger impact on the barrier performance of the materials. For example, one explanation for the cited observation could lay on results from a previous work, which reported a maximum in barrier properties for these copolymers at about 30%RH[18]. Thus, it was reported that moisture, present at this low sorption level, is thought to block the free volume of the polymer via hydrogen bonding, in a regime that extends between the dry state and the extensive polymer plasticization taking place at medium and high RH. Consequently, the observed improvement in barrier properties for these samples, arising after recovery from retorting, could be attributed to the sample falling in the optimum barrier regime. Although this optimum barrier regime does also exist for the low ethylene content copolymers, these samples may either not fall on it and/or the more extensive crystallinity

deterioration seen for these materials may override the cited positive effect. Another potential factor to be considered is the potential modification of the structural polypropylene layers during retorting. DSC experiments showed higher crystallinity (reflected in a higher melting enthalpy) after retorting for the polypropylene (see Table 3). Consequently, an increase in crystallinity for the thicker structural layers after retorting may also contribute to produce lower permeability for the retorted sample after recovery. Nevertheless, Table 3 also shows that the permeability improvement undergone by the polypropylene structural layers is only of about 1% and thus it cannot account for the more significant reductions observed in the multilayer structure.

**Table 3.** DSC results and oxygen transmission rate for treated polypropylene specimens

| | Tm (ºC) | ?H (J/g) | Peak width (ºC) | OTR (cc/m$^2$day) |
|---|---|---|---|---|
| PP non treated | 164.3 | 82.3 | 14.9 | 23.375 |
| PP oven | 164.1 | 94.4 | 16.4 | - |
| PP retorted | 163.7 | 91.1 | 17.2 | 23.125 |

Another curious observation in Table 2 for these higher ethylene content samples is the higher permeability of annealed specimens versus those untreated or retorted and then dried. For these annealed samples the crystallinity was found to be higher by FT-IR compared to untreated and retorted and then dried samples (results not shown). The structure and thermal characteristics of annealed polypropylene were also analyzed and the enthalpy of fusion of this specimen was found to be higher than for untreated and retorted polypropylene (see Table 3). The polypropylene layers were also analyzed using FT-IR. The absorbance peak at 841 cm$^{-1}$ was identified in the literature[19] as a crystalline peak and the peak at 973 cm$^{-1}$ was used as internal standard because it has proved to be insensitive to chain conformation, that is, to the amorphous/crystalline ratio[19,20]. Figure 6 confirms the previous DSC results and suggests that the higher crystallinity is for the annealed sample, followed closely by the retorted specimen and by the untreated specimen. The crystallinity content thus does not explain the unexpected barrier behavior for annealed EVOH38, EVOH44 and EVOH48. For these samples either a relative humidity or a morphology differential argument must be considered as explained above.

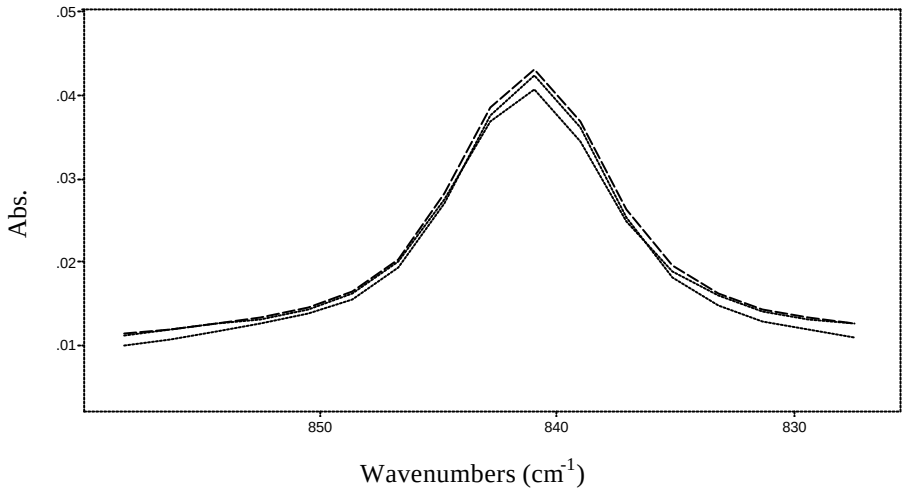


**Figure 6.** Normalized crystallinity band at 841 $cm^{-1}$ of, from higher to lower intensity: heated in the oven at 120ºC during 20 minutes, retorted and untreated polypropylene

From the above results and from an applied problem solving perspective, it clearly appears that a drying step after sterilization of the package can restore or even improve the barrier performance of the materials by removing sorbed moisture and by rebuilding a more favorable morphology. Whether this additional step is viable to an industrial scale is beyond the scope of the present study. Nevertheless, being aware of the implications of crystallinity and its morphology on barrier properties and of the ability of water sorption to modify the polymer morphology, it was thought of interest to study the influence of the initial thermal history on the materials performance upon retorting. To do so, specimens of all samples were given an annealing treatment prior to the retorting process and were then analyzed in their resistance against morphology alterations upon retorting.

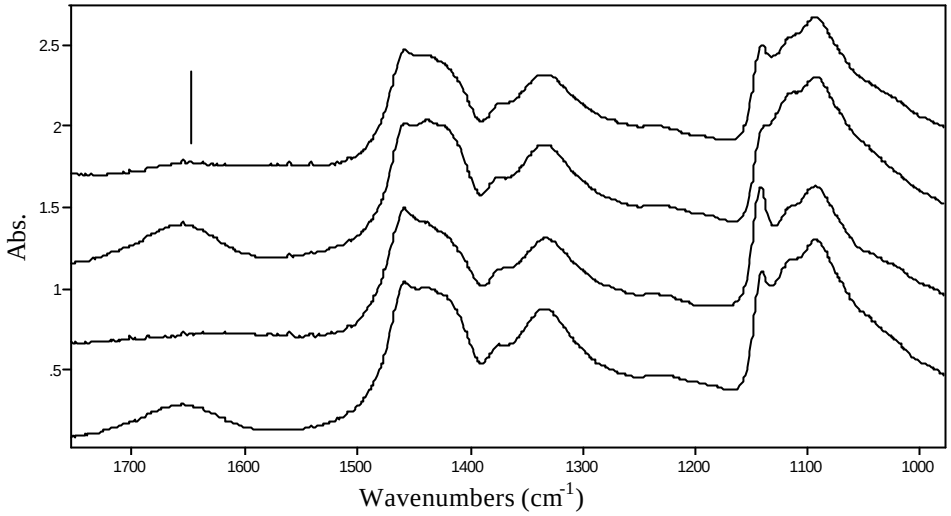


**Figure 7.** FT-IR spectra of, from top to bottom, untreated, retorted, annealed at 160ºC during 20 min and annealed and then retorted EVOH26 specimens

To validate the adequacy of this methodology, the different multilayer structures were first annealed for 20 minutes in an oven at a selected optimum temperature, which had previously been determined through FT-IR (160ºC for the EVOH26, EVOH29, EVOH32 and EVOH38, and 140ºC for EVOH44 and EVOH48); then, the specimens were retorted in the autoclave, delaminated and the EVOH layer FT-IR recorded. The optimum temperature was set at a temperature beyond which crystallinity was seen to decrease through annealing due to extensive melting and fast recrystallization. The rationale behind this annealing experiment was to provide the most adequate polymer morphology in terms of crystallinity content and robustness, i.e. higher crystalline density, before retorting. Variations in crystallinity were estimated through the ratio of the absorbance of the crystallinity band at 1140 cm-1 to that of the band at 1333 cm-1. The values of this ratio for the various copolymer grades and thermal histories are displayed in Table 4.

**Table 4.** FT-IR absorbance of the 1440 $cm^{-1}$ peak divided by the absorbance of the 1333 $cm^{-1}$ reference peak

| | Not treated | Annealed | Retorted | Annealed and retorted | Retorted and dry |
|---|---|---|---|---|---|
| EVOH26 | 1.26 | 1.45 | 1.13 | 1.25 | 1.28 |
| EVOH29 | 1.25 | 1.43 | 1.12 | 1.20 | 1.28 |
| EVOH32 | 1.24 | 1.40 | 1.14 | 1.16 | 1.26 |
| EVOH38 | 1.21 | 1.38 | 1.19 | 1.19 | 1.25 |
| EVOH44 | 1.21 | 1.34 | 1.19 | 1.19 | 1.24 |

From the results, it can be seen that pre-annealed EVOH26, EVOH29 and EVOH32 specimens can reach a higher level of crystallinity after retorting than just retorted specimens. In fact, preannealed sample EVOH26 (see Fig. 7) even shows a degree of crystallinity after retorting similar to that of the untreated specimen (dried in a vacuum at 70$^{o}$C for 1 week). For EVOH 38, EVOH44 and EVOH48 (see Fig. 8 for EVOH38), prior annealing of the specimens did not lead to improved morphology compared to that of untreated specimens.

Figure 7 also shows that after sterilization of annealed EVOH26, there is less water sorbed in the structure of the polymer than in the untreated specimen after retorting. This is reflected by the lower intensity of the 1658 $cm^{-1}$ in-plane OH bending band of water.

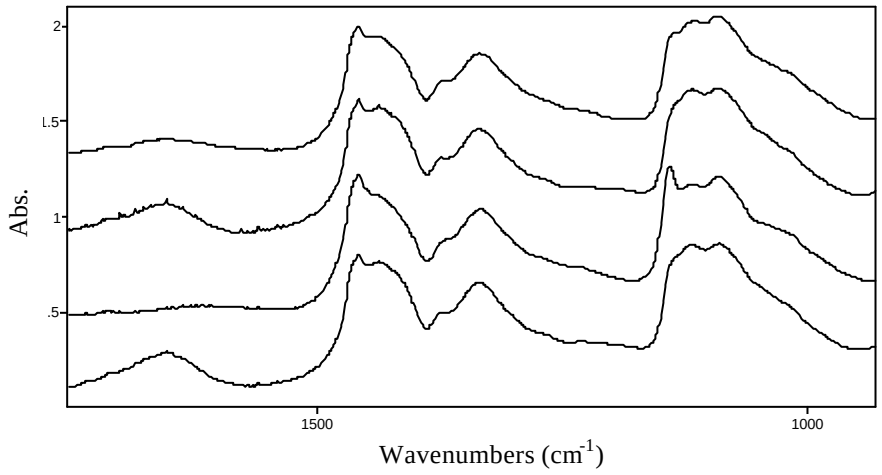


**Figure 8.** FT-IR spectra of, from top to bottom, untreated, retorted, annealed at 160ºC during 20 min and annealed and then retorted EVOH38 specimens

**ACKNOWLEDGEMENTS**

The authors would like to thank Mr. Y. Saito of Central Research Laboratory of Nippon Gohsei for fruitful discussions and financial support.

REFERENCES

[1] Zhang, Z.; Britt, I.J.; Tung, M.A. *Journal of Polymer Science Part B: Polymer Physics* 1999, 37, 691.

[2] Lagarón, J. M.; Powell, A. K.; Bonner, G. *Polymer Testing* 2001, 20, 569.

[3] Aucejo, S.; Marco, C.; Gavara, R. *Journal of Applied Polymer Science* 1999, 74, 1201.

[4] Zhang, Z.; Britt, I.J.; Tung, M.A. *Journal of Applied Polymer Science* 2001, 82, 1866.

[5] Zhang, Z.; Britt, I.J.; Tung, M.A. *Plastic Film and Sheeting* 1998, 14, 287.

[6] Tsai, B.C.; Wachtel, J.A. In *Barrier Polymers and Structures.* American Chemical Society: Washington D.C., 1990, p. 192.

[7] Alger, M.M; Stanley, T.J.; Day, J. *Barrier Polymers and Structures*. American Chemical Society: Washington D.C., 1990, p. 203.

[8] Lagarón, J. M.; Giménez, E.; Saura, J. J.; Gavara, R. *Polymer* 2001, *42*, 7381.

[9] Lagarón, J.M.; Giménez, E.; Altava B.; Del-Valle, V.; Gavara, R. *Macromolecular Symposia* 2003, *198*, 473.

[10] Lee S.Y.; Kim S.C. *Journal of Applied Polymer Science* 1998, 67, 2001.

[11] Yeo J.H.; Lee C.H.; Park C.-S.; Lee K.-J.; Nam J.-D.; Kim S.W. *Advances in Polymer Technology* 2001, *20*, 191.

[12] Del Nobile, M.A.; Laurienzo, P.; Malinconico M.; Mensitieri G.; Nicolais L. *Packaging Technology and Science* 1997, 31-30, 95.

[13] Farrell, C.J.; Tsai, B.C.; Wachtel, J.A. 1983. Patent nº 4,407,897.

[14] Artzi, N.; Nir, Y.; Narkis, M.; Siegmann, A. *Journal of Polymer Science Part B: Polymer Physics* 2002, *40*, 1741.

[15] López-Rubio, A.; Lagarón, J.M.; Giménez, E.; Cava, D.; Hernandez-Muñoz, P.; Yamamoto, T.; Gavara, R. *Macromolecules* 2003, *36*, 9467.

[16] Lagarón, J.M.; Catalá, R.; Gavara, R. *Materials Science and Technology* 2004, *20*, 1.

[17] Matsuyama, H.; Iwatani, T.; Kitamura, Y.; Tearamoto, M.; Sugoh, N. *Journal of Applied Polymer Science* 2001, *79*, 2449.

[18] Aucejo, S.; Catalá, R.; Gavara, R. *Food Science and Technology International* 2000, *6*, 159.

[19] Tadokoro, H.; Kobayashi, M.; Ukita, M.; Yasufuku, K.; Murahashi, S.; Torii, T. *The Journal of Chemical Physics* 1965, *4*, 1432.

[20] Lamberti, G.; Brucato, V. *Journal of Polymer Science Part B: Polymer Physics* 2003, *41*, 998.

[21] Hedenquist, M.; Angelstok, A.; Edsberg, P.; Larsson, T; Gedde, U.W. *Polymer* 1996, *37*, 2887.

# CHARACTERIZATION OF THE EFFECT OF RETORTING ON BLENDS OF EVOH WITH AMORPHOUS POLYAMIDE AND NYLON-CONTAINING IONOMER

## INTRODUCCIÓN AL ARTÍCULO III

Este artículo se encuentra en preparación y, por tanto, únicamente se mostrarán los resultados obtenidos hasta el momento.

Con este artículo se completa el segundo objetivo planteado, en el que la estrategia para la disminución de los efectos dañinos del tratamiento en autoclave se concreta en el uso de mezclas de EVOH con ionómero y poliamida amorfa.

Los materiales objeto de este estudio fueron las mezclas binarias y la ternaria descritas en el apartado de "materiales y métodos" y los cambios producidos en los mismos tras la esterilización se estudiaron mediante DSC, FT-IR, experimentos de difracción de rayos X (en el sincrotrón) y medidas de permeabilidad al oxígeno.

## SHORT INTRODUCTION

Binary and ternary blends of amorphous PA and ionomer with EVOH have proven to have beneficial effects such as improved processability during thermoforming. More in particular, the ternary blends were found to be the most adequate materials for this application. Even when these blends were found to be immiscible, a good phase dispersion and adhesion at the interphase were generally found in earlier work[1]. The interest of testing these blends for its suitability in retortable food packaging applications lays on the fact that these blending components were found to be more moisture resistant than EVOH. Moreover and from a barrier perspective, the materials have a positive deviation from the Maxwell equation in oxygen permeability, therefore, leading to better barrier properties than expected due to the rather ellipsoidal morphology of the blending components.

## RESULTS AND DISCUSSION

When EVOH copolymers are submitted to a retorting experiment in an autoclave without the hydrophobic protection of, for instance, some polyolefinic layers, the damaging effect of this treatment becomes noticeable to the naked eye. The specimens, just after retorting, loose dimensional stability, whiten to a large extent and become rubbery from a mechanical view-point (see Photo 1).

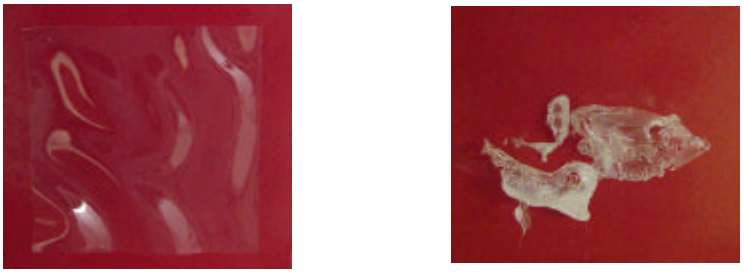

**Photo 1.** EVOH32 before (left) and after (right) retorting in autoclave

Thus, previous to a more exhaustive characterization of the materials, a visual inspection was also carried out on the blend materials to check whether the dimensional integrity and appearance were maintained after the treatment.

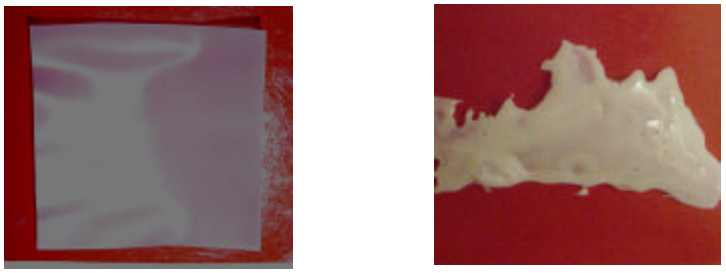

**Photo 2.** EVOH32/aPA blend before (left) and after (right) retorting in autoclave

The blends with amorphous polyamide are not transparent but opaque, which can limit the application of these materials in certain food packaging applications.
From Photo 2, it appears that, although the loss of integrity is less pronounced than that of EVOH alone, the blend sample also shows extensive plasticization, which could be expected because of the hydrophilic character of both materials.

**Photo 3.** EVOH32/ionomer blend before (left) and after (right) retorting in autoclave

The integrity of the EVOH32/ionomer is largely maintained (see Photo 3), although voids and bubbles are present in the retorted specimen. The ionomer semicrystalline fraction of the blend has low higroscopicity and it is characterized by the presence of ionic groups randomly dispersed in the polymeric matrix. However, as the temperature increases, the attractions between ionic groups disappear and the polymeric chains are allowed to freely move. Moreover, the melting point of this

fraction was found to be of around 95ºC[1], which means that during the autoclaving of the blend, the ionomer fraction completely melts. After retorting and during the cooling of the sample, the ionomer fraction will probably crystallize due to fast cooling after retorting and the whole process may promote some voids.

Finally, Photo 4 shows the performance of a ternary blend. This sample gives similar results as the binary blend with ionomer. However, the presence of aPA in the blend, apart from the whitish colour, makes the specimen more water sensitive and the sample is somewhat more damaged after the retorting treatment.

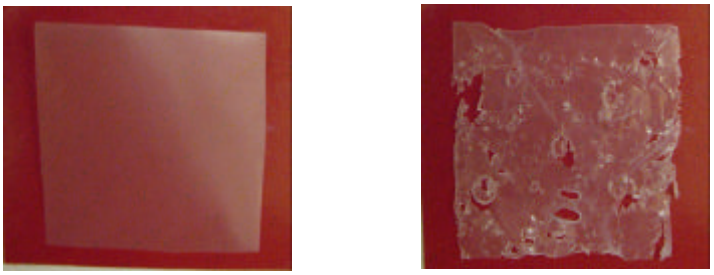

**Photo 4.** EVOH32/aPA/ionomer blend before (left) and after (right) retorting in autoclave

**Thermal characterization**

Previous characterization work in these blends by DSC, WAXS, DMA, SEM, microhardness and tensile testing indicated that the miscibility of this high barrier EVOH32 (with melting point, $T_m$ = 183ºC) with the amorphous polyamide is very poor, an clear phase segregation throughout composition was shown by DSC, DMA and SEM[2]. A two phase structure was also observed in the EVOH/ionomer blends, but from the results a better phase compatibility was inferred. This compatibility was thought to be enhanced by the presence of crystalline Nylon in the formulation of the ionomer. This lack of compatibility of EVOH with other materials is probably due to the fact that EVOH copolymers are strongly self-associated, while the inter-association of the hydroxyl groups of EVOH with, for instance, the carbonyl groups of complementary polymers is comparatively weak[3]. As previously observed in other studies[4,5] as a consequence of retorting, this strong interaction is greatly reduced by

water molecules intercepting inter- and intramolecular hydrogen bonding. It is, therefore, of great interest to ascertain what structural changes underlay the morphological observations pictured above.

In Table 1 the DSC parameters of the three blends before and after autoclaving are displayed. All the specimens were dried in a vacuum oven before the DSC measurements in order to eliminate sorbed water and, thus, be able to compare the enthalpies of the materials. The first heating run (from 50ºC to 250ºC) of the DSC experiments shows that, in agreement with previous results[1], the melting point of the blends was found to be lower than that of the pure EVOH32. But, in contrast to the effects of retorting observed for neat EVOH, the EVOH blends displayed similar and even higher melting point than the untreated specimens. For every blend it seems that retorting induces the formation of crystals, reflected in higher enthalpies after autoclaving and, moreover, in both blends containing ionomer, a more homogeneous crystalline structure is observed, as the broadness of the melting peaks is greatly reduced after autoclaving. The peak width of the EVOH/aPA blend, however, remains the same after the treatment. These results for the blends contrast with those previously obtained for the neat copolymer, which suffered from a decrease in the melting enthalpy after retorting and an increase in the peak broadness.

Table 1. DSC parameters of the different samples before and after retorting. Neat EVOH data is included for comparison purposes

| | | 1st heating run | | | Cooling run | | | 2nd heating run | | |
|---|---|---|---|---|---|---|---|---|---|---|
| | | $T_m$ (ºC) | $?H_m$ (J/g) | Peak width (ºC) | $T_c$ (ºC) | $?h_c$ (J/g) | Peak width (ºC) | $T_m$ (ºC) | $?H_m$ (J/g) | Peak width (ºC) |
| **EVOH** | **untreated** | 187.0 | 83.5 | 13.6 | 158.9 | -78.0 | 10.1 | 183.9 | 82.5 | 12.8 |
| | **retorted** | 183.3 | 82.2 | 22.0 | 158.5 | -71.0 | 11.6 | 183.8 | 80.1 | 15.2 |
| **EVOH/aPA/Ionomer 80/10/10** | **untreated** | 179.9 | 75.9 | 16.3 | 156.6 | -64.7 | 4.5 | 181.9 | 65.5 | 6.8 |
| | **retorted** | 180.2 | 90.8 | 13.6 | 157.0 | -61.8 | 4.5 | 182.4 | 68.9 | 6.8 |
| **EVOH/aPA 80/20** | **untreated** | 181.9 | 61.5 | 9.3 | 156.5 | -65.3 | 3.9 | 182.3 | 69.7 | 6.4 |
| | **retorted** | 182.4 | 75.9 | 9.3 | 156.6 | -76.8 | 3.9 | 182.4 | 82.5 | 6.4 |
| **EVOH/Ionomer 80/20** | **untreated** | 179.9 | 79.5 | 16.3 | 156.3 | -58.7 | 4.0 | 182.0 | 72.5 | 6.3 |
| | **retorted** | 181.2 | 87.9 | 12.8 | 157.2 | -56.7 | 5.3 | 182.0 | 73.9 | 6.4 |

After the cooling run in which the samples were crystallized at 10ºC/min, the second heating run confirms that, in terms of thermal properties, every blend appears to

behave better after retorting than pure EVOH, because the thermal parameters of the retorted samples are similar or even improved with respect to the untreated specimens. Although it appears that the retorted samples are somehow more crystalline, no signs of enhanced compatibility, however, are observed from the DSC thermograms

**Structural characterization**

In figures 1-3 the WAXS diffraction patterns of the dry and retorted blends are displayed. The presence of ionomer both in the binary and in the ternary blends seems to have a beneficial effect on the retorted samples from a crystalline morphology point of view. The diffraction peak is somewhat narrower after the retorting treatment indicating that, instead of a harmful effect over the structure, these conditions of combined temperature and humidity lead to a more robust crystalline order.

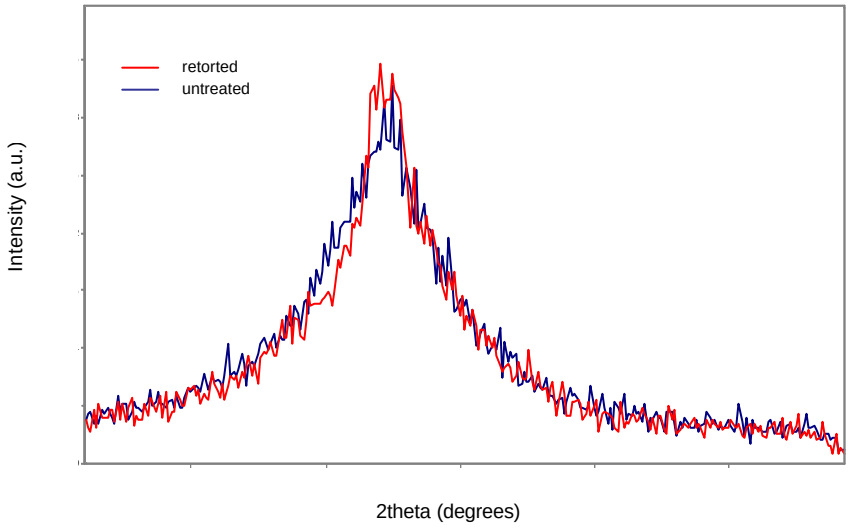


**Figure 1.** WAXS diffraction patterns of the binary blend EVOH/Ionomer 80/20

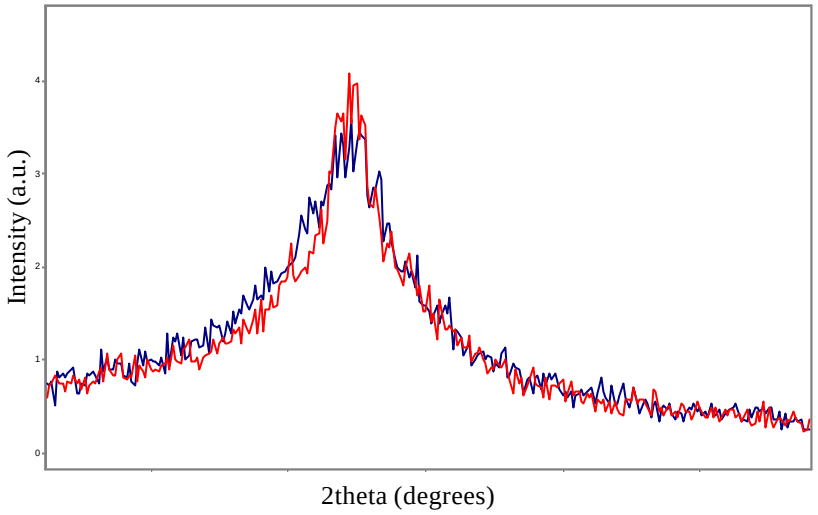


**Figure 2.** WAXS diffraction patterns of the ternary blend EVOH/aPA/Ionomer 80/10/10

On the other hand, the binary EVOH/aPA specimen diffracts in a different manner after autoclaving. First of all, water sorption has been observed to be much more pronounced in EVOH and aPA than in the ionomer[1] and, therefore, it is expected to observe a more plasticized structure in this blend after retorting. The diffraction peak after retorting becomes broader which would seem to indicate in agreement with the effects observed for pure EVOH, some crystal deterioration and fractionation.

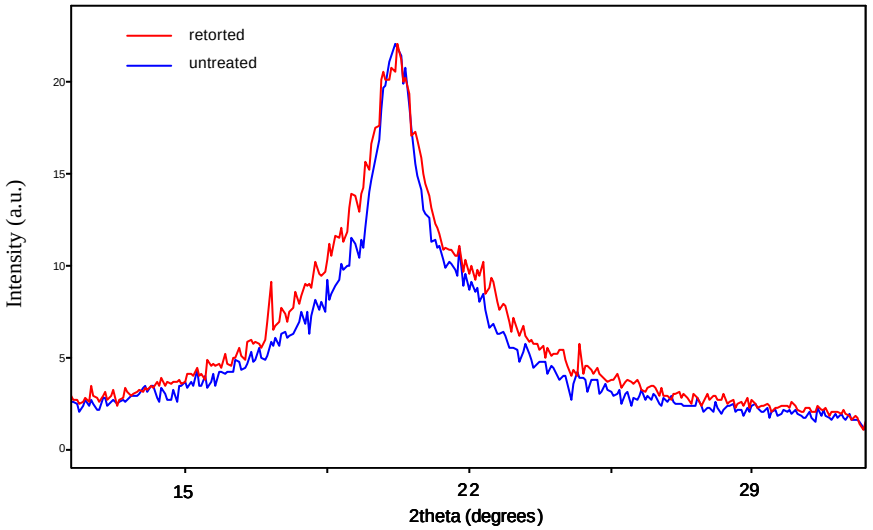


**Figure 3.** WAXS diffraction patterns of the binary blend EVOH/aPA 80/20

But, on the other hand, as it can be observed in Table 1, the enthalpy of fusion of the EVOH/aPA blend is increased after retorting, so a possible explanation is that new, but rather imperfect crystals should have been formed as a consequence of autoclaving.

In a previous study[6] it was observed that crystalline order was induced in amorphous polyamide as a consequence of retorting and, therefore, it is feasible that it also crystallizes when blended with EVOH. It was also reported that the crystals formed were rather imperfect and heterogeneous in size, which could be attributable to the increase in WAXS diffraction peak broadness. But if the fraction of amorphous polyamide crystallizes, it should be observed as new endothermic peaks in the first DSC run. However, as the aPA fraction is relatively low (20%), it is possible that the crystals formed are not discernible by this technique. Other possibility would be that retorting enhances the compatibility between the EVOH and aPA fractions and that segments of both polymers are able to co-crystallize, but this hypothesis needs to be confirmed through, for example, scanning electron microscopy (SEM).

Further analysis of the morphological changes of the EVOH blends was carried out by ATR-FTIR spectroscopy given the fact that the excessive thickness of the samples overabsorbed. Facing again the EVOH/aPA blend morphological transformations, in Figure 4b the spectra of the specimen dry, retorted and retorted and dry is showed. For comparison purposes, in Figure 4a the spectra of the pure fractions dry and retorted are also displayed.

For EVOH32 the most significant changes after autoclaving are, first of all, the presence of sorbed water reflected by the increase in the 1658 $cm^{-1}$ in-plane OH bending water band, and the decrease in the "crystallinity band" of EVOH at 1140 $cm^{-1}$ (see arrows in Figure 4a). In the case of amorphous polyamide, it was observed that during retorting some sort of molecular rearrangements or new interactions took place, which were ascribed to changes in several absorption bands[6] (changes in shape, position and/or relative intensity). For example, the amide I and II bands at 1630 and 1535 $cm^{-1}$ respectively, are displaced towards lower wavenumbers in the retorted specimen indicating that stronger intermolecular interactions do take place for these groups

a)

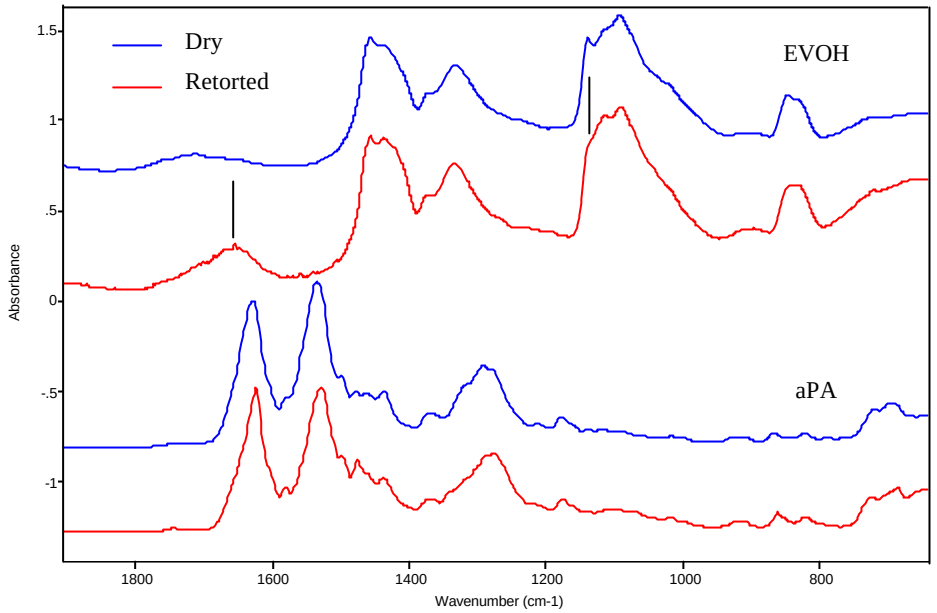


b)

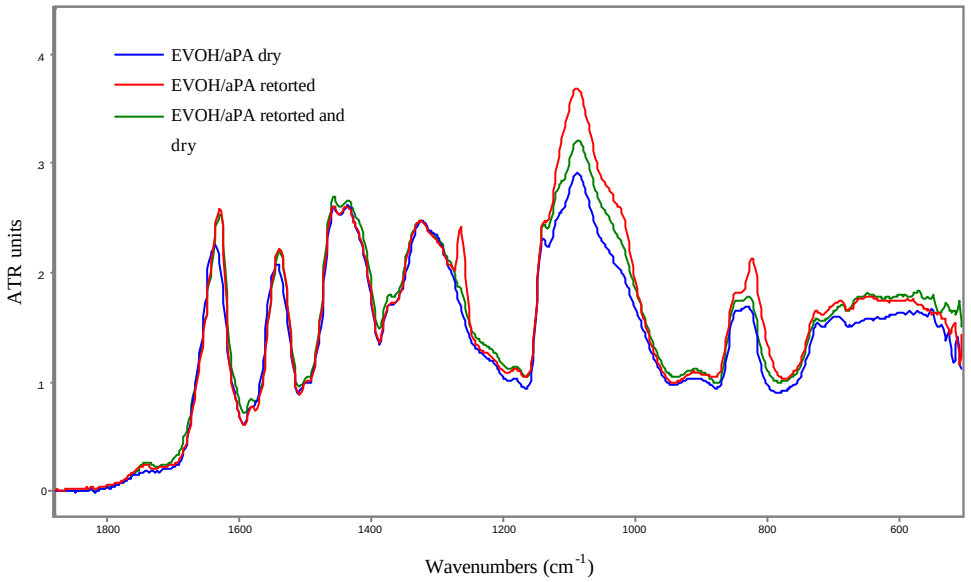


**Figure 4.** ATR-FTIR spectra of (a) EVOH32 dry and retorted (upper spectra) and aPA dry and retorted (lower spectra) and (b) dry, retorted and retorted and dry binary blend EVOH/aPA 80/20

In Figure 4b, it is clearly observed that, in the autoclaved specimens, the amide I and II bands are also displaced, so it is possible that the combined temperature and

pressurized water vapor treatment induces molecular order in the aPA fraction of the polymeric blend. Furthermore, in the just retorted sample, new bands arise at ca. 1263 and 822 $cm^{-1}$. These bands were neither present in the dry pure fractions nor in the retorted ones. From DSC results, no signs of co-crystallization are observed and, therefore, they may have changed as a consequence of the molecular "environment" and electronic perturbations[7], indicating that molecular changes as a result of new interactions have probably occurred. Water is seen to have an important role in the observed changes, as after drying the sample these new bands disappear.

The increase in intensity of the bands adjacent to the "crystallinity" band of EVOH in the autoclaved blends makes difficult a comparison for the latter band. After drying the autoclaved blend sample, the spectrum of this specimen, in general, resembles more that of the dry blend. However, even after drying, the amide I and II bands at 1630 and 1535 $cm^{-1}$ respectively, remain displaced towards lower angle, just as it was previously observed for the retorted aPA suggesting strong intermolecular interactions between components.

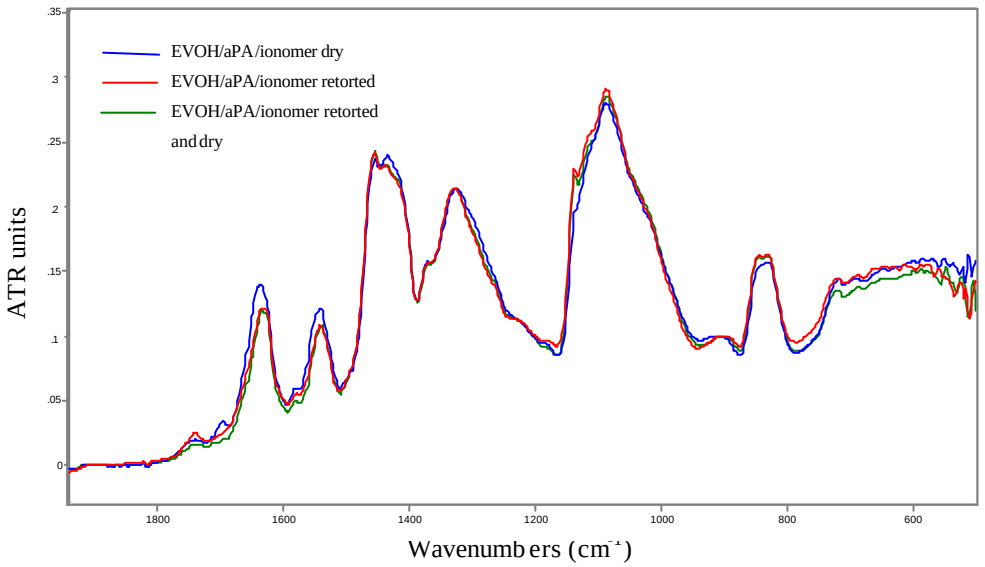


**Figure 5.** ATR-FTIR spectra of the ternary blend EVOH/aPA/Ionomer 80/10/10

In Figure 5 the FT-IR spectra of the dry, retorted and retorted and dry ternary blend are displayed. From the spectrum of the dry specimen it is deduced that the presence of both aPA and polyamide-containing ionomer fractions difficult the crystallization

of the EVOH fraction (see band at 1140 $cm^{-1}$). After retorting, however, this band is seen to increase, suggesting that, again, this treatment favours the mobility of the polymeric chain fractions, weakening the EVOH strong self-association and allowing the reorganization of the chains. Apart from the increase in the crystallinity of the EVOH fraction, it seems that aPA is also able to crystallize in the ternary blend as a consequence of autoclaving. As previously commented, upon retorting the bands corresponding to the amide I and II modes shift towards lower wavenumbers and the peaks are observed to narrow to some extend.

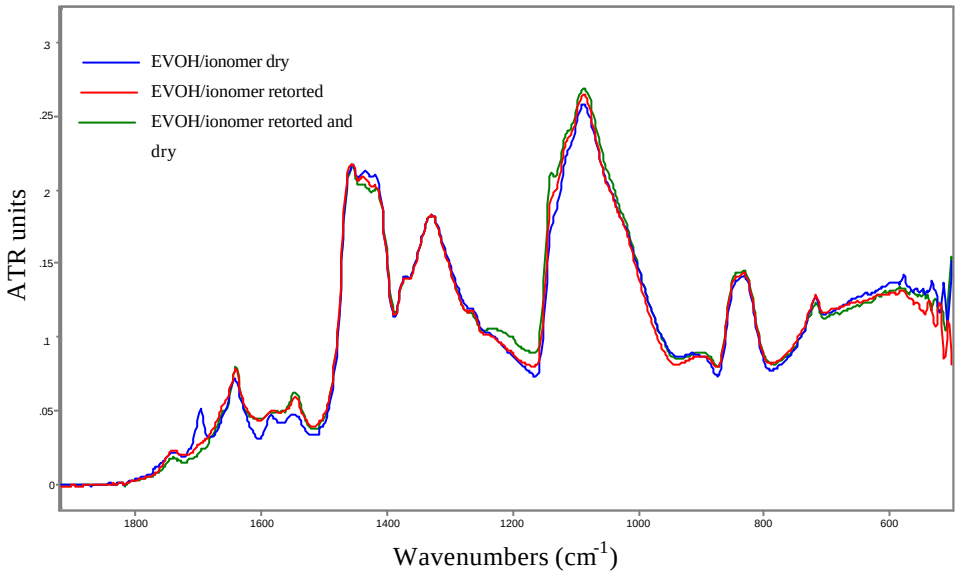


**Figure 6**. ATR-FTIR spectra of the binary blend EVOH/Ionomer 80/20

Substantial changes are also observed between the dry and retorted binary blend EVOH/ionomer. As previously occurred with the ternary blend, autoclaving leads to the development of crystallinity in the EVOH fraction, and the subsequent drying process further increases the intensity of the 1140 $cm^{-1}$ band. The 1500-1800 $cm^{-1}$ range of the spectra is also greatly affected by retorting. The band at 1700 $cm^{-1}$ completely and irreversibly disappears while there is a general increase in intensity of this range.

**Permeability measurements**

Figure 7 shows the oxygen permeability measured at 0% RH and 45ºC of binary and ternary blends before and after the retorting treatment.

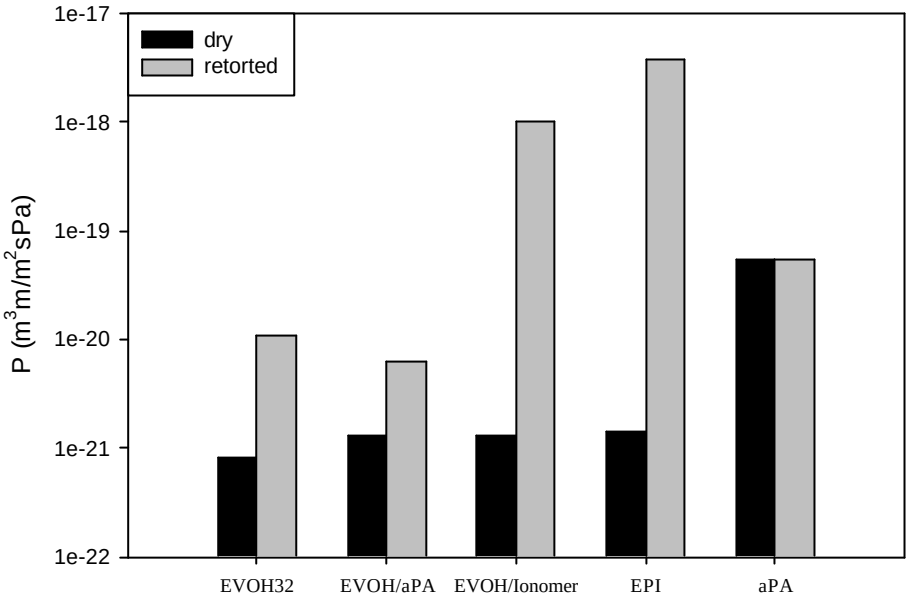


**Figure 7.** Oxygen permeability of pure components and blends measured at 0% RH and 45ºC before and after retorting

From the results, it is observed that dry EVOH displays the lower oxygen permeability, although it is also very low for the dry blends. After retorting every polymeric sample undergoes an increase in permeability except the amorphous polyamide. It was reported in a previous chapter that during retorting this material is able to crystallize and this crystallization, together with the special interaction of this polymer with water, leads to an improvement in barrier properties. It is known that, in this material, moisture sorption does not disrupt the originally existing hydrogen bonding structure, but rather links to free amide moieties being the majority of the sorbed water in the form of clusters[8]. These clusters are able to fill the available free volume, conducting hence to a decrease in the permeability on the basis of a competing mechanism. Interestingly, the EVOH/aPA blend shows the lowest permeability after retorting probably due to crystallization of aPA and enhanced blend interaction as observed by FTIR. On the other hand, the oxygen permeability

of the blends with ionomer greatly increased upon retorting, probably due to the melting and recrystallization of the ionomer which may weaken and generate heterogeneities in the blend structure. As a result, only EVOH/aPA blends appear to generate enough synergies at a molecular level to enhance the barrier properties of EVOH after retorting.

## REFERENCES

[1] E. Giménez. *Desarrollo y caracterización de sistemas de alta barrera basados en un copolímero de etileno y alcohol vinílico (EVOH) para su aplicación en estructuras multicapa termoconformadas en la industria del envasado.* Doctoral Thesis, Universitat Jaume I, 69 (2001)

[2] J.M. Lagaron, E. Giménez, J.J. Saura, R. Gavara. *Polymer 42*, 7381 (2001)

[3]J.M. Lagaron, E. Giménez, B. Altava, V. Del-Valle, R. Gavara. *Macromolecular Symposia 198*, 473 (2003)

[4] B.C. Tsai, J.A. Wachtel. In: *Barrier Polymers and Structures.* W.J. Koros, ed. American Chemical Society: Washington DC, 192 (1990)

[5] A. López-Rubio, J.M. Lagarón, E. Giménez, D. Cava, P. Hernández-Muñoz, T. Yamamoto, R. Gavara. *Macromolecules 36*, 9467 (2003)

[6]A. López-Rubio, R. Gavara, J.M. Lagaron. Aceptado para publicación en el *Journal of Applied Polymer Science*

[7]D. Steele. *Theory of vibrational spectroscopy*. W.B. Saunders, ed. London, 134 (1971)

[8] J.M. Lagarón, E. Giménez, R. Catalá, R. Gavara. *Macromolecular Chemistry and Physics 204*(4), 704 (2003)

# GAS BARRIER CHANGES AND STRUCTURAL ALTERATIONS INDUCED BY RETORTING IN A HIGH BARRIER ALIPHATIC POLYKETONE TERPOLYMER

## INTRODUCCIÓN AL ARTÍCULO IV

En este artículo, que ha sido aceptado para publicación en el *Journal of Applied Polymer Science*, se describen los efectos de la esterilización en autoclave sobre unos de los polímeros alta barrera seleccionados como potenciales alternativas a los copolímeros de etileno y alcohol vinílico (EVOH) para aplicaciones en envases esterilizables. Este artículo, por tanto, se enmarca dentro del tercer objetivo planteado y, como veremos a continuación, demuestra que las policetonas alifáticas muestran mucha mejor resistencia a los procesos de esterilización industrial aplicados a alimentos, utilizados incluso como monocapa, es decir, sin ser atrapados entre polímeros hidrofóbicos como el polipropileno. Si bien es verdad que durante estos procesos combinados de temperatura y vapor de agua a presión, el agua penetra en su estructura plastificándolos y provocando un aumento en la permeabilidad a oxígeno, este aumento no es tan exagerado como en el caso de los copolímeros EVOH y, además, la recuperación de las propiedades barrera es prácticamente total.

**ABSTRACT**

Analysis of the consequences of a typical humid thermal plastic food packaging sterilization (retorting) process (at 121$^{o}$C during 20 minutes in the presence of pressurized water vapour) over the crystalline morphology and gas barrier properties of a high barrier aliphatic polyketone terpolymer was carried out by in-situ simultaneous synchrotron WAXS and SAXS experiments an by DSC, ATR-FTIR spectroscopy and oxygen transmission rate measurements. From a structural view point, it was observed that the retorting process led to a less crystalline material, however crystallinity was fully restored by a post-drying process. The humid thermal treatment also favoured the sorption of moisture in the amorphous phase to a saturation level, i.e. 2% water uptake. Synchrotron X-ray analysis during in-situ retorting of the sample indicated that the crystalline morphology withstood well the retorting process, but that the humid heating seemed to lead to a somewhat more pronounced crystallinity deterioration and higher repeat distance (long period) than dry heating. From a barrier perspective, transport properties (P, D and S) to oxygen were measured at 21$^{o}$C (around $T_g$) and at 48$^{o}$C (well above $T_g$). The oxygen permeability at 21$^{o}$C was observed to increase by ca. nine times immediately after the humid treatment, but the barrier character was observed to quickly recover over time. From the results, it is suggested that a simple post-drying process at relatively moderate temperatures can restore morphology and barrier properties. In the overall, it is also suggested that aliphatic polyketones withstand far better the process of retorting in comparison with, for instance, other high barrier polymers such as ethylene-vinyl alcohol copolymers reported earlier and, therefore, can offer even as a monolayer a solid alternative in retortable food packaging applications.

**Keywords:** Aliphatic polyketones, Retortable packaging, Barrier properties.

## INTRODUCTION

Many oxygen sensitive food products undergo thermal processes such as hot filling or sterilization (retorting) inside plastic packages. Therefore, it is a general requirement for the selected packaging system to have high oxygen barrier and resistance to wet and humid thermal treatments. Sterilization processes which make use of heated water vapour as the heat transfer medium (retorting treatment), can potentially alter the package structure compromising the barrier properties, and hence, the shelf-life of the packaged product. Previous works on multilayer structures containing ethylene-vinyl alcohol (EVOH) copolymers as the high barrier element, indicated that during standard industrial food packaging sterilization processes, some of the pressurized water vapour was capable of traversing the external hydrophobic layers made of polypropylene, sorbed into and subsequently increase the EVOH intermediate layer oxygen permeability by up to three orders of magnitude depending on grade, leading to a long standing decrease in barrier properties, and hence, compromising packaged food quality and safety. In this context, many studies have been carried out to ascertain the effects of water sorption[1,2,3] and retorting[4,5,6] over the permeability and thermal properties of these EVOH copolymers. More recent works, however, also showed that retorting can also be able to catastrophically disrupt the original polymer crystallinity leading to a more permeable morphology[7], and that the polymer morphology can be optimised to make these materials more resistant to these processes[8]. It is, therefore, of great industrial and academic interest to test and understand the retorting behaviour of high barrier polymer based packaging materials with potential advantages in retortable food packaging applications.

Aliphatic polyketones are a family of polymers prepared by the polymerisation of olefins and carbon monoxide, in a perfectly alternating sequence, by means of palladium-based catalysts[9,10]. As a consequence the mol-ratio olefins/carbon monoxide is always one across composition. In order to tailor final polymer properties, a second olefin (propene, butene, etc.) is introduced in the polymerisation reaction substituting randomly for ethene. The introduction of the second olefin results in a range of new materials with very attractive physical characteristics for commercial purposes. These semicrystalline thermoplastic materials have a unique

combination of mechanical, high temperature, chemical resistance, wear and barrier properties. Aliphatic polyketones, therefore, have significant potential in a broad range of engineering, barrier packaging, fibre and blend applications[11,12]. In this work, it is reported for the first time about the impact of a typical humid thermal treatment applied to plastic food packages over the crystalline structure and oxygen barrier of an aliphatic polyketone terpolymer.

## EXPERIMENTAL

### *Materials*

The aliphatic polyketone terpolymer used in this study was synthesised at BP Chemicals (UK) using a proprietary palladium-based catalyst. The material was supplied in powder form (as obtained from the production process).

Films of ca. 120 µm thickness were compression moulded at a temperature above the melting point, using an electrically heated hydraulic press and cooled under pressure at 15°C/min to room temperature. The PK sample is a perfectly alternating ethene/propene/CO terpolymer where the propene substitutes randomly for ethene. In this material the mol percent of CO is always 50 mol% across composition and the amount of the second olefin was not specified. The weight average molecular weight ($M_w$) determined by gel permeation chromatography is around 130,000, relative to PMMA standards and the polydispersity index is around 2.3. Water uptake was reported by the manufactured to be of 2% (w/dryw) and the $T_g$ was measured to be at 20°C by DMA. All samples were, unless otherwise stated, dried at 75°C overnight in a vacuum oven prior to testing.

Specimens of the material were retorted in a sterilization autoclave using industrial standard conditions at 121ºC during 20 minutes and were, subsequently, vapour purged, removed from the autoclave and allowed to cool down at room temperature conditions.

*Methods*

DSC experiments were carried out in a Perkin Elmer DSC 7 calorimeter at a heating speed of 10°C/minute from 50 to 240°C on typically 4 mg of sample cut from the compression moulded films. The calibration of the DSC was carried out with a standard sample of indium and the thermograms were subtracted from the signal of an empty capsule before evaluation.

ATR-FTIR experiments were recorded with a Bruker Tensor 37 instrument with 4 $cm^{-1}$ resolution and equipped with an ATR (Golden Gate, Specac) accessory.

Simultaneous WAXS and SAXS experiments were carried out at the synchrotron radiation source in the soft condensed matter beam at HASYLAB (DESY) in Hamburg (Germany). Scattering patterns were recorded using a one dimensional detector and an incident radiation wavelength, ?, of 0.15 nm. WAXS and SAXS data were corrected for detector response and beam intensity and calibrated against PET and rat tail standards, respectively. Determination of the long period was derived from background substracted and Lorentz corrected SAXS data[13]. Temperature scans were carried out at 5°C/min on dry and wet conditions. Water saturating conditions during the temperature experiment were ensured by sealing a sample in excess of moisture between aluminium films and O-ring rubber seals inside screwed rectangular cell compartments designed for functioning as miniautoclaves to carry out temperature experiments in the presence of liquids[7]. Experiment success was checked by observation of constant background intensity over the experiment and presence of moisture in the cell after termination of the thermal runs, which indicated that moisture did not leak off the cell during the temperature run. Under dry conditions, the specimens were heated up from 25°C to well above the melting point of the polymer at 5°C/min. In the wet specimens, a typical humid thermal sterilization experiment was simulated, in which the sample was heated at 5°C/min up to 121°C and maintained at 121°C for 20 min.

Oxygen transmission rate ($O_2$TR) measurements were performed in an OX-TRAN® 2/20 (Mocon, US) at 0% RH and two different temperatures, i.e. 21ºC and 48°C.

## RESULTS AND DISCUSSION

*Crystalline morphology*

The retorting process leaves the yellowish coloured PK film apparently unharmed with no signs by visual inspection of changes in appearance, colour or in dimensions. This behaviour is in sharp contrast with for instance the retorting of EVOH monolayers, which leads to extensive whitening, i.e. losses in transparency, and significant deterioration in dimensional stability as a result that the sample melts during the actual retorting process[2,7].

Figure 1 shows the DSC thermograms of untreated and retorted specimens of the terpolymer.

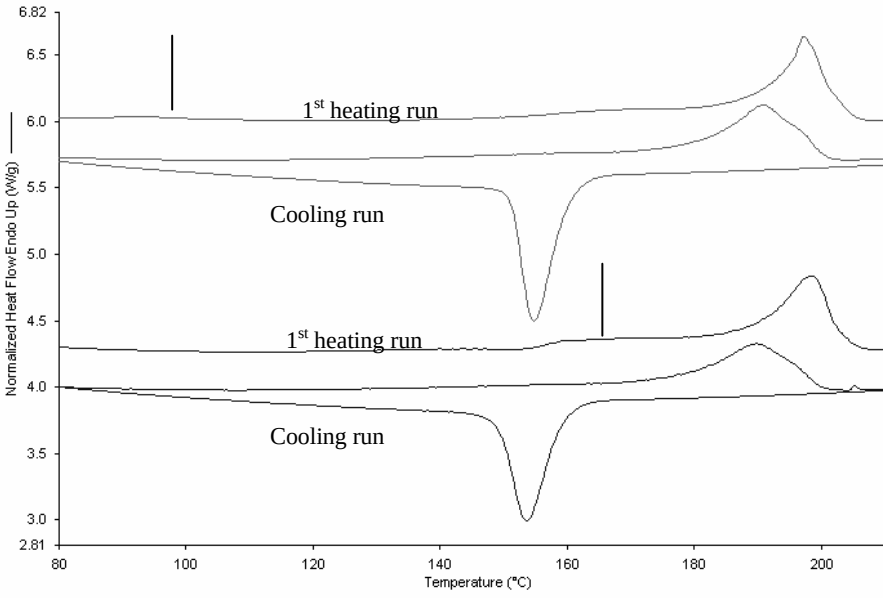


**Figure 1** DSC thermograms during heating-cooling-reheating cycle of retorted and untreated (upper figure) PK specimens. Arrows indicate the annealing peaks as a consequence of drying at 75ºC (untreated sample) and retorting at 121ºC.

In the first and third heating run of this Figure, the specimens shows a broad and multiple endotherm which is characteristic of the melting behaviour of these materials[14]. The third run shows that as the sample has not been properly stabilized

by adequate additives, the thermogram exhibits lower melting point and a broader melting peak result of chemical modifications produced during the first heating scan up to well above the melting point[14]. The crystalline polymorphism and the chemical modifications undergone by aliphatic polyketones are very complex and strongly depend upon a number of factors which have been outlined and discussed previously[14,15]. The low melting point shoulder seen at 90°C in the untreated sample is the result of crystal thickening and melting and recrystallisation of crystals with melting point below the temperature set for drying the material. Likewise, the low melting point shoulder observed at around 160°C in the retorted specimen is again the result of crystal perfection and melting and recrystallization of low melting point crystals due to the retorting process; process which is, in essence, a humid thermal treatment. Surprisingly, however, the position of the melting shoulder at 160°C appears quite high in temperature compared to the annealing temperature used at 121°C. This melting tail -reflect of the annealing process- does generally appear immediately above the annealing temperature used and usually not so distant apart in temperature[15]. This behaviour is attributed to the water vapour pressure (2 atm.) generated over the sample during the retorting process. In the reheating run (2nd heating run) the annealing peaks are no longer seen neither in the untreated nor in the retorted specimens.

**Table 1**. DSC melting ($T_m$) and crystallization ($T_c$) temperatures (ºC) and their corresponding enthalpies (J/g) for untreated and retorted PK specimens

| | **PK untreated** | | | **PK retorted** | | | **PK retorted and dry** | | |
|---|---|---|---|---|---|---|---|---|---|
| | **$T_m$** | **$T_c$** | **DH** | **$T_m$** | **$T_c$** | **DH** | **$T_m$** | **$T_c$** | **DH** |
| **1st heating run** | 197.4 | | 76.6 | 198.2 | | 67.5 | 197.5 | | 74.6 |
| **cooling run** | | 154.8 | -63.6 | | 153.6 | -61.1 | | 153.5 | -63.6 |
| **2nd heating run** | 190.7 | | 66.6 | 189.7 | | 59.3 | 189.7 | | 62.9 |

Table 1 shows melting and crystallization points and melting and crystallization enthalpies during a typical heating-cooling-reheating cycle of untreated, retorted and retorted and vacuum dry at 75°C specimens. From this Table and Figure 1, it appears that although in the retorted sample the melting point is slightly higher and the melting peak has broadened towards higher temperature as a result of crystal

thickening, there is a reduction in the overall melting enthalpy. This reduction in melting enthalpy is, however, no longer seen in the retorted and dry specimen, suggesting that it is the result of impaired re-crystallization of the crystalline fraction with lower melting point (small and defective crystals) as the sample is rapidly taken out of the retorting autoclave. Thus, it is important to realize that some crystallinity reduction (ca. 12%) may be occurring immediately after retorting if the sample is quickly removed (quenched) from the autoclave. Aside this effect of crystallinity reduction on the small and defective crystalline fraction which melts below the retorting temperature, the retorting process does not appear to damage the crystalline morphology but to rather promote an annealing effect on the most robust crystalline morphology.

Figure 2 shows the ATR-FTIR spectra of untreated and retorted PK specimens. The retorted sample was thoroughly blotted (excess water was thoroughly wiped with a tissue) after the treatment and immediately measured. From Figure 2 it can be seen that there is no major changes in the polymer spectrum of the specimens. However, there is a clear increase in the relative intensity of features centred at 3500 $cm^{-1}$ and 1625 $cm^{-1}$ which arise from water OH stretching and OH in-plane bending, respectively (see arrows). Figure 2 also shows a zoom of the OH stretching spectral range of sorbed water in untreated, retorted and water saturated specimens of the terpolymer. These spectra suggest that during the retorting treatment, an amount of water similar to that present in a fully water saturated specimen penetrates the polymer amorphous phase, thus leading within 20 minutes of treatment to a completely water plasticized specimen. This result was further corroborated by gravimetric measurements, which revealed that the retorting process increased the weight of the sample by 2% w/w.

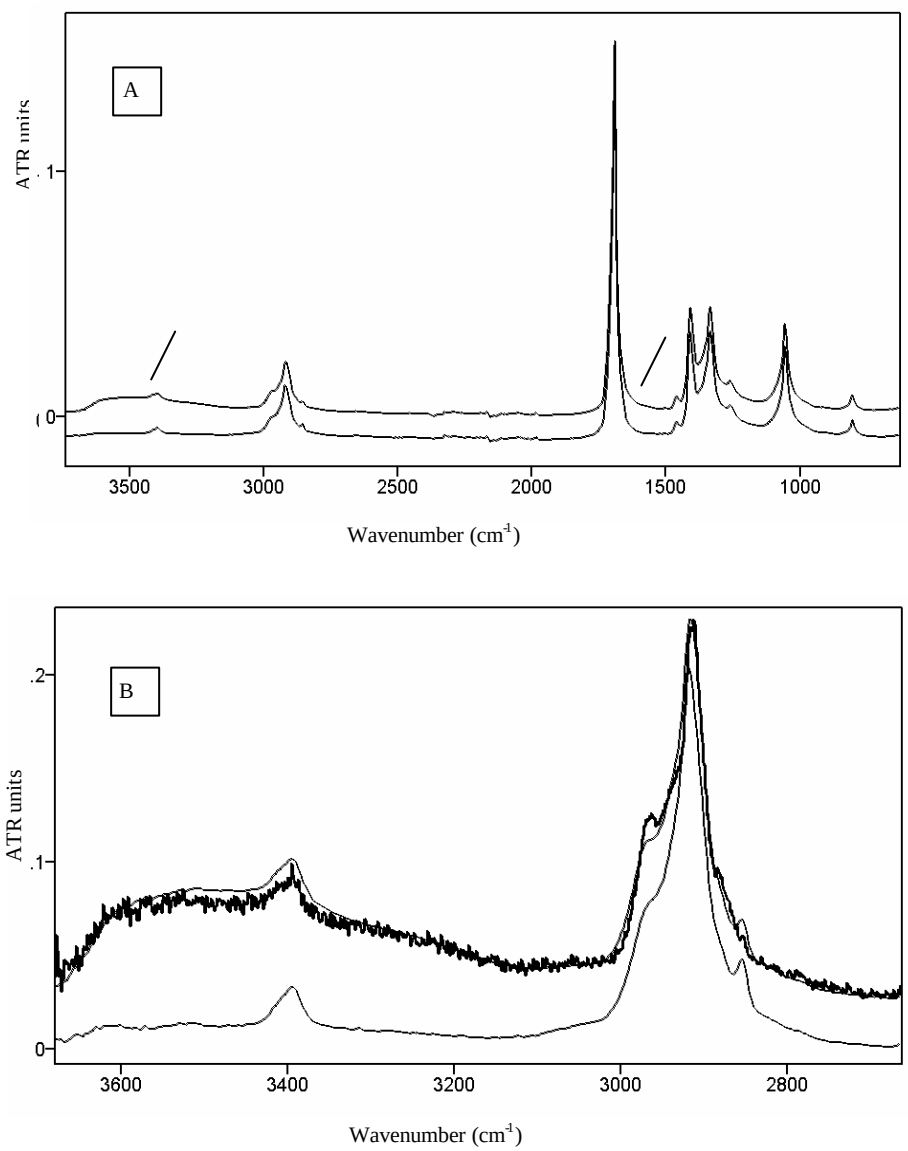


**Figure 2** (A) ATR-FTIR spectra of PK untreated (bottom) and retorted (up) specimens, arrows indicate where water bands can be clearly seen. (B) Spectral zoom in the OH stretching range of untreated (bottom), water saturated (thicker line) and retorted specimens of the PK sample.

The infrared active carbonyl stretching band is known to be a conformationally sensitive mode and, therefore, it has previously been used to estimate molecular order and, therefore, crystallinity content and crystallinity variations in polymers containing this chemistry[16]. By looking into the shape of the carbonyl stretching (see Figure 3) band at 1690 $cm^{-1}$ of the untreated and of the vacuum dry retorted sample

there appears to be no significant changes in the overall crystallinity in agreement with the DSC results reported in Table 1.

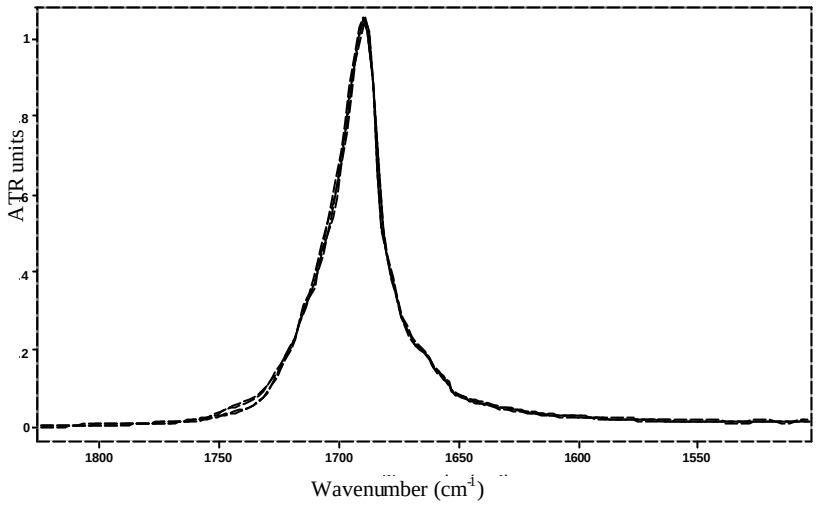


**Figure 3.** ATR- FTIR spectra of untreated and retorted and dry (dashed line) specimens of the PK terpolymer in the carbonyl range.

Figure 4 shows the crystalline patterns of a dry specimen during heating to the melting point and during a typical retorting experiment. The synchrotron methodology permits the real time monitoring of the crystalline patterns during typical thermal ramps and, therefore, allows, among many other cases, for simulation studies during in-situ application of industrial thermal processes.

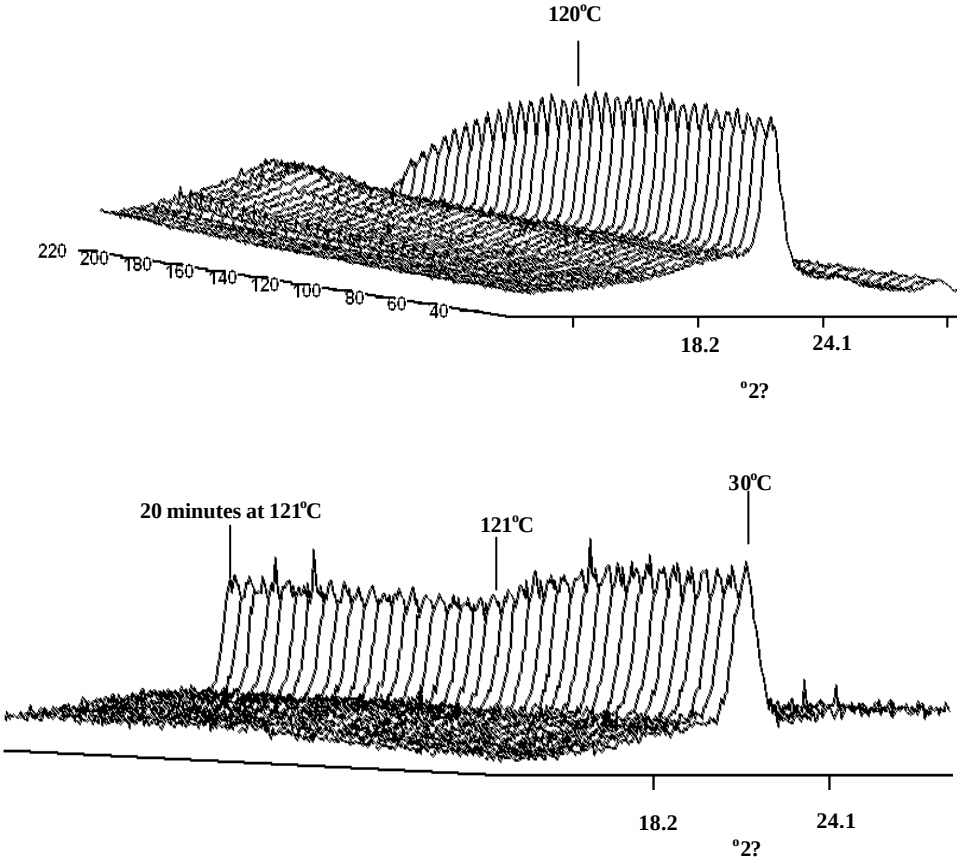


**Figure 4** Synchrotron WAXS traces versus temperature (°C) taken during heating up to the melting point (top figure) and during a typical retorting run of PK specimens (bottom figure).

Figure 5 shows the corresponding evolution of the normalized intensity of the main diffraction peak at 21.5° during dry heating of the sample to the melting point and during the above mentioned retorting experiment. From Figure 4, it can be seen that the crystalline morphology of the terpolymer is typically made of the so-called beta phase[14] and that it remains so during the retorting experiment. This orthorhombic polymorph is known to be dominant in specimens containing a second olefin resulting in branches, whereas the so-called alpha phase is a more thermodynamically stable morphology that becomes dominant in the copolymer and in terpolymers with very low additions of ethylene as second olefin[15]. In the dry specimen, the normalized intensity of the main crystalline diffraction peak is seen to decrease slightly up to about 150°C and from there onwards it decreases more

abruptly to the total melting of the sample at around 205°C, in agreement with DSC results. There appears to be a regime between 70 and 100°C where the intensity of the diffraction peaks rises slightly as a result of annealing.

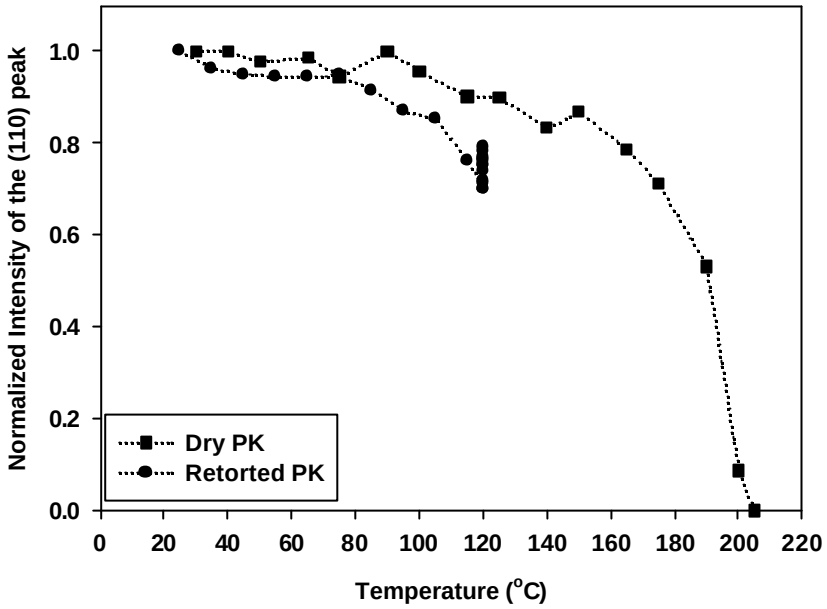


**Figure 5.** Evolution of the main crystalline peak as a function of temperature for dry and retorted specimens of PK.

From the normalized evolution of the intensity of the main diffraction peak during the retorting experiment, it can also be seen that the intensity of this plane decreases with temperature up to reaching 121°C due to partial melting; nevertheless, it increases slightly again during the isothermal run at 121°C suggesting that an annealing positive effect may take place on the crystallinity. Figure 5 further indicates that the decline of the main crystalline pattern with temperature could be slightly higher for the retorted terpolymer than for the dry sample. Nevertheless, caution should be taken when interpreting relative changes in the intensity of the main crystalline peak in terms of crystallinity changes, because this reflects just changes in the height of the main crystalline diffraction peak, and not necessarily similar changes in area. The crystallinity content could not be unambiguously determined in the retorted specimen because the presence of water is modifying the

background of the diffraction patterns and, therefore, the integration method described earlier[15] was not found consistent throughout the experiment.

Figure 6 shows the Lorenz-corrected SAXS patterns evolution with increasing temperature for the dry (in-situ heating to near the melting point, i.e. 175ºC) and wet (during the retorting experiment) specimens and the simultaneous evolution of the repeat distance or long period (L, average sum of the thicknesses of the crystalline lamella and the amorphous inter-lamellar layer) as determined from the maximum of the SAXS patterns for both experiments ($L=1/s_{max}$). As expected, the dry sample shows an increase in long period (seen by a decrease in the scattering vector for the maximum of the peak, $s_{max}$) as it approaches the melting point due to progressive melting of the smaller/defective crystalline morphology and the subsequent increase in the repeat distance. The long period increase with temperature seems more abrupt above ca. 140$^{o}$C. Furthermore, and in accordance with the usual behaviour, as the SAXS peak shifts to lower values of the scattering vector it increases in intensity and, accordingly, it can be more easily resolved, as can be observed in Figure 6. Figure 6 also shows that during the retorting process, the maximum of SAXS cannot be clearly discerned in the neighbourhood of room temperature, however, as temperature rises this becomes more easily detectable. This is the reason why long period data for the retorted sample is only shown above 80$^{o}$C. The evaluation of the maximum of SAXS in Figure 6 suggests that the long period increases to a larger extent above 80$^{o}$C during heating in the presence of water than in dry conditions; however, during the isothermal treatment at 121$^{o}$C it is seen to decrease slightly.

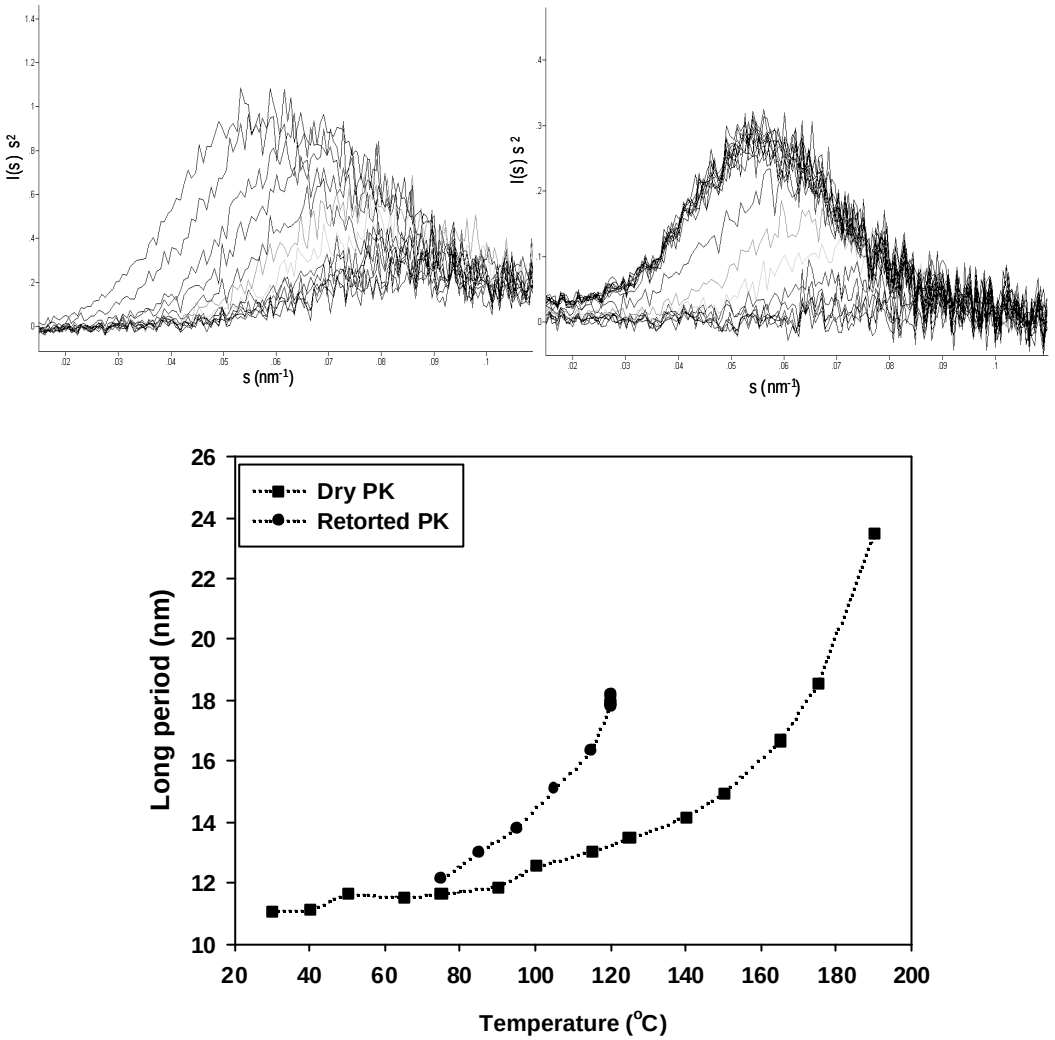


**Figure 6** Lorenz-corrected SAXS curves as a function of temperature for the dry specimen during in-situ heating experiment up to 175°C (left graph) and the wet specimen during the in-situ retorting experiment (right graph). In both graphs the SAXS peak shifts towards lower scattering vector (s) values as the temperature is increased. The lower graph shows the evolution of the long period as determined from the maximum of SAXS peaks ($1/s_{max}$) in the top graphs as a function of temperature for untreated and retorted specimens of PK.

As in Figure 5 the intensity of the main diffraction peak was seen to decrease somewhat more steeply above 80°C for the retorted sample, it is possible to attribute this larger rise in long period above 80°C to a larger decrease in crystallinity. However, as the sample sorbs water in the amorphous phase which disrupts the

inter- and intra-chain dipolar interaction, it may also be possible that the long period increase could be related to swelling and subsequent relaxation or unravelling of the amorphous phase. This behaviour of increased long period during humid heating of the sample has also been reported earlier in ethylene-vinyl alcohol copolymers during retorting[7].

*Oxygen barrier*

Transport properties to oxygen were measured at two temperatures (21 and 48ºC), and values are gathered in Table 2.

**Table 2.** Permeability (P in cc mm/m$^2$ day atm), diffusivity (D in m$^2$/s) and solubility (S in cc/cm$^3$ atm) values at 21 and 48$^o$C at 0%RH for dry untreated specimens and Equation 1 parameters for the retorted specimens

| Sample | P | D | S | $P_¥$ | a | b |
|---|---|---|---|---|---|---|
| **21ºC** | 0.05±0.01 | $2.95\ 10^{-13}$ | $2.05\ 10^{-3}$ | 0.09 | 0.35 | 0.001 |
| **48ºC** | 4.50±0.08 | $2.17\ 10^{-12}$ | $1.29\ 10^{-2}$ | 4.77 | 0.94 | $3.21\ 10^{-4}$ |

Figure 7 shows the normalized (for comparison purposes) permeability built-up with time up to the steady state at 21 and 48$^o$C. From these curves, it can easily be seen that the diffusion of oxygen goes much faster at the higher temperature as expected. In this case, it should also be taken into account that, even when diffusion and permeability are temperature activated processes, a differentiating effect from the $T_g$ could also be expected, as this temperature lays for this polymer around room temperature (i.e. 20$^o$C as determined by DMA by the manufacturer). Thus, while at 21$^o$C the polymer is at the borderline between glassy and rubbery semicrystalline polymer, at 48$^o$C it is clearly expected to behave like a rubbery semicrystalline polymer. This discontinuity in molecular structure marked by the $T_g$ may accentuate the differences in diffusion and permeability at the two temperatures. Table 2 shows numerical values for the diffusivity (D) and solubility (S) coefficients, which indicate that these parameters are higher at 48ºC. Diffusivity was calculated from the so-called half-time method ($t_{0.5}$, i.e. time value at $P/P_e$=0.5) as described elsewhere and solubility from the relation P = D S.[17]

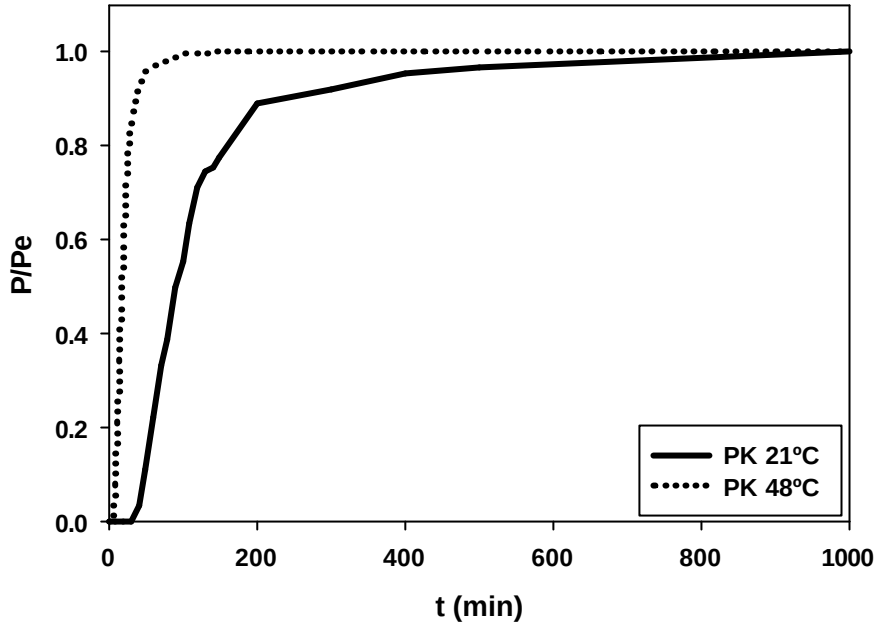


**Figure 7**. Normalized oxygen permeability (P/Pe) vs. time of untreated PK at 21$^{o}$C and 48$^{o}$C at 0R%H.

Figure 8 shows, as an example, the permeability evolution over time at 21$^{o}$C for the terpolymer after the retorting process. This figure indicates that retorting leads to a decrease in barrier properties for the specimen (ca. 9 times higher permeability), but that this is relatively small in comparison with the major changes (three orders of magnitude) undergone by other benchmark high barrier polymers such as EVOH copolymers[8]. Based on the above results, this increase in permeability is most likely caused by water vapour ingress and subsequent drop in inter and intramolecular cohesion (plasticization) of the amorphous phase, albeit it may also have a contribution from the reported decrease in crystallinity undergone by the polymer due to fast cooling after the treatment. Albeit there are some polymers and low humidity regimes for which water sorption may lead to antiplasticization due to water molecules filling the available free volume and impairing or blocking the transport of oxygen, this mechanism is not dominant in the experiments described here due to the observed barrier deterioration after retorting[18]. However, as the permeability is seen to recover over time, water desorption and the subsequent increase in molecular cohesion or self-association leading to barrier improvement is the predominant recovery mechanism.

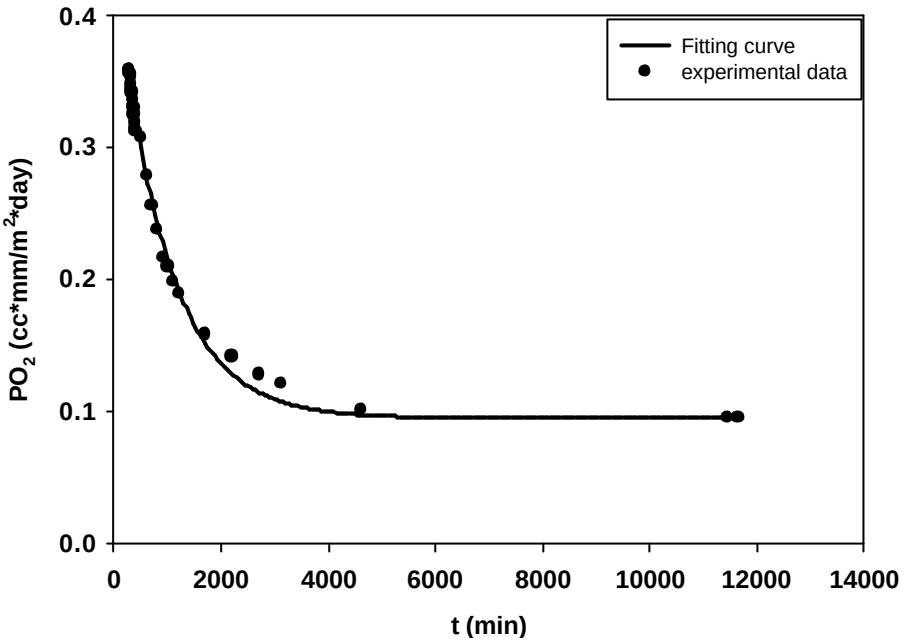


**Figure 8.** Permeability recovery as a function of time at 21°C of retorted PK.

The permeability recovery in the range plotted in Figure 7 appears to follow, in agreement with previous results for EVOH copolymers, an exponential decay as expressed by equation (1).

$$P(t) = P_e + a\, e^{-bt} \qquad (1)$$

In equation 1, $P_e$ is the equilibrium permeability after retorting, "a" is the maximum permeability rise from the equilibrium permeability value at time zero after retorting and "b" is related to the kinetics of the permeability recovery, i.e. the higher the value the faster the process. The parameters of equation 1 for the retorted specimens are gathered in Table 2 for the two temperatures. From the values of "a" in this table, plasticization, barrier deterioration due to water sorption and subsequent drop in intermolecular cohesion during retorting (see long period increase), is clearly higher at 21°C, as expected. At 48°C moisture sorption effect on permeability has a lower impact for three reasons namely, the permeability is higher at this temperature, the moisture content is lower because the sample dries out more quickly and promotes

annealing of the crystalline morphology. The barrier character appears to recover to a large extent, particularly at 48°C, during oxygen testing at both temperatures (see $P_e$ values), albeit it does not seem to reach completely the original permeability values of the untreated samples ($P_0$) probably as a result of the crystallinity deterioration and also due to the existence of some remnant water molecules sorbed in the specimens. These two effects are expected to be smaller at higher temperatures, viz. at 48°C, as observed in Table 2. From all the above observations, it is further substantiated that a post-drying process after retorting can help restore the barrier character by developing the originally present crystallinity and by removing more strongly bound moisture.

**ACKNOWLEDGMENTS**

The authors would like to thank Dr. A.K. Powell and Dr. J.G. Bonner (BP Solvay Polyethylene, Belgium) for supplying samples and for fruitful discussions. This study was supported by MCYT (project MAT2003-08480-C03) and the work performed at the synchrotron facility in Hamburg (Hasylab, Germany) was supported by the IHP-Contract HPRI-CT- 1999-00040/2001-00140 of the European Commission. Finally the authors would also like to acknowledge Dr. S.S. Funari and Mr. M. Dommach (Hasylab, Germany) for experimental support.

## REFERENCES

[1] Lagaron, JM; Powell, AK; Bonner, G. Polymer Testing 2001, 20, 569.

[2] Aucejo, S; Marco, C; Gavara, R. Journal of Applied Polymer Science 1999, 74, 1201.

[3]Zhang, Z; Britt, IJ; Tung, MA. Journal of Applied Polymer Science 2001, 82, 1866.

[4]Zhang, Z; Britt, IJ; Tung, MA. Plastic Film and Sheeting 1998, 14, 287.

[5]Tsai, BC; Wachtel, JA. *Barrier Polymers and Structures.* American Chemical Society: Washington D.C., 1990, 192-202.

[6] Alger, M.M; Stanley, T.J.; Day, J. In: Barrier Polymers and Structures. American Chemical Society: Washington D.C., 1990, 203-224.

[7] López-Rubio, A; Lagaron, JM; Gimenez, E; Cava, D; Hernández-Muñoz, P; Yamamoto, T; Gavara, R. Macromolecules 2003, 36, 9467.

[8] López-Rubio, A; Hernández-Muñoz, P; Giménez, E; Yamamoto, T; Gavara, R; Lagaron, JM. Journal of Applied Polymer Science 2005, 96, 2192.

[9] Drent, E; Budzelaar, PHM. Chemical Reviews 1996, 96, 633.

[10] Sommazzi, A; Garbassi, F. Progress in Polymer Science 1997, 22, 1547.

[11] Bonner, JG; Powell, AK. "213th National American Chemical Society Meeting", ACS Materials Chemistry Publications, Washington, 1997.

[12] Bonner, JG; Powell, AK."New Plastics'98 Conference Proceedings", CSIR, London 1998.

[13] Balta-Calleja, FJ; Vonk, CG. X-ray scattering of synthetic polymers, Amsterdam, Elsevier, 1980.

[14] Lagaron, JM; Vickers, ME; Powell, AK; Bonner, JG. Polymer 2002, 43, 1877.

[15] Lagaron, JM; Lopez-Quintana, S; Rodriguez-Cabello, JC; Merino, JC; Pastor, JM; Polymer 2000, 41, 2999.

[16]Lagaron, JM; Powell, AK; Davidson, NS. Macromolecules 2000, 33, 1030.

[17]Crank, J. The Mathematics of Diffusion. 2nd ed. New York: Oxford Science Publications, 1975.

[18]Lagaron, J.M.; Catala, R.; Gavara, R. Materials Science and Technology 2004, 20, 1

# ON THE UNEXPECTED CRISTALLIZATION OF AMORPHOUS POLYAMIDE AS INDUCED BY A PACKAGED FOOD RETORTING TREATMENT AND ITS IMPLICATIONS IN BARRIER PROPERTIES

## INTRODUCCIÓN AL ARTÍCULO V

En la búsqueda de nuevos materiales alta barrera que pudiesen sustituir a los copolímeros de etileno y alcohol vinílico en envases esterilizables, encontramos que en el caso de la poliamida amorfa, en la que la disposición de los isómeros ácidos en la cadena principal rompen la regularidad impidiendo en principio la cristalización del polímero, cuando se somete a un tratamiento combinado de temperatura y humedad, se consigue un ordenamiento regular de segmentos de las cadenas que queda reflejado en endotermas de fusión en el termograma obtenido por DSC, así como a la aparición de bandas cristalinas por difracción de rayos X. Como ya se explicó en la introducción, la presencia de cristales en la estructura de materiales poliméricos influye en las propiedades de transporte actuando, por un lado, como diminutos bloques impermeables al paso de gases y otros compuestos de bajo peso molecular y, por otro lado, limitando la movilidad de la fase amorfa adyacente, lo cual afecta de forma positiva a los parámetros de transporte. En este artículo se estudiaron también, de modo comparativo, la permeabilidad al oxígeno, así como la sorción de agua en la poliamida amorfa antes y después de la esterilización ("retorting") en autoclave.

**ABSTRACT**

In this study, it is presented for the first time, the characterization of an amorphous polyamide after having been subjected to humid thermal conditions such as these typically applied in the industrial sterilization of packaged foods. From a fundamental point of view it was fortuitously found that the combination of heat and water, with and without pressure built up, was capable of inducing some crystallization in the otherwise amorphous polymer. Characterization of the crystallization process was carried out by DSC, FT-IR and simultaneous time-resolved SAXS and WAXS synchrotron experiments. The crystallization of the polymer began as characterized by DSC in the presence of humidity at ca. 90$^{o}$C and extended up to 120$^{o}$C under autoclave conditions, ant it is thought to be the result of heated water being able to disrupt the intense amide groups self-association brought in by hydrogen bonding. The thermally activated molecular structure is thought to become plasticized by the presence of moisture which, in turn, provokes sufficient segmental molecular mobility in the system to promote some degree of lateral order. Propertywise, the resulting consequences of this behavior are an increase in the barrier properties to oxygen and a reduction in water sorption. From an applied view point, it is suggested that this unexpected behavior could make this polymer of significant interest in retortable food packaging applications.

Keyworks: Amorphous polyamide, retorting, barrier properties, FT-IR, SAXS-WAXS, crystallization

## INTRODUCTION

Due to the excellent properties of polymers as packaging materials, there is a trend in the food industry towards the replacement of classic packages manufactured with materials like glass or tinplate, with lighter, cheaper and versatile plastic packages. These polymeric structures must, however, assure the quality and safety of the packaged products without compromising their shelf-life.

Many food products are to be packaged with high-barrier polymeric materials because oxygen is a ubiquitous element involved in many food deterioration reactions, such as fat oxidation, vitamin loss, etc. But furthermore, several food products, like the continuously increasing demanded precooked foods (ready-to-eat products), require a retorting treatment inside the package before being commercialized (typically 121ºC during 20 minutes in an industrial autoclave, i.e. in the presence of pressurized water vapor). Thus, apart from the already mentioned high-barrier conditions, plastic packages must withstand such kind of processes without suffering undesirable changes.

Ethylene-vinyl alcohol (EVOH) copolymers are a family of semicrystalline high-barrier materials commonly used in retortable packaging structures. Due to their high water sensitivity, derived from the presence of hydroxyl groups in their structure, EVOH copolymers are used as intermediate high-barrier layer in multilayer structures protected from the external relative humidity by at least two layers of a hydrophobic material such as polypropylene. However, it is common knowledge that, even protected between these hydrophobic materials, retorting processes have a tremendous impact on the gas barrier performance of the copolymers. Tsai and Jenkins[1] reported that the oxygen barrier of retortable packages containing an EVOH barrier layer was initially reduced by two orders of magnitude when these containers were subjected to steam or pressurized water during thermal processing and, during long term storage (>200 days), the barrier was partially recovered (by a factor of ten). In a more recent work[2], it was demonstrated that this huge increase in permeability was not only caused by the plasticization of the EVOH structure, as it had been previously reported[1, 3], but that also a deterioration of the copolymer crystallinity takes place in multilayer structures during the retorting process[4]. Real time experiments during in-situ retorting of EVOH monolayers showed that the

material melts around 100°C, which implies that the polymer melts 83°C earlier than expected in the presence of heated water vapour[2]. This behavior clearly proves the strong moisture sensitivity of the material even in multilayer structures.

As a consequence of the detrimental effects of common retorting processes over the structure and permeability of the EVOH copolymers, alternative high-barrier materials are being studied as potential substitutes in retortable food packaging structures. Aliphatic polyketones and amorphous PA are high and medium-high barrier materials with potential in retortable applications. A very recent study has already proven that the aliphatic polyketones are adequate materials to withstand packaged food retorting conditions, as the deterioration in oxygen barrier suffered by these polymers even in monolayer structures is very small compared to the deterioration suffered by EVOH based multilayer structures[5]. Amorphous polyamides, on the other hand, offer favorable properties such as dimensional stability, good dielectric and barrier properties and low mould shrinkage[6], and, furthermore, exhibit an antiplasticization behavior at high relative humidity conditions. Thus, it is known that the oxygen barrier performance of this material increases at high relative humidity conditions in contrast with the behavior of most polar polymers, including most polyamides, aliphatic polyketones and EVOH[7]. It is, therefore, of significant relevance to study the effect of common humid thermal processes for this polymer regarding its potential inclusion in retortable food packaging structures.

In this overall context, this pioneering study reports on the structural and oxygen barrier alterations suffered by a commercial amorphous polyamide material during temperature, humidity and combined temperature and humidity (autoclaved or retorting) treatments by means of DSC, FTIR, oxygen transmission rate and simultaneous WAXS and SAXS experiments via synchrotron radiation.

## MATERIALS AND METHODS

An amorphous polyamide experimental grade (so-called UX-2034) from Dupont (U.S.) polymerized by the condensation of hexamethylene diamine and a mixture of 70:30 isophthalic and terephthalic acids was used in a film extruded form. Alternatively, multilayer structures were obtained by vacuum sealing the amorphous polyamide (aPA) between polypropylene layers with a typical nominal thickness of the barrier layer around 45 microns. As no tie layers were used, the intermediate aPA barrier layer studied here could be easily peeled off after the treatment for testing. Unless otherwise stated, all the samples were kept in a dessicator for a week before testing.

*Thermal treatments*

The materials were thermally treated under dry and humid conditions in a conventional oven (annealing) and in an autoclave (retorting), respectively. The standard treatment given to the samples, both in the oven and in the autoclave, was 120ºC during 20 minutes. The material was also heated in boiling water for 20 minutes to discriminate the water vapour pressure effect from the combined temperature and humidity effect.

*Oxygen transmission rate*

$O_2$TR values were obtained from an OXTRAN model DL200 of Mocon (US). The samples were placed in a 5 $cm^2$ test cell and the measurements were made using a gas flux of 10 mL/min, ambient temperature (around 24ºC) and a relative humidity of 0%. The $O_2$TR values were corrected with the thickness of the films and with the pressure gradient of the experiment, i.e. 1 atm. The oxygen transmission rate of the untreated aPA was measured in dry until equilibrium permeability was reached. A similar sample was vacuum sealed between two polypropylene (PP) layers and retorted in the autoclave during 20 minutes at 120ºC. After the retorting treatment the multilayer structure was delaminated and the aPA intermediate layer was immediately placed in the OX-TRAN cell and its oxygen transmission rate was measured as a function of time.

*ATR/FT-IR Spectroscopy*

Atenuated total reflexion (ATR) infrared (IR) experiments were carried out in the FT-IR mode of the Perkin-Elmer spectrum 2000 system with a spectroscopic resolution of 4$cm^{-1}$. Typical acquisition times were about 10 seconds.

*Differential Scanning Calorimetry*

DSC experiments were carried out in a Perkin-Elmer DSC-7 calorimeter. The heating and cooling rate for the runs was 10ºC/min, being the typical sample weight around 4 mg. Calibration was performed using an indium sample. All tests were carried out, at least, in duplicate to check for repeatibility. The temperature range of the assays was from 50 to 250ºC and from -80 to 250ºC (using liquid nitrogen as cooling medium) in order to distinguish the glass transition temperature ($T_g$) of the retorted aPA. From the thermograms, the glass transition temperature was determined from the temperature of half the change of the specific heat. Apart from the aluminum pans used to perform the previous experiments, pressure proof steel pans were also used to simulate a retorting process. The steel pans are designed to resist the vapor pressure built up exerted during temperature experiments with liquids or solids and, therefore, it can serve as a calorimetric autoclave to follow in situ the enthalpic changes taking place during the retorting experiment. A sample of aPA was placed inside the pan with 10 µL of water where it was heated from 50 to 120ºC at 10ºC/minute and then it was held at 120ºC during 20 minutes. A steel reference pan with indium was used for calibrating the equipment, and another one as a reference pan containing the exact amount of water present in the sample pan to eliminate the water signal from the DSC thermograms.

*X-Ray diffraction*

Simultaneous wide and small angle X-ray scattering (WAXS and SAXS) experiments were carried out at the synchrotron radiation source in the polymer beam A2 at Hasylab (DESY) in Hamburg (Germany). Scattering patterns were recorded using a one-dimensional detector and an incident radiation wavelength, ?, of 0.15 nm. WAXS and SAXS data were corrected for detector response and beam intensity and calibrated against PET and rat tail standards. Temperature scans were also carried out at 5 °C/min on dry (sandwiched between aluminum foil) and in water saturation simulating an industrial retorting process. Water saturation conditions

during the temperature experiment were ensured by sealing a water-saturated aPA specimen in excess of moisture between aluminium windows and O-ring rubber seals inside screwed rectangular cell compartments designed for measuring liquids as a function of temperature specifically designed for the experimental setup[2]. Experiment success was checked by observation of constant background intensity over the experiment and presence of moisture in the cell after termination of the thermal experiments, which indicated that moisture did not leak off the cell during the temperature run.

*Sorption measurements*

Water uptake was analyzed by immersing the previously dried (vacuum oven, 70ºC) untreated and retorted aPA directly into the solvent. Weight gain measurements were carried out in an analytical balance model Mettler AE240. Before each measurement, the polymer surface was thoroughly wiped off with a tissue to eliminate excess solvent. The experiments were carried out in duplicate to check for reproducibility and average values were fitted to the appropriate solution of the second law of Fick to determine diffusion coefficients.

## RESULTS AND DISCUSSION

### Structural characterization

After humid thermal autoclaving of an aPA specimen it was observed that the originally transparent film became more rigid and whitish to some extent. As a result, the structural and/or morphological characteristics of the material were thought to change during the applied process. Figure 1 shows the DSC curves obtained during a typical DSC experiment (heating-cooling-heating runs) of untreated, heated in the oven, heated in boiling water and retorted aPA specimens.

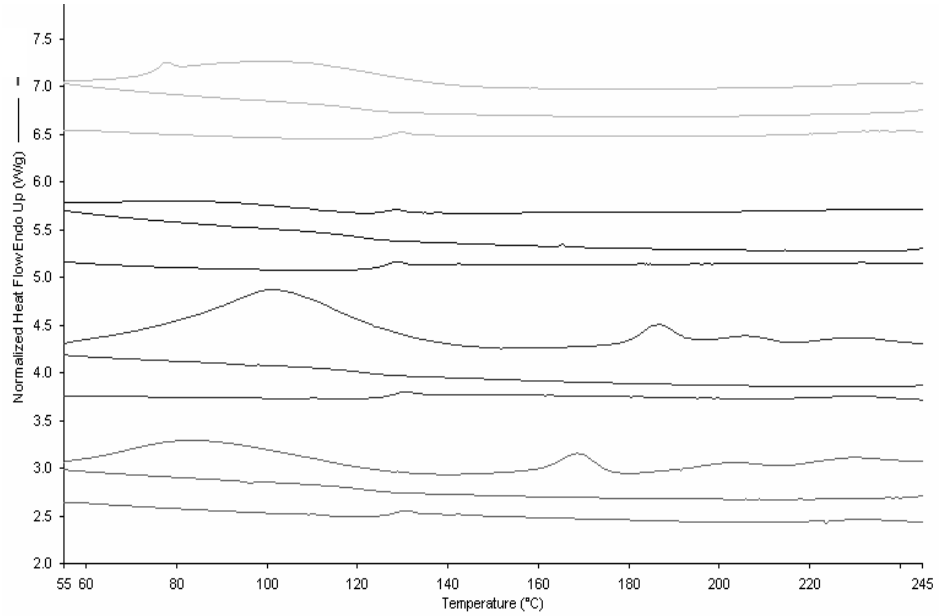


**Figure 1.** DSC thermograms of (from top to down): Untreated aPA, aPA heated in the oven at 120ºC during 20 minutes, aPA retorted and aPA heated in boiling water for 20 minutes. The three runs of each experiment are shown in the picture being the top one the first heating run, the middle one the cooling run and the bottom one the second heating run.

The second heating scan shows that in all cases the glass transition temperature ($T_g$) of the untreated aPA is around 126ºC. In all experiments, but in the annealed specimen, the evaporation of sorbed moisture impeded the observation of the $T_g$ event in the first heating scan. It is assumed that as the sorption of moisture is known

to decrease the $T_g$ of the polymer, this is not observed by the presence of the dominant sorbed moisture endothermic signal covering the range from 50ºC up to about 120°C[7,8].

Surprisingly, the retorted sample displays three endothermic features, which suggests that during the combined treatment with temperature and pressurized water vapor, some degree of crystallization develops in the polymer. In the case of the high-barrier ethylene-vinyl alcohol copolymer (EVOH), the vapor pressure generated inside the autoclave during the autoclaving cycle was found to be decisive in the total disruption of the EVOH crystals. Thus, this study was also aimed to ascertain whether the crystallization process takes place as a result of temperature, presence of humidity or the specific pressurized water vapor conditions. For this purpose, further analysis was carried out in samples that had undergone different conditionings. From Figure 1 it is observed that the annealing process in the oven only conducts to the elimination of strongly bound water, and that aside from temperature, water is needed to achieve lateral molecular order. The effect of vapor pressure on the development of crystallinity was checked by heating an specimen of aPA in boiling water, and if compared with the autoclaved polyamide, the sample also displays three endothermic peaks in the DSC but displaced towards lower temperatures (± 15ºC lower), pointing out that smaller or more defective crystals are formed when no pressure is exerted. The enthalpy of fusion of the retorted aPA is also higher ($?H_m$[retorted]=36.2J/g; $?H_m$[heated in water]=33.1J/g), indicating that a higher degree of crystallization takes place in the specimen. Another curious observation is that in the first heating run of some samples a small endothermic transition was seen around 125°C, which from observation of the third heating scan appears as a molecular relaxation associated to the $T_g$ event in the polymer. However, it is also known that the $T_g$ of the polymer decreases in the presence of water up to a value of 54°C in a water equilibrated sample. Thus, in order to check for the effect that the relative humidity has on the first DSC thermogram, the material was equilibrated at different relative humidities and scanned by DSC. Figure 2 shows the first heating run of the samples equilibrated at different relative humidities. From this figure, it is seen that the above endothermic feature is located at approximately the same temperature across humidity, therefore, ruling out the possibility of being associated with a $T_g$ event in the polymer. The origin of this signal is unknown but it could be

associated with a molecular relaxation process not being affected by moisture or could related to a moisture induced signal.

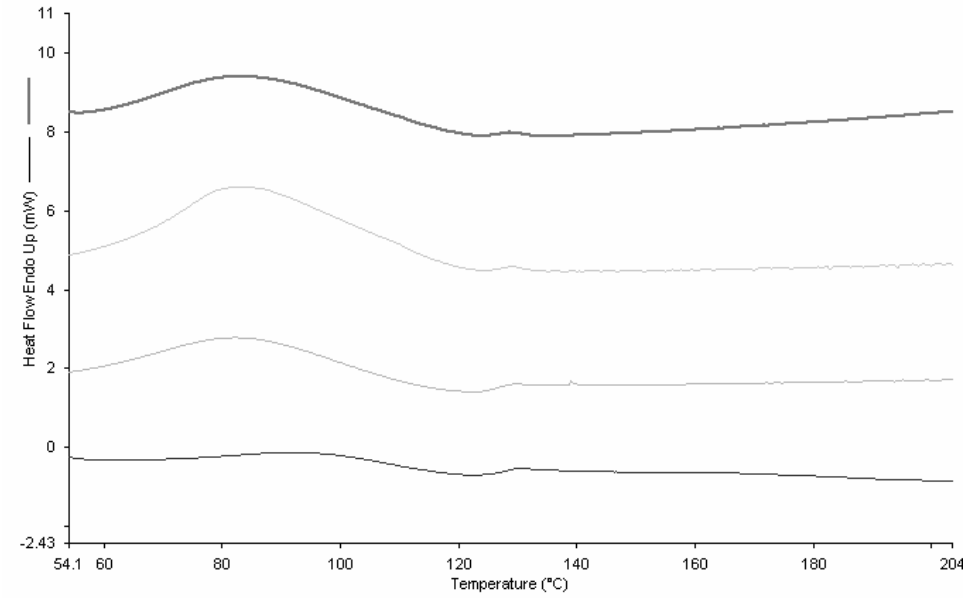


**Figure 2.** First heating DSC scans of aPA at different relative humidities. From top to bottom: 100%, 75%, 23% and 0% RH

What appears obvious from the DSC experiments is that the crystallinity appears to be heterogeneous in size or perfection due to the multiple melting endotherms observed, and that this does only occur in the presence of humidity, because in the crystallization and subsequent second melting step under nitrogen atmosphere this is no longer detected (see Figure 1). From previous work, it was found that the polymer is not able to disrupt the originally present hydrogen bonding between amide groups as a result of moisture sorption[7]. From the present results, however, it seems apparent that this material requires of heated moisture to weaken the strong inter- and intra-molecular bonding network established between the amide groups needed to rearrange certain chain segments as to yield lateral order.

The molecular structure of the autoclaved amorphous polyamide was also analyzed through the use of FT-IR spectroscopy. The FT-IR spectra of dry aPA and retorted aPA specimens are presented in Figure 3. The assignment of the major infrared bands of interest is summarized in Table 1.

**Table 1.** aPA FT-IR bands of interest and their most likely assignments

| Wavenumbers ($cm^{-1}$) | Band assignment |
|---|---|
| 3444 | "free" N-H stretch |
| 3310 | hydrogen-bonded N-H stretch |
| 3070 | aromatic C-H stretch |
| 2930 | asymmetric $CH_2$ stretch |
| 2850 | symmetric $CH_2$ stretch |
| 1630 | amide I mode |
| 1535 | amide II mode |
| ~1290 | amide III mode |
| 700 | amide V mode |

Figure 3a shows the $CH/CH_2$ and NH stretching range normalized to the intensity of the $CH_2$ symmetric stretch band at 2850 $cm^{-1}$ for comparison purposes. The intensity of the latter band has been found to be unaffected by water sorption and has been used before as internal standard for this polymer[8]. However, due to the partial crystallization of the autoclaved specimen this band is no longer adequate as internal standard in this study as it is usually sensitive to conformational changes. Irrespective of that, it is clear from observation of this Figure that several absorption bands have changed shape, position and/or relative intensity. It is known that, when a polymer sample crystallizes either new absorption bands and/or narrowing of the spectral features is often observed due to an increase in conformational regularity and other resulting effects like factor group splitting, etc.[9]. From observation of the spectrum, new bands and narrowing of some spectral feature does take place (see Figure 3).

a)

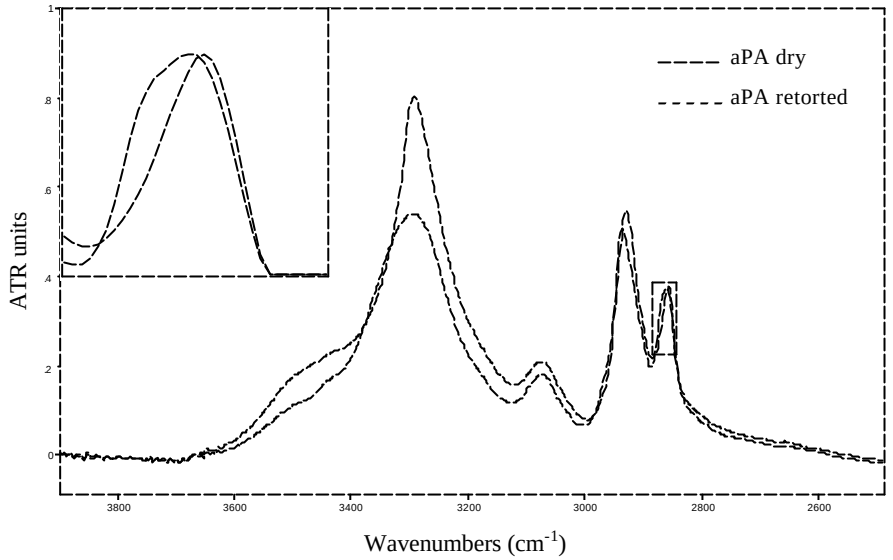


b)

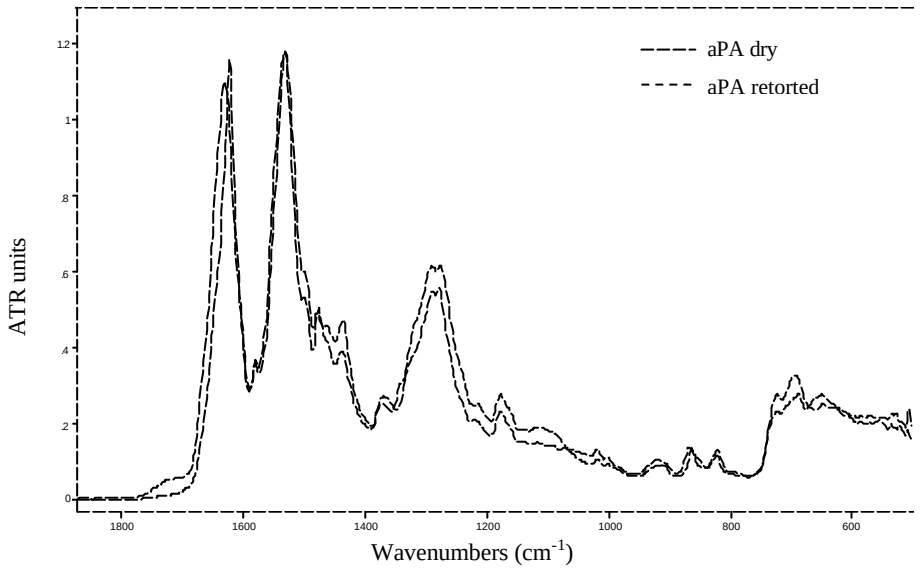


**Figure 3.** ATR-FT-IR spectra of dry (connected) and retorted (dotted) aPA specimens. (a) N-H and C-H stretching regions in the range 2600-3800 $cm^{-1}$; (b) amide I, II, III and V regions in the range 600-1800 $cm^{-1}$

The main difference between the spectra is observed in the N-H stretching region, which covers a range of about 3100-3500 $cm^{-1}$. The N-H stretching vibration is not a conformationally sensitive mode, but it is strongly sensitive to changes in hydrogen bonding. In a simplistic interpretation, the broad band envelope can be considered to be composed of two bands, namely, a dominant band centered at 3310 $cm^{-1}$ attributed to a distribution of hydrogen-bonded N-H groups, and a higher frequency small

shoulder band centered at 3444 $cm^{-1}$ attributed to "free" N-H groups. In the presence of humidity other water bands are observed in this vibrational range. In a previous study dealing with the FTIR spectrum of this sample[7], up to five different bands were found to constitute the complex band profile underlying this range.

The broadness of the hydrogen-bonded N-H band reflects, in large part, the distribution of hydrogen-bonded N-H groups of varying strengths dictated by distance and geometry. Given the "spaghetti-like" nature of random chain molecules, it is expected that there will be a distribution of distances and geometries of these hydrogen bonds formed between complementary N-H and C=O moieties[10]. However, after retorting, the highly absorbent N-H stretching mode at 3310 $cm^{-1}$ gets narrower; this indicates a more regular distribution and geometry of the N-H group vibrations. Moreover, the mentioned band appears to increase relative intensity and has slightly shifted towards lower wavenumbers. This tendency is opposite to that observed in the work of Skrovanek[11] et al., which described the effect of temperature in the FT-IR spectrum of an amorphous polyamide. In the latter work, the authors found that with increasing temperature, the IR active NH stretch band was found to shift towards higher wavenumbers and to decrease in intensity. The band shift reflects a decrease in the average NH bond length due to temperature-induced weakening of the polymer self-association, while the reduction in area of the hydrogen bonded N-H stretching mode with increasing temperature was mainly attributed to a decrease in the absorption coefficient. The latter result can be explained by the strong dependence found between the absorptivity coefficient and the hydrogen bond strength. Therefore, the apparently higher intensity displayed by this band in the retorted specimen would indicate both a narrowing effect of the band and a higher hydrogen bond strength which, in turn, will result in a more regular conformational state of the aPA polymer chains as in crystals.

Although both aPA samples (untreated and retorted) were dried in a dessicator before taking the IR spectra, the water band displayed in both spectra at approximately 3491 $cm^{-1}$, overlaps with the "free" N-H groups making difficult their quantification.

In contrast with the results observed in the case of water sorption[7], after autoclaving, the aromatic CH stretching band at 3075 $cm^{-1}$ is seen to shift to lower wavenumbers,

and the band corresponding to the CH symmetric stretching seems to split into two different components due to probably correlation field splitting or factor group splitting effects (see inset in Figure 3a). The latter observation strongly points again to the presence of crystalline order in the polymer.

The amide I and II modes are conformationally sensitive and, therefore, frequency shifts of these bands can also be related to changes in the polymer chains conformation. However, unlike the essentially isolated N-H stretching vibration, the amide I and II modes are more complex vibrations containing contributions from different functional groups (bond vibrations) and, as a result, the changes observed are difficult to interpret.

The amide I mode at 1630 $cm^{-1}$ which is considered to be comprised of contributions from mainly the C=O stretching but also from the C-N stretching and the C-C-N deformation vibrations, shifts towards lower wavenumbers and gets narrower after the retorting of the material. The amide II mode is a mixed mode containing contributions from the N-H in-plane bending, the C-N stretching and the C-C stretching vibrations. This band at 1535 $cm^{-1}$ also gets narrower and shifts towards lower wavenumbers after autoclaving. In general, it can be stated that narrower bands are related with more homogeneous bonds features, and therefore, with more ordered polymer structures. The displacement towards lower wavenumbers of both, amide I and II modes are related with an increase in bond length. These results are thus consistent with the shift observed for the hydrogen bonded NH stretching band. The displacement towards lower wavenumbers of, both, the hydrogen-bonded NH stretching band and the amide I band, are related with an increase in the bond length, and can be explained by the enhanced hydrogen bonding interactions established in the crystals and, therefore, with the presence of crystallinity.

Several changes in band shape, position and intensity are also observed in the amide III and V modes, which indicate the substantial changes that take place in the aPA structure as a consequence of retorting. However, these modes are highly mixed and will not be discussed further in this study.

The presence of crystallinity in the retorted amorphous polyamide was again confirmed by means of simultaneous SAXS and WAXS experiments on the polymer films. Figure 4 shows the WAXS patterns of an untreated, heated in boiling water and retorted aPA specimen. From this Figure it can be seen, that two crystalline peaks arise in the retorted sample: a more intense one at 2? ~18º and a weak band at 2? ~26º (see arrows). In agreement with DSC results, X-ray scattering studies did also reveal the presence of crystals in the specimen heated in boiling water. In agreement with the DSC results, the crystallinity diffraction peaks are less clearly defined for the latter sample and are, in general, poorly defined suggesting heterogeneity in crystal size and perfection. By curve-fitting determination of the area of the crystalline peaks under the amorphous halo of the WAXS pattern, it was found that the crystallinity of the retorted polymer film is around 5%.

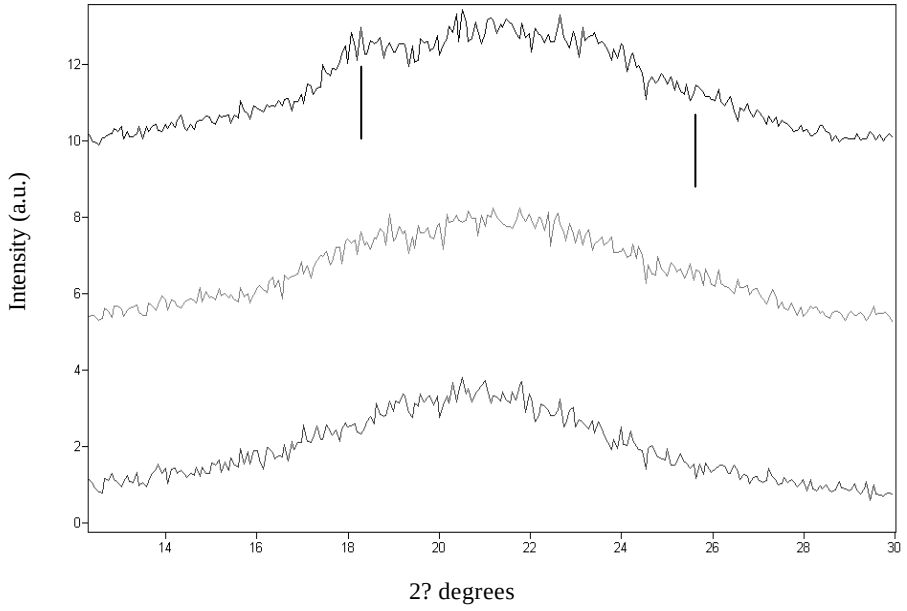


**Figure 4.** From top to bottom WAXS diffraction patterns of retorted, heated in boiling water and untreated amorphous polyamide

The presence of a periodic structure in the retorted aPA was further confirmed by a very weak shoulder that appears in the SAXS pattern of the retorted sample (see Figure 5). From this plot the maximum of the SAXS peak was determined to yield an average long period value ($L=L_c+L_a$) of 94 nm. By multiplying the repeat distance (L) by the determined crystallinity fraction, an average crystal thickness value ($L_c$) of

approximately 4.7 nm can be derived for the retorted specimen. This suggests indeed a very ill defined crystalline morphology for the sample.

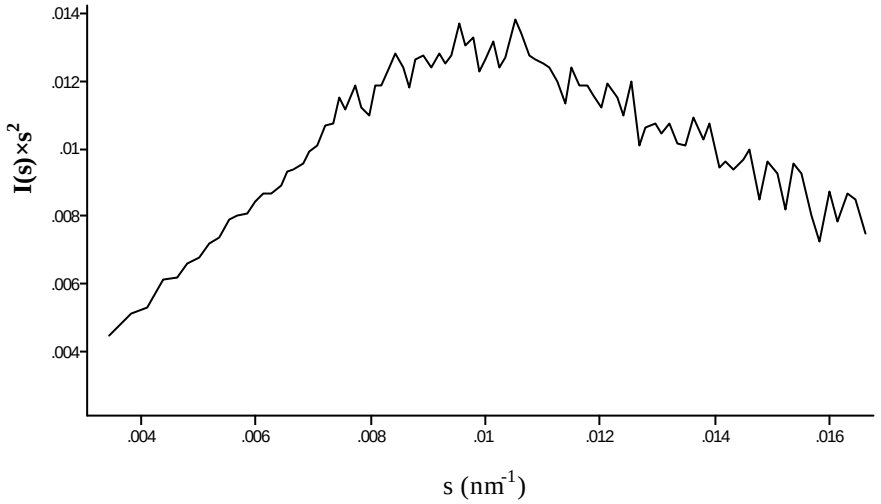


**Figure 5.** Lorentz-corrected SAXS pattern of retorted aPA

In order to determine how does the crystallinity develop in the sample, in-situ time-resolved simultaneous WAXS and SAXS synchrotron experiments were carried out both on dry aPA and on the sample specimen encapsulated in the presence of water. The evolution of the WAXS patterns of the untreated (heated up to 250ºC) and retorted aPA (during a typical in-situ retorting experiment) are displayed in Figure 6. Despite the relatively high noise signal born out of the fact that the film is a low scatterer specimen, it is observed that, in contrast with the amorphous halo seen along the heating of the untreated specimen, a crystalline peak at 2? ~18º develops in the autoclaved sample and becomes clearly detectable at around 110$^{o}$C. The latter peaks stays in the sample along the whole retorting experiment in agreement with the fact that after retorting the sample remains crystalline as determined by DSC.

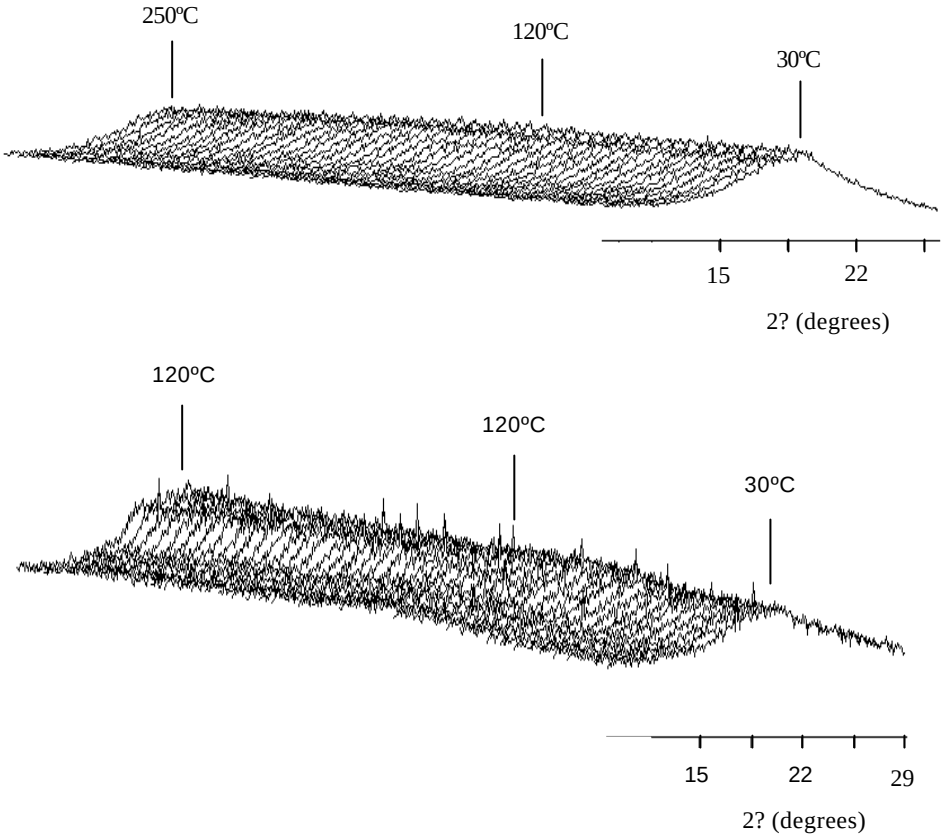


**Figure 6.** WAXS diffraction patterns of an amorphous polyamide during an in-situ heating experiment up to 250ºC of a dry specimen (top figure) and during an in-situ retorting experiment in the presence of water (bottom figure)

Further in-situ retorting experiments were also performed by DSC using sealed steel pans as retorting miniautoclaves. Figure 7a shows that during the initial heating step, an exothermic peak develops at ca. 90$^{o}$C and extends up to about 120$^{o}$C with maximum at ca. 105$^{o}$C and with a crystallization enthalpy of 28 J/g. During the 20 minutes isothermal step (Figure 7b) no further crystallization appears to take place in the sample and this indicates that the crystallization process extends in water along only the heating ramp and that the crystallization endset is around 115$^{o}$C. Given the relative broadness of the crystallization peak it is not surprising to find that the crystals formed during the autoclave process are of varying sizes and/or perfection.

**a)**

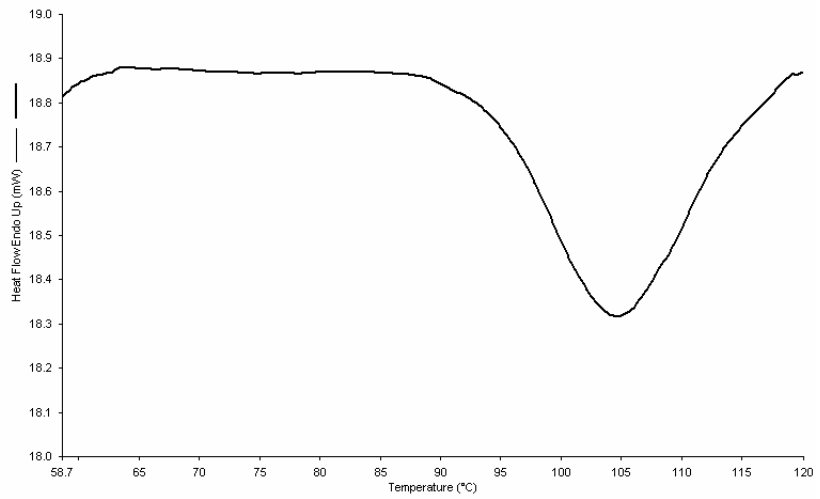


**b)**

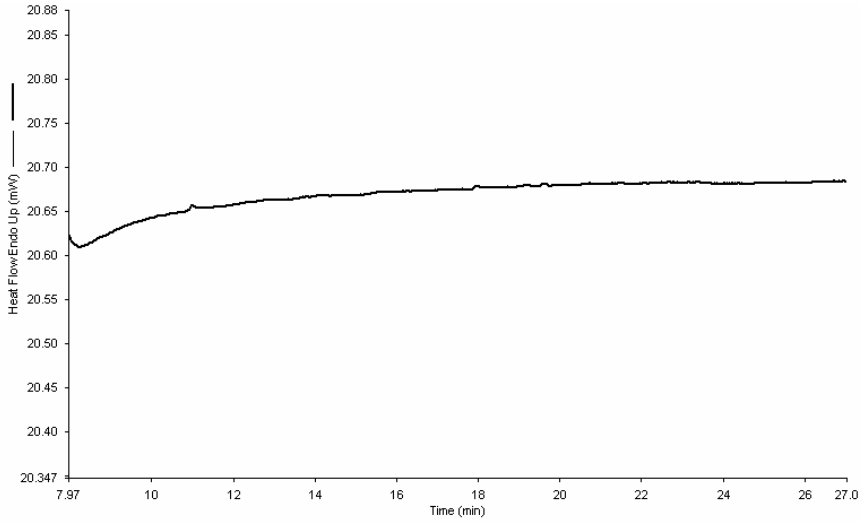


**Figure 7.** DSC curves of an amorphous polyamide during an in-situ retorting experiment. (a) Heating-curve showing the formation of crystals. (b) Holding-curve at 120ºC during 20 minutes

## Effect on transport properties

As crystallinity defines many properties, and this material is being currently studied, in among other applications, for food packaging, it was considered that a very relevant property for the application would be the barrier behavior for its strong implications in food quality and safety issues.

Because the material becomes very brittle when is retorted as a monolayer and that makes difficult to clamp the film to the oxygen permeability kit without failure, the sample was retorted protected between polypropylene layers, which is the usual multilayer configuration in retortable food packaging applications. Thus, the polyamide film was vacuum sandwiched between two layers of polypropylene (PP) before retorting, after that the PP was delaminated and the barrier layer released for barrier testing. The sample retorted between PP also underwent crystallization (checked by DSC enthalpy of fusion) but to a lesser extent (36.2 J/g of the aPA retorted without protection layers vs. 20 J/g of the aPA retorted between PP). The reason for this behavior is that even when PP offers barrier to water at ambient conditions, it is known to allow sufficient passage of moisture through it during retorting to have an impact on the barrier layer[2].

Figure 8 shows the $O_2$TR curves corrected for the thickness of the aPA films. From Figure 8, it can be observed that not only the permeability coefficient reached a clearly lower value for the retorted specimen, but also that the diffusion coefficient was found to be slightly lower for the "crystalline" aPA ($D_{untreated\ aPA}$= $8.24*10^{-14}$ $m^2/s$; $D_{retorted\ aPA}$= $7.85*10^{-14}$ $m^2/s$). As crystals are impermeable elements, they necessarily diminish solubility and diffusivity, the latter due to a more tortuous path for the permeant to travel across the thickness. In the equilibrium, the oxygen permeability values are 0.46±0.001 and 0.40±0.001 (cc*mm*atm)/($m^2$*day) for the untreated and retorted aPA respectively, that is, after retorting there is a reduction of around 10% of the original $O_2$ permeability value which, in turn, results in a better barrier performance of the retorted specimen.

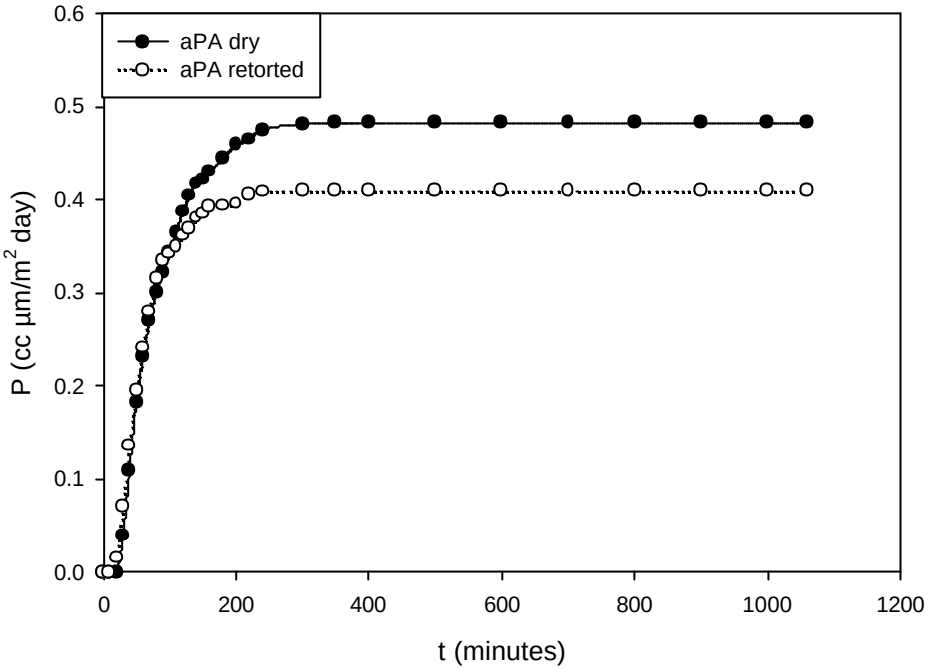


**Figure 8.** Oxygen permeability of untreated and retorted aPA

Figure 9 shows the water sorption curves obtained for the untreated and retorted aPA and, as expected, the sorption of this solvent was lower in the latter sample. While the uptake of sorbed water is about 8.1% ($W/W_{dry}$) for untreated aPA (in accordance with previous works[11]), the retorted specimen only sorbed 4.3%. The reason why the effect in water is stronger than in oxygen has probably got to do with the fact that the sample being tested for oxygen was autoclaved between PP protected layers and for water sorption was directly exposed.

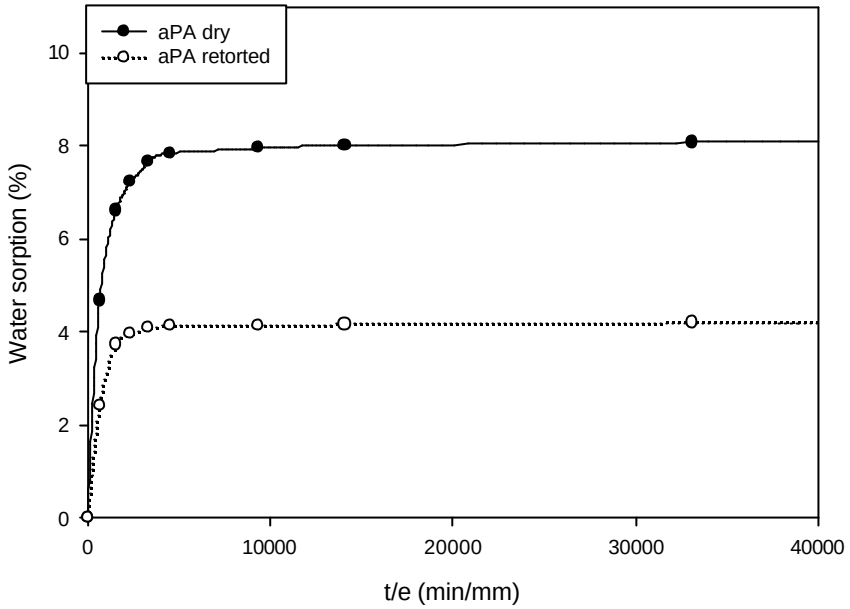


**Figure 9**. Water sorption of aPA dry (solid curve) and aPA retorted (dotted curve)

**ACKNOWLEDGMENTS**

The work performed at the synchrotron facility in Hamburg (Hasylab, Germany) was supported by the IHP-Contract HPRI-CT-1999-00040/2001-00140 of the European Commission and the authors acknowledge Dr. S. Funari and Mr. M. Dommach (Hasylab) for experimental support. ALR acknowledges the Spanish Ministry of Education and Science for the award of a FPI grant assigned to the project AGL2003-07326-C02-01.

## REFERENCES

[1] Tsai, B.C.; Jenkins, B.J. *Journal of Plastic Film and Sheeting* **1988**. *4*, 63-71.

[2] López-Rubio, A.; Lagarón, J.M.; Giménez, E.; Cava, D.; Hernandez-Muñoz, P.; Yamamoto, T.; Gavara, R. *Macromolecules* **2003**, *36*, 9467-9476.

[3] Zhang, Z.; Britt, I.J.; Tung M.A.. *Journal of Polymer Science Part B: Polymer Physics* **1999,** *37*, 691-699.

[4] López-Rubio, A.; Hernandez-Muñoz, P.; Giménez, E.; Yamamoto, T.; Gavara, R.; Lagarón, J.M. *Journal of Applied Polymer Science* **2005**, *96*, 2192-2202.

[5] López-Rubio, A.; Giménez, E.; Gavara, R.; Lagarón J.M. Accepted for publication in *Journal of Applied Polymer Science*.

[6] Granado, A.; Eguiazábal, J.I.; Nazábal, J. *Macromolecular Materials and Engineering* **2004**, *289*, 281-287.

[7]Lagarón, J.M.; Giménez, E.; Catalá, R.; Gavara, R. *Macromolecular Chemistry and Physics* **2003,** *204* (4), 704-713.

[8] Hernández, R.J.; Giacin, J.R.; Grulke, E.A. *Journal of Membrane Science* **1992**. *62*, 187-199.

[9] Mallapragada, S.K.; Narasimhan, B. Infrared Spectroscopy in Analysis of Polymer Crystallinity. *Encyclopedia of Analytical Chemistry*. R.A. Meyers (Ed.) **2000**. Copyright John Wiley & Sons Ltd.

[10] Skrovanek, D.J.; Howe, S.E.; Painter, P.C.; Coleman, M.M. *Macromolecules* **1985**, *18*, 1676-1683.

[11] Lagarón, J.M.; Giménez, E.; Gavara, R.; Saura, J.J. *Polymer* **2001**. *42***,** 9531-9540.

# EFFECT OF HIGH PRESSURE TREATMENTS ON THE PROPERTIES OF EVOH BASED FOOD PACKAGING MATERIALS

## INTRODUCCIÓN AL ARTÍCULO VI

En este artículo, publicado en la revista *Innovative Food Science and Emerging Technologies* (vid Anexo 3), se presentan los efectos de uno de los tratamientos de conservación de alimentos alternativos a la esterilización en autoclave sobre la estructura y propiedades de los copolímeros EVOH. Los tratamientos de conservación con altas presiones hidrostáticas, además de los ya comentados beneficios sobre la preservación de la calidad sensorial y nutritiva de los alimentos han demostrado no afectar de un modo negativo a las propiedades físicas del EVOH, incluso causando una ligera mejora en la morfología cristalina que se refleja en una disminución de la, ya de por sí, baja permeabilidad del material seco. Este artículo se engloba dentro del cuarto y último objetivo de la tesis.

**ABSTRACT**

The effects of different high pressure processing (HPP) treatments on EVOH based packaging materials were studied and they were compared with the morphological effects produced by a more traditional food preservation technology, i.e. sterilization. The samples were high pressure processed at 400 and 800 MPa, during 5 and 10 minutes at two different temperatures, 40 and 75ºC. Sterilization was carried out in an autoclave at 120ºC during 20 minutes. Oxygen barrier and morphological properties of the treated packaging structures were analyzed and compared with those of the untreated samples. The results proved that HPP scarcely affects packaging materials, especially when compared with the detrimental consequences of retorting.

Keywords: High pressure processing, EVOH, packaging materials, oxygen permeability, morphological properties

## INTRODUCTION

In many food industrial processes, food is packaged prior to the application of the preservation technology (like thermal treatments) in order to optimize preservation processes and minimize product manipulation. Therefore, the package is incorporated in the same production line and the preservation technologies are applied to the already packaged product. Commonly employed heat treatments, like pasteurization and sterilization, require airtight high-barrier retortable materials, such as film structures containing ethylene-vinyl alcohol copolymers (EVOH). These copolymers are one of the most widely used families of semicrystalline materials because, apart from being an excellent barrier to oxygen and aroma compounds, they also have high chemical resistance to organic compounds (aroma components or ink solvents), excellent chemical and optical characteristics, good thermal resistance and very fast crystallization kinetics. The high oxygen barrier characteristic of EVOH materials is provided by the hydroxyl groups of their structure which confer them with a high cohesive energy, reducing the free volume between the polymeric chains available for gas exchange. However, these hydroxyl groups make the copolymers water sensitive and, therefore, in high relative humidity environments, their barrier characteristics is greatly impaired. For that reason, in most packaging applications, EVOH is used in multilayer structures, sandwiched between at least two layers of an hydrophobic material such as polyethylene or polypropylene. Previous studies carried out in our lab showed that, even protected by hydrophobic layers, the oxygen permeability of the copolymers is greatly deteriorated during sterilization processes (López-Rubio, Lagarón, Giménez, Hernández-Muñoz, Yamamoto & Gavara, in press; Lagarón, López-Rubio, Giménez, Catalá, Yamamoto, Saito et al., 2004).

On the other hand, consumer preferences towards mildly preserved, high quality and more fresh-like products are leading to the substitution of these traditional thermal treatments by other emerging preservation technologies based on the application of irradiation, microwave pasteurization, electric fields, high hydrostatic pressure and their combination with mild thermal treatments.

Among these emerging technologies, high pressure processing (HPP) is receiving a great deal of attention due to its unique advantages over conventional thermal treatments, including application at low temperatures, which improves the retention

of food quality. High pressure treatments are independent of product size and geometry and their effect is uniform and instantaneous (Palou, López-Malo, Barbosa-Cánovas & Swanson, 1999). Most of the HPP equipments work in batch processes. Foodstuffs are packaged at the end of the production line and then, they are pressurised at hundreds MPa levels to produce a high nutritional and sensorial quality product, with more desirable texture and longer shelf-life (Ledward, 1995). The application of high pressure to a food product during a short period of time results in enzyme deactivation and reduction of microorganisms, effects which are intensified when the process is combined with temperature (40-75ºC) (Roberts & Hoover, 1996).

To increase the efficiency of the process, the package and the packaging process must be carefully selected. First, the package must be flexible enough to transfer the pressure to the food product without fracture or distortion of the package (Mertens, 1993) since, generally, the high pressure package is the retailer package and, therefore, it must have consumer appeal. Additionally, vacuum packaging is the selected packaging technology since the presence of voids with air produces a non-uniform treatment and can lead to food or package distortion. Finally, transparency of the film may add marketing advantages. Once the product has been correctly packaged, the food can be high pressure processed irrespective of size and geometry. To increase the shelf-life of processed foods, the package must be designed with an adequate oxygen barrier material. Among potential solutions, polyamides and EVOH copolymers add good and excellent barrier to oxygen, respectively, without compromising flexibility or transparency (Catalá & Gavara, 1996; Ozen & Floros, 2001).

It is then crucial to understand the effects of high pressure on relevant properties of plastic materials to assure the safety of the foodstuffs along their shelf-life but, at the present moment, there are very few studies dealing with this subject.

In this work, EVOH-based packaging structures have been HPP treated at various hydrostatic pressures, temperatures and periods of exposure. The effect of HPP on permeability and morphology of the selected materials has been studied and compared to the effect of thermal sterilization.

## EXPERIMENTAL

### Materials

Two commercial ethylene-vinyl alcohol (EVOH) copolymers supplied by the Nippon Synthetic Chemical Industry Co. Ltd (Nippon Gohsei, Osaka, Japan) were analyzed: EVOH26 and EVOH48, where the number indicates the mol percentage of ethylene in the copolymer composition. Coextruded multilayer structures comprising polypropylene (PP)(100µm)/EVOH(10µm)/PP(100µm) (with adhesive) were used as received. Monolayer 10µm EVOH26 and EVOH 48 films were also subject of study. These materials were shipped as PP/EVOH/PP structures without adhesive. PP layers protect EVOH films during the treatments and are easy to peel off before testing.

### Methods

*High Hydrostatic Pressure Processing*

The films were cut into 10 x 10 cm pieces and placed inside polyethylene pouches. Each pouch was then filled with 150 mL distilled water and sealed, without headspace, using a Multivac 021-336 impulse sealer (Busch, Switzerland). Thus, the tested films did not directly contact the high pressure transmission fluid. Three replicates were prepared for each film and HPP condition.

HPP was performed with a QFP-6 Flow Batch High Pressure Food Processor (Flow Autoclave System, Columbus, OH). This equipment had a 1 L pilot-scale processing vessel measuring 6.0 cm in diameter and 18.8 cm in length. The high pressure transmission fluid used in this equipment was Houghto-Safe 620-TY (Houghton International, Valley Forge, PA), a glycol/water mixture. The HPP conditions were 400 and 800 MPa, for 5 and 10 min, at 40 and 75°C.

*Oxygen Transmission Rate*

The oxygen transmission rate through the extruded specimens was measured at 45ºC under dry conditions using an Oxtran 2/20 instrument (Modern Control Inc., Minneapolis, MN, USA).

*Differential Scanning Calorimetry*

DSC experiments were carried out in a Perkin-Elmer DSC-7 calorimeter. The heating and cooling rate for the runs was 10ºC/min, being the typical sample weight around 8 mg. Calibration was performed using an indium sample. All tests were carried out, at least, in duplicate. The temperature range of the assays was from 15 to 220ºC. From the thermograms, the melting temperature was determined from the maximum of the endotherm.

*Fourier Transform Infrared Spectroscopy*

Transmission FT-IR experiments were recorded with a Bruker Tensor 37 equipment with 4 $cm^{-1}$ resolution and 4s as typical acquisition time. Before FT-IR tests, films were dried at 70$^{o}$C in vacuum for over a week (preconditioning given to all samples before testing).The samples were placed into the measuring chamber which was continuously purged with a high flux of $N_2$ to maintain a constant dry and inert environment.

*X-Ray diffraction*

Simultaneous wide and small angle X-ray scattering (WAXS and SAXS) experiments were carried out at the synchrotron radiation source in the polymer beam A2 at Hasylab (DESY) in Hamburg (Germany). Scattering patterns were recorded using a one-dimensional detector and an incident radiation wavelength, ?, of 0.15 nm. WAXS and SAXS data were corrected for detector response and beam intensity and calibrated against PET and rat tail standards.

## RESULTS AND DISCUSSION

After the high pressure treatment, both the PP-protected structures and the unprotected EVOH films showed no signs of damage and did not present whitening or blistering, consequences which have been reported in samples retorted at temperatures above 100ºC (Aucejo, Catalá & Gavara, 2000; Koros, 1990; Tsai & Wachtel, 1990).

### *Oxygen transmission rate*

Table 1 shows the oxygen transmission rate values obtained for the different samples. As stated before, the excellent barrier property of EVOH copolymers is provided by their vinyl alcohol fraction and, therefore, it is logical that the structures containing higher vinyl alcohol content copolymers (i.e. PP/EVOH26/PP) display lower oxygen transmission rates. However, when compared with higher ethylene content copolymers, such as EVOH48, their oxygen barrier is clearly more deteriorated after sterilization and the original value of oxygen permeability is not completely recovered even after 150 hours of continuous testing at 45ºC. In contrast with the tremendous impact of sterilization over the permeability of the copolymers (see the oxygen transmission rate values for the just-retorted samples), HPP does not alter significantly the oxygen permeability of EVOH. Moreover, for almost every high-pressure treatment given to the polymeric structures, slightly better barrier properties are observed, being this improvement more pronounced for the copolymer with lower ethylene content, i.e. EVOH26.

**Table 1.** Oxygen transmission rate (cc/m$^2$day) of multilayer structures PP//EVOH//PP high-pressure processed, retorted and untreated

| | EVOH26 | EVOH48 |
|---|---|---|
| non treated | 0.60 | 40.88 |
| 400MPa, 40ºC, 5' | 0.44 | 39.24 |
| 400MPa, 75ºC, 5' | 0.36 | 41.00 |
| 800MPa, 40ºC, 5' | 0.50 | 39.63 |
| 800MPa, 75ºC, 5' | 0.62 | 37.50 |
| 400MPa, 40ºC, 10' | 0.50 | 37.00 |
| 400MPa, 75ºC, 10' | 0.48 | 38.25 |
| 800MPa, 40ºC, 10' | 0.58 | 39.38 |
| 800MPa, 75ºC, 10' | 0.59 | 38.13 |
| retorted | 392.00 | 645.00 |
| retorted (after 150h) | 1.63 | 28.55 |

Masuda (1992) also investigated the oxygen permeability of the same basic packaging structure (PP/EVOH/PP) and of oPP/EVOH/PE, PVDC-coated oPP/cPP and PET/Al/cPP. They found that the high-pressure treatment applied did not change initial oxygen barrier properties. Similar studies carried out have confirmed that, in general, the barrier properties of plastic packaging structures are not significantly affected by the common high-pressure treatments employed in food processing (Lambert, Demazeau, Largeteau, Bouvier, Laborde-Croubit & Cabannes, 2000; Schauwecker, Balasubramaniam, Sadler, Pascall & Adhikari, 2002). On the other hand, packaging structures containing metallized layers are susceptible to suffer from permeability changes as a result of high-pressure processes, as demonstrated by Caner (2000). This increase in permeance observed, can be explained by the lower compression rate of metals which can provoke delamination of the packaging structures or discontinuities in the metal coating caused by the low mechanical resistance of the thin aluminum layer.

*Morphological characterization*

DSC experiments were carried out to compare the thermal characteristics of the different samples. This technique provides information on several parameters related

to polymer morphological features like crystallinity or crystal size. The results obtained for the EVOH26 and the EVOH 48 are displayed in Table 2.

**Table 2.** DSC results for the EVOH26 and EVOH48 samples non-treated, retorted and HHP processed. Tm (melting point in ºC), ΔH (enthalpy of fusion in J/g) and width (peak width in ºC) covering 70ºC from the endset

| | EVOH26 | | | EVOH48 | | |
|---|---|---|---|---|---|---|
| **Treatment** | **Tm** | **ΔH** | **Width** | **Tm** | **ΔH** | **Width** |
| Non-treated | 193.67 | 71.97 | 13.79 | 155.33 | 58.27 | 18.50 |
| Retorted | 191.61 | 58.60 | 18.64 | 154.39 | 57.99 | 19.69 |
| 400MPa, 40ºC, 5min | 193.58 | 77.89 | 14.60 | 156.50 | 59.16 | 18.19 |
| 400MPa, 40ºC, 10min | 194.67 | 73.98 | 14.70 | 154.83 | 69.33 | 17.64 |
| 400MPa, 75ºC, 5min | 194.33 | 78.75 | 14.15 | 155.00 | 56.26 | 18.65 |
| 400MPa, 75ºC, 10min | 193.75 | 73.02 | 13.66 | 155.33 | 56.64 | 18.00 |
| 800MPa, 40ºC, 5min | 193.83 | 68.12 | 14.82 | 154.83 | 65.63 | 16.19 |
| 800MPa, 40ºC, 10min | 193.08 | 75.28 | 14.08 | 155.50 | 59.28 | 17.69 |
| 800MPa, 75ºC, 5min | 193.67 | 75.67 | 13.75 | 155.17 | 60.59 | 17.31 |
| 800MPa, 75ºC, 10min | 194.25 | 73.88 | 14.64 | 155.00 | 64.55 | 18.07 |

The reported increase in permeability for the retorted EVOH26 copolymer can be understood by direct comparison of the DSC data obtained for the retorted and the untreated sample. The lower melting point and enthalpy of fusion of the retorted film point out the lower crystal size and less crystallinity, respectively. Moreover, the thermograms (shown in figure 1) also reflected a broader melting peak of the retorted sample. This can be the result of a crystal fractionation which yields a broader distribution of crystal sizes, a higher crystal heterogeneity, and consequently a wider melting temperature range. In contrast, the melting behavior of HPP EVOH26 samples is not significantly different from that of the untreated material. In several specimens even a slight increase in the melting point is observed. Higher melting enthalpies were also obtained for most of the high pressure processed samples, which suggest a pressure-induced crystallinity development (see peak width column in Table 2 and thermogram in Figure 1).

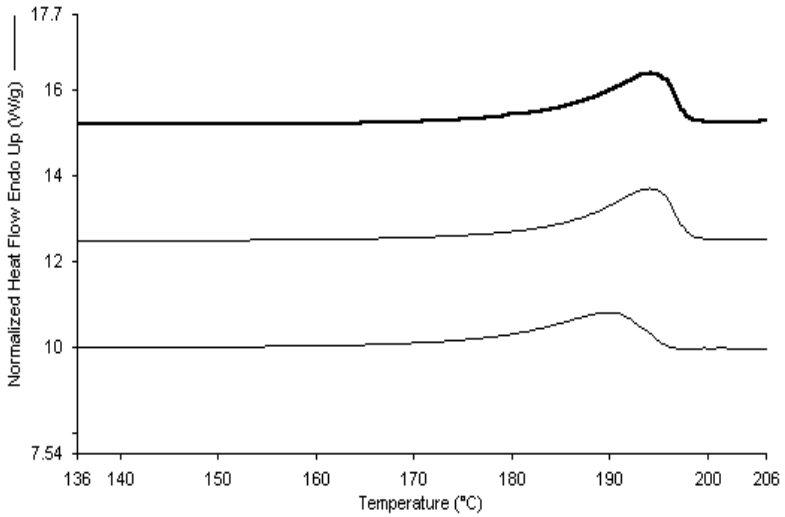


**Figure 1.** DSC thermograms of EVOH specimens delaminated from PP/EVOH/PP structures after the following treatments: from top to bottom, untreated, HPP at 400MPa, 40ºC, 5 minutes and retorted.

Similar results were obtained for the EVOH48, but in this case fewer differences are observed, both for the retorted sample and for the high pressure treated polymers. As mentioned before, sterilization is not so harmful for this copolymer grade. The differences between DSC parameters are less pronounced and barrier properties are totally recovered after a certain period of time (see Table 1). In fact, after 150 hours following sterilization, the oxygen transmission rate of the retorted EVOH48 is better than that of the untreated specimen. The explanation of this phenomenon is still unclear (it is, at the present moment, under investigation). From the results, there is no evident correlation between the changes observed and the different HPP variables (pressure applied, temperature and time of exposure).

Thermal characteristics of EVOH have also been analyzed after submitting a multilayer structure of nylon/EVOH/polyethylene to 690 MPa at 95ºC during 10 minutes (Schauwecker et al, 2002). DSC results showed no differences in the heat flow curves between controls and EVOH films treated. It is not specified the copolymer grade used for this study, but EVOH32 is usually employed as it is the copolymer of choice for most commercial applications.

X-ray experiments performed using a Synchrotron radiation source demonstrated the poor resistance to temperature of the copolymers in the presence of water. Through time-resolved experiments it was proven that a dry sample of EVOH32 melts around 183ºC (in accordance with DSC results), but when the same copolymer grade was heated in the presence of water (simulating a retorting process), the crystalline patterns completely disappeared at ca. 100ºC, i.e. 83ºC below its actual melting point (López-Rubio, Lagarón, Giménez, Cava, Hernández-Muñoz, Yamamoto et al., 2003). As an example, in Figure 2, the diffractograms of EVOH26 untreated and retorted are presented. After retorting, the peak becomes broader and less defined, indicating the disruption of the crystalline structure which is, obviously, more heterogeneous, probably due to crystal fractionation. These results are in agreement with the wider melting temperature range observed by DSC, previously commented.

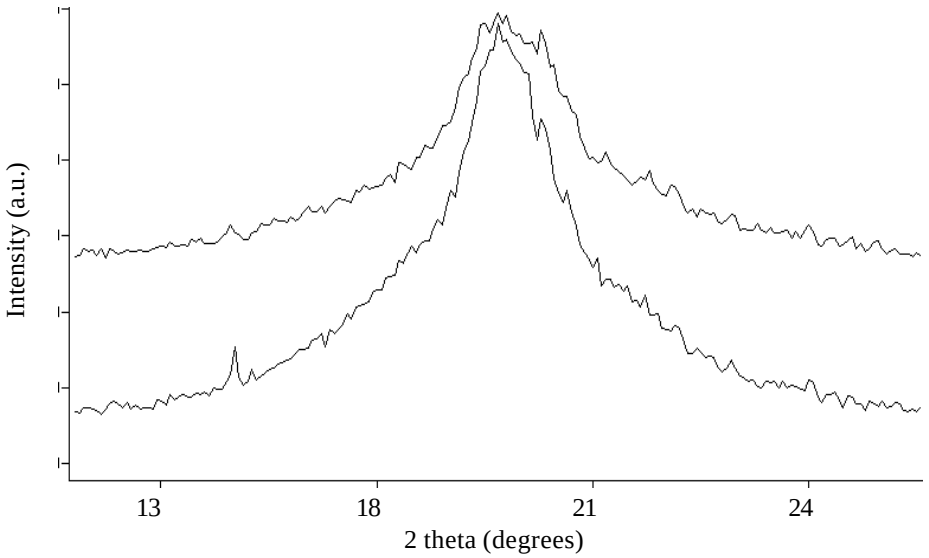


**Figure 2.** Diffractograms of untreated (down) and retorted (upper peak) EVOH26 specimens

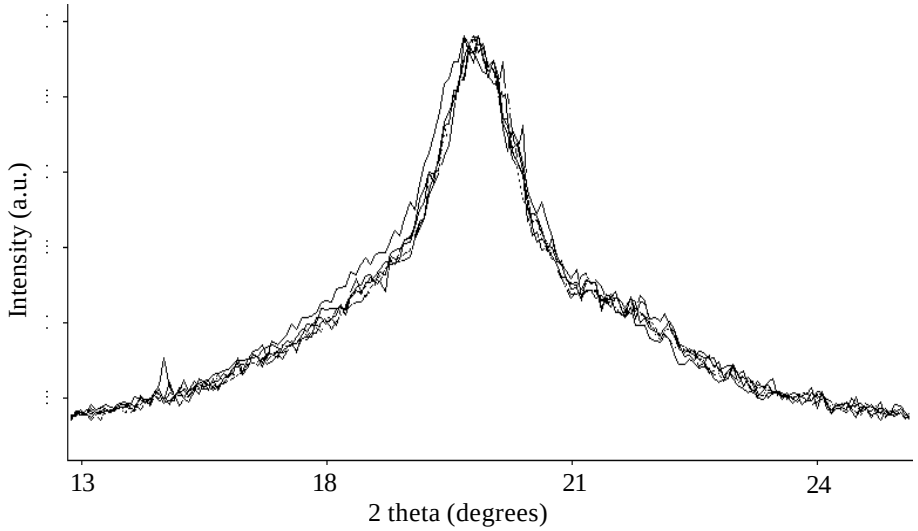


**Figure 3.** Diffractograms of untreated (peak slightly displaced towards lower angle) and HPP treated EVOH26 specimens

Few changes are observed between the diffractograms of untreated and HPP copolymers. Figures 3 and 4 show the crystalline peaks obtained for the various EVOH26 and EVOH48 samples, respectively. In the case of EVOH26, peaks corresponding to the high pressure treated samples are a bit narrower and slightly displaced towards higher angles, what may indicate a certain improvement of their crystalline structure.

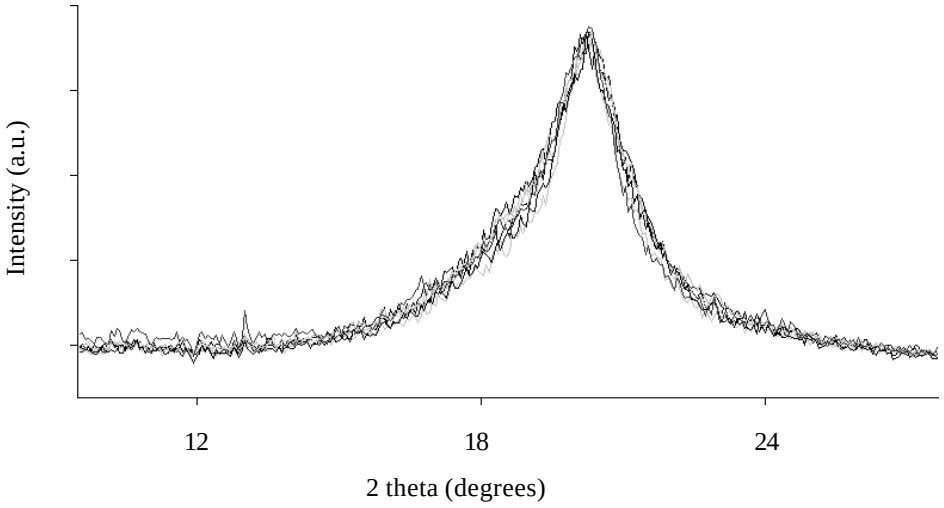


**Figure 4.** Diffractograms of untreated and high pressure processed EVOH48 specimens

In order to corroborate all previous results, FT-IR experiments were also carried out, because this spectroscopy technique has been proven to be a very useful tool to analyze the crystalline structure of EVOH copolymers, due to its sensitivity to detect both, crystallinity alterations through the use of the 1140 $cm^{-1}$ band (likely assigned to C-O-C stretching or to C-C stretching coupled with a C-O stretching mode) and the presence of humidity in the sample through observation of the OH in plane bending band at 1650 $cm^{-1}$. The 1333 $cm^{-1}$ band is considered an internal standard as the intensity of this band does not appear to change. Therefore, the absorbance of the 1140 $cm^{-1}$ band divided by that of the internal standard at 1333 $cm^{-1}$ can give us an indication of potential alterations in crystallinity after the various treatments irrespective of differences in optical path and of minor thickness variations between different specimens. These values are collected in table 3.

**Table 3.** FT-IR absorbance of the crystallinity band (1140 $cm^{-1}$), internal standard band (1333 $cm^{-1}$) and their ratio for EVOH26 specimens non treated and high pressure processed.

| | 1333 $cm^{-1}$ | 1140 $cm^{-1}$ | 1140/1333 |
|---|---|---|---|
| 400MPa, 40ºC, 5' | 0.8640 | 1.1069 | 1.2811 |
| 400MPa, 40ºC, 10' | 0.8640 | 1.1063 | 1.2804 |
| 400MPa, 75ºC, 5' | 0.8640 | 1.0933 | 1.2654 |
| 400MPa, 75ºC, 10' | 0.8640 | 1.1145 | 1.2899 |
| 800MPa, 40ºC, 5' | 0.8640 | 1.1066 | 1.2808 |
| 800MPa, 40ºC, 10' | 0.8640 | 1.1194 | 1.2956 |
| 800MPa, 75ºC, 5' | 0.8640 | 1.0927 | 1.2647 |
| 800MPa, 75ºC, 10' | 0.8640 | 1.1110 | 1.2858 |
| non treated | 0.8640 | 1.0801 | 1.2501 |
| retorted | 0.8640 | 1.0028 | 1.1606 |

Figure 5 shows FT-IR spectra obtained for untreated and retorted EVOH26 specimens. From these experiments, the previous rationalization of the retorting effects is now confirmed. During sterilization, pressurized water is capable of traversing the hydrophobic polypropylene layers, reaching the intermediate EVOH layer and sorbs onto it, as it is reflected by the increase in the 1650 $cm^{-1}$ band. Moreover, the lower intensity in the 1140 $cm^{-1}$ band displayed by the retorted sample and the lower ratio between the 1140/1133 bands, clearly indicates the loss in crystallinity as a consequence of the combined effect of water vapor and temperature.

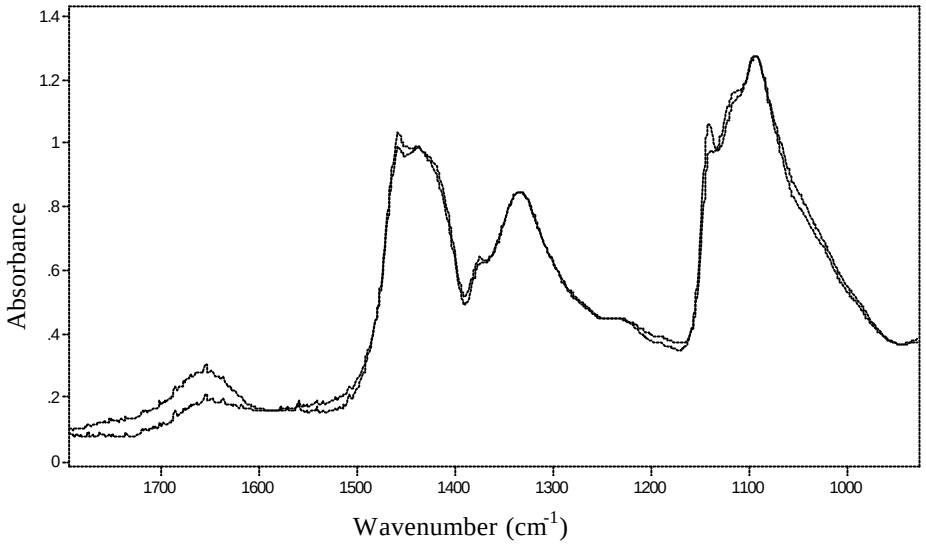


**Figure 5.** FT-IR spectra of EVOH26 specimens untreated (dotted line) and retorted

In the case of HPP samples, the FT-IR spectra showed equivalent functional group absorbance bands. The average of these bands for the EVOH48 did not change significantly after the treatments (results not shown). On the other hand, Figure 6 clearly shows an increase in the absorbance of the crystallinity band (i.e. 1140 $cm^{-1}$ band) for the high pressure treated EVOH26 specimens. Although EVOH samples were surrounded by water during the pressurization there is not an increase in the absorbance of the 1650 $cm^{-1}$ band as in the case of the retorted sample (see insert in Figure 6). In order to quantify the crystallinity changes observed as a consequence of the various treatments applied, the ratios between the crystallinity band and the internal standard band were calculated. The results, displayed in Table 3, indicate that for every high pressure treatment applied to PP/EVOH26/PP packaging structures, the crystallinity of the high barrier material is higher than that of the as-received material. Both, figure 6 and table 3 also reflect that this effect is more significant at higher pressures and longer exposure periods.

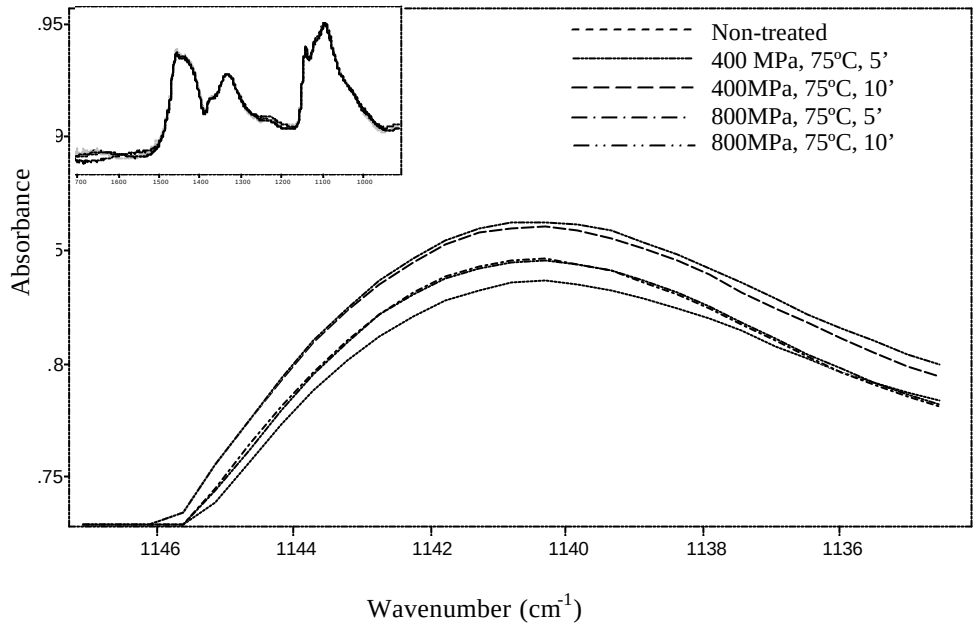


**Figure 6.** FT-IR spectra of EVOH26 specimens untreated (dotted line) and high pressure treated at the region of the 1140 $cm^{-1}$ band. Broader spectral range is shown as an insert.

## CONCLUSIONS

From the results obtained in this work, it is possible to assert that plastic packaging structures containing EVOH as barrier layer are suitable to be used in high pressure treatments of food. In contrast to sterilization processes which cause a crystallinity disruption of ethylene-vinyl alcohol copolymers, HPP does not affect significantly the structure of the copolymers with high ethylene content (EVOH48) and, moreover, a slight improvement in crystalline morphology is observed for the EVOH26, which results in even better barrier properties than the non treated material.

## REFERENCES

Aucejo, S., Catalá, R. & Gavara, R. (2000). Interactions between water and EVOH food packaging films. *Food Science and Technology International, 6,* 159-164.

Caner, C., Hernandez, R.J. & Pascall, M.A. (2000). Effect of High-pressure Processing on the Permeance of Selected High-barrier Laminated Films. *Packaging Technology and Science, 13,* 183-195.

Catalá, R. & Gavara, R. (1996). Alternative high barrier polymers for food packaging. *Food Science and Technology International, 2,* 281-291.

Koros, W.J. (1990). Barrier Polymers and Structures: Overview. In W.J. Koros, *Barrier Polymers and Structures* (1-21). ACS Symposium Series 423, Washington DC.

Lagarón, J.M., López-Rubio, A., Giménez, E. Catalá, R., Yamamoto, T., Saito, Y. & Gavara, R. A novel understanding of industrial retorting in ethylene-vinyl alcohol copolymers used in retortable food packaging applications. In *Conference ANTEC2004,* Chicago, 16-20 May 2004.

Lambert, Y., Demazeau, G., Largeteau, A., Bouvier, J.M., Laborde-Croubit, S. & Cabannes, M. (2000). Packaging for High-pressure Treatments in the Food Industry. *Packaging Technology and Science, 13* (2), 63-71.

Ledward, A.D. (1995). High pressure processing - the potential. In A.D. Ledward, D.E. Johnston, R.G. Earnshow & A.P.M. Hasting, *High Pressure Processing of Foods* (pp. 1-5). Nottingham University Press, Nottingham.

López-Rubio, A., Lagarón, J.M., Giménez, E., Cava, D., Hernández-Muñoz, P., Yamamoto, T. & Gavara, R. (2003). Morphological alterations induced by Temperature and Humidity in Ethylene-Vinyl Alcohol Copolymers. *Macromolecules, 36,* 9467-9476.

López-Rubio, A., Lagarón, J.M., Giménez, E., Hernández-Muñoz, P., Yamamoto, T. & Gavara, R. Gas barrier changes and morphological alterations induced by retorting in ethylene-vinyl alcohol based food packaging structures. *Journal of Applied Polymer Science,* in press.

Masuda, M., Saito, Y., Iwanami, T. & Hirai, Y. (1992). Effect of hydrostatic pressure on packaging materials for food. In C. Balny, R. Hayashi, K. Heremans & P. Masson, *High Pressure and Biotechnology* (pp. 545-548). John Libbey Eurotex: Paris.

Mertens, B. (1993). Packaging aspects of high-pressure food processing technology. *Packaging Technology and Science, 6,* 31-36.

Ozen, B.F. & Floros, J.D. (2001). Effects of emerging food processing techniques on the packaging materials. *Trends in Food Science and Technology, 12,* 60-67.

Palou, E., López-Malo, A., Barbosa-Cánovas, G.V. & Swanson, B.G. (1999). High-Pressure Treatment in Food Preservation. In M. S. Rahman, *Handbook of Food Preservation* (pp. 533-576). Marcel Dekker, New York.

Roberts, C.M. & Hoover, D.G. (1996). Sensitivity of Bacillus coagulans spores to combinations of high hydrostatic pressure, heat, acidity and nisin. *Journal of Applied Bacteriology, 81,* 363-368.

Schauwecker, A., Balasubramaniam, V.M., Sadler, G., Pascall, M.A. & Adhikari, C. (2002). Influence of High-pressure Processing on Selected Polymeric Materials and on the Migration of a Pressure-transmitting Fluid. *Packaging Technology and Science 15* (5), 255-262.

Tsai, B.C. & Wachtel, J.A. (1990). Barrier Properties of Ethylene-Vinyl Alcohol Copolymer in Retorted Plastic Food Containers. In W.J. Koros, *Barrier Polymers and Structures* (192-202). ACS Symposium Series 423, Washington DC.

# RADIATION-INDUCED OXYGEN SCAVENGING ACTIVITY IN EVOH COPOLYMERS

## INTRODUCCIÓN AL ARTÍCULO VII

A continuación se muestran los efectos de la irradiación sobre la estructura y propiedades de los copolímeros de etileno y alcohol vinílico (EVOH). Con este artículo se cubre el objetivo final de la tesis, en el que se muestran los efectos de otro tratamiento emergente de conservación de alimentos (aparte de la esterilización y las altas presiones) que también se aplica sobre los productos ya envasados.

Este artículo, como el artículo 3, se encuentra en fase de preparación.

En los resultados presentados se pone un especial énfasis en el fenómeno de absorción de oxígeno observado tras la irradiación del material y que, aunque en principio pudiera ser considerado de interés en el envasado de alimentos sensibles a este gas, deriva de un daño morfológico irreversible en el que una vez han reaccionado todos los radicales libres con el oxígeno permeante, deja una estructura más "abierta" y menos cohesionada con peores propiedades barrera que las presentadas por el material original.

## INTRODUCTION

Irradiation of prepackaged foodstuffs using gamma and electron beam radiation is gaining ground as a method of food preservation. Although widely used in USA, the commercialization of irradiated products in many European countries is rather limited due to strict regulations concerning the labeling of the food products and to the lack of information given to consumers about the harmlessness of irradiated food over consumers' health.

In order to enhance the protection offered by irradiation, foodstuffs are usually prepackaged in flexible packaging materials prior to the treatment and, in that way, subsequent recontamination by microorganisms is prevented. Moreover, this technique is also being used for the sterilization of flexible packages utilized later on in aseptic packaging technology[1].

The advantages of this technique include:

- It can be used at room temperature and therefore the nutritional characteristics of the food products are maintained
- The treatment offers a reliable sterilization
- The operation is safe and relatively easy and
- The irradiation dose and dose rate can be easily controlled[2].

However, irradiation also presents a number of limitations:

- The irradiation doses allowed for food sterilization cannot inactivate enzymes and, thus, it is necessary to use it in combination with heat, for example, to achieve a complete stabilization of food products
- The irradiation is neither capable of inactivating viruses and microbial toxins and, therefore, in certain applications it cannot totally assure food safety[3]
- Irradiation can induce organoleptic changes, specifically in fatty products. For example, the irradiation in milk is not feasible because doses of 0,5 kGy provoke aroma alterations[4]
- Due to the variability of the food products, it is difficult to standardize the treatment[5, 6].
- As a consequence of irradiation, radiolysis products from the packaging materials may be liberated to the inner package atmosphere and affect the sensory properties and even the safety of prepackaged food products[7].

Concerning this last aspect, plastics are affected in various ways when exposed to high-energy radiation. The polymer chains may exhibit scission, cross-linking[8], free radical production[9,10], formation of gases and low molecular weight radiolysis products[11], discoloration and formation of unsaturated bonds[12]. The dominant effect depends on the particular material, additives used in the plastic, radiation dose and irradiation conditions[13]. Obviously, physical and chemical changes in plastics as a result of irradiation are of prime importance since they can affect the quality of the packaged food products. Probably due to the lack of information, there are limited number of polymers approved under current regulatory standards of the United States Food and Drug Administration (USFDA)[14]. USFDA states that any dietary constituent is below the threshold of regulation (TOR) if it occurs at less than 0.5ppb in the diet[15], and it has been demonstrated that all the radiolytic and non-radiolytic products of ethylene-vinyl alcohol (EVOH) copolymers are within this TOR (safe limit), so in principle, this confirms the safety of irradiated EVOH as a food contact material.

Although apart from the formation of radiolytic compounds, changes in structure and properties have been already studied for EVOH, to the best of our knowledge the radiation-induced oxygen scavenging activity that show these copolymers has not been described before.

The aim of this paper is to study the potential structural modifications that explain the curious behaviour observed in EVOH copolymers as a consequence of electron beam irradiation.

## EXPERIMENTAL

### Materials

A commercial grade of an ethylene-vinyl alcohol copolymer containing a 29 mol percentage of ethylene in the copolymer composition (Soarnol® EVOH29) was supplied by the Nippon Synthetic Chemical Industry Co. Ltd (Nippon Gohsei, Osaka, Japan).. The films of two different thicknesses (ca. 10 and 60 µm) were shipped individually vacuum packaged in aluminium bags in order to keep their properties after irradiation as constant as possible. Non-irradiated samples were also supplied for the sake of comparison.

### Methods

*Irradiation*

The monolayer films of 10 and 60 µm of EVOH 29 were irradiated using an electron beam at doses of 30 and 90 KGy. Irradiation was carried out at room temperature in the presence of air with an Electrocurtain CB250/15/180L (Eye Graphics Co. Ltd.) in the Central Research Laboratory (Nippon Gohsei, Japan) with an acceleration voltage of 200 KV and an irradiation current of 1.4 mA. Irradiation doses were measured using an Eye Graphics Co. Ltd. method.

*Oxygen transmission rate*

Oxygen transmission rate ($O_2$TR) measurements were performed in an OX-TRAN® 2/20 (Mocon, US) at a temperature of 45ºC and 0% RH. High temperature assays were carried out in order to increase the permeability of the EVOH films and, thus, be able to measure it with higher certainty, given the very high barrier character of these materials with 29 mol% of ethylene content.

*Differential Scanning Calorimetry*

DSC experiments were carried out in a Perkin-Elmer DSC-7 calorimeter. The heating and cooling rate for the runs was 10ºC/min, being the typical sample weight around 4 mg. Calibration was performed using an indium sample. All tests were carried out, at least, in duplicate. The temperature range of the assays was from 50 to

200ºC. From the thermograms, the melting temperature was determined from the maximum of the endotherm.

*Fourier Transform Infrared Spectroscopy*

Transmission FT-IR experiments were recorded with a Bruker Tensor 37 equipment with 4 $cm^{-1}$ resolution and 4s as typical acquisition time. The samples, previously vacuum dried were placed into the measuring chamber which was continuously purged with a high flux of $N_2$ to maintain a constant dry and inert environment.

*Gas chromatography/mass spectrometry (GC/MS)*

The identification of organic compounds released by the irradiated films when exposed to air was carried out by gas chromatography coupled to mass spectroscopy. A film sample was introduced in a glass vial closed with a mininert valve (Supelco, Belafonte, PA, USA) and kept at room temperature during 10 days. The volatile compounds released in the vial headspace were concentrated by using a solid phase microextraction (SPME) device equipped with a 65 µm PDMS/DVB fiber (Supelco, Belafonte, PA, USA). The SPME system was introduced in the vial through the mininert port and the fiber was exposed to the headspace during 20 min. Then, the fiber was introduced in the injection port of a G1800A GC/MS (Agilent Technologies, Palo Alto, CA) where the volatile compounds were thermally desorbed and identified by comparison with mass spectra from a library database (Wiley 138K) and posterior verification with pure standards. The chromatographic conditions were: Injector temperature, 220ºC; Helium flow rate, 1 mL/min; GC-mass spectrometer interface temperature, 280ºC; initial oven temperature, 40ºC during 3 min; first temperature ramp at 3ºC/min to 60ºC; second ramp at 10ºC/min; final temperature, 250ºC for 5 min. The GC was equipped with a TRB-Meta X5 capillary column (30 m, 0.32 mm i.d., 0.25 µm film thickness, Teknokroma, Barcelona, Spain). Mass spectra were obtained by electron impact at 70 eV, and data were acquired across the range 34–400 uma.

## RESULTS AND DISCUSSION

*Oxygen scavenging capacity of irradiated EVOH*

Despite the extensive characterization of the effects of irradiation over polymeric materials, to the best of our knowledge, there has not been any previous report about the induced capacity of oxygen scavenging in any polymeric material which, specially in the case of plastics for food packaging applications (like EVOH copolymers used as high-barrier materials for oxygen-sensitive products) is of paramount importance.

This oxygen scavenging phenomenon of the irradiated EVOH29 was observed by placing the polymeric film samples in the OX-TRAN immediately after opening the aluminum bags supplied. The oxygen transmission rate ($O_2$TR) of the materials was recorded as a function of time until equilibrium was reached. Figure 1 shows the $O_2$TR evolution of the irradiated films in comparison with the non-irradiated polymer. In this case, as the thickness of the film samples analyzed is identical (10 microns), $O_2$TR values can be directly compared. From this figure it can be observed that the oxygen transmission rate of the EVOH29 irradiated at 90 KGy is close to zero during the first 50 hours and, in the case of the copolymer irradiated at 30 KGy, the passage of oxygen is “blocked” during more than 30 hours.

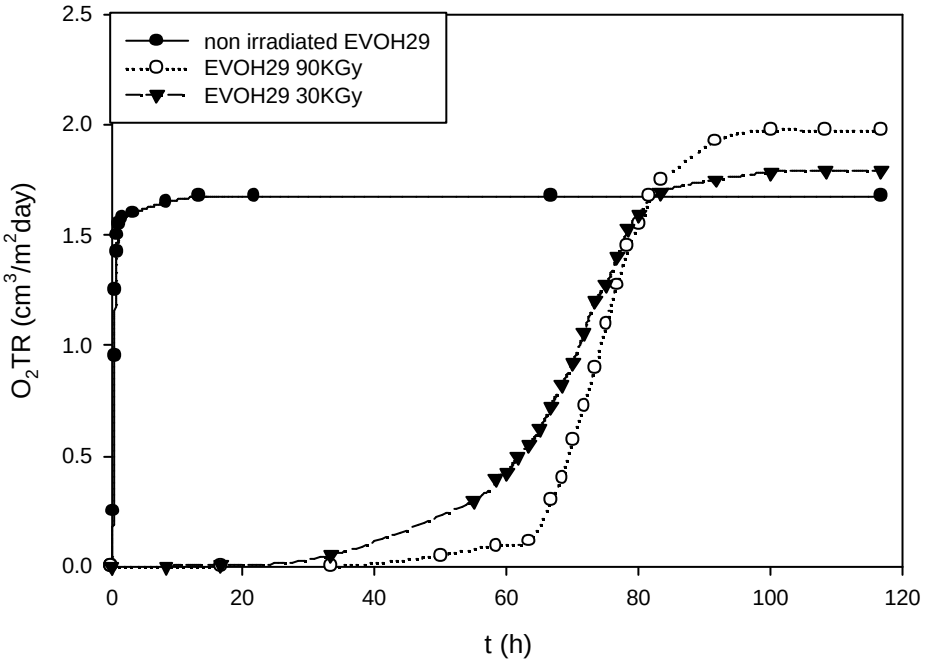

**Figure 1.** Oxygen transmission rate curves of EVOH29 non-irradiated and irradiated at 30 and 90 KGy

However, the equilibrium permeability of the irradiated films is higher (about 18% and 7% respectively) than that of the non-irradiated specimen and, therefore, it seems that the oxygen scavenging induced capacity is directly related with changes in the polymeric structure, because the higher the irradiation dose, the longer the time the polymer blocks oxygen and, concurrently, the higher the equilibrium permeability attained.

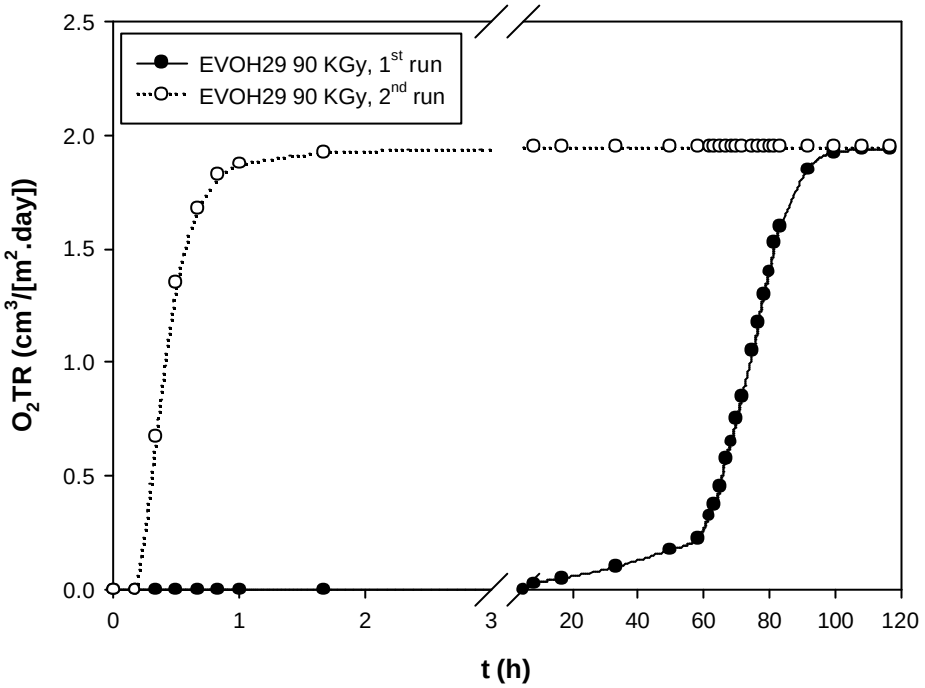


**Figure 2.** Oxygen transmission rate curves of EVOH29 irradiated at 90 KGy obtained immediately after opening (1st run), and once the scavenging effect is exhausted (2nd run).

After measuring their oxygen scavenging capacity, the irradiated films were exposed to dry nitrogen and a new $O_2$TR experiment was initiated. Figure 2 shows the first and second tests run on a sample irradiated at 90 KGy. In the second experiment, the curve profile, instead of reflecting the oxygen blocking capacity, was similar to that shown by the non-irradiated sample, although the final transmission rate was identical to that observed in the first experiment.

From the second run curve, it is possible to determine the diffusion coefficient (D) by curve fitting to the Pasternak's solution to the Fick's laws with the boundary conditions of the permeation experiment[16] :

$$\frac{F(t)}{F(\infty)} = \frac{4}{\sqrt{p}}\sqrt{\frac{\lambda^2}{4 \cdot D \cdot t}}\sum_{n=1,3,5}^{\infty}\exp\left(\frac{n^2\lambda^2}{4 \cdot D \cdot t}\right)$$

where F is the transmission rate at any time (t) and at equilibrium (8), and l is the film thickness. Considering that the Permeability coefficient is the product of D times the solubility coefficient (S) as defined be Henry's law, it is possible to characterize the oxygen transmission through the irradiated sample. Table 1 lists the values of the three coefficient for a non-irradiated sample and that irradiated at 90 KGy.

Table 1. Oxygen Permeability (P), diffusion (D) and solubility (S) coefficient values for non-irradiated and irradiated EVOH29 films

| | Non-irradiated | Irradiated 90 KGy |
|---|---|---|
| D (m2/s) | 8e-15 | 1.1e-14 |
| Permeability (m3.m/m2.s.Pa) | 1.94e-21 | 2.43e-21 |
| S (m3/m3.Pa) | 2.42 e-7 | 2.21e-7 |

As it can be observed, the irradiation slightly decreases the solubility to oxygen of the polymer but significantly increases the oxygen diffusion coefficient through the film. This last parameter appears to be the main responsible of the observed increment in $O_2$TR, and therefore in the permeability coefficient.

In figure 2, the area limited by the two curves (the oxygen scavenging film and that with this capacity exhausted), the $O_2$TR at equilibrium and the baseline can be an indirect measurement of the oxygen scavenging capacity of the film. For the 90 kGy irradiated film, this capacity has been estimated in about 5 $cm^3/m^2$ of film.

*Thermal and structural variations as a consequence of irradiation*

If the crystalline polymeric phase is affected by the irradiation treatment, it is expected that the thermal characteristics also change. Both the non-irradiated and irradiated copolymer samples were temperature scanned and the thermograms obtained are collected in Figure 3. The first heating runs of the three samples analyzed (upper curve of each experiment) display a rather broad melting endotherm but the maximum of the peak is displaced towards lower temperatures in the irradiated samples (the higher the dose used during irradiation, the lower the melting point). For the sake of clarity, the DSC parameters (melting and crystallization temperatures, enthalpies of fusion and crystallization and peak width) obtained for the different experiments are showed in Table 2.

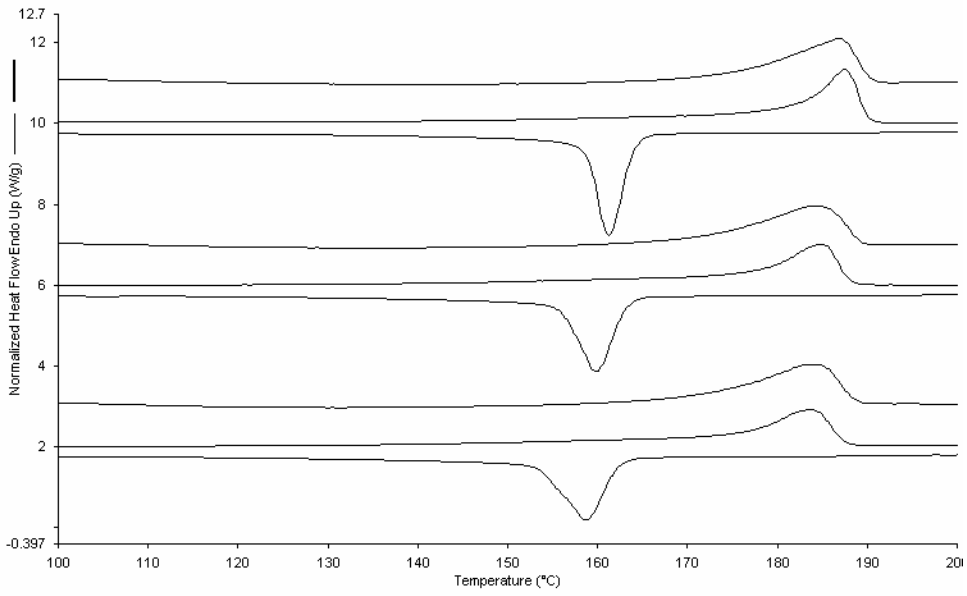


**Figure 3.** DSC thermograms of (from up to down): non-irradiated, irradiated at 30KGy and irradiated at 90KGy EVOH29. The three runs of each experiment are showed together in the figure, being the upper one the first heating run.

From Figure 3 it is apparent that there are induced structural changes and, moreover, that those morphological modifications caused by irradiation are irreversible. Again, the effects prove to be dose-dependent as, for example, the crystallization

temperature range is more extended after irradiation and if comparing between both treatments, the higher dose, i.e. 90 KGy shows the broadest crystallization peak.

**Table 2.** DSC parameters of non-irradiated, irradiated at 30KGy and irradiated at 90KGy EVOH29, being $T_m$ the melting point, $T_c$ the crystallization temperature, $\Delta H_f$ the enthalpy of fusion and $\Delta H_c$ the enthalpy of crystallization

| | | Non-irradiated | Irradiated at 30KGy | Irradiated at 90KGy |
|---|---|---|---|---|
| **1st HEATING RUN** | **$T_m$ (ºC)** | 187.00 | 184.00 | 183.83 |
| | **D$H_f$ (J/g)** | 70.84 | 74.06 | 76.47 |
| | **Peak width (ºC)** | 16.23 | 17.25 | 15.80 |
| **COOLING RUN** | **$T_c$ (ºC)** | 161.30 | 159.80 | 158.80 |
| | **D$H_c$ (J/g)** | -70.67 | -69.56 | -67.86 |
| | **Peak width (ºC)** | 5.32 | 7.57 | 8.97 |
| **2nd HEATING RUN** | **$T_m$ (ºC)** | 187.53 | 184.87 | 183.70 |
| | **D$H_f$ (J/g)** | 74.03 | 70.79 | 67.39 |
| | **Peak width (ºC)** | 8.07 | 11.16 | 12.41 |

In table 2 the dose-dependent irreversible morphological changes induced by irradiation are clearly discernible. From the second heating rate it is observed that the higher the irradiation dose, the lower the melting point and the enthalpy of fusion and the broadest the melting peak. That is, as the irradiation dose is increased the crystallinity appears to decrease and the crystals formed appear to be more heterogeneous.

Among the previously commented chemical reactions that arise after irradiation, the formation of free radicals has been observed to be the predominant path responsible for the structural changes in polymers irradiated with electron beam[17].
FT-IR analysis was carried out in the irradiated sample in order to detect potential structural changes. Previous infrared studies were made on irradiated EVOH, but as a part of a multilayer packaging structure[2] and, in that case, no significant changes were observed between the non-irradiated and irradiated IR spectra.

In Figure 4, FT-IR spectra in the range 900-1800 $cm^{-1}$ of EVOH29 non-irradiated and irradiated at 30KGy and 90KGy are represented. The spectra have been normalized to the intensity of the 1333 $cm^{-1}$ band for comparison purposes. From this figure, two remarkable changes are observed. First of all, from previous studies[18] it is

known that the band at 1140 $cm^{-1}$ in the spectra of EVOH copolymers can be related with their crystallinity, in a way that an increase in that band indicates an increase in the molecular order of the materials. The Figure 4b shows an enlargement of this range in which the decrease in the crystallinity band is hardly discernible in the case of EVOH29 irradiated at 30KGy, but for the copolymer irradiated at 90 KGy, a clear fall of the 1140 $cm^{-1}$ band is observed, indicating a loss of crystallinity due to the high-dose irradiation treatment.

**a)**

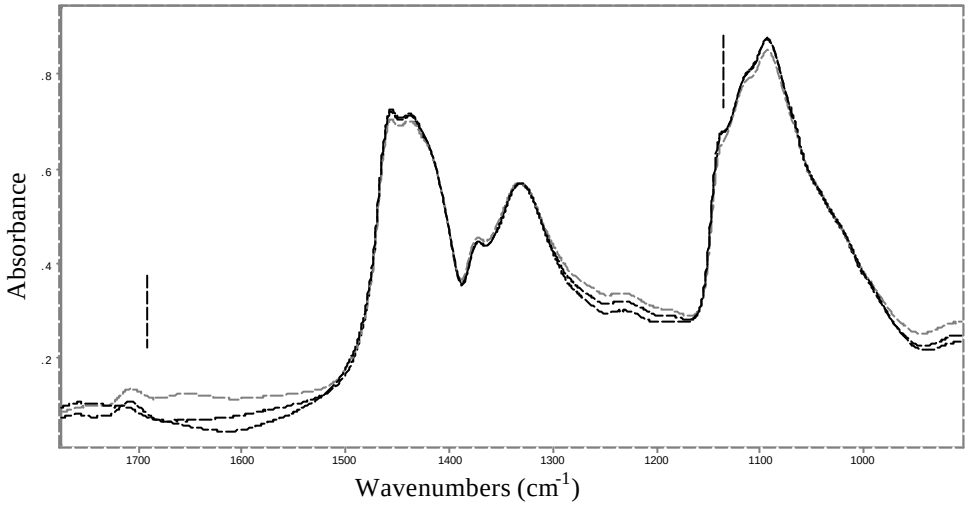


**b)**

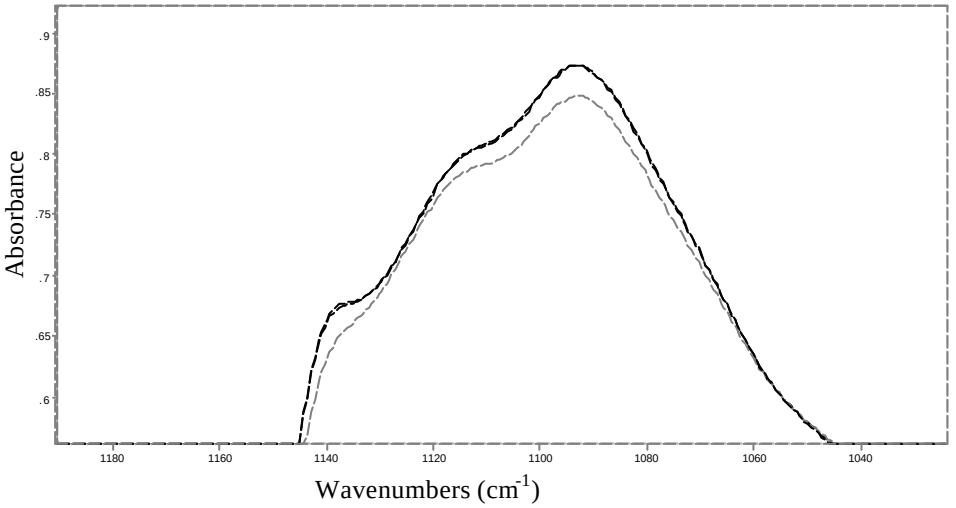


**Figure 4.** (a) FT-IR spectra of EVOH29 dry (continuous black line), irradiated at 30KGy (dashed black line) and irradiated at 90 KGy (grey line) in the range 900-1800 $cm^{-1}$. (b) Enlargement of the "crystallinity band" range

The second important change is a new band arising at around 1700 $cm^{-1}$ in both irradiated EVOH spectra. This band probably corresponds to the formation of degradation products, such as aldehydes and ketones. In fact, the C=O stretching mode of both aldehydes and ketones generates IR bands in the range 1680-1750 $cm^{-1}$. Those bands have been also observed at high irradiation doses in LDPE, and have been described to arise from the interaction of oxygen with free radicals of the polymer[19]. It would be, therefore, expectable that as oxygen molecules interact with the free radicals formed during the irradiation process, the intensity of this spectral range increase. The confirmation of this hypothesis was carried out with the 60 µm EVOH29 specimens that were measured in the transmission mode to get the absolute absorbance in the range of interest. Figure 5 shows the evolution of this range with time for a sample of EVOH29 irradiated at 90 KGy. To obtain the figure, the sample was recorded immediately after opening the vacuum sealed aluminum bag and between measurements it was stored mounted on the sample holder (to avoid changes in sample thickness or optical path) in a dessicator in order to keep the film dry.

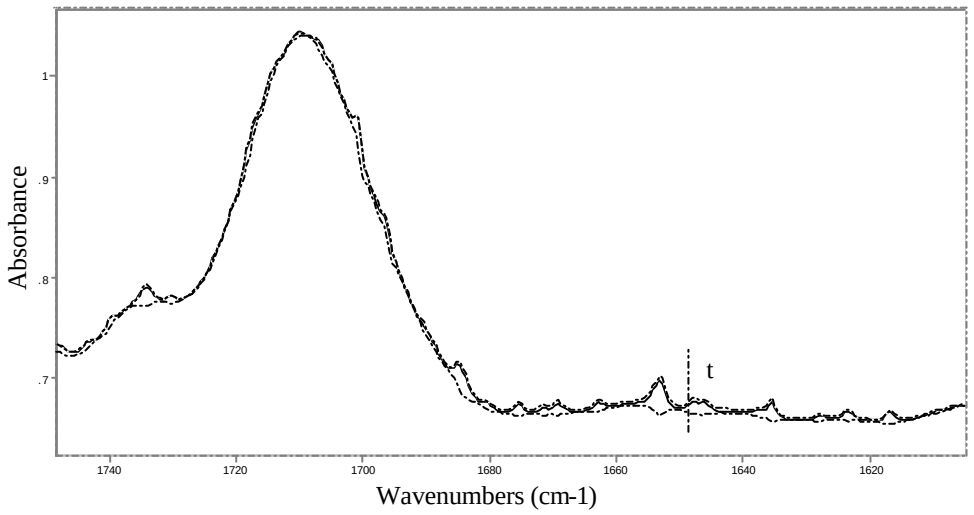


**Figure 5.** FT-IR spectra in the range 1600-1750 $cm^{-1}$ of an EVOH29 (60 microns thick) measured at various times after irradiation. The arrow indicate the formation of new degradation products as a function of time

From observation of Figure 5, the intensity of this spectral range increases with time as oxygen reacts with the free radicals of the sample. However this increase is rather small, indicating that most of the free radicals have already reacted with oxygen.

The formation of these compounds was further confirmed by gas chromatography coupled to mass spectrometry and, as an example, Figure 6 shows the chromatogram obtained following the methodology described in the experimental section. A piece of ca. 10 $cm^2$ of the 60 µm film irradiated at 90 KGy was introduced in an airtight vial and stored for 10 days at room temperature. A PDMS-DVB SPME device was used to concentrate the compounds desorbed by the irradiated film. A similar experiment was carried out with a non-irradiated sample to identify the compounds which desorption is caused just by the irradiation process or the posterior oxygen scavenging effect. No relevant peaks were obtained from the non-irradiated samples (results not shown). However, in the case of the irradiated sample, a number of volatile compounds were detected. Figure 6 shows a chromatogram obtained for this sample. As it can be seen, several linear aldehydes and ketones were identified as radiolytic compounds. The difference between these results and those observed by Kothapalli and Sadler[11] could be easily explained by the different methodology used. They extracted the radiolysis compounds from the EVOH samples with liquid solvents used as food simulants, while in this work only volatile compounds released by the film in the vial headspace and trapped by the SPME fiber were analyzed.

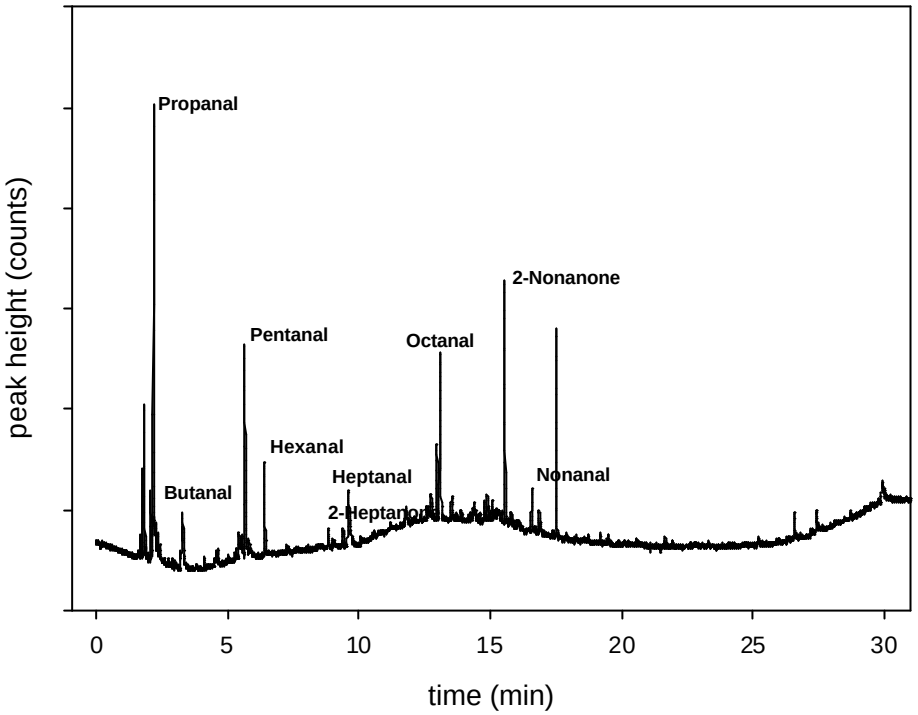


**Figure 6.** Gas chromatogram highlighting the most relevant volatile compounds, released by an EVOH29 film irradiated at 90 kGy, using the experimental conditions described in the experimental section.

## REFERENCES

[1] Azuma, K. Hirata, T. Tsunoda, H. Ishitani, T. Tanaka, Y. Identification of the volatiles from low density polyethylene film irradiated with an electron beam. *Agricultural and Biological Chemistry 47*(4), 855 (1983)

[2] Riganakos, K.A., Koller, W.D., Ehlermann, D.A.E., Bauer, B. & Kontominas, M.G. Effects of ionizing radiation on properties of monolayer and multilayer flexible food packaging materials. *Radiation Physics and Chemistry 54*, 527 (1999)

[3] Farkas, J.. Irradiation as a method for decontaminating food. A review. *International Journal of Food Microbiology 44*, 189 (1998)

[4] Urbain, W.M. In: *Advances in Food Research*. Academic Press, Nueva York, 155 (1978)

[5] Loaharanu, P. In: *New methods of food preservation*. G.W. Gould, ed. Champman & Hall, Londres, 90 (1995)

[6] Rahman, M.S. *Handbook of Food Preservation*. Marcel Dekker, Inc. Nueva York (1997)

[7] Merrit, C. Qualitative and quantitative aspects of trace volatile components in irradiated foods and food substances. *Radiation Research Reviews 3*, 353 (1972)

[8] Killoran, J.J. Chemical and physical changes in food packaging materials exposed to ionizing radiation. *Radiation Research Reviews 3*, 369 (1972)

[9]Komolprasert, V., McNeal, T.P., Agrawal, A., Addikari, C., Thayer, D.W. Volatile and non-volatile compounds in irradiated semi-rigid crystalline poly(ethylene terephtalate) polymers. *Food Additives and Contaminants 18*, 89 (2001)

[10] Krzymien, M.E., Carlsson, D.J., Deschenes, L., Mercler, M. Analysis of volatile transformation products from additives in gamma-irradiated polyethylene packaging. *Food Additives and Contaminants 18*, 739 (2001)

[11] Kothapalli, A., Sadler, G. Determination of non-volatile radiolytic compounds in ethylene co-vinyl alcohol. *Nuclear Instruments and Methods in Physics Research B 208*, 340 (2003)

[12] Thayer, D.W. Chemical changes in food packaging resulting from ionizing radiation. *Food and Packaging Interactions.* J.H. Hotchkiss, ed. ACS Symposium Series No.365, Washington, 181 (1988)

[13] Keay, J.N. The effect of irradiation doses of gamma irradiation up to 16 Mrad on plastic packaging materials for fish. *Journal of Food Technology 3*, 123 (1968)

[14] USFDA 21CFR 179.45

[15] Kuznesof, P.M., VanDerveer, M.C. In: *Plastics, Rubber, and Paper Recycling*, ACS Symposium Series No. 609, Washington, 389 (1995)

[16] Gavara, R., Hernández, R.J. Consistency test for continuous flow permeability experimental data. *Journal of Plastic Film and Sheeting 9*, 126 (1993)

[17] Sadler, G., Chappas, W., Pierce, D.E. Evaluation of e-beam, gamma- and X-ray treatment on the chemistry and safety of polymers used with pre-packaged irradiated food: a review. *Food Additives and Contaminants 18*(6), 475 (2001).

[18] López-Rubio, A., Lagaron, J.M., Gimenez, E., Cava, D., Hernandez-Muñoz, P., Tomoyuki Yamamoto, T., Gavara., R. Morphological alterations induced by temperatura and humidity in ethylene-vinyl alcohol copolymers. *Macromolecules 36*, 9467 (2003)

[19]Goulas, A.E., Riganakos, K.A., Badeka, A., Kontominas, M.G. Effects of ionizing radiation on the physicochemical and mechanical properties of commercial monolayer flexible plastics packaging materials. *Food Additives and Contaminants 19* (12), 1190 (2002)

# IMPROVING PACKAGED FOOD QUALITY AND SAFETY BY SYNCHROTRON X-RAY ANALYSIS

## INTRODUCCIÓN AL ARTÍCULO VIII

En este artículo, publicado en la revista *Food Additives and Contaminants* (vid Anexo 4), se pretende enfatizar el potencial de la técnica de difracción de rayos X utilizando una fuente de radiación sincrotrón para el estudio de diversos problemas relacionados con la calidad alimentaria, en la que los envases juegan un papel fundamental. Esta técnica, que se viene utilizando ampliamente en diversos estudios básicos fundamentalmente centrados en la dilucidación de estructuras (bien sean polímeros, bien proteínas) puede, sin embargo, ser utilizada para abordar problemas diversos en los que la rapidez del método, alta resolución, carácter no destructivo y la posibilidad de realizar experimentos resueltos en el tiempo simulando diversos procesos, la convierten en una herramienta muy interesante.

Sin lugar a dudas, los estudios de rayos X mediante radiación sincrotrón han sido decisivos en muchos de los resultados presentados en la tesis y, por ello, hemos considerado interesante incluir este artículo en el que, aunque aparecen algunos de los estudios ya mostrados, se introduce la técnica resaltando algunas de sus propiedades y se comentan sus aplicaciones.

**ABSTRACT**

The objective was to demonstrate, as an example of an application, the potential of synchrotron X-ray analysis to detect morphological alterations that can occur in barrier packaging materials and structures. These changes can affect the packaging barrier characteristics when conventional food preservation treatments are applied to packaged food. The paper presents the results of a number of experiments where time-resolved combined wide-angle X-ray scattering and small-angle X-ray scattering analysis as a function of temperature and humidity were applied to ethylene-vinyl alcohol co-polymers (EVOH), polypropylene (PP)/EVOH/PP structures, aliphatic polyketone terpolymer (PK) and amorphous polyamide (aPA) materials. A comparison between conventional retorting and high-pressure processing treatments in terms of morphologic
alterations are also presented for EVOH. The impact of retorting on the EVOH structure contrasts with the good behaviour of the PK during this treatment and with that of aPA. However, no significant structural changes were observed by wide-angle X-ray scattering in the EVOH structures after high-pressure processing treatment. These structural observations have also been correlated with oxygen permeability measurements that are of importance when guaranteeing the intended levels of safety and quality of packaged food.

Keywords: Plastics packaging, synchrotron X-ray analysis, food preservation, processing

## INTRODUCTION

When evaluating the quality and safety of food products, several parameters have to be taken into account. Food safety is usually referred to the absence of foodborne pathogens, while food quality comprise, not only microbial quality, but also sensorial or organoleptical quality and, of course, nutritional quality. In packaged foods, quality also extends to the appearance and preservation of the functional properties of the package. Among the agents that can cause food spoilage, micro-organisms, enzymes and chemical reactions are the most relevant. In order to control the action of these alterating agents, diverse preservation methods are applied to food products which seek to destroy unwanted enzymes and micro-organisms while maintaining original texture and nutritional characteristics.

Nowadays, packages play a significant role in food quality preservation and, among them, plastic packages are gaining importance due to their balanced characteristics (transparency, flexibility, versatility, low cost, easy of processing, etc.) and the wide variety of formulations which allow the development of packaging structures for specific product requirements. Many food products are commercialized inside plastic packages which, in fact, constitute a critical parameter in determining their shelf-life because, unlike other traditional packaging materials, such as glass or tinplate, polymers are permeable to gases and low molecular weight substances. Today, many preservation processes are applied to the already packaged food products and, therefore, the package characteristics must be tailored and controlled to withstand such processes and to guarantee the quality of products along shelf-life. Chemistry is in polymers one of the most important factors defining structure and, therefore, end properties (Lagarón et al., 2004). Polymer morphology is for a given chemistry an important structural parameter in itself, because it defines and controls many characteristics, being the most relevant one for the purpose of this study the barrier properties to gases, water and organic vapours.

Synchrotron X-ray radiation is, in general, a high brilliant source of energy capable of unravelling the state of matter at different molecular scales. Several characteristics make this tool one of the most powerful techniques available for exploring matter, namely:

- The intensity of the radiation can be of the order of a billion times greater than radiation from a typical laboratory x-ray source.
- The emerging beams can be extremely fine (just a few microns across).
- The beam is highly collimated, that is, divergence is very low.
- The radiation spectrum can span from infra-red to hard x-rays.
- Provides intense brightness and tenability across the spectrum.
- Synchrotron radiation is pulsed (pulses of 10-100 picoseconds separated by 10-100 nanoseconds).

Due to their outstanding characteristics, synchrotron light is a very good technique for pure and applied research in a great variety of areas. Specifically, in the food research area, it has been used to examine diverse quality-related subjects such as the presence of mercury in fish (Harris et al., 2003), the polymorphism of cocoa-butter to avoid fat bloom in chocolate (Kalnin et al., 2002; Schenk and Peschar, 2004) or to ascertain how starch granules react to heat and frost (Donald et al., 2001). For the study of the structure of polymers, however, synchrotron radiation is an indispensable tool. The polymer morphology, particularly the crystalline phase, is of paramount importance in defining the physical and chemical properties of polymers. This can be resolved by small angle X-ray scattering (SAXS) and wide angle X-ray scattering (WAXS) experiments. While SAXS experiments allow the determination of the averaged repeat distance between beginning and end of two adjacent lamellar crystals, i.e. thickness of the lamellar crystal plus the thickness of the intermediate amorphous phase, and also provides important information about the polymer morphology; the crystal structure and the content of crystallinity are usually deduced from the position and intensity of the peaks in the WAXS pattern (Ryan et al., 1994). Nevertheless, the most important aspect of synchrotron X-ray analysis in polymers is that because it is a high brilliance source, it allows to monitor simultaneously WAXS and SAXS experiments and permits to follow time-resolved processes in line such as crystallization, chemical reactions, processing and industrial process monitoring, etc..

The potential of synchrotron light as in-process analyzer and to assure food quality and safety issues from a food packaging point of view is demonstrated in this work through the application of time resolved X-ray experiments to monitor typical industrial retorting processes and after high pressure treatment of various barrier materials.

## MATERIALS AND METHODS

*Materials*

The barrier polymeric materials selected for this study are:

Two commercial ethylene-vinyl alcohol (EVOH) copolymer grades (Soarnol®), EVOH32 and EVOH26, where the numbers indicate the mol percentage of ethylene in the copolymer composition. The EVOH samples were supplied by The Nippon Synthetic Chemical Industry Co., Ltd. (NIPPON GOHSEI) (Japan), co-extruded between polypropylene layers but without adhesive.

The aliphatic polyketone (PK) terpolymer used in this study was synthesized at BP Chemicals (UK) using a proprietary palladium-based catalyst. The PK sample is a perfectly alternating ethene/propene/CO terpolymer (EPCO) where the propene substitutes randomly for ethene. In this material the mol percent of CO is always 50 mol% across composition and the amount of the second olefin was not specified.

Finally, a Selar amorphous polyamide UX-2034 from Dupont (U.S.A) polymerized by the condensation of hexamethylene diamine and a mixture of 70:30 isophthalic and terephthalic acids was also studied.

*Food preservation processes*

Sterilization of the materials was carried out in an autoclave at 121ºC during 20 minutes.

High pressure processing (HPP) was performed with a QFP-6 Flow Batch High Pressure Food Processor (Flow Autoclave System, Columbus, OH). The HPP conditions were 400 and 800 MPa, for 5 and 10 min, at 40 and 75°C (López-Rubio et al., 2005).

*Methods*

Simultaneous WAXS and SAXS experiments were carried out at the synchrotron radiation source in the soft condensed matter beam (A2 station) at Hasylab (DESY) in Hamburg (Germany). Scattering patterns were recorded using a one dimensional detector and an incident radiation wavelength, ?, of 0.15 nm. WAXS and SAXS data were corrected for detector response and beam intensity and calibrated against PET and rat tail standards, respectively. Temperature scans were also carried out at 5$^{o}$C/min on dry and in the presence of water excess in films of the samples. Presence

of water vapour during the temperature experiments were ensured by sealing the film specimens in excess of moisture between thick aluminum layers and O-rings rubber seals inside a screwed rectangular cell compartment specifically designed for functioning as an autoclave (López-Rubio et al., 2003). Experiment success was checked by observation of constant background intensity over the experiment and presence of moisture in the cell after termination of the thermal experiments, which indicated that moisture did not leak off the cell during the temperature run. The cited conditions are thought to closely simulate circumstances occurring during industrial retorting processes.

Oxygen transmission rate ($O_2$TR) measurements were performed in an OX-TRAN® 2/20 (Mocon, US) at a temperature of 48$^{o}$C and 0% RH. Permeability tests were carried out above room temperature in order to increase the permeability of the films and, thus, be able to measure it with higher certainty, given the very high gas barrier character of these materials.

**RESULTS AND DISCUSSION**

Figure 1 show, as an example, the simultaneous WAXS and SAXS diffraction patterns of a dry specimen of EVOH32 as a function of temperature (López-Rubio et al., 2003). From this experiment it can be seen that, as temperature increases in the polymer the WAXS and SAXS patterns rise due to annealing at first but, later, vanish at the melting point of the polymer. The polymer melts at around 180$^{o}$C, in agreement with DSC data.

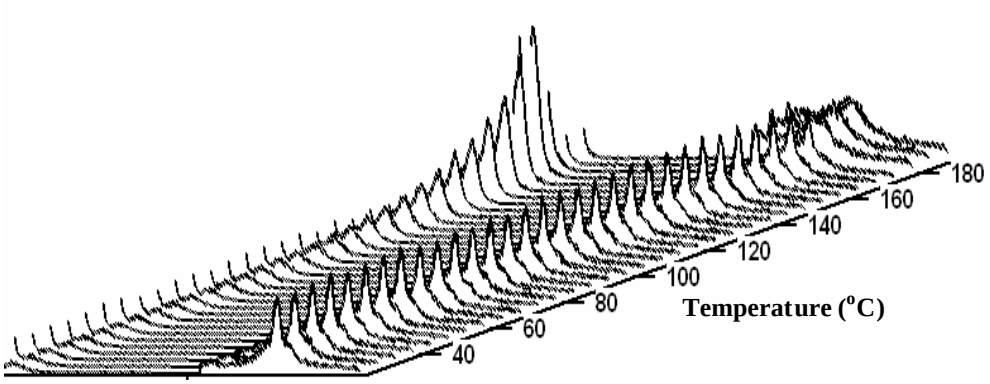


**Figure 1.** Typical synchrotron simultaneous WAXS and SAXS traces as a function of temperature for a dry sample of EVOH32.

Figure 2 shows the long period calculated from the maximum of the SAXS peak after Lorentz correction, for a dry and for a sample retorted in situ within the cell as described in the experimental section. This Figure shows that, as the sample melts, the long period rises just before total disappearance (see SAXS in Figure 1); in the case of the dry sample the long period disappears at around 180$^{o}$C in agreement with the melting point of the polymer by DSC and WAXS. However, the sample retorted shows a much earlier melting at around 100$^{o}$C, which is 83$^{o}$C below the actual melting point of the polymer.

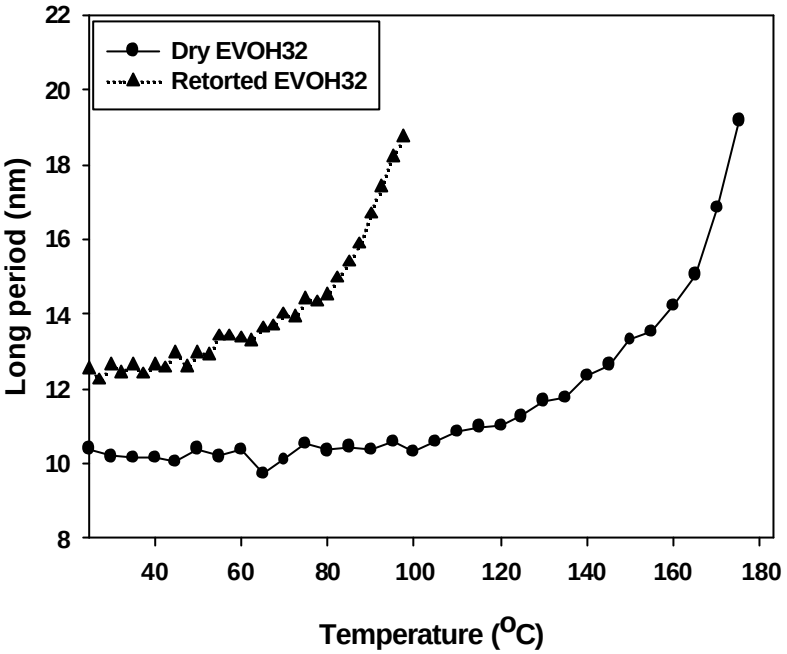


**Figure 2.** Evolution of the long period of dry and in-situ retorted EVOH32 specimens.

This structural deterioration caused by the retorting process has a direct impact on the barrier performance of the copolymer, compromising, therefore, the shelf-life of the packaged product in case an EVOH monolayer was used as the barrier layer.

This dramatic crystallinity deterioration suffered by EVOH films during retorting can be partially overcome by efficient protection between water barrier polymers like polypropylene (PP). From our studies with synchrotron radiation, it was observed that by appropriate shielding of the EVOH layer between polypropylene layers of a critical thickness (40 microns) the EVOH integrity was found to be largely maintained during a typical retorting process (see Figure 3). The experiments were carried in the retorting cell with polypropylene layers of varying thickness, until no significant structural damage of the barrier polymer was seen. In Figure 3, the arrow indicates the presence of the (110) crystalline peak of EVOH in the structure during the whole retorting experiment, suggesting that the barrier layer does not melt in a multilayer structure. Nevertheless, the complex diffraction pattern of the multilayer makes difficult a quantitative analysis to determine to what extent the degree and

morphology of the crystallininity is affected during the experiment. Of course, it is well known that even if the crystallinity of the polymer remains intact after the retorting process, a significant plasticization of the amorphous phase does still occur due to some water ingress through the PP layers, which leads to a decrease in barrier properties (see Table 1). This Table indicates that a very strong plasticization takes place in the polymer as a result of water sorption and morphological damage. To overcome these problems some solutions have been provided (López et al., 2005a), whereby by increasing the thickness of the PP layer further, pre-annealing of the EVOH layer to strengthen crystals and/or subsequent drying of the packaged food after retorting, the effect can be partially or totally counteracted.

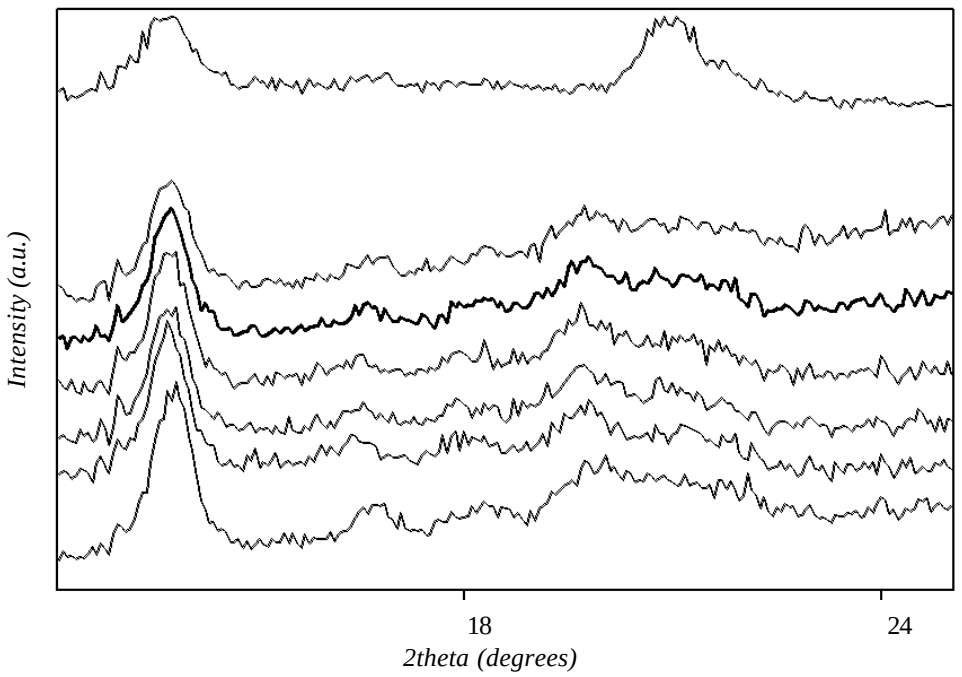


**Figure 3.** WAXS patterns of PP, EVOH32 and of PP/EVOH/PP structures during different stages of the retorting process.

In contrast to the high water sensitivity of the morphology of ethylene-vinyl alcohol copolymers, the aliphatic polyketone terpolymer was found to retain its crystalline structure along the in-situ sterilization process carried out at the synchrotron station, as it can be observed from Figure 4. Figure 4 shows that the main crystalline diffraction peak of the PK sample is retained over time during the retorting

experiment suggesting that the crystalline morphology of the polymer does not suffer deterioration during retorting even in a monolayer situation. Detailed observation of Figure 4 indicates that a small decrease in the intensity of the crystalline peak is seen at around 100°C; however, this is due to partial melting of the polymer because it can also be seen in the dry sample (results not shown). Table 1 indicates that some plasticization, oxygen barrier decrease, takes place in the polymer after retorting, which is most likely the result of water sorption in the amorphous phase and, therefore, has no morphological origin. In fact, and unlike EVOH, after drying the PK sample does recover the original permeability.

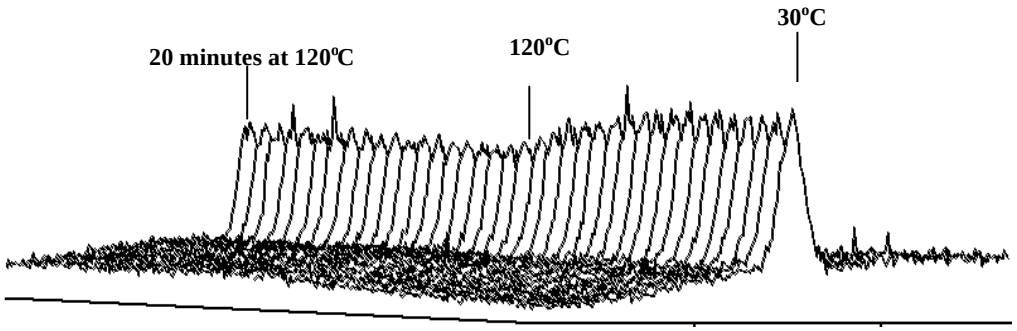


**Figure 4.** WAXS patterns of a PK specimen taken during a typical retorting experiment.

A third situation in terms of morphological alterations during retorting is observed for the case of the amorphous polyamide (aPA). This material develops during retorting some crystallinity as can be observed from observation of Figure 5.

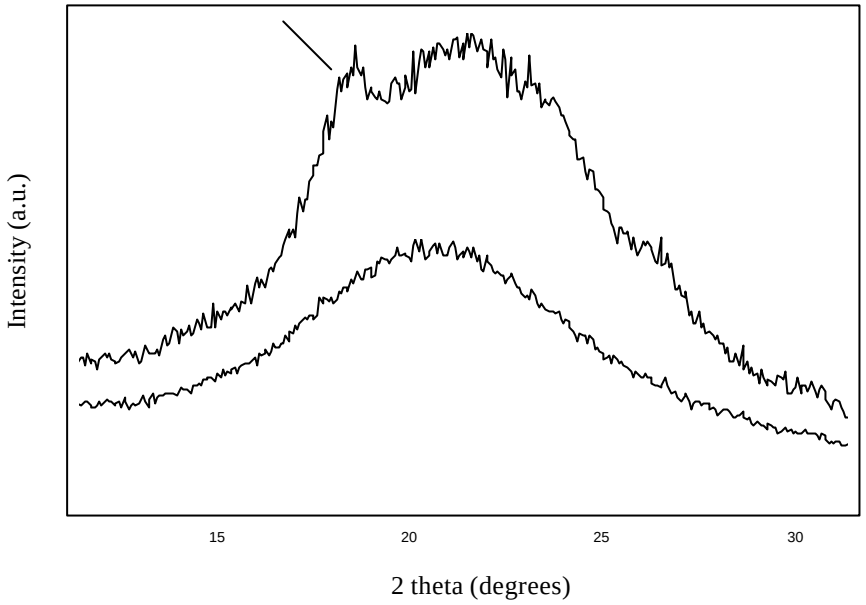


**Figure 5.** WAXS diffraction patterns of retorted (top curve) and untreated (bottom curve) amorphous polyamide.

Figure 5 shows that the amorphous halo of the dry sample is different in the retorted sample. In the latter sample, a small crystalline diffraction peak appears at 2? ≈ 18º. The small shoulder seen at 27º is an artefact coming from the cell. These observations suggest that retorting allows some organization of the polyamide chains to establish some degree of molecular order, which is, at the moment under investigation and that will be reported more in detail elsewhere. Oxygen barrier deterioration after retorting of this sample is almost negligible (see Table 1).

In another context, current consumption trends towards mildly preserved, high quality and more fresh-like products are leading to an increased interest in the substitution of more conventional aggressive thermal treatments such as retorting, by other emerging preservation technologies such as high-pressure processing (HPP), irradiation or microwave processing. As an example, one important objective of this synchrotron study was to compare the morphological and barrier properties effects suffered by EVOH subjected to high pressure treatments as opposed to the damaging retorting processing.

Figure 6 shows the diffractograms of EVOH26 untreated and retorted (a) and untreated and high-pressure processed (b). After retorting, as stated before, the peak becomes broader and less defined, indicating the disruption of the crystalline structure which is, obviously, more heterogeneous, due to crystal fractionation. On

the other hand, few changes are observed between the diffractograms of untreated and HPP copolymers.

Table 1 also indicates that no alterations in barrier properties are observed after application of HHP[9]. Synchrotron experiments during in situ high pressure treatments are being planned at the moment to study the actual changes that can occur in the packaged food during HPP processes.

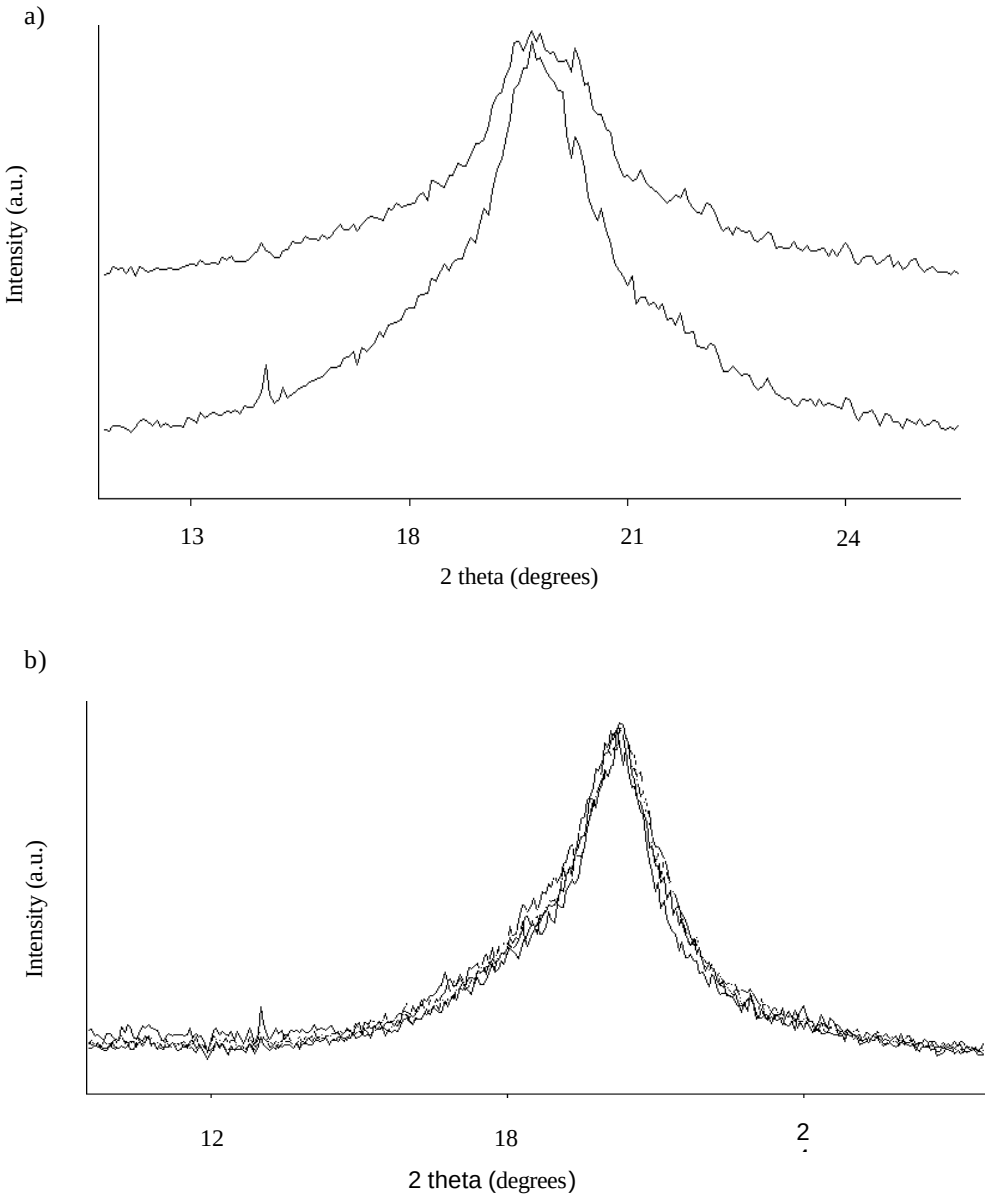


**Figure 6.** (a) Synchrotron WAXS diffractograms of untreated (bottom) and retorted (up) EVOH26 specimens and (b) Diffractograms of untreated and high-pressure processed EVOH26 specimens.

## CONCLUSIONS

Synchrotron X-ray analysis is a very powerful source of structural information to study in situ potential alterations in foods and food packaging materials during application of industrial processes. In this work, the technique has been applied to ascertain potential structural damages suffered by high barrier materials during retorting, and that can have a significant impact in food quality and safety of packaged foods. This type of studies is very useful prior to the selection of suitable materials for specific applications or to estimate the limiting conditions of use and, moreover, the morphological results obtained can also be related to property changes such as barrier properties.

**Acknowledgements**

The authors would like to acknowledge Mr. Y. Saito of The Nippon Synthetic Chemical Industry Co. Ltd. (NIPPON GOHSEI), Japan for supplying EVOH and for financial support and to Dr. Graham Bonner, BP Solvay Polyethyelene, Belgium for supplying the PK material. The work performed at the synchrotron facility in Hamburg (Hasylab, Germany) was supported by the IHP-Contract HPRI-CT-1999-00040/2001-00140 of the European Commission and the authors would also like to acknowledged Dr. S.S. Funari and Mr. M. Dommach (Hasylab) for experimental support.

## REFERENCES

Donald, A.M.; Kato, K.L.; Perry, P.A.; Waigh, T.A. (2001). Scattering studies of the internal structure of starch granules. Starch 53, 504-512.

Harris, H.H.; Pickering, I.J.; George, G.N. (2003).The chemical form of mercury in fish. Science 301: 1203

Kalnin, D.; Garnaud, G.; Amenitsch, H.; Ollivon, M. (2002). Monitoring fat crystallization in aerated food emulsions by combined DSC and time-resolved synchrotron X-ray diffraction. Food Research International 32, 927-934.

Lagarón, J.M.; Catalá, R.; Gavara, R. (2004) Structural characteristics defining high barrier properties in polymeric materials. Materials Science and Technology 20 (1), 1-7

López-Rubio, A.; Lagarón, J.M.; Giménez, E.; Cava, D; Hernández-Muñoz, P.; Yamamoto, T.; Gavara, R. (2003). On the morphological alterations induced by temperature and humidity in ethylene-vinyl alcohol copolymers. Macromolecules 36, 9467-9476.

López-Rubio, A.; Lagarón, J.M.; Hernández-Muñoz, P.; Almenar, E.; Catalá, R, Gavara R, Pascall MA. 2005. Effect of high pressure treatments on the properties of EVOH based food packaging materials. Innovative Food Science and Emerging Technologies 6:51–58.

Lopez-Rubio, A; Gimenez, E; Hernandez-Muñoz, P; Tomoyuki, Y; Gavara, R; Lagaron, JM (2005). Morphological and Barrier Properties Alterations in EVOH Copolymers as a Result of Packaged Food Retorting Processes. Accepted for publication in J. Appl. Polym. Sci.

Ryan, A.J.; Bras, W.; Mant, G.R.; Derbyshire, G.E. (1994). A direct method to determine the degree of crystallinity and lamellar thickness of polymers: application to polyethylene. Polymer 35, 4537-4544.

Schenk, H.; Peschar, R. Understanding the structure of chocolate. Radiation Physics and Chemistry 71 (2004), 829-835.

## 5 CONCLUSIONES

La presente tesis ha profundizado en el estudio de los daños provocados por los tratamientos de esterilización en autoclave sobre los copolímeros de etileno y alcohol vinílico (EVOH), y ha propuesto y establecido diferentes estrategias y alternativas para asegurar la conservación de alimentos sensibles al oxígeno de larga duración envasados en estructuras plásticas.

Del trabajo realizado se pueden resaltar las siguientes conclusiones:

1. Los tratamientos de temperatura aplicados entre la temperatura de transición vítrea del material y su temperatura de fusión (lo que se conoce como “recocido”, “templado” o “annealing”) provocan una mejora en la estructura cristalina de los copolímeros EVOH. Al aumentar la temperatura de recocido, aumenta el período largo, siendo este aumento más pronunciado en aquellos copolímeros con mayor contenido en etileno, que se explica por su menor temperatura de fusión. Por otra parte, la sorción de agua en los copolímeros EVOH conduce a una disolución parcial de los cristales más defectuosos que no se recupera tras la desorción. Cuanto mayor es el contenido en alcohol vinílico y, por tanto, la afinidad al agua de los copolímeros, mayor es la caída en la cristalinidad en presencia de humedad.
2. Los tratamientos de esterilización en autoclave sobre los copolímeros EVOH, conducen a una estructura cristalina más defectuosa y heterogénea y mediante experimentos de radiación sincrotrón simulando una esterilización in-situ, se observó que en presencia de vapor de agua a presión, la cristalinidad y por tanto la consistencia del EVOH32 (32% en moles de etileno) comienza a disminuir al calentar por encima de temperatura ambiente y funde por completo alrededor de 100ºC, es decir, 83ºC por debajo de su punto de fusión.
3. Independientemente de su composición, inmediatamente después de la esterilización, tiene lugar un enorme deterioro en las propiedades barrera a oxígeno de los copolímeros. En el caso de los copolímeros con mayor contenido en alcohol vinílico (>62%), la permeabilidad original de los materiales no llega a recuperarse por completo debido al daño estructural provocado por el tratamiento y este fenómeno es tanto más acusado cuanto mayor es el contenido en alcohol

vinílico del material. Curiosamente, sin embargo la permeabilidad a oxígeno en el equilibrio alcanzada tras la esterilización de los copolímeros con mayor contenido en etileno (EVOH44 y EVOH48) es incluso menor que su permeabilidad original.

4. Un secado posterior a la esterilización (70ºC a vacío) conduce, en todos los copolímeros EVOH estudiados, a una mejora de las propiedades barrera, siendo esta mejora más pronunciada para los copolímeros con mayor contenido en etileno. Este fenómeno puede explicarse considerando que durante el tratamiento de secado tiene lugar una fusión de los cristales más pequeños y defectuosos, y una posterior reorganización y recristalización de los segmentos de cadena dando lugar a una estructura cristalina mejorada más impermeable.
5. El tratamiento de recocido previo a la esterilización (optimizado en función de la composición del copolímero), mejora la resistencia a estos procesos de los materiales con mayor contenido en alcohol vinílico (EVOH26, EVOH29 y EVOH32). Incluso en el caso del EVOH26, se observó que tras el recocido y posterior esterilización en autoclave, el grado de cristalinidad era similar al de la muestra sin tratar y además que el nivel de sorción de agua era menor que en la muestra que no había sido previamente recocida.
6. Las mezclas estudiadas de EVOH con poliamida amorfa y con poliamida e ionómero mejoran la resistencia de los copolímeros a la esterilización en términos de propiedades térmicas y estructura cristalina. Sin embargo, las propiedades barrera de sistemas multicapa solo son mejores para el caso de la mezcla de EVOH con PA amorfa debido a la gran interacción entre componentes y potencialmente a la cristalizacion parcial de la PA.
7. A diferencia de los daños que provoca la esterilización en los copolímeros EVOH, las policetonas alifáticas estudiadas, al ser sometidas a este tratamiento combinado de temperatura y vapor de agua a presión, sólo mostraron sorción de agua que, al plastificar la estructura, resultó en un aumento de la permeabilidad a oxígeno. Este aumento fue relativamente menor que en el caso del EVOH ya que, a diferencia de éste, apenas hubo daño estructural y, por tanto, la recuperación de las propiedades barrera de las policetonas tras la esterilización es prácticamente total.
8. También se comprobó que la poliamida amorfa, que fue otro de los materiales de alta barrera estudiados frente a la esterilización, es capaz de desarrollar cierto

orden cristalino al ser sometido a tratamientos combinados de temperatura y humedad, como en el caso de la esterilización. La morfología cristalina formada, aunque bastante imperfecta y heterogénea, consigue ofrecer mejores propiedades barrera a oxígeno e, incluso, mejora las propiedades barrera a agua de este polímero originalmente amorfo.

9. A diferencia de los tratamientos de esterilización, los tratamientos de conservación mediante altas presiones hidrostáticas no afectan significativamente a los copolímeros EVOH, conduciendo incluso a una mejora de la estructura cristalina y, paralelamente, a una disminución de la permeabilidad a oxígeno, en aquellos copolímeros con mayor contenido en alcohol vinílico.
10. Los tratamientos de conservación mediante irradiación con electrones acelerados, que también se aplican sobre los alimentos previamente envasados, producen en los copolímeros EVOH una alteración en su estructura que conduce durante las primeras horas tras el tratamiento, a un bloqueo del oxígeno en su estructura, debido a la interacción de este gas con los radicales libres formados durante el tratamiento. Sin embargo, la permeabilidad final que alcanza el material en el equilibrio, es decir, tras la reacción del oxígeno con todos los radicales libres formados durante la irradiación, es sustancialmente superior a la permeabilidad original de los copolímeros. Esta mayor permeabilidad al oxígeno de los materiales irradiados se deriva del daño estructural provocado como resultado de la irradiación.